The potential therapeutic benefit of targeting S-phase kinase-associated protein 2 (SKP2) in neuroblastoma.

Laura Elizabeth Evans

Thesis submitted for the degree of Doctor of Philosophy

Newcastle University

Faculty of Medical Sciences

Northern Institute for Cancer Research

September 2014

Abstract

S-phase kinase-associated protein 2 (SKP2) is the substrate recognition subunit of the SCF E3 ubiquitin ligase complex which monitors the G_1/S transition of the cell cycle. SKP2 is a positive regulator of cell cycle progression targeting tumour suppressor proteins for degradation, primarily the cyclin-dependent kinase inhibitor $p27^{KIP1}$. An oncogenic protein, SKP2 is frequently overexpressed in human cancers and contributes to malignant progression. S*KP2* has previously been identified as a possible MYCN target gene in neuroblastoma and based on these reports it is hypothesised that SKP2 is a potential therapeutic target in *MYCN* amplified disease.

In this study a positive correlation between MYCN expression and *SKP2* mRNA expression was shown in the SHEP-Tet21N MYCN-regulatable cell line and in a panel of *MYCN* amplified and non-amplified neuroblastoma cell lines. In chromatin immunoprecipitation and reporter gene assays, MYCN bound directly to E-box DNA binding motifs within the *SKP2* promoter, and induced transcriptional activity which was decreased by the removal of MYCN and mutation of the E-boxes.

SKP2 knockdown induced cell cycle arrest and apoptosis in non-*MYCN* amplified neuroblastoma cell lines independent of the p53 pathway. The G_1 arrest induced was rescued in-part by the knockdown of $p27^{KIP1}$ confirming the importance of the SKP2/p27 axis in cell cycle progression in neuroblastoma.

Structure-activity relationship analysis identified a sub-set of putative SKP2 inhibitors which inhibited growth and suppressed SKP2-mediated p27 degradation in HeLa cells. Additionally, treatment of the MYCN regulatable SHEP-Tet21N cell line with commercially available direct or indirect modulators of SKP2 activity identified a MYCN-dependent sensitivity.

In conclusion these data show that *SKP2* is a direct transcriptional target of MYCN and suggests that SKP2 is a potential therapeutic target in neuroblastoma.

Dedication

I dedicate this thesis to Harry Mitchelson and George, Stephen and Carolyn Evans.

Acknowledgements

To individually thank everyone that have helped me throughout my PhD would add another chapter to my thesis, however, several people cannot go un-named. Firstly I would like to thank my supervisors Professor. Herbie Newell and Professor. Deborah Tweddle for their support and confidence in me throughout this project and for constantly finding a positive spin for when my 'realistic view' of my results got the better of me. I would also like to thank Elaine who was instrumental in actually getting me into a white lab coat and was a constant presence and sounding board when I was finding my feet. Thank you for volunteering yourself for that role. I am also incredibly grateful to Professor Giovanni Perini, Giorgo Milazzo and Dr. Samuele Gherardi for providing the ChIP data, Professor Raymond Stallings for the ChIP-chip array data and finally to Andrew Shouksmith for his endless stream of freshly synthesised compounds.

I am under no illusion that one of the main reasons I have managed to actually complete my PhD is thanks to Dr. Lindi Chen. Her constant support both in and out of the lab and her never ending patience, even when I was asking the simplest of questions, has been my saviour. Most importantly I thank her for providing the daily banter which was instrumental in keeping my sanity intact over the past 4 years, and for teaching me the art of making a unicorn out of a donkey. I would also like to thank Liam for remaining supportive and not letting the Atlantic prevent him from being someone I can always lean on, even when he couldn't get a word in edgeways.

I consider myself extremely lucky to be able to have done my PhD in an institute full to the brim of friendly and helpful people, where there is always someone around to have a cup of tea with and on those more challenging of days a gin & tonic. It has been a pleasure to spend 4 years here.

Finally I would like to thank Cancer Research UK for funding this study.

Contents

List of Figures

List of Tables

Abbreviations

µg/µl	Microgram/microlitre
4-OHT	4-Hydroxytamoxifen
AKT	Protein Kinase B
ALK	Anaplastic lymphoma kinase
APC/C	Anaphase Promoting Complex/Cyclosome
APC11	Anaphase Promoting Complex subunit 11 (RING protein)
APC2	Anaphase Promoting Complex subunit 2 (Cullin Protein)
ARF	Alternative Reading Frame
ASN	Antisense strand
ATRA	All-trans retinoic acid
ATRX	ATP-dependent helicase / X-linked helicase II
AURKA	Aurora A Kinase
β-TRCP/FBXW1	F-box/WD repeat-containing protein 1A
BAD	BCL-2-associated death promoter protein
BAX	BCL-2-associated X protein
BCA	Bicinchoninic Acid
BCL-2	B-cell lymphoma 2
BH3	BCL-2 homology domain 3
B-HLH	Basic helix-loop-helix
BRCA2	Breast cancer 2, early onset
BMP	Bone Morphogenetic proteins
BrdU	Bromodeoxyuridine
CAK	CDK-activating kinase
cAMP	Cyclic adenosine monophosphate
CAND1	Cullin-associated NEDD8-dissociated protein 1
CBF1	C-promoter binding factor 1
CBP	cAMP-response element binding protein
CD44	Lymphocyte homing receptor
CDC	Cell division cycle
CDC20	Ubiquitin conjugating enzyme E2 R1 (Human)
CDH1	Cadherin-1
CDK	Cyclin dependent kinase
cDNA	Complementary DNA
CDT1	Chromatin licensing and DNA replication factor 1
ChIP	Chromain Immunoprecipitation
CHX	Cycloheximide
CK1	Casein Kinase 1
CKS1	Cyclin-dependent kinase regulatory subunit 1
CLU	Cluterin
CML	Chromic myeloid leukaemia
CMV	Cytomegalovirus
CNS	Central nervous system
CRL	Cullin-RING complex
Ct	Cycle threshold
CUL1	Cullin 1

DAM	DNA adenine methylation
Db	Doubling time
D-box	Degron
DCM	DNA cytosine methylation
ddH_20	Double-distilled water
DFMO	Difluoromethylornithine
DKK3	Dickkopf-3
DMSO	Dimethyl sulfoxide
DNA	Deoxyribose nucleic acid
dNTP	Deoxyribosenucleotide triphosphate
DOX	Doxycycline
DVED	Amino acid sequence: aspartic acid-valine-glutamic acid-aspartic acid
E1	Ubiquitin-activating enzyme
E2/UBC	Ubiquitin conjugating enzyme
E3	Ubiquitin ligase
E2F	E2F transcription factor
EC50	Half maximal effective concentration
EBRT	External beam radiation therapy
ECL	Enhanced chemiluminescence
EDTA	Ethylenediaminetetraacetic acid
EFNB2/B3	Ephrin-B2/B3
EFS	Event free survival
EGFP	Enhanced green fluorescent protein
ELK-1	ETS domain-containing protein
EM1	Early mitotic inhibitor 1
EMT	Epithelial-mesenchymal transition
EPH	Ephrin receptor
EPHB6	EPH tyrosine kinase-type B6
ER	Oestrogen receptor
ERBB2/HER2	v-erb-b2 avian erythroblastic leukaemia viral oncogene homolog 2
ETS	Transcription factor Ets
FACS	Fluorescence-activated cell sorting
FAM	6-carboxyfluorescein amidite
FBL	F-box/Leucine-rich repeat protein
FBS	Fetal bovine serum
FBW	F-box/WD repeat domain containing protein
FBX	F-box
FISH	Fluorescence in situ hybridization
FOXM1/O1/3a	Forkhead box protein M1/O1/3a
FOXP3	Forkhead box protein P3
FRET	Fluorescence resonance energy transfer
FSC	Forward Scatter
G0	Cellular quiescence
G1/G2	Gap Phase
GABP	GA-Binding Protein
GAPDH	Glyceraldehyde 3-phosphate dehydrogenase

GD2	Ganglioside G2
GI50	Half maximal growth inhibitory concentration
Glu	Glutamic acid
GLUT1	Glucose transporter 1
GM-CSF	Granulocyte-macrophage colony-stimulating factor
GN	Ganglioneuroma
GNB	Ganglioneuroblastoma
GSK3β	Glycogen synthase kinase 3β
Gy	Gray
HAT	Histone Acetyle-transferases
HBD	Hormone binding domain
HDAC1	Histone Deacetylase 1
HECT	Homologous to E6-associated protein C-terminus
HES1	Hairy and enhancer of split-1
HIF	Hypoxia-inducible factors
HIPK2	Homeodomain-interacting protein kinase 2
HLH-LZ	Helix-loop-helix-leucine zipper
HRP	Horseradish peroxide
Hrs	Hours
HSCT	Hematopoietic stem cell transplantation
HSR	Homogenously staining region
HSV	Herpes Simplex Virus
H-TWIST	Human Twist-related protein 1
HuD	ELAV-like protein 4
ID2	Inhibitor of DNA binding 2
IDRF	Image Defined risk factors
IKK	IκB-inducing Kinase
IL-2 or 6	Interleukin-2 or 6
ING3	Inhibitor of growth family member 3
INK4	Inhibitory Kinase 4
INRC	International neuroblastoma response criteria
INRG	International neuroblastoma risk group
INSS	International neuroblastoma staging system
IR	Irradiation
I-Type	Intermediate-type (neuroblastoma cell type)
JAK	Janus kinase
KAT	Potassium antimony tartrate
KIP1	Kinase Inhibitor protein 1
KPC	Kip1 ubiquitination-promoting complex
kV	Kilovolts
LB	Luria broth
LOH	Loss of Heterozygosity
Lys	Lysine
MAb	Monoclonal antibody
MAD	MAX dimerization protein
MASH1	mammalian achaete-scute homog-1
MAX	MYC association factor X
MB1/2	Myc-boxes 1/2

MCS	Multiple cloning site
MDM2	Mouse double minute 2 homologue
MDR	Multiple drug resistance
MEF	Mouse embryonic fibroblasts
MIBG	Meta-Ido-Benzyl-Guanidine
miRNA	MicroRNA
MIZ-1	MYC-associated transcription factor
MNT	MAX network transcriptional repressor
MRD	Minimal Residual Disease
MRN	Mre11-Rad50-Nb1 complex
mRNA	Messenger RNA
MXI1	MAX interactor 1, dimerization protein
MYC	v-myc avian myelocytomatosis viral oncogene
MYCN	v-myc avian myelocytomatosis viral oncogene, neruoblastoma derived
NAE	NEDD8-activating enzyme
NCL	Newcastle
NCS	Negative control siRNA
NGFR	Nerve growth factor receptor
NF-κB	Nuclear factor kappa-light-chain-enhancer of activated B cells
NLS	Nuclear localisation sequence
nM	NanoMole
nm	Nanometre
NRAS	Neuroblastoma RAS viral (v-ras) oncogene homolog
N-Type	Neuroblastic (neuroblastoma cell type)
NY	New York
ODC1	Ornithine decarboxylase 1
ONPG	Orhto-Nitrophenyl-β-galactosidase
ORC1	Origin recognition complex subunit 1
PAX3	Paired box 3
PBS	Phosphate buffered saline
PC	Polyclonal
PCR	Polymerase chain reaction
PHOX2a/b	Paired mesoderm homeobox protein 2a/b
PI	Propidium Iodide
PI3K	Phosphoinositide 3-kinase
PPM1D	Protein phosphatase Mg2+/Mn2+ dependent 1D
pRB	Retinoblastoma protein
Pre-RC	Pre-replication complex
pTEF-β	Positive transcription elongation factor
PTEN	Phosphatase and Tensin Homolog
PTPN11	Protein tyrosine phosphatase non-receptor type 11
PUMA	p53 upregulated modulator of apoptosis
qRT-PCR	Real-time PCR
RARα	Retinoic acid receptor α
RAG2	Recombination activating gene 2
RBX1	RING-box protein 1

RhoA	Rho-associated protein kinase
RING	Really Interesting New Gene
RISC	RNA-induced silencing complex
RLT	RNesy Lysis buffer
Rn	Reaction
RNA	Ribonucleic Acid
ROX	Passive reference dye for Taqman® qRT-PCR
RPE	RNesy buffer for washing membrane bound RNA
RT-PCR	Reverase transcription PCR
RUNX3	Runt-related transcription factor 3
RW1	RNesy buffer for washing membrane bound RNA
SAGE	Serial analysis of gene expression
SCA	Segmental chromosome alterations
SCF	Skp1-Cul1-F box protein
SDS	Sodium dodecyl sulfate
SDS-PAGE	SDS-Polyacrylamide gel electrophoresis
SEM	Standard error of mean
Ser	Serine
shRNA	Small hairpin RNA
siRNA	Small interfering RNA
SIRT3	Sirtuin-3
SKP1	S-phase Kinase-associated protein 1
SKP2	S-phase Kinase-associated protein 2
SN	Sense strand
SOX9/10	SRY (sex determining region Y)-box 10
SRB	Sulforhodamine B
SSC	Side scatter
STAT3	Signal Transducer and Activator of Transcription 3
S-Type	Substrate adherent (neuroblastoma cell type)
TAD	Transactivation domain
TAMRA	Tetramethylrhodamine
TBI	Total body irradiation
TBP	TATA-binding protein
TBST	Tris-buffered saline and Tween 20
TCA	Trichloroacetic acid
TET	Tetracycline
TetR	Tetracycline repressor
TetO	Tetracycline operator sequences
TGF	Transforming growth factor
Thr	Threonine
THZ1	Covalent inhibitor of CDK7
TIE	TGF-β inhibitory site
TIP60	Tat-interactive protein-60
TOB1	Transducer of ERBB2, 1
TP53INP1	Tumour protein p53-inducible nuclear protein 1
TRE	Tetracycline response element
TrkA	Tryosine Kinase receptor A (neurotrophic)
TRRAP	Transformation/transcription domain-associated protein

Tta	Transcriptional activator
UbcH5c	Ubiquitin conjugating enzyme E2 D3 (Human)
UK	United Kingdom
UPS	Ubiquitin proteasome system
USA	United States of America
VLS	Virtual ligand screening
WAF1/CIP1	Wild-type activating fragment-1
WEE1	WEE1 G2 checkpoint kinase
WNT	Wingless/integrated
wt	Wild type
XTT	2,3-bis-(2-methoxy-4-nitro-5-sulfophenyl)-2H-tetrazolium-5-carboxanilide

Chapter 1.
Introduction

1.1. Neuroblastoma

An embryonal tumour, neuroblastoma is the most common cancer in children less than 1 year, and accounts for 22% of all childhood cancer diagnosed at this age in the UK. Accounting for approximately 6% of all childhood malignancies diagnosed in patients younger than 15 years, i.e. ~95 cases annually (www.cancerresearchuk.org), it is responsible for a disproportional percentage of paediatric cancer deaths, i.e. ~15% all paediatric oncology deaths (Maris, 2010).

Neuroblastoma is a neoplasm of the neural crest of the sympathoadrenal lineage (sympathetic nervous system), and as such has a wide variation of presentation (Figure 1.1). Often arising in the adrenal medulla, primary tumours are commonly found as mass lesions in the neck, chest, abdomen or pelvis. An extremely heterogeneous disease, the clinical presentation ranges from asymptomatic tumours which spontaneously regress without therapy, to extremely aggressive malignant tumours which are non-responsive to current intensive therapeutic options (Maris, 2010; Davidoff, 2012).

Understanding the heterogeneity of neuroblastoma is of great interest, and although a number of key genetic and biological features have been identified, due to the complex nature of the disease it is proving difficult to identify which markers are of independent prognostic value and warrant additional investigation (Riley *et al.*, 2004).

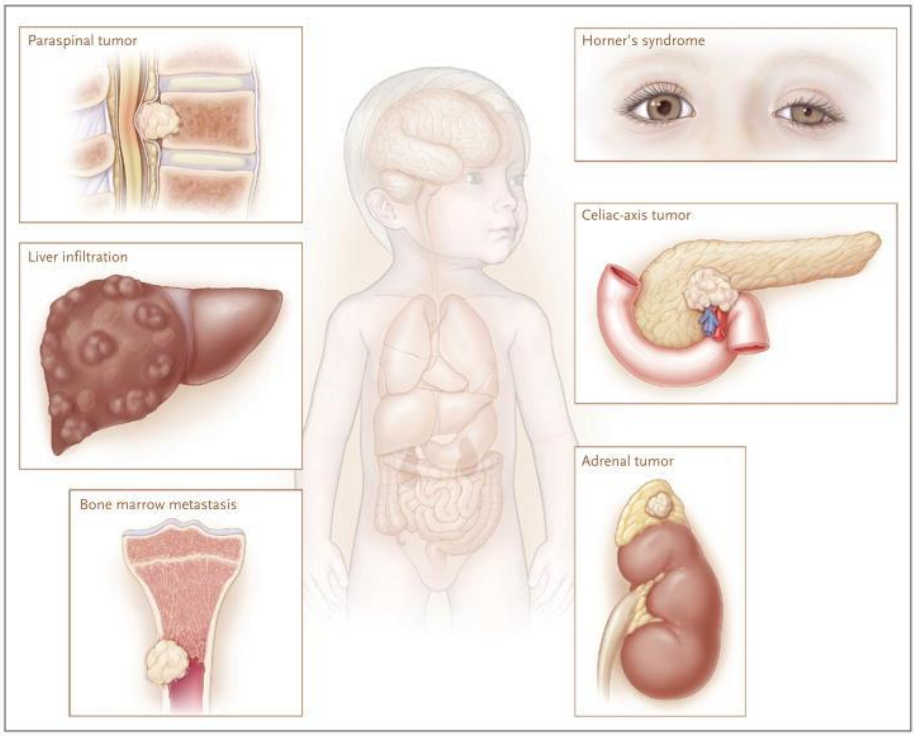

Figure 1.1 **Clinical presentation of neuroblastoma (Maris, 2010).** Originating from sympathetic nervous tissue, neuroblastoma typically presents in the adrenal medullar or paraspinal nerve tissue between the neck and pelvis. Common sites of disease include the neck, chest and pelvis with thoracic tumours capable of extending the neck to produce Horner's syndrome. Over half of patients present with advanced disease with metastasis to distant sites such as cortical bone, bone marrow and liver.

1.1.1. *Neural crest development of neuroblastoma*

Due to the frequency of tumours presenting in the paraspinal ganglia and adrenal medulla in the abdomen, neuroblastoma is identified as a tumour of sympathoadrenal lineage neural crest cells. The neural crest arises from the dorsal-most portion of the closing neural tube beneath the overlying ectoderm (Gilbert, 2000). During development of the neural crest multipotent progenitor cells are able to migrate and differentiate into a variety of lineages depending on regulation by intrinsic and extrinsic factors. Lineage studies have identified the sympathetic nervous system as arising from the trunk region of neural crest cells which, following the expression of PAX3, SOX9 and SOX10 transcription factors, undergo epithelial to mesenchymal transition (EMT) and migrate ventrally from the neural tube to the dorsal aorta. Here they are exposed to signals for Bone morphogenetic proteins (BMPs) which initiate the differentiation programme directing the cells to the sympathoadrenal lineage (Huber *et al.*, 2002; Betters *et*

al., 2010). Following BMP expression, differentiation into sympathetic neurones is regulated by the transient expression of basic helix-loop-helix (B-HLH) transcription factors which include MASH1, HES1, MYCN, HIF1α and HuD, in addition to homeobox genes such as *PHOX2A* and *PHOX2B*, and the p53 paralogue p73. The upregulation or amplification of some of these genes has been identified in aggressive neuroblastoma linking the molecular development of sympathetic neurones to that of neuroblastoma biology (Figure 1.2) (Nakagawara and Ohira, 2004).

Although the precise mechanism of neuroblastoma development is still largely elusive, advancements in genomic analyses have mapped genetic abnormalities and gene expression changes in neuroblastoma to specific regions involved in neurone development and differentiation. An improved understanding of the development of normal sympathetic neurones has also allowed the transcript profiles of these differentially expressed genes to be determined, identifying important groups of genes which drive neuroblastoma development. The use of functional analysis can further define their biological characteristics, potentially identifying therapeutic targets (Nakagawara and Ohira, 2004).

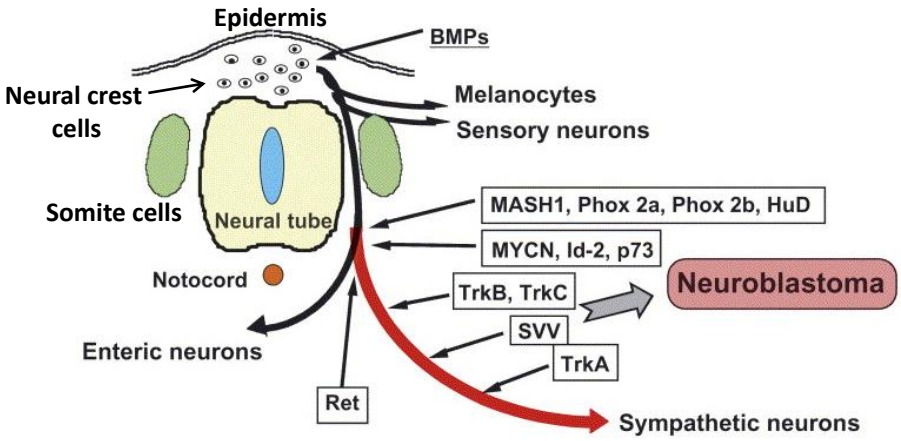

Figure 1.2 The differentiation pathway of sympathetic neurones (Nakagawara and Ohira, 2004). During formation of the neural tube the original ectoderm is organised into somite pairs either side of the forming neural tube, which will eventually provide cells for skin, muscle and skeletal formation, the externally positioned epidermis of the skin and the transient neural crest. Neural crest cells migrate in both a ventrolateral direction (between somites and neural tube), and dorsolateral direction (between somites and epidermis), during which they receive signals which initiate differentiation processes.

1.1.2. *Tumour cell biology*

Neuroblastoma belongs to the peripheral neuroblastic tumour subgroup of childhood solid tumours. Histologically mature tumours are comprised of two main cell populations, neuroblastic/ganglion cells and non-neuronal stromal cells, which include Schwann, perineurial and satellite cells (Figure 1.3).

Schwann cells are derived from the neural crest and form a myelin sheath around axons of the peripheral nervous system to provide support and insulation (Gilbert, 2000). Schwann cells in neuroblastoma are not considered to be neoplastic, and unlike the neuroblastic/ganglion cell population have a diploid DNA content and in mature variants of neuroblastoma cannot be distinguished from normal Schwann cells (Ambros *et al.*, 1996). Consequently, alongside the grade of differentiation of the neuroblastic component and nuclear pathology i.e. the mitosis-karyorrhexis index, the number of Schwann cells is related to disease outcome and applied along with age at diagnosis as prognostic indicators used to assign treatment in subtypes of neuroblastoma (Shimada *et al.*, 1984).

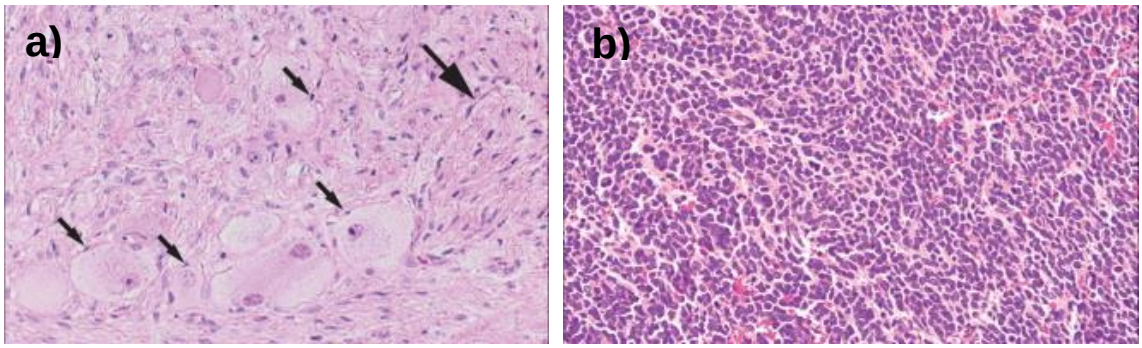

Figure 1.3 Hematoxylin and eosin stain of neuroblastoma tumour cells with varying degrees of differentiation. a) Schwann cells (large arrow) and ganglion cells (small arrows) which are prominent in stroma-rich differentiated neuroblastoma. **b)** Undifferentiated neuroblastoma with densely packed small round blue cells and little cytoplasm or Schwannian stroma (Maris et al., 2007)

1.1.3. *Cell type*

Consistent with its origins from the multi-potent neural crest cells, neuroblastoma cell lines have been categorised into three cell subtypes depending on their morphological and biological characteristics (Biedler *et al.*, 1973); N-type (neuroblastic), S-type (substrate adherent) and the intermediate I-type (Table 1.2). Each cell type can differentiate predictably along specific neural crest

lineages in response to particular morphogens, and are therefore useful models for understanding the cellular heterogeneity of neuroblastoma (Ross *et al.*, 2003).

Cell Type	Description
I-Type	• Stem cells with morphological features of both N- and S-type • Prominent nuclei, like N-type but with more cytoplasm and occasional neurites • Attach equally well to substrate and other cells forming focal aggregates
N-Type	• Neuroblastic / immature neuroblasts with small refractile cell bodies • High nucleur-to-cytoplasmic ratio and short neurites • High saturation density which form cell aggregates • Present at various differentiation states
S-Type	• Schwannian precursors / non-neuronal • Large flattened cells with prominent oval nuclei, abundant cytoplasm and no neurites • Adhere tightly to substrate, form monolayers and have contact inhibition • May be tumour-derived *in vitro* but not *in vivo*

Table 1.1 Neuroblastoma cell line subtypes (Ross *et al.*, 2003)

1.2. Genetic predisposition to neuroblastoma

Accounting for 1-1.5% of cases, familial neuroblastoma is thought to follow an autosomal dominant pattern of inheritance arising from a germline mutation consistent with Knudsons two-hit hypothesis (Knudson and Strong, 1972). Familial neuroblastoma is diagnosed at an early age, and until recently the genetic aetiology of the disease was largely unknown.

The paired-like homeobox 2B (*PHOX2B)* gene plays a vital role in the differentiation and development of the sympathoadrenal phenotype (Huber, 2006). Mutations are often found in neuroblastoma cases associated with other disorders of neural crest-derived tissues such as congenital central hypoventilation syndrome and/or Hirschsprung disease (Mosse *et al.*, 2004; Trochet *et al.*, 2004), although somatic mutations of this gene are rare. Activating *ALK* mutations are found in the majority of familial cases and ~8% of sporadic neuroblastoma across all subtypes and risk groups (Maris, 2010), and the aggressive *ALK(*F1174L) variant has been described as a key driver in

neuroblastoma development from neural crest cells (Schulte *et al.*, 2013a). A receptor tyrosine kinase, ALK is thought to participate in the regulation of neuronal differentiation (Iwahara *et al.*, 1997) and is generally accepted as the main cause of familial susceptibility to neuroblastoma in healthy families (Mosse *et al.*, 2008).

1.3. Genetics of sporadic neuroblastoma

A number of genetic aberrations occur in sporadic cases of neuroblastoma, some of which influence disease severity. Genome wide association studies have shown enrichment of a common genetic variation at chromosomes 6p22 and 2q35 as well as a copy-number variation at 1q21 with the development of neuroblastoma. However, individually, these variations are thought to have a relatively modest effect on susceptibility (Maris *et al.*, 2008; Diskin *et al.*, 2009; Pugh *et al.*, 2013).

1.3.1. *MYCN amplification*

A member of the MYC family of proto-oncogenes, MYCN maps to the short arm of chromosome 2p24 and is found to be amplified (>10 copies per cell) in ~20% of primary tumours (Schwab *et al.*, 1983). Corresponding with high MYCN protein levels, *MYCN* amplification contributes to neoplastic transformation (Schwab *et al.*, 1985a) and is sufficient to drive neuroblastoma tumorigenesis in mice (Weiss *et al.*, 1997).

The most common focal genetic lesion in sporadic neuroblastoma, *MYCN* amplification strongly correlates with high-risk, advanced stage disease and is used as a genetic marker of poor prognosis and for treatment stratification (Brodeur *et al.*, 1984). The biological significance of *MYCN* amplification is supported further by the poor outcome seen in otherwise favourable disease patients, e.g. those with localised tumours, supporting its central role in neuroblastoma tumour progression (Cohn *et al.*, 1995).

The amplification of *MYCN* is suggested to follow the episome model where the DNA segment is excised, circularised, and amplified by mutual recombination, to produce double minute chromosomes which can integrate into somatic chromosomes to form homogeneously staining regions (hsr) (Storlazzi *et al.*,

2010). Amplification is often associated with other genetic abnormalities such as allelic loss of 1p or 17q gain (Bown, 2001), and fluorescence in situ hybridisation studies (FISH), have shown that 17q genetic material frequently flanks integration sites for *MYCN*, suggesting it is an area for preferential *MYCN* recombination (O'Neill *et al.*, 2001).

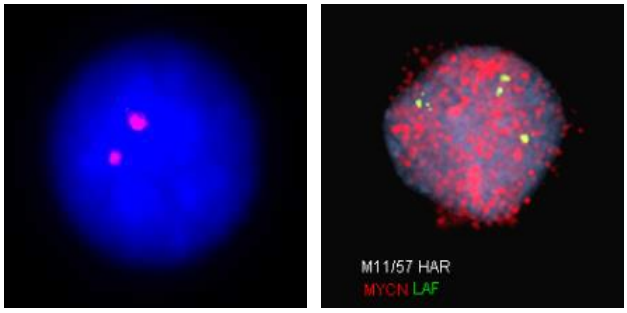

Normal **Amplified**

Figure 1.4 *MYCN* amplification as double minutes detected in a neuroblastoma tumours by fluorescence *in situ* hybridisation (FISH).

1.3.2. *Segmental chromosome alterations (SCA)*

A number of segmental chromosome alterations have been reported in neuroblastoma, with deletions thought to harbour tumour suppressor genes and gains harbouring putative oncogenes. Although these alterations have been shown to be of prognostic impact individually, multivariate analysis has identified combinations of genetic alterations which define specific clinical and prognostic characteristics independently of *MYCN* amplification (Schleiermacher *et al.*, 2011). Consequently these SCA genomic profiles are used for risk stratification, particularly in non-*MYCN* amplified disease (Schleiermacher *et al.*, 2012)

1.3.2.1. 1p deletion

Deletions and chromosomal rearrangements of the short arm of chromosome 1 are found in 25 - 35% of neuroblastoma and are associated with aggressive metastatic disease (Caron *et al.*, 1996). The most common deletion is at 1p36 following the unbalanced translocation of 17q: t(1:17)(p36;q11-12), suggesting the region contains tumour suppressor genes (Bown *et al.*, 2001). Although in multivariate analysis 1p loss of heterozygosity (LOH) is a predictor of poor event free survival, it has been shown to have no effect on overall survival, especially

in high risk groups where it is often associated with *MYCN* amplification (Fong *et al.*, 1989; Maris *et al.*, 2000).

1.3.2.2. Gain of 17q

Occurring in over 50% of neuroblastoma, gain of 17q is often the consequence of unbalanced translocations between chromosomes 1 and 11, and is thus frequently associated with the loss of 1p or 11q (Lastowska *et al.*, 1997; Bown *et al.*, 2001). Although 17q gains often correlate with a more aggressive disease, due to the involvement of these translocation partners, the independent prognostic significance is not strong. However, when combined with *MYCN* status 17q gain does provide a reliable prediction of patient outcome (Spitz *et al.*, 2003b). Although cytogenetic analysis of 17q translocations has identified breakpoint heterogeneity, the gain of a region from 17q22-qter suggests that several candidate genes map to the region and are possibly overexpressed by a gene dose effect (Van Roy *et al.*, 1997). For example, the amplification of *PPM1D* on 17q23 results in overexpression of the p53-inducible phosphatase which reduces p53 phosphorylation, attenuating apoptotic cell death (Saito-Ohara *et al.*, 2003).

1.3.2.3. Loss of 11q

Allelic loss of 11q most frequently occurs at 11q23 and is found in 22 - 44% of neuroblastoma. Inversely correlated with *MYCN* amplification, it is a poor prognostic indicator for non-amplified disease (Guo *et al.*, 2000). Moreover 11q alterations are an independent marker of decreased event free survival in all risk groups, and strongly correlate with metastatic relapse (Spitz *et al.*, 2003a; Spitz *et al.*, 2006).

1.3.3. *DNA Ploidy*

DNA content in neuroblastoma is used as a prognostic marker for disease behaviour. Hyperdiploidy of tumour cells is significantly more frequent in lower risk tumours and is associated with Schwann and ganglion cell differentiation, a better response to chemotherapy, and a more favourable prognosis (Look *et al.*, 1984; Gansler *et al.*, 1986; Brenner *et al.*, 1989). DNA diploid tumours on the other hand are more common in metastatic, high-risk tumours and have been

found to act as a poor prognostic indicator when combined with *MYCN* amplification status (Muraji *et al.*, 1993). However, DNA aneuploidy has been shown to not correlate with age and stage of disease but has been found to associate with decreased long-term survival in patients older than 24 months post-operation, and with advanced disease (Nakazawa, 1993).

1.3.4. *ALK mutations*

Missense mutations of anaplastic lymphoma kinase, *ALK*, are found in 6 -10% of sporadic neuroblastoma with an additional 3 - 4% showing high levels of *ALK* amplification (Cheung and Dyer, 2013). Activating mutations in the kinase domain promotes hyper-phosphorylation and increased activity, enhancing proliferation and tumorigenesis, especially in the presence of *MYCN* amplification. MYCN has been shown to cooperate with ALK gain-of-function mutations, and reports have identified ALK as a direct transcriptional target of MYCN and able to stimulate MYCN gene transcription thereby contributing to MYCN-mediated disease progression (Schonherr *et al.*, 2012; Hasan *et al.*, 2013). Inactivation of ALK induces apoptotic cell death and impairs proliferation, identifying the kinase as an attractive therapeutic target (Chen *et al.*, 2008b; George *et al.*, 2008; Janoueix-Lerosey *et al.*, 2008). Preclinical data have recently validated the use of the ALK inhibitor crizotinib in neuroblastoma, and further clinical trials are currently in progress with a second generation inhibitor, LDK-378 (Schulte *et al.*, 2013b).

1.3.5. *Additional genetic aberrations*

Additional genes with significant mutated frequencies in somatic high-risk neuroblastoma are *PTPN11* (2.9%), *ATRX* (2.5%) and *NRAS* (0.83%) (Pugh *et al.*, 2013). Mutations in the α-thalassaemia/mental retardation syndrome X-linked (*ATRX* gene), while not sufficient to promote neuroblastoma formation alone, are significantly linked with the age of diagnosis. *ATRX* mutations are associated with an absence of the ATRX protein and long telomeres due to its role as a chromatin remodelling protein. They are more commonly found in older patients with 44% of cases found in patients older than 12 years who have a poor prognosis. However, due to cohort size further analysis is required into the prognostic impact of *ATRX* mutations (Cheung *et al.*, 2012).

1.3.6. *Favourable neuroblastoma genes*

Transcripts encoding certain tyrosine kinases (*TrkA, p75NTR* and *EFNB3*) and cell surface molecules (*CD44, EFNB2* and *EFNB3*) are all established favourable markers in neuroblastoma, as their expression predicts a favourable outcome in tumours lacking *MYCN* amplification and suppresses the malignant phenotype of unfavourable disease in xenograft models (Tang *et al.*, 2000a; Tang *et al.*, 2000b). High-level expression *EPHB6*, and its ligands *EFNB3* and *EFNB2*, predict a favourable outcome with more precision when combined together with data for *TrkA* expression. Interestingly, there is a distinct pattern with *TrkA* and *ERNB2* expression being associated with both age and stage of disease, and *EPHB6* and *EFNB3* expression with age only (Tang *et al.*, 2000b). *TrkA* is often considered the more informative prognostic marker (Nakagawara *et al.*, 1993; Suzuki *et al.*, 1993), and has been shown to be predictive of 5-year survival when associated with high MYCN expression, in a non-*MYCN* amplified setting (Tang *et al.*, 2006b). Although the role of *p75NTR* in neuroblastoma is less clear, *TrkA* and *p75NTR* expression has been shown to be repressed by MYCN, suggesting a role in MYCN-driven tumour progression (Schulte *et al.*, 2009; Iraci *et al.*, 2011).

1.4. Treatment stratification and risk classification

Many factors have been found to determine heterogeneity in neuroblastoma outcome, such as age at diagnosis, stage of disease, as well as the other histopathological and genetic features described in Section 1.3 and below. Identifying and understanding the clinical significance of these risk-factors has allowed for improved pre-treatment risk and treatment stratification.

1.4.1. *International Neuroblastoma Staging System (INSS)*

The International Neuroblastoma Staging System (INSS) and International Neuroblastoma Response Criteria (INRC) were originally developed in 1988, (Brodeur *et al.*, 1988), and revised in 1993, (Brodeur *et al.*, 1993), and are used to confirm diagnosis and predict response to therapy (Table 1.2). However, the INSS is based on the extent of tumour removal and thus its utility is strongly dependent on the individual surgeon. Furthermore, localised disease which is expected to spontaneously regress cannot be properly staged as it is not removed due to ‘treatment’ being observation. To address these limitations

adaptations have been implemented and a new clinical staging system developed by the International Neuroblastoma Risk Group (INRG). Based on rigorously defined surgical risk factors, (IDRFs: image defined risk factors), localised disease was divided into two subgroups (Table 1.3) removing previous limitations. Not intended to replace the INSS risk assessment, the two staging systems are used in conjunction with one another (Monclair *et al.*, 2009).

1.4.2. *International Neuroblastoma Risk Group (INRG) classification system*

To overcome variation in factors selected to define pre-treatment risk across the different international cooperative groups, the INRG developed a new classification system in an attempt to standardise neuroblastoma diagnosis. Based on INRG stage, age, histologic category, grade of tumour differentiation, *MYCN* status, presence/absence of 11q aberrations and tumour ploidy, 16 statistically and/or clinically different pre-treatment designations were identified (Table 1.4). Four main prognostic groups were then defined according to percentage cut-offs of 5-years event-free survival (EFS). These were; very low-risk (≥ 85%), low-risk (≥ 75% to ≤ 85%), intermediate risk (≥ 50% to ≤ 75%) and high risk (≤ 50%). It was hoped that using these classifications across the international groups would ensure that children were allocated into homogenous pre-treatment groups and hence allow for a better comparison of future clinical trials data (Cohn *et al.*, 2009).

Tumour Stage	Description
1	Localised tumour with complete gross excision, with or without microscope residual disease; representative ipsilateral lumpy nodes negative for tumour microscopically. Nodes attached to and removed with primary tumour may be positive
2A	Localised tumour with incomplete gross excision; representative ipsilateral non-adherent lymph nodes negative for tumour microscopically
2B	Localised tumour with or without complete gross excision, with ipsilateral non-adherent lymph nodes positive for tumour; enlarged contralateral lymph nodes negative microscopically
3	Unresectable unilateral tumour infiltrating across the midline (beyond the opposite side of the vertebral column) with or without regional lymph node involvement, or midline tumour with bilateral extension via infiltration (unresectable) or lymph node involvement
4	Any primary tumour with dissemination to distant lymph nodes, bone, bone marrow, liver, skin, and/or other organs (except as defined for stage 4S disease). Distant metastatic disease
4s	Localised primary tumour (as defined for stage 1, 2A or 2B disease) with dissemination limited to skin, liver, and/or bone marrow (limited to infants younger than 1 year, marrow involvement of less 10% of total nucleated cells, and MIBG scan negative in the marrow). Favourable outcome over stage 4 disease when in absence of *MYCN* amplification

Table 1.2 Original description of INSS tumour stages (Brodeur *et al.*, 1993). MIBG: Metaidobenzylguanidine

Tumour Stage	Description
L1	Localised tumour not involving vital structures, as defined by the list of IDRFs, and confined to one body compartment
L2	Local-regional tumour with presence of one or more IDRFs
M	Distant metastatic disease (except stage MS tumour)
MS	Metastatic disease in children younger than 18 months, with metastases confined to skin, liver and/or bone marrow

Table 1.3 Descriptions of INRG pre-treatment classification (Monclair *et al.*, 2009). L: localised, M: metastatic, S: Special, and 1: with and 2: without surgical risk factors.

INRG stage	Age in months	Histological category	Grade of tumour differentiation	*MYCN*	11q abberations	Ploidy	Pretreatment risk group
L1/2		GN maturing; GNB intermixed					Very Low
L1		Any, except GN maturing or GNB intermixed		Not Amp			Very Low
				Amp			High
L2	≤ 18	Any, except GN maturing or GNB intermixed		Not Amp	No		Low
					Yes		Intermediate
	≥ 18	GNB nodular;	Differentiating	Not Amp	No		Low
					Yes		Intermediate
			Poorly differentiated or undifferentiated	Not Amp			
				Amp			High
M	≤ 18			Not Amp		Hyper-Diploid	Low
	≤ 12			Not Amp		Diploid	Intermediate
	12 to ≤ 18			Not Amp		Diploid	Intermediate
	≤ 18			Amp			High
	≥ 18						High
MS	≤ 18			Non Amp	No		Very Low
					Yes		High
				Amp			High

Table 1.4 The INRG classification system. (GN – ganglioneuroma, GNB – ganglioneuroblastoma. (Cohn et al., 2009).

1.5. Current Treatment (as reviewed by (Ora and Eggert, 2011))

Following the tumour profiling of molecular markers and risk assessment, the appropriate treatment plan can be initiated based on the clinical classification.

1.5.1. *Observation*

As most of INSS 4s neuroblastomas spontaneously regress, patients without symptoms or unfavourable prognostic markers are closely observed without

active treatment. A clinical trial randomising a 'wait-and-see' approach vs. surgery for INSS stage 1 and 2 (with no unfavourable prognostic markers) showed 47% of tumours regress spontaneously while a second found only 17 out of 53 required treatment (Hero *et al.*, 2008; Tanaka *et al.*, 2010).

1.5.2. *Surgery*

As a solid tumour, neuroblastoma surgery provides local control, helps confirm diagnosis and allows tissue acquisition for histological and molecular classification. Although surgery is the treatment of choice for localised disease, chemotherapy is sometimes required initially to shrink the tumour before surgery.

1.5.3. *Chemotherapy*

A large proportion of neuroblastoma patients present with metastatic or advanced disease and require chemotherapy. Treatment options include alkylating agents (cyclophosphamide, busulfan and melphalan), platinum analogues (cisplatin and carboplatin), vinca-alkoids (vincristine), epipodophyllotoxins (etoposide and VP16-213), and anthracyclines (doxorubicin) as all have well established activity against neuroblastoma. Combinations of existing drugs and novel agents are also being investigated in ongoing Phase II trials for relapsed, refractory and chemo-resistant neuroblastoma (Kushner *et al.*, 2010; Bagatell *et al.*, 2011). Treatment for high-risk neuroblastoma (*MYCN* amplified disease and INSS stage 4 ≥ 12 months) is as follows:

1. *Dose intensive therapy to reduce tumour burden**:*** Combinations of chemotherapeutic drugs at high doses, e.g. cisplatin, carboplatin, etoposide or doxorubicin. Topetecan is also used if initial treatment is insufficient.

2. *Consolidation treatment to removal residual tumour and metastases:* Following surgical resection of the primary tumour, high dose myeloablative chemotherapy with combinations of busulfan, melphalan, carboplatin and etoposide and autologous stem cell rescue.

3. *Maintenance treatment to eliminate minimal residual disease:* As local or systemic relapse of high-risk disease is often due to minimal residual disease (MRD), maintenance treatment focusses on biological therapies to induce

terminal differentiation, such as retinoid derivatives (13-cis retinoic acid), or cytocidal immunotherapy. Specifically, monoclonal antibodies against the surface glycolipid GD2, which have recently been assessed in Phase I and II trials. GD2 is a target for immunotherapy due to its high level of expression on neuroblastoma, and the protection of healthy neurones in the CNS by the blood-brain barrier. In an attempt to enhance response rates cytokines have also been combined with anti-GD2 therapy to increase cytotoxicity. Clinical trials have shown an increase in 2-year EFS for anti-GD2 therapy when combined with IL-2, GM-CSF and isotretinoin (Yu *et al.*, 2010).

1.5.4. *Radiation treatment*

Neuroblastoma is a radiosensitive disease, although external beam treatment is usually only given for high risk disease during the consolidation phase, or for a palliative treatment to sites of relapse. Radiation is often given at the site of the primary tumour using external beam radiotherapy (EBRT) with total body irradiation (TBI) being replaced by effective chemotherapeutic methods. A second approach includes iodine^{131}-labelled metaiodobenylguanidine (^{131}I-MIBG). A norepinephrine analogue selectively taken up by neuroblastoma tumours, haematological toxicity has restricted its use, although certain regimes use it prior to hematopoietic stem cell rescue/transplant (HSCT) conditioning regimens (French *et al.*, 2013) .

1.5.5. *Treatment of recurrent disease*

Patients with low- and intermediate-risk disease can benefit from conventional treatment such as surgery with or without moderately intensive chemotherapy. Unfortunately recurrence of high-risk disease is extremely difficult to treat and no treatment options are currently available which offer long term cure.

1.6. The MYC family of transcription factors

The MYC proto-oncogene family is a group of basic-helix-loop-helix-leucine zipper (b-HLHZ) transcription factors which arise from five distinct gene family members, *c-MYC*, *MYCN*, *L-MYC*, *B-MYC* and *s-MYC*. Although, only *c-MYC*, *L-MYC* and *MYCN* are expressed in mammalian cells and reported to have neoplastic potential (Nesbit *et al.*, 1999). B-MYC and s-MYC are both members of the rat MYC gene family yet share extensive homology with the amino termini of the MYC family, however, B-MYC shares more similarities with c-MYC (Ingvarsson *et al.*, 1988), and s-MYC shows a greater resemblance to murine MYCN (Sugiyama *et al.*, 1989).

Although c-MYC, L-MYC and MYCN all function in a similar manner though association with the HLH-LZ phosphoprotein MAX, as discussed in Section 1.6.2, the presence of three distinct gene sequences suggests each has unique functional roles. This is supported by findings of differential expression of MYC proteins in a stage and tissue-specific manner during human and murine differentiation, in addition to the specific cancer types in which they are overexpressed (Zimmerman *et al.*, 1986).

MYC expression is tightly regulated with each step of protein synthesis being intensely controlled by positive and negative inputs which respond to appropriate growth factor signalling as reviewed by (Tansey, 2014). All MYC proteins are broadly expressed at high levels during early embryogenesis, and given their conservation have been found to overlap in gene targets resulting in a certain level of functional redundancy in early embryonic development (Malynn *et al.*, 2000). As development continues their distribution becomes more spatial and restricted to specific cell types. During midgestation c-MYC expression is the most broadly distributed, although is most abundant in areas of high proliferative activity and following full development is found at low levels in adult tissues with a high proliferative capacity (e.g. skin epidermis and gut, (Schmid *et al.*, 1989)). MYCN expression is more prominent in postmitotic cells undergoing neuronal differentiation (Galderisi *et al.*, 1999; Edsjo *et al.*, 2004) and is found in low levels in many neuronal tissues following its downregulation during differentiation. L-MYC has a similar tissue distribution to MYCN and is found in both proliferative

and differentiative compartments on the brain and neural tube and has also been shown to be present in the developing kidney and lungs (Schmid *et al.*, 1989). However, no unique role in development has yet to be determined for L-MYC, with homozygous null L-MYC mice found to be viable (Hatton *et al.*, 1996). Conversely, homozygous deletion of either c-MYC or MYCN results in embryonic lethality, with c-MYC knockouts showing abnormalities in the heart and a delay in embryonic turning (Davis *et al.*, 1993), and MYCN knockouts showing developmental deformities in the lungs and central and peripheral nervous tissue (Stanton *et al.*, 1992).

The importance of the spatio-temporal expression of c-MYC and MYCN is notable in their association with tumour development. Deregulated c-MYC expression is recognised as an essential aspect of human Burkitt's lymphoma (Spencer and Groudine, 1991), yet has been found to be broadly overexpressed in both blood and solid tumours. MYCN on the other hand is more frequently overexpressed in solid cancers of neural origin, such as neuroblastoma, and L-MYC most commonly found overexpressed in small cell lung carcinoma (Tansey, 2014). Although overexpression of the MYC family is recognised as a key oncogenic event, with gain-of-function experiments identifying them capable of promoting transformation (Adams *et al.*, 1985; Rosenbaum *et al.*, 1989), it is still not fully understood to what level they contribute to oncogenic activity due to the plethora of genes which they both activate and repress. Known to play critical roles in proliferation, differentiation and apoptosis the oncogenic behaviour of the MYC family could potentially be a result of their enhanced expression, although it is still not fully understood how MYC behaviour is different in cancer versus normal cells.

1.6.1. *MYC protein structure*

As with all MYC members the N-terminal transcriptional activation domain (Figure 1.5, TAD) is essential for Myc-induced transcriptional activation following its fusion with a DNA binding domain (Kato *et al.*, 1990). The TAD region is also accepted to be where MYC contacts RNA polymerase II-associated proteins (Tansey, 2014) and is responsible for signalling the ubiquitin-mediated degradation of MYC proteins (Salghetti *et al.*, 1999). The amino-terminus also contains the Myc-boxes (MB), of which MB1 and MB2 are conserved across all

3 family members indicating they are critical for MYC biology. The C-terminus contains a basic DNA binding region (Figure 1.5, B), alongside a helix-loop-helix and leucine zipper region (Figure 1.5, HLH-LZ), which mediates the interaction with the smaller BHLH-LZ protein MAX, and the physiological recognition of the DNA target sequences (Wenzel *et al.*, 1991). Dimerization of MYCN/MAX is essential for transcriptional activation, and mediates the DNA affinity of MYCN. The resultant MYCN/MAX heterodimer binds to canonical 5' CACGTG or non-canonical 5' CANNNG E-box sequences upstream of the target promoter where MYCN is able to activate transcription (Adhikary and Eilers, 2005) (Schwab *et al.*, 1983; Wenzel and Schwab, 1995). Less is understood about the central portion of the MYC proteins with deletion mutants failing to identify regions critical for MYC activity (Heaney *et al.*, 1986; Biegalke *et al.*, 1987).

As MYC family members have a shorter half-life than the constitutively expressed MAX proteins, the regulation of MYC family genes is limited to the control of MYC levels as reviewed by (Grandori *et al.*, 2000). This greater stability of MAX proteins aids their role as MYC antagonists. Thus, along with cofactors MAD, MNT and MXI1, MAX forms homodimers that represses MYC-regulated genes by binding to the E-boxes. This repression is then lost following formation of MYC/MAX heterodimers on cell cycle entry and the increase in MYC expression, as reviewed by (Adhikary and Eilers, 2005).

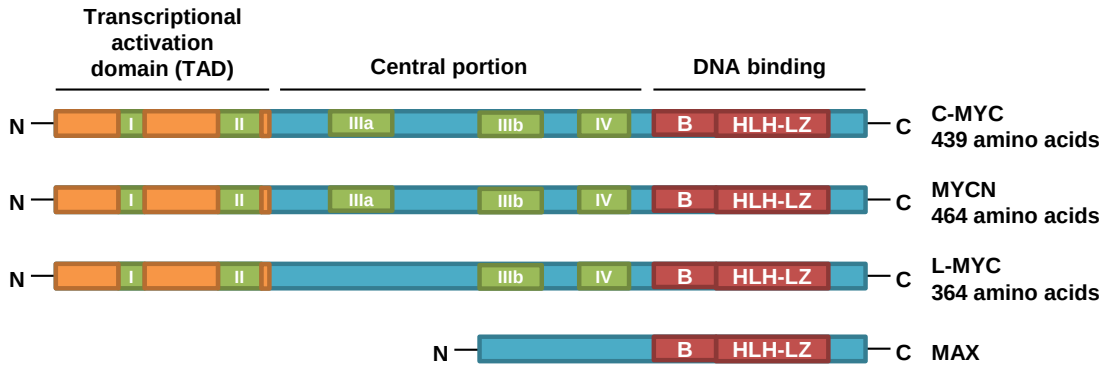

Figure 1.5 Schematic representation of the protein structure of the MYC family and Max. Transactivation domain (TAD) and conserved Myc boxes (MBI and MBII) at the N-terminus, central portion and basic region (B) / helix-loop-helix / leucine-zipper (HLH-LZ) at the C-terminus. Proteins vary in size due to differences in the length of nonconserved sequences but are drawn to highlight the relative location of the Myc boxes (Tansey, 2014).

1.6.2. *Transcriptional regulation by MYC*

MYC proteins can transcriptionally activate and repress numerous target genes. Although many c-MYC target genes have been identified, as listed at http://mycancergene.org/sit/mycTargetDB.asp (Zeller *et al.*, 2003), fewer MYCN-regulated genes are known. However, due to the homology between the two transcription factors, progress is being made in identifying the direct and indirect downstream targets of MYCN, (http://medgen.ugent.be/MYCNot) (Kumps *et al.*, 2013). Transcriptional regulation by MYC proteins relies on their dimerization with MAX. The MYC/MAX heterodimer interacts with a large number of proteins, suggesting that DNA recognition by the C-terminal domain and transcriptional regulation by the N-terminal domain is not solely reliant on MAX. Although both BHLH-LZ and transactivation domains (TAD) are known to be required for MYCN activity, how these activate transcription is still poorly understood (Sakamuro and Prendergast, 1999). Binding of the nuclear cofactor TRRAP to N-terminal domain MBII of MYCN is essential for its transactivation activity, and promotes the recruitment of histone acetyl transferases (HAT) such as GCN5 and TIP60 and the CBP component (cAMP-response element binding protein) of the p300/CBP complex, to form large multiprotein complexes (McMahon *et al.*, 1998; McMahon *et al.*, 2000; Vervoorts *et al.*, 2003; Martínez-Cerdeño *et al.*, 2012). These HATs have been shown to promote histone acetylation and chromatin remodelling, creating a euchromatin conformation. This conformation allows the docking of transcriptional machinery such as the TATA-binding protein (TBP), a member of the transcriptional pre-initiation complex, implying MYC/MYCN is able to recruit pol II machinery to activate transcription (Barrett *et al.*, 2005). As all HATs mentioned are able to acetylate MYCN, and thus enhance its stability and transcriptional latency, it is argued that MYCN may play a more generic role in the maintenance of an open nucleosomal landscape, in addition to the transcriptional activation of specific genes (Cotterman *et al.*, 2008).

MYC/MYCN have also been shown to promote transcript elongation by recruitment of the positive transcription elongation factor b (PTEFb). A complex consisting of CDK9 and its regulatory subunit cyclin T1 (Peng *et al.*, 1998), P-TEFb phosphorylates the Ser2 residue at the carboxyl-terminal-domain of RNA polymerase II, stimulating transcription (Majello *et al.*, 1999; Gargano *et al.*,

2007). Using the target gene *CAD* as an experimental model Eberhardy *et al* showed that P-TEFb mediated MYC-mediated transcriptional activation through the binding of cyclin T1 to the conserved Myc Box I (MBI) domain (Eberhardy and Farnham, 2002). Argued to be the rate limiting step in MYC/MYCN transactivation, MYCN is predicted to participate in this functional interaction due its homology with c-MYC

Although most genes that are regulated by the MYC family are activated, the N-terminal TAD has been implicated in transcriptional repression through its interaction with the two zinc-finger transcription factors; MYC-associated transcription factor (MIZ-1) (Staller *et al.*, 2001), and basal transcription factor 1 (SP1). MYCN has since been shown to require the formation of a MYCN/MIZ1/SP1 complex to silence gene expression, which promotes a hetrochromatin conformation by recruiting histone deacetylases (e.g. HDAC1) and switching off gene expression (Iraci *et al.*, 2011). Alternatively MYCN has been found to bind to the EZH2 component of the polycomb repressive complex 2 (PRC2) (Corvetta *et al.*, 2013). A histone methyltransferase, EZH2 expression has been associated with epigenetic silencing in neuroblastoma and its upregulation able to suppress the expression of several tumour suppressors including *CLU*, *NGFR* and *RUNX3* (Wang *et al.*, 2012a).

In addition to the presence of an E-box motif, MYC binding has been shown to be influenced by the chromatin characteristics showing a stronger preference towards areas with a high density of CpG islands which often define regions of open, active chromatin (Kundu and Rao, 1999). MYC binding is also heavily influenced by epigenetic marks as E-boxes buried in tightly compacted chromatin will be overlooked for those which are associated with histone modifications identifying as transcriptionally ‘active’ e.g. methylation on histone H3 at lysine 4 and 79 (Guccione *et al.*, 2006).

MYC has been shown to regulate gene transcription independent of the E-box and act as a transcriptional facilitator by directly interacting with other transcription factors. This has recently been shown for retinoic acid responsive genes where the MYC/MAX dimer is able to transcriptionally repress genes required for differentiation in leukaemia cells by interacting with the retinoic acid receptor-α (RARα). Concomitantly, during retinoic acid induced differentiation

phosphorylation of c-MYC in the C-terminal helix-loop-helix domain results in MAX being displaced and co-activators being recruited. MYC can therefore act as a switch from promoting to supressing leukaemia tumorigenesis (Uribesalgo *et al.*, 2011).

An alternative approach to the transcriptional role of the MYC family is that they work as universal amplifiers of already expressed genes rather than acting as sequence-specific transcriptional activators. In a model recently described for c-MYC, tumour cells expressing low levels were found to have the transcription factor almost exclusively bound to the E-boxes in core promoters. However, in tumour cells with elevated levels of c-MYC it was found to occupy both the core promoters and large regulatory elements, termed enhancers, of these genes at additional low affinity E-box like sequences (Nie *et al.*; Lin *et al.*, 2012). Furthermore, clusters of enhancers densely packed with transcription factors, cofactors and chromatin regulators (Hnisz *et al.*), have been recently identified as a feature of deregulated MYCN. These 'super enhancers' facilitate the high-level expression of genes and have been found to sensitise *MYCN* amplified cells to the CDK7 inhibitor THZ1. A covalent inhibitor it prevents the phosphorylation and activation of RNA polymerase II thus reducing the expression of MYCN-driven super enhancer-associated oncogenic drivers (Chipumuro et al., 2014). By amplifying the tumour cell's gene expression program this enhancer model helps to explain the diverse effects of overexpressed MYC on gene expression, and the lack of a common *MYC* transcriptional signature. However, this model requires further refinement as it is not clear whether the increases in transcriptional output are through direct or indirect transcriptional activities of c-MYC, additionally the model does not account for the ability of c-MYC to repress the transcription of select genes.

1.6.3. The MYCN *oncogene in neuroblastoma*

MYCN encodes a 60-64kDa nuclear phosphoprotein which has been found to play an important role in the differentiation pathways of neuronal progenitor cells and the development of tissues of the nervous system (Knoepfler *et al.*, 2002). MYCN has been repeatedly demonstrated to have a crucial role in neuroblastoma. MYCN over-expression studies highlighted the requirement for MYCN down-regulation to allow terminal differentiation of neurones (Wakamatsu

et al., 1997), while conditional MYCN expression was found to promote the transformation of neuroblasts in transgenic mice, and enhance the proliferation and metastatic ability of tumour-derived cell lines (Lutz *et al.*, 1996; Weiss *et al.*, 1997). However, MYCN expression also sensitises cells to apoptotic cell death, providing a pathway which can be exploited therapeutically by inducing a p53 response (Gamble *et al.*, 2012; Petroni *et al.*, 2012). The defects in the apoptotic pathways seen in *MYCN*-amplified neuroblastoma may therefore be a mechanism of evading MYCN-induced apoptosis (Hogarty, 2003).

As a consequence of the ability of MYCN to both drive cellular proliferation and induce apoptosis, the impact of *MYCN* amplification is dependent on the net integration of the two signalling pathways. This paradox is observed histologically by the high mitosis-karyorrhexis index (MKI) in human *MYCN* amplified tumours. MKI is a combined measure of proliferation (mitoses) and apoptosis (karyorrhexis; degeneration of the nucleus) and is hence used in the cellular classification of neuroblastoma (Shimada *et al.*, 1995; Shimada *et al.*, 1999).

Regulation of genes associated with cell cycle progression

MYCN promotes the G_1/S cell cycle transition, and in an attempt to identify potential MYCN target genes involved in this process microarray analysis following MYCN siRNA knockdown was previously performed, and the results confirmed in a regulatable MYCN expression system (Bell *et al.*, 2007).

ODC1: Ornithine decarboxylase (ODC) is the rate-limiting enzyme in polyamide biosynthesis and has been found to be co-amplified with 19% of *MYCN*-amplified neuroblastoma due to its position ~5.5 Mb from the *MYCN* locus on chromosome 2p24 (Hogarty *et al.*, 2008). A direct transcriptional target of MYCN, ODC is also required for the degradation of $p27^{KIP1}$ by promoting the MYC-induction of CKS1 (Keller *et al.*, 2007), an accessory protein of the E3 ligase complex which targets $p27^{KIP1}$ for degradation. However, interestingly, treatment with the ODC inhibitor alpha-difluoromethylornithine (DFMO) impairs cell proliferation by increasing levels of $p21^{CIP1/WAF1}$, not $p27^{KIP1}$, which enhances the G_1 population of tumour cells and survival of *TH-MYCN* transgenic mice (Hogarty *et al.*, 2008; Rounbehler *et al.*, 2009). The efficacy and safety of DMFO as a single agent and in

combination with etoposide has since been evaluated in patients with relapsed and high-risk disease (Sholler *et al.*, 2013)

E2F: Central regulators of cell cycle progression, E2F transcription factors are negatively controlled by the retinoblastoma protein (pRB) pathway and target a variety of genes including those required for S-phase transition. E2F proteins are known to regulate *MYCN* expression in neuroblastoma (Strieder and Lutz, 2003), and E2F genes are direct transcriptional targets of c-MYC. However, although E2F1 expression has been shown to decrease after MYCN knockdown, it remains yet to be confirmed as a direct MYCN target gene (Woo *et al.*, 2008).

MDM2: The negative regulator of p53, *MDM2* is a direct MYCN target gene (Slack *et al.*, 2005). By binding to the P2 region of the *MDM2* promoter, MYCN up-regulates MDM2 expression providing a mechanism for the evasion of p53-induced apoptosis in *MYCN*-amplified neuroblastoma (Slack *et al.*, 2005). MDM2 expression has also been found to have a functional role in the MYCN-mediated centrosome amplification observed following DNA damage in the SHEP-Tet21N MYCN expression system (Slack *et al.*, 2007).

DKK3: Dickkopf-3 (DKK3) is a member of the DKK family of secreted WNT antagonists, and is a candidate tumour suppressor gene due to its down-regulation in a variety of malignancies (Kuphal *et al.*, 2006; Katase *et al.*, 2013; Lin *et al.*, 2013). Ectopic expression of DKK3 has been shown to inhibit cell proliferation in neuroblastoma cell lines (Koppen *et al.*, 2007), with MYCN suggested to indirectly supress DKK3 expression by directly up-regulating the microRNA miR-17-92 cluster (De Brouwer *et al.*, 2012).

ID2: An inhibitor of differentiation, DNA-binding protein inhibitor 2 (ID2) promotes the G_1/S transition by binding to hypo-phosphorylated pRB, promoting the release of the E2F transcription factors, and antagonising the growth-suppressive activities of $p16^{INK4A}$ and $p21^{CIP1/WAF1}$ (Lasorella *et al.*, 1996). The clinical relationship between MYCN and ID2 expression remains unclear as some reports observe no correlation between the two oncogenes (Wang *et al.*, 2003), while others identify ID2 as a potential MYCN target gene (Woo *et al.*, 2008).

SKP2: S-phase kinase-associated protein 2 (SKP2) is the F-box protein for the SCF E3 ubiquitin ligase complex which monitors the G_1/S transition (Carrano *et al.*, 1999; Nakayama *et al.*, 2004). MYCN siRNA knockdown studies decreased SKP2 expression at the transcript and protein level identifying it as a potential MYCN transcriptional target (Bell *et al.*, 2007).

Regulation of genes associated with apoptosis

The ability of MYCN to enhance apoptosis following cellular stress, while not fully understood, involves the upregulation of multiple pro-apoptotic proteins.

p53: The 'guardian of the genome' (Lane, 1992), p53 plays a crucial role in the maintenance of genomic stability and tumour suppression by monitoring several mechanisms, including the G_1/S transition and induction of apoptosis. MYCN directly regulates p53 transcription (Westermann *et al.*, 2008; Chen *et al.*, 2010b), and this relationship is thought to play an important role in the mechanism by which MYCN sensitises cells to apoptosis.

p14^{ARF}: A central component of the p53 pathway, p14^{ARF} antagonises MDM2 and thus activates and stabilises p53. Homozygous deletions of p14^{ARF} have been reported in neuroblastoma indicating that it promotes the progression of *MYCN* amplified disease (Caren *et al.*, 2008; Carr-Wilkinson *et al.*, 2010a). Although there are no reports showing MYCN sensitising cells to p14^{ARF} driven apoptosis, p14^{ARF} is reported to inhibit the transcriptional activity of c-MYC/MYCN by directly binding to the proteins promoting their nucleolar sequestration (Qi *et al.*, 2004; Amente *et al.*, 2007).

H-TWIST: Human Twist-related protein 1 (H-TWIST) is an embryonic transcription factor of the B-HLH family that is essential for neural crest development (Chen and Behringer, 1995). H-TWIST proteins inhibit apoptosis by directly interacting with p53, suppressing its DNA-binding activity (Maestro *et al.*, 1999; Shiota *et al.*, 2008). Although not identified as a direct MYCN transcriptional target, high levels of H-TWIST are observed in *MYCN*-amplified tumours suggesting oncogenic cooperation between the two proteins, and that H-TWIST

is a MYCN-derived mechanism which disrupts the ARF/p53 pathway in neuroblastoma (Valsesia-Wittmann *et al.*, 2004).

PUMA: The p53 upregulated modulator of apoptosis (PUMA) is a member of the BCL-2 protein family which activates the BH3-only pro-apoptotic protein, inducing the canonical mitochondrial apoptotic pathway (Yu and Zhang, 2008). PUMA plays an essential role in p53-dependent and -independent apoptosis, triggering cell death in *in vivo* and *in vitro* models (Jeffers *et al.*, 2003; Villunger *et al.*, 2003; Yu *et al.*, 2003), and its expression has been shown to be reduced following MYCN knockdown by siRNA (Chen *et al.*, 2010b).

BCL2 and BAX: Overexpression of the anti-apoptotic proteins BCL-2 and BCL-X_L has been shown to inhibit apoptosis by preventing mitochondrial permeability (Kroemer *et al.*, 1997). In contrast, overexpression of the pro-apoptotic protein BAX can induce mitochondrial permeability releasing pro-apoptotic proteins such as cytochrome C, thereby activating the caspase cascade (Pastorino *et al.*, 1998). MYCN has also been shown to cooperate with cytotoxic drug treatment to increase BAX protein levels, while not affecting BCL-2 levels, to alter the ratio of the opposing proteins in favour of apoptosis (Fulda *et al.*, 1999).

MYCN regulation of noncoding RNAs

The noncoding portion of the genome, noncoding RNA (ncRNA), identifies functional RNA molecules which are not translated into proteins yet still play an important role in cellular processes. Split into the 2 classes of small ncRNAs (i.e. miRNAs and siRNAs ≤200 nt) and long ncRNAs (lncRNA ≥ 200 nt) their deregulation has been found to be involved in several diseases including cancer (Esteller, 2011). MicroRNAs are an abundant ncRNA which negatively regulate protein expression and whose expressional changes profoundly affect the protein composition of a cell (Baek *et al.*, 2008). Although their precise mechanism of action is still elusive, the miRNA-mRNA regulatory network is highly complex. Given the ability of single miRNAs to target several different mRNAs they have been found to regulate a broad spectrum of cellular processes including proliferation, differentiation, and apoptosis (reviewed by (Huang *et al.*, 2011)). MYCN has been reported to upregulate and repress miRNA expression. The

MYCN-induced miRNAs, (*mir17-92* cluster, *mir*-9 and *mir-421*) have been identified to target genes involved in proliferation and the inhibition of apoptosis and differentiation, while the miRNAs which inversely correlate with MYCN expression (*mir-184* and *mir-542-5p*) are identified as tumour suppressor miRNAs (reviewed by (Buechner and Einvik, 2012)). Interestingly ncRNAs are also reported to target MYCN expression and the overexpression of *mir-34a* has been shown to directly target MYCN resulting in growth inhibition and increased apoptosis (Wei *et al.*, 2008). Conversely MYCN expression is stabilised by the *MYCN cis*-antisense RNA *NCYM*. Initially thought to be a lncRNA it has since been identified as a *de novo* evolved protein which inhibits the GSK3β-mediated degradation of MYCN resulting in a positive feedback loop and aggressive phenotype in *MYCN/NCYM*-amplified tumours (Suenaga *et al.*, 2014).

1.6.4. *The clinical significance of MYCN expression in neuroblastoma*

Although *MYCN* amplification is a strong poor prognostic indicator, high levels of MYCN expression in a non-amplified setting, although not an independent prognostic factor, is associated with a favourable outcome (Cohn *et al.*, 1995; Tanaka *et al.*, 2004; Tang *et al.*, 2006b). Often a result of increased protein stabilisation, it is speculated that in the absence of *MYCN* amplification the apoptosis-inducing function of MYCN is dominant over proliferation-inducing effects and vice versa in amplified disease.

MYCN protein has a short half-life (~2hrs) and is targeted for proteasomal degradation by the SCF^{FBXW7} E3 ubiquitin ligase complex (Yada *et al.*, 2004), which is dependent on the phosphorylation of Thr58 by glycogen synthase kinase 3β (GSK3β), following phosphorylation at Ser62 by the cyclin B/CDK1 complex which acts as a priming site for GSK3β (Sjostrom *et al.*, 2005). As GSK3β is negatively regulated by the PI3K/AKT pathway, PI3K inhibitors have been exploited as an approach to target MYCN therapeutically by promoting its degradation (Chesler *et al.*, 2006). Conversely high levels of Aurora A kinase (*AURKA*), have been shown to uncouple MYCN degradation from PI3-kinase-dependent signalling in neuroblastoma, stabilising the protein (Otto *et al.*, 2009). The expression of *AURKA* has also been shown to be elevated in *MYCN*-amplified neuroblastoma potentially creating a positive feedback loop (Berwanger *et al.*, 2002).

The clinical significance of high levels of MYCN expression in low-risk, non-amplified disease requires further definition. One such study defined a functional MYCN signature by integrating the *in vitro* regulation by MYCN protein with the *in vivo* correlation to *MYCN* mRNA levels. Following the silencing of MYCN in a *MYCN* amplified neuroblastoma cell line, 422 up- and 463 down-regulated genes were identified. The selected genes were then compared to the *MYCN* expression profile in a series of 88 neuroblastoma tumours resulting in the identification of 157 genes which showed an expression profile which correlated with *MYCN* mRNA levels. Acting as a prognostic signature, this MYCN-157 signature marked the influence of stabilisation of MYCN at the protein level separating itself from the amplified/non-amplified classifications, and consequently was found to predict poor outcome in neuroblastoma with and without *MYCN*-amplification (Valentijn *et al.*, 2012).

1.7. The cell cycle

The eukaryotic cell cycle is an intricate and carefully regulated sequence of events which culminates in mitosis. Central to this process is the sequential activation of the cyclin-dependent kinases (CDKs) which when in a complex with their activating cyclins regulate the progression towards cell division (van den Heuvel and Harlow, 1993; Pines, 1994; Malumbres and Barbacid, 2005; Malumbres *et al.*, 2009). The cell cycle is divided into four successive stages; M phase (mitosis) where the parental cell divides to give two daughter cells; S phase (DNA synthesis), where the DNA is replicated; and the two gap phases G_1 and G_2 during which there are crucial checkpoints to ensure genomic structure and integrity before the cell is committed to DNA replication and mitotic division, respectively (Figure 1.6)

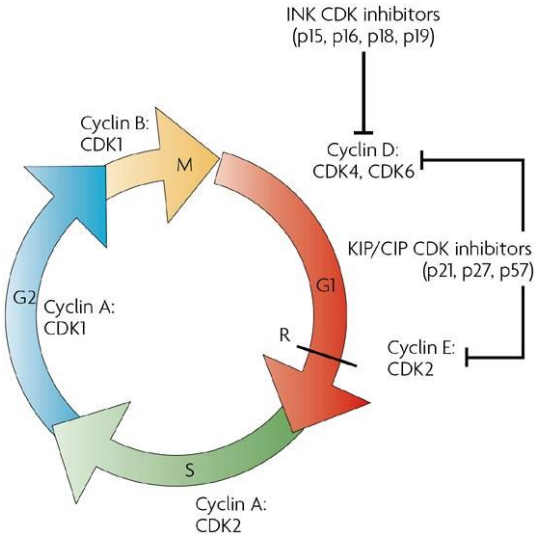

Figure 1.6 Cell cycle control and regulation. Progression through the cell cycle is regulated by different cyclin-CDK complexes which are in turn controlled by a combination of processes, including transcriptional activation of cyclin expression, post-translational modifications and inhibition by specific cyclin dependent kinase inhibitors (CKDI).(Dehay and Kennedy, 2007)

1.7.1. *The G_1 to S transition*

Progression through the G_1 phase requires constant stimulation by mitogenic signals and a high rate of protein synthesis, interruption of either resulting in the rapid exit from the cell cycle into G0 (cellular quiescence) (Bertoli *et al.*, 2013). The G_1 to S phase transition is primarily regulated by the retinoblastoma protein (pRB) which in its hypo-phosphorylated form sequesters the E2F family of transcription factors thereby repressing E2F-responsive genes. Following mitogenic stimulation, pRB is initially phosphorylated by cyclin D-CDK4/6 complexes in early G_1 releasing the cell from a quiescent state. Phosphorylation partially inactivates pRB resulting in E2F-induced expression of cyclin E, which following the activation of CDK2 drives the cells though the G_1 phase by promoting the sequential phosphorylation of pRB, liberation of E2F proteins, and activation of a plethora of genes required for S phase (Lundberg and Weinberg, 1998; Ezhevsky *et al.*, 2001). The positive feedback loop created by the cyclin E-CDK2 complex increases levels of the complex above that of the CDK inhibitors $p27^{KIP1}$ and $p21^{WAF1/CIP1}$, and this shift in complex equilibrium plays an important role in the commitment of the cell to mitotic division as once past the restriction point cell cycle progression is independent of mitogenic and inhibitory signals (Zetterberg *et al.*, 1995).

1.7.2. *Inhibitors of the G_1 to S transition*

Two main families of cyclin-CDK inhibitors have been characterised, the INK4 protein family (inhibitors of CDK4), and the CIP/KIP family. The INK4 class specifically inhibit CDK4 and CDK6 and include; $p16^{INK4a}$, $p15^{INK4b}$, $p18^{INK4c}$ and $p19^{INK4d}$, while the CIP/KIP family affect a broader spectrum of cyclin-CDKs and include $p27^{KIP1}$ (p27 hereafter) and $p21^{WAF1/CIP1}$ (p21 hereafter), as reviewed by (Sherr and Roberts, 1999). The periodic expression of cyclins and CDK inhibitors thereby acts as the driving force of the cell cycle and loss of CDK inhibitors provides a selective advantage to tumour development. Although p27 is a recognised CDK2 inhibitor, it has also been demonstrated to help trigger replication origins and promote the assembly and activation of cyclin D-CDK4. High levels of p27 and p21 in early G_1 have also been shown to be sequestered by cyclin D-CDK4 complexes preventing the inhibition of cyclin E-CDK2 (Cheng *et al.*, 1999; Larrea *et al.*, 2008). In addition to ubiquitin-mediated proteasomal degradation of CDK inhibitors, CDK activity is regulated by a variety of positive phosphorylation events by CDK-activating kinases (CAK) and negative phosphorylation events catalysed by kinases such as Wee1 (Perry and Kornbluth, 2007). Further regulation is also brought by the removal of inhibitory phosphates from cyclin A/E-CDK2 complexes by the phosphatase Cdc25, thus promoting entry into S phase (Bertoli *et al.*, 2013).

1.7.3. *S phase to M phase transition*

DNA replication is confined to the S phase of the cell cycle. Initiated by the assembly of the pre-replicative complexes (pre-RC) on multiple DNA origins, origin firing, formation of replication forks, and DNA synthesis is tightly regulated by CDK activity. Regulation includes inhibition of pre-RC assembly so to ensure that origins only fire once per S phase (Takeda and Dutta, 2005). The S to G_2 phase transition is regulated by cyclin A-CDK1/2 complexes and CDK1 which, thought to monitor the firing of pre-RC, is regulated by the phosphatase Cdc25 which in turn is controlled by cyclin A-CDK2 activity (Mitra and Enders, 2004). Cyclin A-CDK2 has also been reported to phosphorylate E2F1 inhibiting its DNA-binding activity and creating a negative feedback loop which switches cyclin A transcription off, allowing progression into S phase (Xu *et al.*, 1994; Kitagawa *et al.*, 1995). The regulation of mitotic progression by CDK1 and CDK2 is not fully

understood and a large number of substrates have been identified as targets, implicating CDK1 and CDK2 in a variety of different signalling pathways such as DNA replication, chromatin packaging and remodelling, spindle assembly and DNA damage signalling and repair (Ubersax *et al.*, 2003; Chi *et al.*, 2008). CDK1 activity is best understood in budding yeast where CDK1 singularly drives the cell cycle progression. The current model for CDK driven cell cycle progression is based upon the substrates wide range of efficiencies for kinase-mediated phosphorylation, with the better substrates being phosphorylated at low CDK activity, and vice versa (Koivomagi *et al.*, 2013). This is further complicated by the multisite nature of the majority of the substrates resulting in several phosphorylation events being required. Recently CKS1 has been identified as a phosphor-adaptor subunit of CDK1 able to facilitate multisite phosphorylation by binding to specific priming sites (Koivomagi *et al.*, 2011), However, the role of CKS1 on CDK1-activity has been shown to depend on the kinetics of the CKS1 consensus sites phosphorylation in the multisite reaction. If the CKS-binding site is phosphorylated early, binding to the remaining sites is triggered followed by enhanced CDK1-activity. However, phosphorylation late in the multisite reaction leaves CKS1 priming non-essential (McGrath *et al.*, 2013). Based on these findings that net phosphorylation is not a singular event and relies on the substrates specificity towards CKS1. Additional substrate parameters have also been identified including the distance between phosphorylation sites, their distribution and the ratio of serine to threonine residues contributing to the understanding of CDK-controlled cell cycle progression.

1.8. The Ubiquitin Proteasome System

The periodic expression of CDK inhibitors acts as a driving force for the cycle and is controlled by ubiquitin-mediated proteolysis. The ubiquitin-proteasome system (UPS) covalently attaches multiple ubiquitin molecules (Ub) to a lysine residue on specific protein substrates. Several rounds of ubiquitination can occur and different lengths of ubiquitin chains have been found to direct the substrate down a particular pathway with polyubiquitination, via lysine 48 or lysine 11, being associated with targeting substrates for degradation by the 26S proteasome (Clague and Urbe, 2010). Ubiquitin ligation is mediated by 3 enzymes; a ubiquitin-activating enzyme (E1), a ubiquitin-conjugating enzyme (E2) and a ubiquitin ligase (E3). While few reports have linked E1 and E2 to cancer development, the

deregulation of E3 has been implicated in numerous human pathologies including malignancy (Nakayama and Nakayama, 2006a). As uncontrolled cell proliferation and insensitivity to growth inhibitory signals are recognised as key 'hallmarks' of cancer development (Hanahan and Weinberg, 2011), alterations in the expression or activity of the UPS regulatory subunits have become of particular interest.

1.8.1. *Ubiquitin ligases and cell cycle control*

E3 ligases are primarily responsible for the recognition of the target protein, specificity and versatility being achieved by the large number of different E3 ligases available with ~600 putative E3s shown to be encoded by the human genome (Li *et al.*, 2008). The E3s are divided into 2 major classes based on their domain structure and substrate recognition; the HECT (homologous to E6-associated protein C-terminus) family, and the largest type the RING (Really Interesting New Gene) family, which can be further subdivided depending on the structure of the RING finger motif (Sun, 2003). The two main E3 ligases involved in cell cycle progression are members of the cullin-based subfamily, a further division of the RING-finger type E3s. The anaphase-promoting complex or cyclosome (APC/C), and SKP1-CUL1-F-box protein (SCF) both share similar core structural components including a scaffold complex, a RING protein and a substrate binding subunit (Figure 1.7). However, APC/C and SCF complexes differ in their cellular functions and substrates which are highlighted by the timing of their activity in the cell cycle.

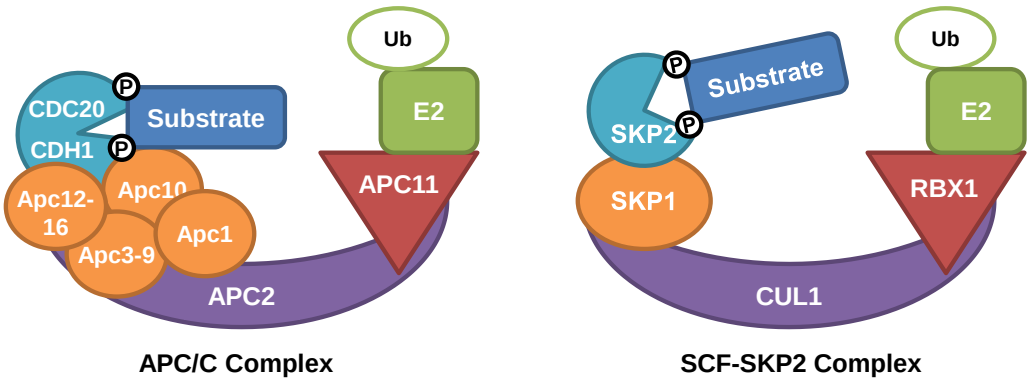

Figure 1.7 Schematic representation of the structure of SCF and APC/C ubiquitin ligases. Members of the cullin-RING ligase superfamily, both complexes have cullin protein scaffolds (APC2) and (CUL1) (Zheng *et al.*, 2002; Barford, 2011). The RING-finger component APC11/RBX1 binds to the N-terminal end and recruits the E2 conjugating enzyme (E2), and the substrate specific subunit attaches to the C-terminal end via an adaptor protein. In the SCF complex the F-box SKP2 binds to the SKP1 adaptor. The APC/C complex has two specificity factors CDC20 and CDH1 which work alongside the 13 different core component subunits (Penas et al., 2011; Bassermann et al., 2014).

APC/C is active from mid M-phase (anaphase), allowing the passage of the cell through G_1, and recognises substrates by a degradation motif or degron (D-box) in the target protein primary sequence. In contrast SCF complexes, although originally thought to primarily regulate the G_1-S transition, are active from late G_1 to early M-phase and utilize F-box subunits to recognise substrates which have often been post-transcriptionally modified though phosphorylation at specific residues (Nakayama and Nakayama, 2006a; Frescas and Pagano, 2008). Although involved in distinct phases of the cell cycle, SCF and APC/C complexes share common substrates and regulate each other by ubiquitin-mediated degradation. This crossover produces a network of positive and negative feedback loops which ultimately control CDK1 and CDK2 activity, allowing mitotic division and the controlled passage though the cell cycle as summarised in Figure 1.8, (Bashir *et al.*, 2004; Wei *et al.*, 2004). Several different SCF complexes regulate the cell cycle and unlike SCF^{SKP2}, which positively regulates cell cycle by targeting CDK inhibitors for degradation, $SCF^{\beta\text{-}TrCP}$ can promote and inhibit proliferation by promoting the degradation the mitotic APC/C activator CDC20, as well as the CDH1 inhibitor EMI1 (Guardavaccaro *et al.*, 2003) and CDK1 inhibitory kinase WEE1 (Watanabe *et al.*, 2004).

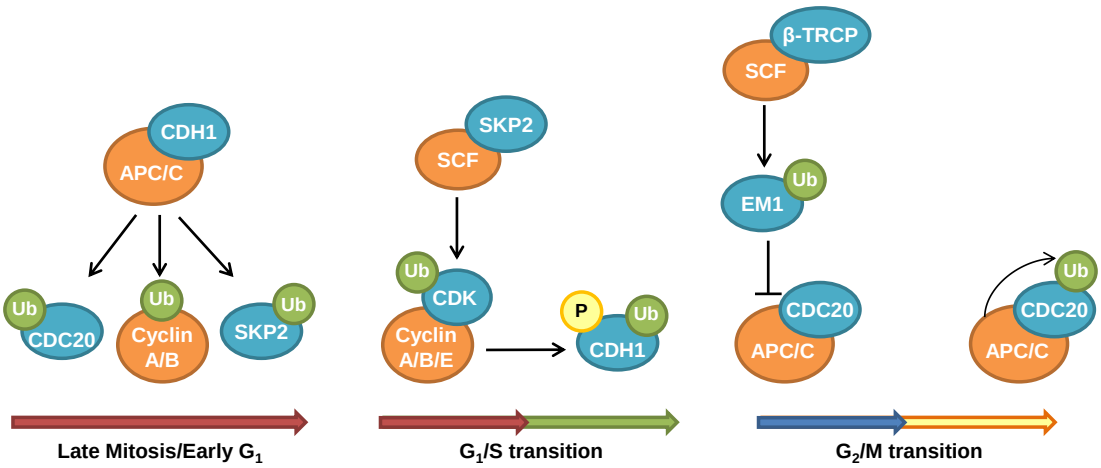

Figure 1.8 Schematic representation of the interplay between the APC and SCF E3 ubiquitin ligase complexes during cell cycle. During early G1 phase the APC/C^{CDH1} complex promotes the degradation of SKP2, its own activator CDC20, and cyclins A and B, which decreases CDK1/2 activity. During the G1 phase levels of SKP2 protein increase, overcome APC/C^{CDH1} degradation and the SCF^{SKP2} complex targets the CDK inhibitors p27 and p21 for degradation, thereby activating CDK1 and CDK2 and promoting progression into S phase. Active cyclin A-CDK complexes in S-phase phosphorylate CDH1 targeting it for degradation by a second SCF complex allowing the formation of APC/C^{CDC20}. In G2 the APC/C^{CDC20} complex is inhibited by the F-box protein EMI1; however, EMI1 alongside the CDK1 inhibitor WEE1 are targeted for destruction by $SCF^{\beta\text{-}TRCP}$ allowing the onset of mitosis. CDC20 is then targeted in a self-catalytic mechanism during anaphase at the spindle-associated checkpoint allowing mitotic progression (Kurland and Tansey, 2004; de Bie and Ciechanover, 2011).

1.9. The SCF^{SKP2} Complex

1.9.1. *SCF^{SKP2} Structure*

SCF complexes consist of the constant components RBX1, CUL1 and SKP1, and a variable component known as the F-box protein. Acting as a rigid scaffold, the cullin protein (CUL1) organises this elongated structure. The RING-box protein (RBX1), which contains the RING zinc-finger domain, binds to the CUL1 protein C-terminal globular α/β domain and forms the catalytic core capable of recruiting the E2 ubiquitin-conjugating enzyme. Two E2 enzymes are associated with the SCF^{SKP2} complex, UbcH5c (Brzovic *et al.*, 2006) and CDC34 (Lisztwan *et al.*, 1998), which are interchangeable and paired with particular targeted proteins bound to the substrate receptor F-box protein such as SKP2.

SKP2 is bound to the N-terminal domain of the CUL1 scaffold protein by the SKP1 adaptor protein. Prior to SKP1-SKP2 docking on CUL1, it is first released from the negative regulator $p120^{CAND1}$ which holds the CUL1-RBX1 structure in a

functionally-immature state. A rate limiting step in SCF assembly, CUL1 is covalently modified by the attachment of the ubiquitin-like protein NEDD8. Termed neddylation, this process dissociates the $p120^{CAND1}$ inhibitor from CUL1 thus promoting SKP1 attachment (Liu *et al.*, 2002).

Early modelling studies revealed that CUL1 adopted a long stalk-like structure, as shown in Figure 1.9, which separated the substrate binding from the catalytic E2 cysteine by approximately 50 Å, implying that the substrates are placed to bridge the gap (Zheng *et al.*, 2002). Neddylation has since been shown to play an important role in both steering RING E3 ligases towards their specific targets and modulating the position of the E2 catalytic centre, although presentation of the acceptor Lysine to the E2 active site has been shown to require further guidance by the substrate itself (Lydeard *et al.*, 2013; Scott *et al.*, 2014).

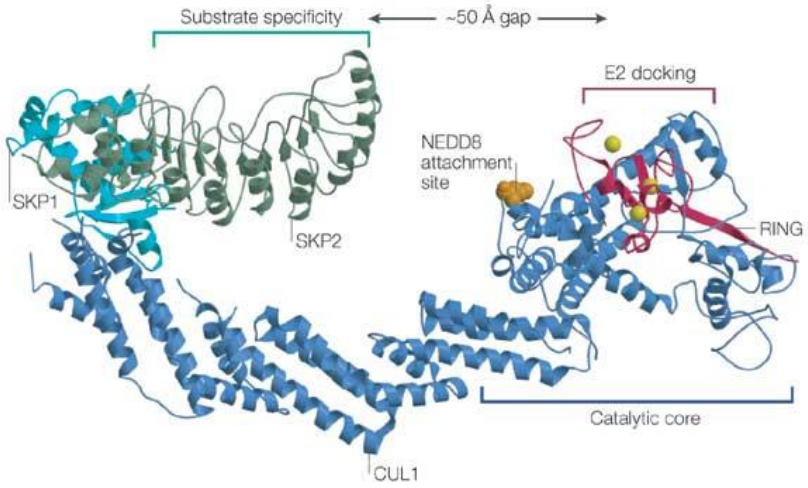

Figure 1.9 The crystal structure of SCF^{SKP2} (Protein Data Bank File 1LDK) Following the attachment of NEDD8, the F-box protein SKP2 binds to the adaptor protein SKP1 and determines the substrate specificity. A 50-Å gap separates the tip of the SKP2 leucine rich repeat domain and the active-site cysteine of the E2 which is docked on the RING protein within the catalytic core. The yellow spheres represent the zinc molecules within the RBX protein (Petroski and Deshaies, 2005).

1.9.2. *The SKP2 F-box protein*

Attached to the SCF complex by the SKP1 adaptor protein, F-box proteins are characterized by a 40 amino acid F-box motif which binds to SKP1, as well as a protein-interaction domain which specifically interacts with target substrates (Bai *et al.*, 1996). F-box proteins are classified into three categories: FBWs containing WD-40 domains, FBLs containing leucine-rich repeats and FBXs which either contain different protein-protein interaction modules or no recognisable motif (Cenciarelli *et al.*, 1999). One of the better characterised mammalian F-box proteins is SKP2 (S-phase kinase-associated protein 2) which belongs to the FBX1 class. First discovered as a complex with cyclin A-CDK2 (Zhang *et al.*, 1995), SKP2 is now known to play an essential role in cell cycle progression through the controlled degradation of S-phase inhibitors. Although SKP2 activity is primarily associated with degradation of the CDK inhibitor p27 (discussed further in Section 1.9.3), it is responsible for promoting the degradation of a number of tumour suppressor proteins (Table 1.5). Recognition of substrates by SKP2 requires the phosphorylation of specific residues and in some cases an accessory protein which enhances the affinity of the substrate for the SCF^{SKP2} complex.

Cellular Role	Reported Substrate	Function	Refs
Cell Cycle Control	$p27^{KIP1}$	CDK2 and 4 inhibitor	(Carrano *et al.*, 1999; Sutterluty *et al.*, 1999; Tsvetkov *et al.*, 1999)
	$p21^{WAF1/CIP1}$	CDK1/2/and 4/6 Inhibitor	(Yu *et al.*, 1998; Bornstein *et al.*, 2003)
	$p57^{KIP2}$	CDK Inhibitor	(Kamura *et al.*, 2003)
	Free Cyclin E	Binds to CDK2 and drives G_1 progression	(Nakayama *et al.*, 2000)
	Cyclin D1	Binds to CDK4/6 and drives G_1 progression	(Yu *et al.*, 1998)
DNA Replication	CDT1	DNA replication factor: helps from pre-RC	(Li *et al.*, 2003)
	ORC1	Origin recognition complex: forms platform for pre-RC	(Mendez *et al.*, 2002)
DNA Repair (double-strand breaks)	BRCA2	Involved in repair of homologous recombinational repair	(Moro *et al.*, 2006)
	RAG2	Cleaves DNA producing signal ends for non-homologous end joining	(Jiang *et al.*, 2005b)
Gene Transcription	TOB1	Transcriptional corepressor and suppressor of cyclin D1 promoter activity	(Hiramatsu *et al.*, 2006)
	p130	pRb pocket protein: activates E2F family of transcription factors	(Tedesco *et al.*, 2002; Bhattacharya *et al.*, 2003)
	FOXO1	Member of the Forkhead box protein family: multi-functional transcription factor	(Huang *et al.*, 2005)
	MEF/ETS	An ETS transcription factor driving G_1/S transition	(Liu *et al.*, 2006)
	c-MYC	Member of the MYC family of TF: Multi-functional	(Kim *et al.*, 2003; von der Lehr *et al.*, 2003)
	E2F1	Multi-functional transcription factor suppressed by pRb	(Marti *et al.*, 1999)
	ING3	Subunit of a Nu4A histone acetyltransferase complex and multi-functional TF	(Chen *et al.*, 2010a)

Table 1.5 Examples of reported substrates of SKP2, summarised from (Frescas and Pagano, 2008).

1.9.3. *Ubiquitin mediated degradation of CIP/KIP family of CDK inhibitors*

The most established SKP2 substrate is the CDK inhibitor p27 which accumulates in *SKP2*$^{-/-}$ knockout mice and is held responsible for the over-replication phenotypes observed, including nuclear enlargement, polyploidy and multiple centromeres (Nakayama *et al.*, 2000; Nakayama *et al.*, 2001). The absence of these abnormalities in *SKP2*$^{-/-}$*p27*$^{-/-}$ double-knockout mice not only identified p27 as a bona fide SKP2 substrate, yet also implied that p27 degradation plays a crucial role in the regulation of the G_1 phase by SKP2. However, as not all phenotypes of *SKP2*$^{-/-}$*p27*$^{-/-}$ and *SKP2*$^{-/-}$ mice were found to be identical, additional important protein substrates are targeted for SKP2-mediated ubiquitination (Nakayama *et al.*, 2004).

Recognition of p27 by SKP2 is dependent on the CDK inhibitor being phosphorylated on a threonine residue (Thr187) by the cyclin E-CDK2 complex (Müller *et al.*, 1997; Sheaff *et al.*, 1997; Vlach *et al.*, 1997), and the SKP2 accessory protein cyclin-kinase-subunit 1 (CKS1) (Ganoth *et al.*, 2001). A cell cycle regulatory protein, CKS1 enhances the affinity of the SCF^{SKP2} complex for p27. Binding to the leucine-rich repeat domain and C-terminal end of SKP2, the interaction does not induce any conformational change in the F-box protein, but provides a substrate-binding site where p27 can dock (Hao *et al.*, 2005). The Glu185 side-chain of p27 inserts between SKP2 and CKS1 which allows the N-terminal end of p27 to interact with SKP2, and the C-terminal end which contains the phosphorylated T187 residue, with CKS1 (Figure 1.10).

In addition to the recruitment of CKS1, SKP2-mediated turnover of p27 has been shown to require the assembly of p27-cyclin A/E-CDK2 complexes. In a non-catalytic role, cyclin A (Montagnoli *et al.*, 1999a) and cyclin E (Ungermannova *et al.*, 2005) have been shown to directly bind un-phosphorylated p27, which is thought to be a necessary step for the recruitment of p27 to the catalytic subunits of the SCF^{SKP2} complex (Zhu *et al.*, 2004; Ungermannova *et al.*, 2005). In addition to presenting p27 to the SKP2-CKS1 binding pocket and phosphorylating Thr187, interactions observed between CKS1 and CDK2 (Bourne *et al.*, 1996) and between SKP2 and cyclin A (Zhang *et al.*, 1995), suggest that the p27-cyclin A/E-

CDK2 trimeric complex may enhance binding within the SKP1-SKP2-CKS1-p27 final configuration (Figure 1.11) (Hao *et al.*, 2005).

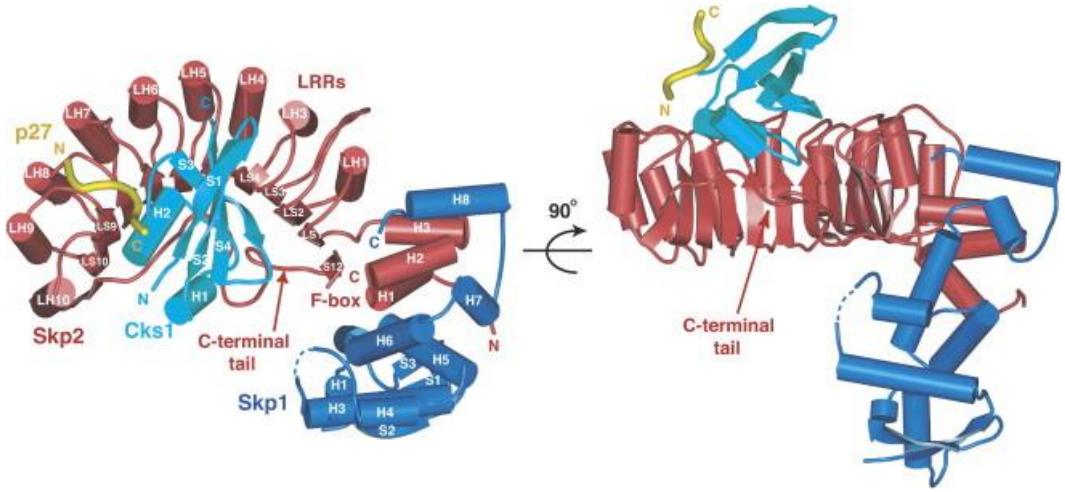

Figure 1.10 Crystal structure of SKP1-SKP2-CKS1-p27 complex. Ribbon diagrams of the complex are shown in views related by a 90° rotation. SKP1, SKP2 CKS1 and p27 are shown in blue, red, cyan and yellow, respectively. (Hao et al., 2005)

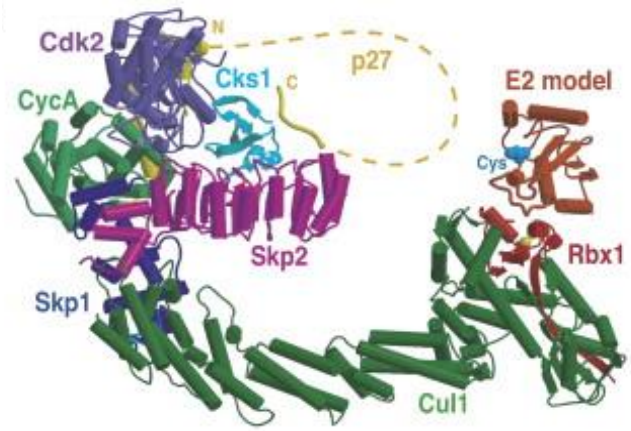

Figure 1.11 Model of SCF^{SKP2} -CKS1-CDK2-cyclin A complex showing that the hypothesised interactions, which have been structurally characterised, can coexist in one complex. SKP1, SKP2 CKS1 and p27 are shown in blue, magenta, cyan and yellow, respectively. The middle region of p27 (yellow) where no structural information exists is shown as a dotted line. Also shown is the docked E2 (orange) and its active site cysteine (cyan) (Hao et al., 2005).

The other members of the CIP/KIP family of CDK inhibitors, p57 and p21, share the conserved N-terminal CDK2-cyclin A/E inhibitory domain with p27, and have also been shown to be targeted for degradation by the SKP1-SKP2-CKS1 complex (Bornstein *et al.*, 2003; Kamura *et al.*, 2003). Extensive homology at the C-terminal end has been described between p27 and p57, suggesting that the mechanism for recognition by SKP2 and recruitment to the SCF^{SKP2} complex are analogous following the phosphorylation of p57 on a threonine residue (Thr310) (Kamura *et al.*, 2003; Hao *et al.*, 2005). In contrast, p21 does not show clear C-terminal domain homology with p27, although similarities have been shown including the requirement for CKS1 and for cyclin E-CDK2 presentation and phosphorylation of a specific residue (Ser130) (Bornstein *et al.*, 2003). The anion-binding site of CKS1 has also been shown to be necessary for p21 ubiquitination, which interacts with a negatively charged glutamine residue in an analogous manner to p27. Interestingly, additional charged residues on p21 have been found to interact with CKS1, and promote ubiquitination in the absence of substrate phosphorylation, implying that p21 Ser130 phosphorylation is not absolutely required for SKP2-mediated degradation. A final difference between p27 and p21 observed was the specificity of E2 enzymes. As discussed in Section 1.9.1, the CUL1 scaffold protein dictates the distance between the SKP2-protein substrate and the catalytically active E2 enzymes CDC34 and UbcH5c. While the SCF^{SKP2}-mediated ubiquitination of p27 was shown to be similar with CDC34 and UbcH5c, a much lower ubiquitination was observed for UbcH5c in the targeting of p21, suggesting that the identity of the SKP2 substrate influences E2 enzyme selected (Bornstein *et al.*, 2003).

1.9.4. *Regulation of SKP2 gene expression*

Isolation and characterisation of the human *SKP2* promoter has identified binding sites for a number of transcription factors suggesting that SKP2 expression is regulated at a transcriptional as well as post-translational level. The cell cycle dependent oscillations of *SKP2* mRNA are often cell context dependent, and both active and repressive regions have been identified in the *SKP2* promoter (reviewed by (Chan *et al.*, 2010b)).

The identification of binding regions for GA-binding protein (GABP), Notch-1 activated CBF1, and SP1/ELK-1 regulatory elements, supports the concept of

cell cycle *SKP2* regulation as these factors are all known to mediate mitogenic signalling. However, as neither GABP or Notch-1 alone were able to bypass mitogen-dependent *SKP2* induction, the accumulation of SKP2 protein during the G_1 cell cycle phase must involve the cooperation of several signalling pathways (Imaki *et al.*, 2003; Sarmento *et al.*, 2005). Interleukin-6 (IL-6) activated signal transducer and activator of transcription 3 (STAT3) mediates the expression of a variety of genes and was found to promote SKP2 transcription in cervical carcinoma cells by recruiting the co-activator p300 to the *SKP2* promoter region (Huang *et al.*, 2012). Furthermore, regulation of *SKP2* gene expression by the PI3K/AKT signalling pathway is implicated by the decrease in *SKP2* mRNA levels following PI3K inhibition or AKT1 knockdown (Auld *et al.*, 2007; Gao *et al.*, 2009). The PI3K/PTEN/AKT signalling pathway modulates many aspects of cell growth and survival, and has been shown to positively (Andreu *et al.*, 2005) and negatively (Mamillapalli *et al.*, 2001) regulate SKP2 transcription in cancer cell models, depending on the levels of AKT activation or PTEN suppression. Moreover, the transcription factors c-MYC and NF-κB are downstream targets of PI3K signalling and have both been shown to bind to the *SKP2* promoter; c-MYC binding to high affinity E-boxes capable of promoting *SKP2* mRNA expression (Bretones *et al.*, 2011). However, the contribution of SKP2-mediated p27 degradation towards c-MYC-driven proliferation was found to be modest when compared to the effect of CKS1 loss, suggesting that other CKS1 targets not linked to the SCF^{SKP2} complex are critical for MYC-driven tumorigenesis (Old *et al.*, 2010).

NF-κB is a family of transcription factors and consists of two structural classes, Class I/NF-κB subfamily (p50/p105 and p52/p100) and Class II/Rel subfamily (RelA and RelB) which bind as homo- or hetero-dimers, and are held in an inactive state by the inhibitory IκB subfamily (IκBα and IκBβ). Following stimulation by extracellular signals, and a series of proximal events, an IκB-inducing kinase (IKKα or IKKβ), is activated which phosphorylates the IκB proteins, allowing their dissociation and the activation of gene transcription (Gilmore, 2006). There are two key pathways leading to NF-κB-mediated transcription, however only the non-canonical pathway is reported to regulate *SKP2* gene expression (Figure 1.12). The IKK catalytic subunits are linked to the cell cycle, and the IKKα subunit has been shown to induce *SKP2* transcription,

and thereby decrease p27 stability, by phosphorylating the p52 precursor p100 leading to its processing to p52, nuclear translocation as a RelB/p52 heterodimer, and exchange with the repressive p50/RelB dimer on the *SKP2* promoter (Schneider *et al.*, 2006). This model is supported by findings of Barré *et al* who observed p52/RelA dimer binding to the *SKP2* promoter during G_1 and S phases following release of the IKKβ subunit by AKT-mediated phosphorylation (Barre and Perkins, 2007). The difference in composition of the activating dimers reflects the complexity of NF-κB pathways. Regulated by a large number of stimuli in a cell context-dependent manner, functional differences are widely observed between the activator and repressor roles of the same NF-κB subunits.

IKKβ has also been shown to negatively regulate the Forkhead FOXO transcription factor FOXO3a, which inhibits SKP2-mediated cell cycle progression by transcriptional repression and disruption of the SCF^{SKP2} complex formation. This again links the PI3K/AKT pathway to SKP2 expression, which has been shown to target FOXO3a for inactivation (Hu *et al.*, 2004; Santo *et al.*, 2013; Wu *et al.*, 2013). Additionally the transcriptional repressor of the *HER2/ERBB2* oncogene in breast cancer Forkhead box P3, FOXP3, is a *SKP2* transcriptional repressor (Zuo *et al.*, 2007).

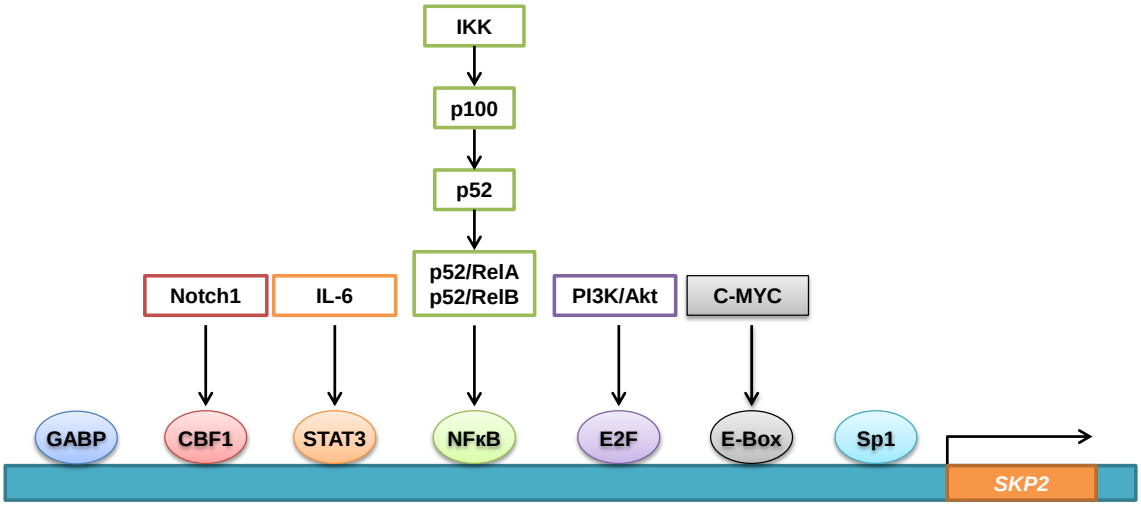

Figure 1.12 Schematic representation of transcription factors reported to regulate *SKP2* gene expression.

1.9.5. *SKP2 and pRB-mediated cell cycle progression*

The identification of functional E2F responsive elements in the *SKP2* promoter implicates pRB in the regulation of *SKP2* at the transcriptional level (Zhang and Wang, 2006). Given that the primary SKP2 target, p27, is a recognised negative regulator of cyclin E/A-CDK2 complexes, and that pRB phosphorylation by CDK2 is required for the E2F release, a positive feedback loop exists between the four components (Figure 1.13).

This interplay between SKP2 and pRB at both the transcriptional and protein levels emphasises the central role of SKP2 in the response to proliferative signals, and progression through the cell cycle towards mitogen independence.

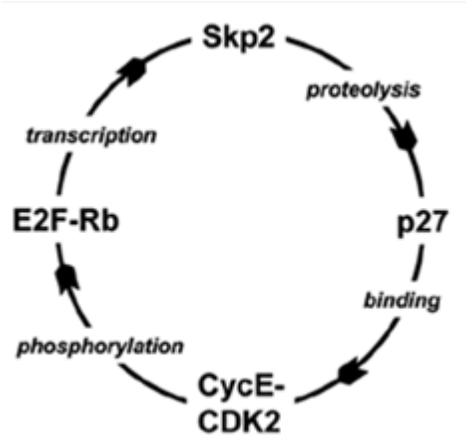

Figure 1.13. The SKP2 autoinduction loop. A positive feedback loop, upon mitogenic stimulation, cyclin D/CDK4/CDK6 complexes perform the initial phosphorylation of pRB allowing E2F1 dissociation and expression of E2F1-dependent genes such as SKP2 and cyclin E. SKP2 and cyclin E/CDK2 phosphorylate and ubiquitinate p27 promoting its degradation and allowing full activation of cyclin E/CDK2 complexes which further phosphorylate pRB enhancing E2F1-dependent gene induction (Ji *et al.*, 2004).

While E2F1 promotes *SKP2* activity, two consecutive E2F sites have been located in tandem with a TGF-β inhibitory site (TIE) on the *SKP2* promoter. This tandem E2F/TIE element is a known transcriptional repressor of *c-MYC* promoter function and has been shown to have a similar role in suppressing *SKP2* gene expression (Appleman *et al.*, 2006; Muth *et al.*, 2010). The pRB-E2F regulation of cell cycle dependent genes occurs by three modes: active induction, de-repression and active repression (reviewed by (Cobrinik, 2005), and the net

impact on *SKP2* expression is dependent on the combination of E2F-binding sites used, as well as the cell type and level of cell differentiation (Chong *et al.*, 2009).

Although pRB is capable of both activating and repressing *SKP2* activity, kinetic studies have demonstrated that the p27 accumulation observed during pRB-mediated G_1 arrest is independent of the repression of E2F targets (Ji *et al.*, 2004). As the outcome of gene regulation depends on the final protein expression levels, and pRB-E2F plays a crucial role in cell cycle progression, it is not surprising that pRB functions at a post-translational level. Direct interaction between pRB and the N-terminus of SKP2 has been demonstrated and found to disrupt SKP2-targeted degradation of p27 (Ji *et al.*, 2004), and the ability of pRB to cooperate with APC/C^{CDH1} in targeting SKP2 for proteasomal degradation (Binne *et al.*, 2007). Additionally the pRB pocket protein p107 has been found to regulate SKP2 proteolysis by a mechanism only partly reliant on the APC/C^{CDH1} complex (Rodier *et al.*, 2005). Together these additional faces of the pRB-SKP2 model highlight a functional cooperation between the two E3 ligases and pRB which contributes to pRB-mediated cell cycle progression, independent of E2F binding.

1.9.6. *Post translational modifications of SKP2*

As discussed in Section 1.8.1, SKP2 is periodically expressed throughout the cell cycle and targeted for proteasomal degradation by the APC/C^{CDH1} complex. Targeted by CDH1, which recognises the D-box in the SKP2 N-terminal domain (Bashir *et al.*, 2004; Wei *et al.*, 2004), post-translational modifications of SKP2 have been shown to disrupt this interaction increasing SKP2 stabilisation. Current literature has identified the phosphorylation of Ser72 by activated AKT as an important mechanism for the regulation of SKP2 stability and activity. Induced by a direct interaction between AKT and the N-terminus of SKP2 (Gao *et al.*, 2009; Lin *et al.*, 2009), Ser72 phosphorylation acts as a molecular switch which, in addition to its ability to increase SKP2 transcription, (Section 1.9.4), identifies PI3K/AKT signalling as a major regulatory pathway of SKP2 activity.

Ser72 phosphorylation has been shown to play a central role in the re-localisation of SKP2 to the cytoplasm and two mechanisms have been described. Firstly, SKP2 phosphorylation promotes binding to the 14-3-3 protein family member 14-

3-3β which regulates AKT-mediated trafficking across the nuclear membrane, and secondly phosphorylation disrupts the nuclear localisation sequence (NLS), inhibiting binding to the nuclear import receptors, importin α5 and α7 (Gao *et al.*, 2009; Lin *et al.*, 2009). Interestingly, restricting SKP2 to the cytoplasm has been found to promote cell migration, identifying an oncogenic role for overexpressed SKP2 independent of its E3 ligase activity as discussed in Section 1.10.3 (Lin *et al.*, 2009).

Contrasting molecular consequences of SKP2 phosphorylation by AKT have been observed. While Lin *et al* proposed that Ser72 phosphorylation is required for efficient SCF^{SKP2} complex formation (Lin *et al.*, 2009), Gao *et al* confirmed the previous observations that Ser72 modification primes SKP2 for phosphorylation on flanking sites Ser64 (by CDK2) and Ser75 (by casein kinase 1), (Rodier *et al.*, 2008). Phosphorylation of these residues was shown to stabilise SKP2 by disrupting its interaction with CDH1, and thus preventing its degradation by the APC/C^{CDH1} complex. However, the dual phosphorylation at Ser74 and Ser75 was more effective in inhibiting CDH1 binding, while Ser64 phosphorylation was found able to stabilise SKP2 in a CDH1 independent mechanism (Gao *et al.*, 2009).

Rodier *et al* did not find Ser72 phosphorylation a requirement for SCF^{SKP2} assembly and activity, however as the authors overexpressed all components of the SCF complex including CKS1, this may have favoured SCF^{SKP2} complex formation (Rodier *et al.*, 2008). Interestingly, although the N-terminal region of SKP2 is dispensable for the assembly of the SCF^{SKP2} complex (Schulman *et al.*, 2000), a SKP2 mutant lacking the N-terminal 90 amino acids was found to form the SCF complex more efficiently than full-length SKP2 (Lin *et al.*, 2009). Based on the model that Ser72 phosphorylation promotes a conformational change of the N-terminus to promote the interaction between SKP2 with SKP1, the phosphorylation of Ser72 may identify a mechanism to which the overexpression of SKP2, seen in human tumours, promotes aggressive proliferation following AKT-mediated phosphorylation (Ecker and Hengst, 2009; Lin *et al.*, 2009). Nonetheless, as CDH1 is more prevalent in the nucleus, the cytoplasmic re-localisation may ultimately play a larger role in SKP2 stabilisation than post-translational modification and structural inhibition.

A second post-translational modification of SKP2 which produces a similar outcome is acetylation. Building upon the known interaction between SKP2 and the transcriptional co-activator/acetyl-transferase p300, SKP2 has been shown to be acetylated at K68 and K71 within the NLS region (Inuzuka *et al.*, 2012). Negatively regulated by the deacetylase SIRT3, the sites are adjacent to Ser72 and acetylation has been shown to prevent the SKP2-CDH1 interaction and promote SKP2 translocation into the cytoplasm, independently of AKT-mediated phosphorylation (Inuzuka *et al.*, 2012).

1.10. SKP2 the proto-oncogene

SKP2 protein overexpression has been identified in a variety of human cancers and found to contribute to the malignant phenotype both as an E3 ligase and through molecular mechanisms independent of its F-box (Figure 1.14).

1.10.1. *Targeting p27 for degradation*

The majority of reports of SKP2 as an oncogenic protein are related to the negative regulation of the CDK inhibitor p27. In the absence of p27, mice have organ hyperplasia and grow ~20%-30% larger than wild-type animals. However, $p27^{-/-}$ mice rarely develop malignancies with exception of the thymus and pituitary glands, which have high endogenous levels of p27 (Blain *et al.*, 2003). A 'dose-dependent' or 'haploinsufficient' tumour suppressor, the loss of a single allele of p27 (*CDKN1B*) increases susceptibility to tumorigenesis in mice when challenged with either carcinogens or paired with oncogenes (Blain *et al.*, 2003; Bloom and Pagano, 2003). The contribution of p27 deficiency to tumorigenesis through enhancing proliferation or reducing apoptosis when $p27^{-/+}$ mice are crossed with $PTEN^{+/-}$ or $RB^{+/-}$ mice, respectively, in addition to the desensitisation to anti-mitogenic stimuli seen in p27 deficient human tumours, highlights the potential clinical benefits of restoring p27 levels (Park *et al.*, 1999; Di Cristofano *et al.*, 2001; Blain *et al.*, 2003). However, although low levels of p27 profoundly impact tumour progression and are associated with a poor prognosis, mutations and deletions of *CDKN1B* are seldom found and mRNA levels often stay constant, implying that the low levels are a result of decreased protein stability and increased degradation (Bloom and Pagano, 2003).

1.10.2. *SKP2 overexpression*

Amplification of the 5p13 locus containing the *SKP2* gene or increased expression of *SKP2* mRNA are only occasionally seen and are often associated with an advanced metastatic state, while increased SKP2 expression is often detected in early oncogenesis (Dowen *et al.*; Yokoi *et al.*, 2004). As previously discussed, a multitude of molecular pathways regulate SKP2 expression at the transcriptional and post-translational level, many of which are found to be constitutively active in human cancers (e.g. PTEN/PI3K/AKT, c-MYC, IL-6/STAT3). Consequently the overexpression of SKP2 is often due to a combination of enhanced *SKP2* gene activation and decreased CDH1- targeted degradation.

SKP2 overexpression has been detected in various types of cancers and directly correlates with tumour aggressiveness and poor prognosis (Hershko, 2008). There is often an inverse relationship between SKP2 and p27 levels, and SKP2 cooperation with H-Ras^{G12V} to promote neoplastic transformation is associated with reduced levels of p27, implying that it is the loss of the CDK inhibitor that promotes malignancy (Gstaiger *et al.*, 2001). Although promoting the accumulation of p27 forms the objective of the majority of inhibitor development programmes targeting SKP2, the importance of the SKP2-p27 axis has been shown to be cell type specific. As SKP2 regulates p27 levels to promote S phase transition and mitogen independence, a point of control that is regulated by multiple pathways, the importance of SKP2 and the impact of SKP2 inhibition is heavily dependent on the significance of p27 degradation on tumour incidence, progression and aggressiveness in each tumour type (Timmerbeul *et al.*, 2006).

Importantly, not all the over-replication characteristics in the *SKP2*$^{-/-}$mice were corrected by the dual knockout of p27, implying that secondary SKP2 targets could also contribute to its oncogenic function (Kossatz *et al.*, 2004).

1.10.3. *SKP2 cytosolic localisation and cell migration*

SKP2 overexpression has been linked to metastatic behaviour in several cancer types including prostate (Drobnjak *et al.*, 2003), breast (Signoretti *et al.*, 2002), melanoma (Rose *et al.*, 2011) and lymphoma (Yokoi *et al.*, 2004), which often

also correlates with increased SKP2 cytoplasmic immunostaining. Although the mechanism is not fully elucidated, the impaired migratory capacity of *SKP2*$^{-/-}$ MEFs compared to their wild-type counterparts suggests that SKP2 is involved in the migratory response (Lin *et al.*, 2009).

SKP2 cytoplasmic localisation induced by Ser72 phosphorylation and K68/K71 acetylation, as discussed in Section 1.9.6, has been shown to contribute to tumour cell migration. Expression of the KLKL acetylation-mimetic SKP2 mutant in *SKP2*$^{-/-}$ MEFs was associated with increased migration compared to wild-type SKP2 MEFs. Additionally, increased expression of E-cadherin was detected both in SKP2$^{-/-}$ MEFs and following the depletion of endogenous SKP2 in a range of epithelial carcinoma cell lines. An important protein which mediates cell-cell adhesion, SKP2 is reported to modulate E-cadherin stability by targeting it for degradation once phosphorylated by casein kinase 1 (CK1) (Inuzuka *et al.*, 2012).

A second model for SKP2-mediated cell migration and metastasis implicates SKP2 in the transcriptional activation of RhoA. A member of the Ras superfamily, Rho GTPases are involved in cancer cell motility by inducing the reorganisation of the actin cytoskeleton (Sahai and Marshall, 2002). Although RhoA transcription is ultimately induced by c-MYC binding to E-box motifs within the proximal promoter, it has been suggested that c-MYC recruits SKP2 to form a MYC-SKP2-MIZ1 transcriptional complex which orchestrates increased RhoA expression and thus enhanced motility (Chan *et al.*, 2010a). Furthermore, p27 has been shown to regulate cell motility by binding to RhoA thus preventing it from interacting with its downstream effectors (Besson *et al.*, 2004). SKP2 overexpression would therefore target RhoA both at the transcriptional and post-translational level, and this interplay has been observed in the regulation of cell motility in gastric cancer cell lines by the IL-6/JAK/STAT3 pathway. Interleukin-6 (IL-6) induced STAT3 activity regulates multiple aspects of cancer development and progression, and is a well-established facilitator of increased invasion and metastasis (Teng *et al.*, 2014). A direct transcriptional target of STAT3 (Section 1.9.4) (Huang *et al.*, 2012), SKP2 links the IL-6/JAK/STAT3 pathway with RhoA activity, as the STAT3-mediated upregulation of SKP2 results in decreased p27 and increased RhoA activity (Wei *et al.*, 2013).

1.10.4. *SKP2 and apoptotic cell death*

Although the oncogenic role of SKP2 is primarily associated with its ability to target proteins for degradation, many of which are established tumour suppressors, there is a growing body of literature describing an oncogenic function for SKP2 independent of its E3 ligase activity. One such mechanism is the involvement of SKP2 in the regulation of apoptosis. The depletion of SKP2 by siRNA or antisense oligonucleotides has been shown to induce apoptosis in several cancer cell lines (Cobrinik, 2005; Jiang *et al.*, 2005a). However, only recently have the molecular mechanisms by which SKP2 suppresses apoptosis started to be understood. The evasion of apoptosis is one of the main hallmarks of cancer development and is often associated with the loss of function of one or both of the two major tumour suppressors, p53 and pRB (Hanahan and Weinberg, 2011), both of which have been shown to have their functional activity modulated by SKP2.

The antiproliferative effects of p53 are exerted through its ability to act as a transcription factor. Often activated by post-translational modifications, the p53-cofactor p300 stimulates transcriptional activity by transferring acetyl groups to conserved lysine residues within the C-terminus subsequently activating p53 DNA-binding (Gu and Roeder, 1997; Gu *et al.*, 1997; Lill *et al.*, 1997). Kitagawa *et al* found that although SKP2 does target p300 for degradation, this role was secondary to the disruption of the p300-p53 interaction. SKP2 directly binds to p300 through the same CH1 and CH3 domain as p53, thereby antagonising the p53-p300 interaction and suppressing p53-mediated cell cycle arrest and apoptosis (Kitagawa *et al.*, 2008). Interestingly, SKP2 deficiency has also been shown to induce senescence in an ARF-p53 independent manner in *ARF*$^{-/-}$ mice and in *PTEN*-deficient prostate, although the authors emphasized the requirement for the SKP2 inactivation to be paired with an oncogenic stress to induce senescence, which was found to be dependent upon the levels of induction of p27, p21 and the activating transcription factor Atf4 (Lin *et al.*, 2010a). Additionally the SKP2 isoform SKP2B, which differs at the C-terminal domain (Radke *et al.*, 2005), is reported to promote the degradation of the potential tumour suppressor protein prohibitin (Chander *et al.*, 2010). Thought to be involved in both cell proliferation and apoptosis, depending on its cellular location,

nuclear prohibitin has been shown to enhance p53-mediated transcriptional activity while repressing E2F1 activity.

In contrast to the p53 pathway which is activated by oncogenic stress, pRB is regulated by phosphorylation, and when active (i.e. hypo-phosphorylated) is often associated with induction of senescence or a G_1 arrest rather than apoptosis. Recently studies have found that the ability of pRB to maintain p27 stability plays an important role in the capacity of pRB to both arrest cells in G_1 and induce cellular senescence (Ji *et al.*, 2004; Binne *et al.*, 2007). Deleting *SKP2* in pRB-deficient cells (*Rb1*$^{+/-}$*Skp2*$^{-/-}$) was found to prevent pituitary tumorigenesis in mice by inducing apoptosis identifying a synthetically lethal interaction which could be targeted to treat RB-deficient tumours (Wang *et al.*, 2010a).

The interplay between p53 and pRB in the response to SKP2 depletion conforms to the existing paradigm whereby p53 is activated in response to pRB-deficiency (Wang *et al.*, 2010a) and conversely, that pRB is activated by p53-deficiency (Lin *et al.*, 2010a). Zhao *et al* demonstrated a p27 safeguarding response where *SKP2* deletion in pRB/p53 doubly deficient tumours established a lasting mitotic block due to the accumulation of p27 protein which subsequently developed into apoptotic cell death (Zhao *et al.*, 2013). This effect of p27 stabilisation has previously been observed in *SKP2*$^{-/-}$ mouse models, where chromosome over-duplication as a result of the accumulation of cyclin E and p27 in *SKP2*$^{-/-}$ MEFs triggered apoptotic cell death (Nakayama *et al.*, 2000). These data suggest that specifically targeting p27 degradation mechanisms would be more effective than targeting SKP2 alone; however, p27 is known to both promote and inhibit apoptosis depending on the cell type and environmental factors (Drexler, 2003). It would therefore be important to first determine the contribution of p27 to tumour progression in each tumour type.

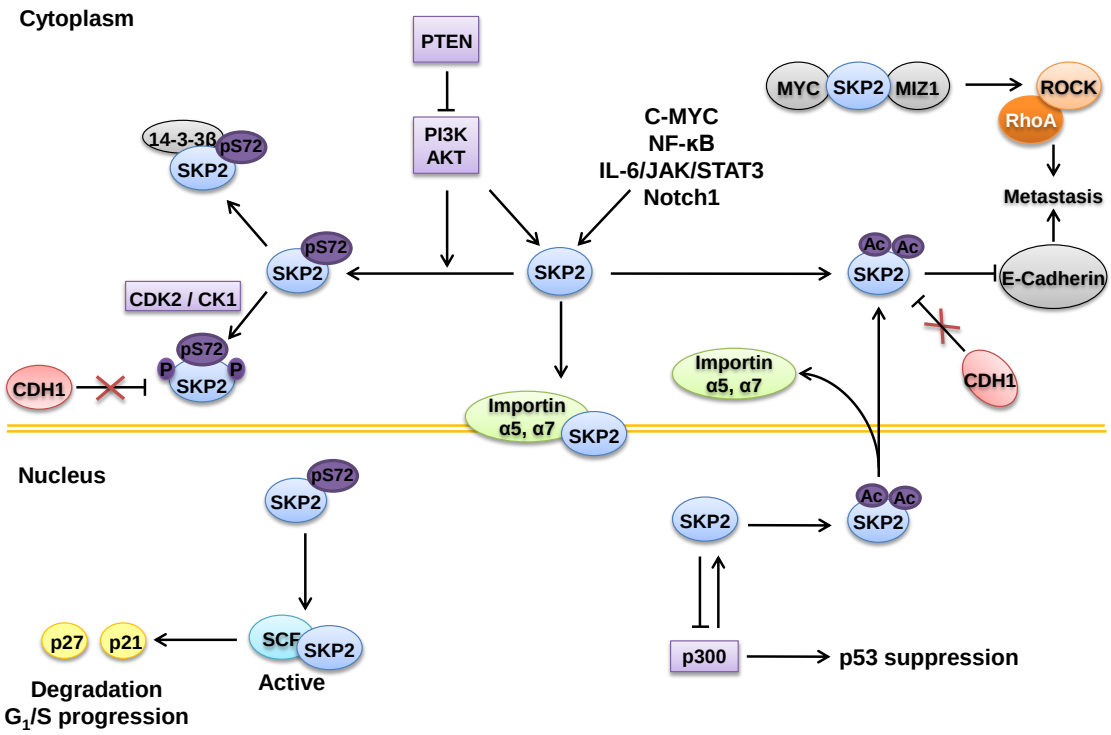

Figure 1.14 Summary of key potential mechanisms by which SKP2 can be overexpressed and potentiate tumour development

1.11. SKP2 in Neuroblastoma

The oncogenic function of SKP2 in neuroblastoma is primarily associated with its role in the ubiquitination and degradation of p27. The mRNA and protein level of p27 is of clinical relevance to the progression of neuroblastoma, and p27 levels have been shown to be predictive for long-term survival and decreased metastasis in neuroblastoma patients (Bergmann *et al.*, 2001; Koomoa *et al.*, 2013). Consequently, p27 accumulation has been associated with a favourable response to treatment in neuroblastoma cell lines with increased p27 levels shown to; prevent chromosomal instability following DNA damage (Sugihara *et al.*, 2006), induce retinoic acid-mediated cell cycle arrest (Nakamura *et al.*, 2003), and play a key role in the potency of the ODC1 inhibitor alpha-difluoromethylornithine (DFMO) towards G_1 arrest and tumour migration (Koomoa *et al.*, 2013).

SKP2 overexpression has previously been observed at the mRNA and protein level in neuroblastoma clinical samples, and is related positively with tumour aggressiveness and inversely with p27 levels. Identifying high risk neuroblastoma independently of established prognostic indicators (e.g. *MYCN* amplification 1p

deletion, 17q gain), the higher levels of SKP2 mRNA and protein found in *MYCN* amplified compared to non-amplified tumours suggests that a regulatory relationship exists between MYCN and SKP2 (Westermann *et al.*, 2007). This suggestion is supported by studies which have found higher SKP2 levels in the presence of ectopic MYCN expression and in *MYCN* amplified cell lines (Sugihara *et al.*, 2006; Bell *et al.*, 2007; Westermann *et al.*, 2007; Muth *et al.*, 2010). Moreover, SKP2 has recently been characterised as a c-MYC target gene confirming the existence of E-box motifs within the *SKP2* promoter (Bretones *et al.*, 2011). Given the overlap often found between target genes of the MYC family members, these previous findings suggest that SKP2 is a candidate gene for direct MYCN regulation in neuroblastoma.

The exact role of SKP2 overexpression in *MYCN* amplified neuroblastoma is not fully understood, yet both genes have been shown to drive uncontrolled proliferation and regulate p53-mediated apoptosis (Kitagawa *et al.*, 2008; Chen *et al.*, 2010b). MYCN-driven deregulated SKP2 expression may therefore attenuate apoptotic cell death as seen for c-MYC (Bretones *et al.*, 2011). However, SKP2 protein expression levels do not correlate with *MYCN* expression in *MYCN* amplified or non-amplified cell lines (Westermann *et al.*, 2007). Furthermore although low p27 expression has been reported to inversely correlate with SKP2, it is of prognostic importance in neuroblastoma independent of *MYCN* status (Bergmann *et al.*, 2001). The role of SKP2 in neuroblastoma pathogenesis may therefore range from being an independent driving force to an essential MYCN-driven mechanism.

1.11.1. *The regulation of SKP2 by c-MYC and MYCN*

Like many transcription factors both c-MYC and MYCN are rapidly turned over by the ubiquitin proteasome pathway. Recently, SKP2 has been shown to participate in the ubiquitin/proteasome-mediated degradation of c-MYC. In a yeast-based screen, Kim *et al* took advantage of the destruction of mammalian c-MYC expressed in *Saccharomyces cerevisiae* by Ub-mediated proteolysis. Through a series of mutations inhibiting the function of different components of the ubiquitin proteasome system, it was found that c-MYC was stabilised in yeast cells lacking Grr1, the yeast ortholog of SKP2 (Kim *et al.*, 2003). This evidence was supported by similar findings from von der Lehr *et al*, confirming that SKP2 participates in c-

MYC degradation. Interestingly, this interaction between c-MYC and SKP2 was also found to stabilise the transcription factor and enhance c-MYC regulated transcription and S-phase entry (von der Lehr *et al.*, 2003). Surprisingly, the interaction and coactivator ability of SKP2 was observed to be dependent upon the presence of the SKP2 F-box motif, implying that the E3 ligase activity plays a role; however, the effect was shown to be independent of p27 degradation or phosphorylation of c-MYC (von der Lehr *et al.*, 2003). SKP2 recruits c-MYC to the SCF^{SKP2} complex by interacting with the N-terminal MYC Box 2 (MB2) and a region within the C-terminal BHLH-Zip domain. As both these regions are required for the transcriptional regulation and oncogenic potential of c-MYC these results indicate that SKP2 plays a critical role in the oncogenic potential of c-MYC by acting a transcriptional cofactor (Kim *et al.*, 2003; von der Lehr *et al.*, 2003). Although the authors were unable to show ubiquitination and degradation of c-MYC occurred at the promoter, the removal of the SKP2 F-box repressed c-MYC induced transcription. These findings therefore suggest that the E3 ligase activity of SKP2 is essential for its coactivator function, supporting the hypothesis that there is a close relationship between the activities of transcription factors and their ubiquitination and degradation.

Moreover SKP2 has been identified as a direct c-MYC target gene, inducing SKP2 accumulation and subsequent p27 degradation in a CML model. Interestingly, c-MYC was also shown to promote the phosphorylation of p27 on the Thr187 residue required for SKP2 recognition through its ability to up-regulate CDK2 and cyclin A and E, therefore reinforcing the importance of c-MYC in controlling p27 levels (Bretones *et al.*, 2011).

Several studies have observed higher *SKP2* expression in the presence of MYCN in neuroblastoma tumours and cell lines (Bell *et al.*, 2007; Muth *et al.*, 2010). The mechanism of MYCN-mediated up-regulation of SKP2 is not fully understood but one report identifies SKP2 as an indirect target of MYCN (Muth *et al.*, 2010). As *SKP2* is a confirmed E2F2 gene target the authors suggested that deregulated SKP2 expression is through the induction of the direct MYCN target gene product *CDK4*, which promotes the SKP2 auto-induction loop by increasing pRB phosphorylation and E2F1 abundance, which consequently decreases the level of repressive pRb-E2F1 complexes on the *SKP2* promoter (Muth *et al.*, 2010).

However, taking into account the recent mapping of two high affinity E-boxes on the *SKP2* promoter to which c-MYC can bind, and the aforementioned homology within the *MYC* family, it is possible that *SKP2* is in fact a direct target of MYCN.

Transcript profiling has established *SKP2* as a prognostic indicator of high risk, aggressive disease independent of the *MYCN* status and disease stage (Westermann *et al.*, 2007). Nevertheless, two independent gene expression microarray analyses have identified an effect on *SKP2* levels from differential *MYCN* expression, with both studies showing an increase in *SKP2* in the presence of *MYCN* (Bell *et al.*, 2007; Muth *et al.*, 2010). Amongst other characteristics, deregulated *MYCN* expression is well known to accelerate cell proliferation by shortening the G_1 phase of cell cycle (Lutz *et al.*, 1996). Several studies have suggested that the enhanced transition into S phase induced by MYCN is in part a result of the reduced expression of cell cycle related genes such as p27 and p21, as their function has been reported to be antagonised by c-MYC (Charron *et al.*, 1992; Wei *et al.*, 2004; Guglielmi *et al.*, 2014). However further research into the relationship between MYCN and p27/p21 implies that high MYCN expression alone is not responsible for their repressed levels (Bell *et al.*, 2006; Guglielmi *et al.*, 2014). As both p27 and p21 are targeted by the SCF^{SKP2} complex for degradation the hypothesised direct regulation of SKP2 by MYCN may contribute to the aggressive phenotype of *MYCN*-amplified tumours.

1.12. Pharmacological inactivation of SKP2

The prognostic significance and potential oncogenic role of SKP2 in several human malignancies, in contrast to its restricted role in mouse development, has led to the classification of SKP2 as a cancer-cell specific drug target. Taken with the observation that SKP2 knockdown only promotes senescence, apoptosis and autophagy in the presence of an oncogenic event, and that SKP2 knockout mice are both viable and fertile, SKP2 inhibition has the potential to be tumour cell specific (Lin *et al.*; Chen *et al.*, 2008a; Kitagawa *et al.*, 2008). Although small molecules which indirectly disrupt SKP2 activity have been developed in an attempt to restore p27 levels, as discussed in Chapter 5, no specific SKP2 inhibitors are currently available. The crystal structure of the SCF^{SKP2} complex identifies interfaces between p27 and SKP2-CKS1, offering the possibility of compounds designed to directly interact with these interfaces in order to inhibit

SKP2-mediated p27 degradation. Ubiquitination of p27 is prevented by introducing a point mutation at Glu185 or Thr187 (Hao *et al.*, 2005), and this site together with clefts at the CKS1-SKP2 interface could be exploited by small molecular inhibitors to disrupt the SKP2-p27 interface (Hao *et al.*, 2005).

Protein-protein interactions are often described as 'undruggable'; however, advances in drug discovery approaches and techniques have opened up new possibilities (as reviewed by (Nero *et al.*, 2014)). In a recent report, Chan *et al* identified candidate compound SZL-P1-41 (compound #25) which specifically inhibited SKP2 activity by blocking the SKP1-SKP2 interaction (Chan *et al.*, 2013). By utilizing virtual high-throughput screening, clusters of residues along the SKP2-SKP1 interaction surface were first identified on the basis of their contribution to the overall binding energy. Termed 'hot spots', a library of potential small molecule inhibitors was then searched, and evaluated for their interaction with the drug target. A knowledge driven approach, virtual-ligand screening (VLS) utilises previously collected information on the 3D structure of the target to establish an understanding of the spatial and energetic criteria required for the interaction. A computational or in silico method, potential inhibitors can then be screened, predictions made based on their calculated binding affinities for the 'hot spots', and lead compounds identified for biological screening and experimental validation (Klebe, 2006). A study has recently utilised this approach to identify inhibitors of the SKP2-CKS1 interface (Wu *et al.*, 2012b), enhancing the specificity to only SKP2 targets which require CKS1 (i.e. CDK inhibitors p27, p21 and p57). Taken together with the small molecule inhibitors identified by Chan *et al*, these studies illustrate potential approaches to specifically target SKP2 activity.

1.13. Summary

MYCN amplified neuroblastoma is a highly aggressive sub-type of disease which has proven difficult to treat successfully. Consequently, downstream effectors of MYCN are being investigated as potential therapeutic targets. SKP2 overexpression is observed in several malignancies including neuroblastoma where it is associated with *MYCN* amplification, suggesting a potential mechanistic link. The substrate recognition factor for the SCF^{SKP2} E3 ligase complex, SKP2 is an important regulator of the G_1/S cell cycle transition, primarily

through its ability to target the CDK inhibitor p27 for degradation. Often correlating directly with tumour progression and inversely with p27 stability, SKP2 is a well-established oncoprotein whose inactivation while compatible with life, has been shown to trigger cell-type specific G_1 arrest, senescence and apoptotic cell death. The present study aims to further validate SKP2 as a potential therapeutic target in neuroblastoma by determining whether it is directly regulated by MYCN, and exploring its role in cancer cell proliferation and survival to inform the discovery and development of SKP2 inhibitors.

1.14. Hypothesis and Aims

Hypothesis:

SKP2 promotes cancer cell proliferation and survival in neuroblastoma identifying it as a potential therapeutic target.

Aims:

1. To determine whether SKP2 is a direct transcriptional target gene of MYCN.

2. To validate SKP2 as a therapeutic target using a panel of neuroblastoma cell lines, and determine whether *MYCN* amplification or *p53* status influence sensitivity to SKP2 inhibition.

3. To investigate the potency and specificity of commercially available and novel compounds reported or designed to directly or indirectly target SKP2.

Chapter 2.
Materials and Methods

2.1. Tissue culture

All neuroblastoma cell lines used in this study were routinely confirmed to be mycoplasma negative using the Mycoalert® detection kit (Lonza, Basel, Switzerland). All tissue culture was carried out using aseptic technique in class II contamination hoods (Biomat2, MedAir® Inc. MA, USA). A list of the neuroblastoma cell lines used in this study is shown in Table 2.1. The conditional MYCN expressing SHEP Tet21N cells and SKNAS-Nmyc-ER cells are discussed in detail in Section 2.2.

2.1.1. *Propagating neuroblastoma cell lines*

All cell lines were grown in RPMI 1640 growth medium with 10% (v/v) foetal bovine serum (FBS) (Sigma, St Louis, MO, USA), 100 units/ml penicillin and 100 µg/ml streptomycin (Sigma) unless otherwise stated. All cell lines were grown at 37°C in 5% CO_2 in a humidified incubator and passaged once 60-70% confluent. The growing surface of the flask was washed with 10 ml sterile PBS and the cells detached by incubation at room temperature with 2 ml of 1x trypsin-EDTA (Sigma). Once the cells were dislodged the trypsin was neutralised using 8 ml of full media and the resulting cell suspension used to seed new flasks at the desired cell density.

2.1.2. *Resurrecting cell lines from liquid nitrogen stocks*

Cells were removed from liquid nitrogen storage and thawed in a 37°C waterbath. The cell suspension was transferred to a sterile universal container and centrifuged at 500 x g for 5 minutes at room temperature, after which the supernatant containing dimethyl sulphoxide (DMSO) was removed and the cell pellet resuspended in 6 ml of fresh full media, previously warmed to 37°C, and transferred to a 25 cm^2 flask (Corning Incorporated, Corning, NY, USA) and incubated at 37°C, 5% CO_2 in a humidified incubator.

Cell Line	Morphology	MYCN Status	*p53* Status	Reference
SHSY5Y	N-type	-	WT	(Biedler *et al.*, 1973)
GIMEN	S>N	-	WT	(Cornaglia-Ferraris *et al.*, 1990)
SHEP	S-Type	-	WT	(Biedler *et al.*, 1978)
SKNAS	S-Type	-	Mutant[1]	(Goldschneider *et al.*, 2006a)
SKNAS-NmycER	N-Type	-	Mutant[1]	(Valentijn *et al.*, 2005)
SK-N-BE(2c)	I-Type	+	Mutant[2]	(Biedler *et al.*, 1973)
IMR-KAT100	N-Type	+	Mutant[3]	(Xue *et al.*, 2007)
IMR32	N-type	+	WT	(Tumilowicz *et al.*, 1970)
LAN5	N-type	+	WT	(Seeger *et al.*, 1982)
SHEP-TET21N	S-type		WT	(Lutz *et al.*, 1996)

Table 2.1 Morphology, *MYCN* and *MDM2* amplification and *p53* status for the panel of neuroblastoma cell lines used in this study. **1** Mutation from alternative splicing downstream of exon 9; leads to truncated β-isoform. 2 Missense mutation at exon 5, codon 135; TGC (cysteine) to TCC (phenylalanine).3 Selected for resistance to potassium antimony tartrate (KAT) leading to point mutation at codon 135 (exon 5); TGC (cysteine) to TCC (phenylalanine). (-) non-amplified, (+) amplified and WT: wildtype.

2.1.3. *Freezing down cells for storage in liquid nitrogen*

For cell stocks a 75 cm^2 flask of cells at ~70% confluency were frozen down. Adherent cells were detached according to Section 2.1.1, centrifuged at 500 x g and resuspended in 10 ml freezing media containing 10% DMSO (v/v) (Sigma, Tissue culture grade), 10% FBS (v/v) and 80% growth media (10% FBS v/v). Cell suspension was aliquoted into cryogenic vials (NUNC™, Rochester, NY, USA) and stored at -80°C for 24 hrs prior to transfer to liquid nitrogen stores.

2.1.4. *Cell counting*

The concentration of cells after detachment was determined using a haemocytometer (Hawksley, Sussex, UK). The cells were dispersed by passage

through a 5 ml COMBITIP® PLUS syringe (Eppendorf, Cambridge, UK) and ~10 µl of cell suspension drawn under the coverslip of the haemocytometer by capillarity action. The haemocytomter has 2 grids for scoring cells, each 1 mm^2 (area) x 0.1 mm (depth). The liquid of 0.1 mm depth covering the 1 mm square therefore has a volume of 10^{-4} ml (0.1 cm x 0.1 cm x 0.01 cm). To calculate the number of cells/ml, the average number of cells from 2 central grids was first calculated and then multiplied by 10^4.

48 cell in counting area = 48 cells per 10^{-4} ml = $48/10^{-4}$ cells per ml = 48 x 10^4 cells per ml).

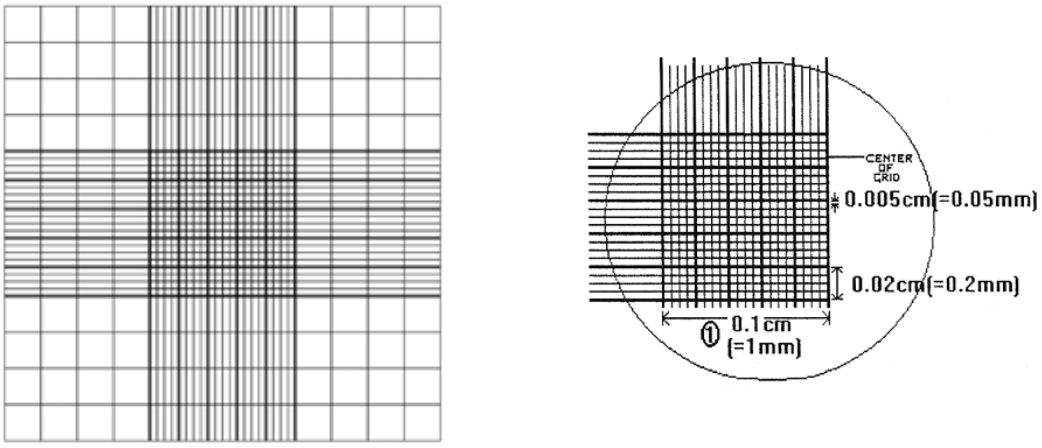

Figure 2.1 Grid layout of the hemocytometer

2.2. MYCN regulatable cell lines

2.2.1. *SHEP Tet21N MYCN expression system*

The SHEP-Tet21N MYCN expression system allows the effect of conditional MYCN expression to be investigated by using a synthetic inducible expression system based around the tetracycline repressor of *E coli*. Stably transfected into the S-type SHEP cells which normally express low levels of *MYCN* mRNA and no detectable protein levels, the expression of MYCN can be controlled through the addition or removal of tetracycline (Lutz *et al.*, 1996).

2.2.2. *Principles of Tet-OFF system*

The Tet-Off system utilises the regulatory elements of the Tn*10*-specified tetracycline-resistance operon of *E. coli* where resistance to the antibiotic tetracycline is negatively regulated by the tetracycline repressor (*tet*R). *Tet*R blocks the transcription of tetracycline resistant genes by binding to the *tet* operator sequences (*tetO*). Upon addition of tetracycline *tet*R is prevented from binding the *tet*O allowing gene activation (Gossen and Bujard, 1992).

By fusing the *tet*R to the C-terminal domain (activation domain) of the VP16 protein found in the Herpes Simplex Virus (HSV), the TetR is converted from a transcriptional repressor to a hybrid transcriptional activator (tTA) which can activate promoters fused to specific *tet*O sequences resulting in an increase in gene expression up to 10^5-fold (Gossen and Bujard, 1992).

In order to express the gene of interest, several identical tetO sequences are placed upstream of a minimal CMV promoter (P_{minCMV}) forming the tetracycline response element (TRE). Therefore, under regular culture conditions the tTA will bind to the specific tetO sequences within the TRE promoting the expression of the gene of interest. Following the addition of tetracycline the TRE-controlled genes are repressed as tetracycline binds to the tTA rendering it incapable of binding the TRE sequences, thereby preventing the transactivation of the gene of interest (figure 2.2).

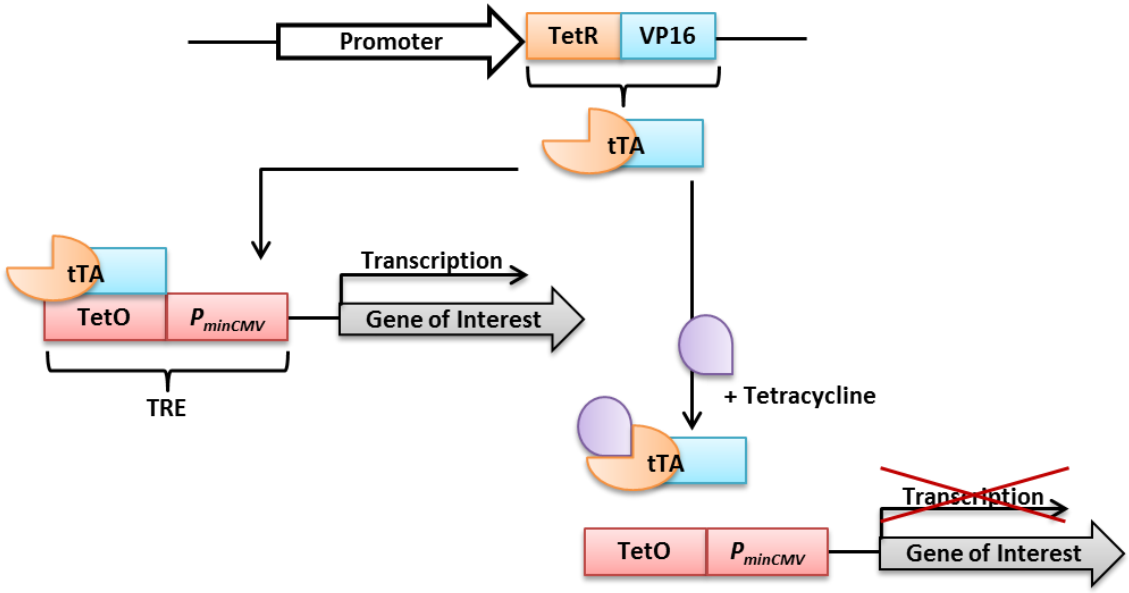

Figure 2.2 The Tet-OFF system

2.2.3. *Generation of SHEP-Tet21N MYCN regulatable cells*

The Tet-OFF SHEP Tet21N cells were originally generated by Lutz et al. (1996). In brief, SHEP cells were first co-transfected with the pUHD15-1 plasmid containing the Tet-responsive reporter units (tTA) and the pSV2neo plasmid which provided neomycin resistance and allowed selection by treatment with G418 sulphate. The clones were then co-transfected with the pUHD10-3/*MYCN* plasmid which had previously had the *MYCN* sequence cloned into the *Eco*R1 site, and the pHMR272 plasmid allowing selection by hygromycin (Figure 2.3). Addition of G418 sulphate and hygromycin in the growth media therefore selected and maintained the growth of transfected clones which expressed MYCN only in the absence of tetracycline (Lutz *et al.*, 1996).

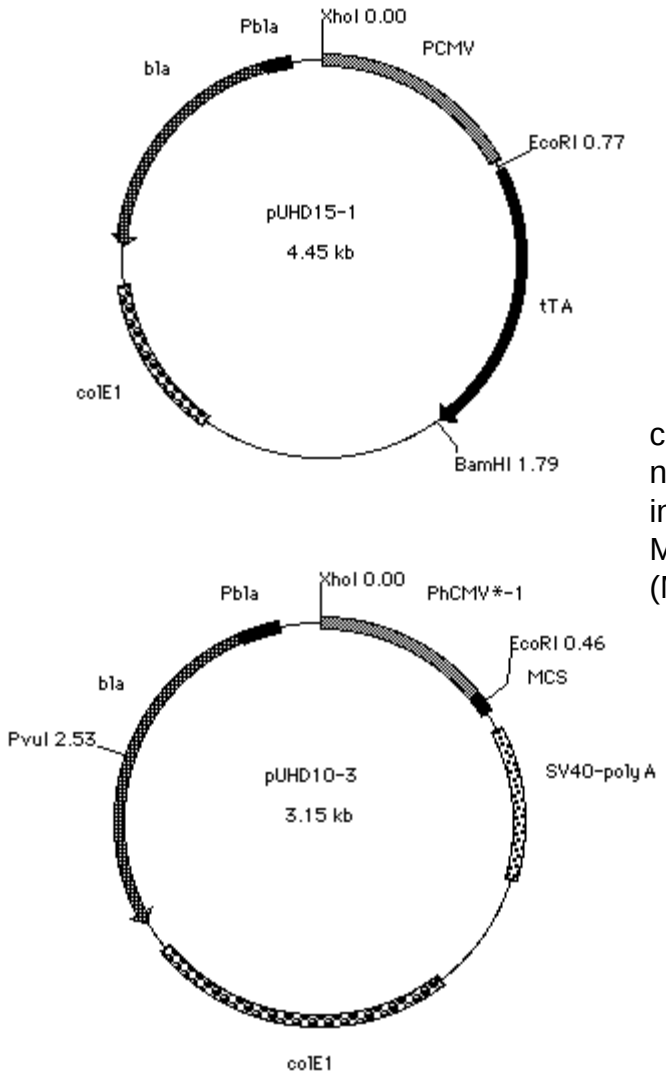

Figure 2.3 Plasmid maps of a. pUHD15-1 and b. pUHD10-3 used to generate the Tet21N cell line (http://www.zmbh.uni-heidelberg.de)

2.2.4. *Culturing of SHEP-Tet21N MYCN regulatable cells*

The SHEP-TET21N cell line was grown in RPMI 1640 growth medium with 10% (v/v) FBS (Sigma) and 200 µg/ml G418 sulfate (Calbiochem, Darmstadt, Germany) at 37°C in 5% CO_2 in a humidified incubator and passaged once 60-70% confluent. Cells were cultured in the presence of 1 µg/ml tetracycline (Sigma) for a minimum of 24 hrs to switch off MYCN expression.

2.2.5. *SKNAS-NmycER cell line*

The SKNAS-NmycER cell line was generated by stably inserting the NmycER chimeric protein into the non-*MYCN* amplified, p53 mutant SKNAS cell line. The C-terminus of mouse MYCN protein is fused to the hormone binding domain

(HBD) of a transcriptionally inactive oestrogen receptor. Harbouring a point mutation (G525R) the receptor is unable to bind to oestrogen yet retains normal sensitivity to the synthetic ligand 4-hydroxytamoxifen. The ability of MYCN to transcriptionally activate its target genes is therefore dependent on the presence of 4-hydroxytamoxifen to promote the movement of MYCN from the cytoplasm into the nucleus (Littlewood *et al.*, 1995).

2.2.6. *Generation of the SKNAS-NmycER cell line*

The SKNAS-NmycER cell line was generated using a pBABEpuro retrovirus vector which contained a puromycin resistance gene and the Nmyc-ER chimeric protein construct. Based on the previous construction of the c-MycER construct a *Bam*HI site was created using PCR at the 5' end of a tamoxifen mutant oestrogen receptor to facilitate the fusion of the MYC protein. The fusion protein was subsequently cloned into a retroviral vector through the generation of an *Eco*RI fragment containing the MycER construct (Figure 2.4) (Littlewood *et al.*, 1995). The retroviral vector pBABEpuro-myc-ER was then transfected into the SKNAS cells by retrovirus transduction, and stable transfectants selected and maintained by continuous exposure to puromycin (Tang *et al.*, 2006a).

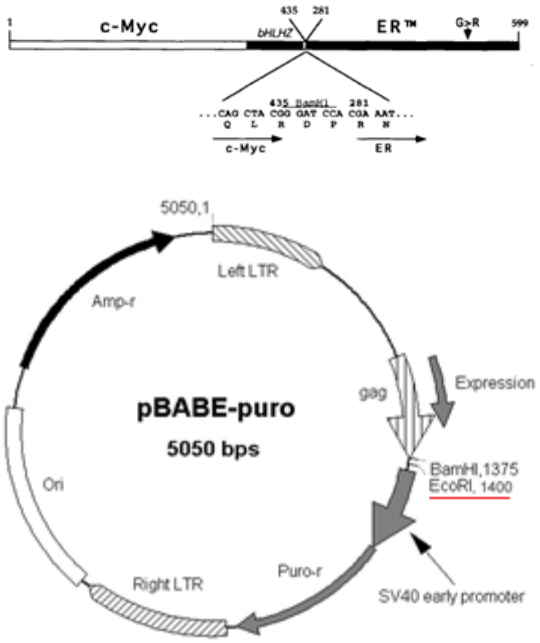

Figure 2.4 Construction of the c-MycER™ chimeric protein and plasmid map of pBABE-puro used to generate the SKNAS-NmycER cell line. The mutant hormone binding domain of the oestrogen receptor containing a single amino acid change from glycine to arginine at position 525 was fused to the C-terminal of human c-Myc to form the c-MycER construct (Littlewood *et al.*, 1995). The *Eco*RI site in which the N-MycER construct is inserted is highlighted (www.addgene.org)

2.2.7. *Culturing the SKNAS-NmycER cell line*

The SKNAS-NmycER cell line was grown in DMEM growth medium with 10% (v/v) FBS (Sigma) and 1 µg/ml puromycin at 37°C in 5% CO_2 in a humidified incubator and passaged once 60-70% confluent. Cells were cultured in the presence of 100 ng/ml 4-hydroxytamoxifen to switch on the transcriptional activity of MYCN.

2.2.8. *Advantages and disadvantages of the MYCN regulatable cell lines*

A number of systems can be employed to control transgene expression in mammalian cells. The Tet-OFF and ER system have tight control over gene expression which is also reversible, unlike knock-out or knock-in systems such as Cre-*lox* recombination were the effect on gene expression is irreversible. The Tet system and ER system are highly sensitive to their corresponding activator molecules and have both been used to study MYCN target genes upon MYCN modulation (Bell *et al.*, 2007; Valentijn *et al.*, 2012). Although, as the Tet-OFF

system represses the transcription of a gene, it will have a slower response time than the ER system which stabilises an already expressed protein inducing its activity, the mutation in the ER fused to MYCN also possesses very low affinity for 17β-oestradiol preventing the activation of the ER-fusion protein by endogenous oestrogen (Littlewood *et al.*, 1995). As the SKNAS cell line harbours a *p53* mutation, the SKNAS-NmycER cell line allows further investigation of the role of MYCN in cell proliferation and apoptosis independent of the p53 pathway.

The main disadvantage of SHEP-TET21N and SKNAS-NMycER cells is the histology of their parental cell lines. Both SHEP and SKANS cells are S-type subclones of the SK-N-SH cell line which have been shown to be the least tumorigenic and to have lower levels of MYCN expression compared to other cell types (Carr-Wilkinson *et al.*, 2011). The induction of MYCN expression may therefore not provide data directly relevant to a *MYCN* amplified cell line. However, for the Tet21N cells, the level of MYCN mRNA and protein expression has been reported to be comparable to that in the *MYCN* amplified cell lines IMR32, CHLA-136 and PER-108. Furthermore the cells respond to DNA damage in a similar manner in the absence of tetracycline (Tet21N MYCN+) (Bell *et al.*, 2006). Additionally, both SHEP and SKNAS cells harbour $p14^{ARF}$ deletions which may provide a selective growth advantage (Dreidax *et al.*, 2013).

2.3. Cycloheximide treatment of the SHEP-Tet21N MYCN regulatable cell line

Cycloheximide is an inhibitor of protein synthesis in eukaryotes. An anti-fungal antibiotic, it interferes with translational elongation and can be used to study the stability of proteins. Cycloheximide (Calbiochem) was prepared at a 200 nM stock solution in 100% ethanol and stored at -20°C for a maximum of one month. Cycloheximide was diluted in cell culture media prior to use to a final concentration of 25 µM and cells treated for the time periods stated.

2.4. RNA Interference

RNA interference via small interfering RNA (siRNA) is a cellular process that can be used to control gene expression in eukaryotic cells. A type of post-transcriptional gene silencing, the siRNA hybridizes to its complementary sequence within the target mRNA initiating its degradation, and therefore preventing protein expression. By exploiting this pathway, the expression of chosen genes can be 'knocked down' through use of appropriately designed synthetic siRNAs (Elbashir *et al.*, 2001a).

2.4.1. *The mechanism of siRNA*

siRNAs are 20-25 nucleotide-long non-translated double-stranded RNA (dsRNA) duplexes, with phosphorylated 5' ends and hydroxylated 3' ends, which have symmetric 2-3 nucleotide overhangs. Formed following the cleavage of long dsRNAs, catalysed by the RNA endonuclease Dicer enzyme, the siRNA molecules are then incorporated into a multiprotein RNA-inducing silencing complex (RISC). One essential component of the RISC is the argonaute family of proteins which act as the main catalytic components. Once the 3' overhang of the siRNA is exposed, the RNA strand with the least thermodynamically stable 5' end is selected by the argonaute protein, the siRNA is unwound, and the chosen strand fed into the RISC complex. With the partner strand then degraded the chosen 'guide strand' is used as a template to recognise complementary mRNA molecules. mRNA strands which display extensive complementarity to the guide strand are then fragmented by activated endonucleases, within the argonaute protein family, ensuring translation cannot take place and therefore preventing protein expression (Figure 2.5).

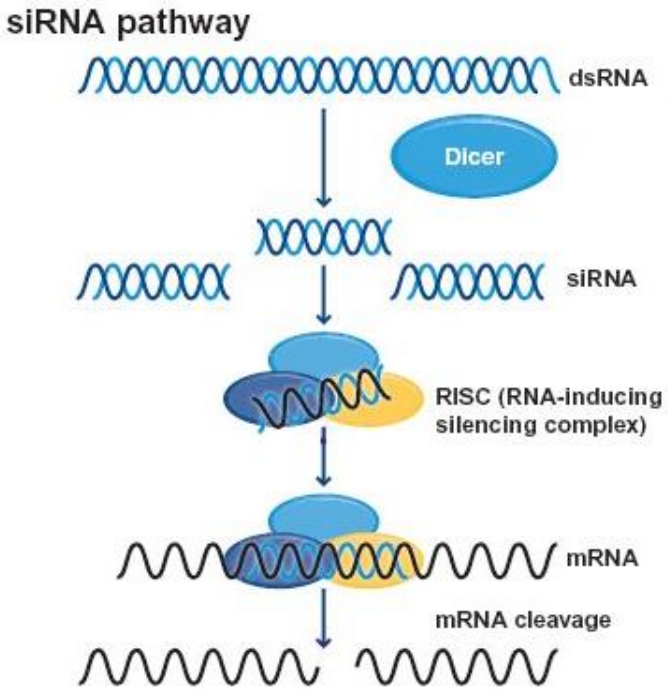

Figure 2.5 A schematic representation of the siRNA pathway
(http://www.abcam.com/index.html?pageconfig=resource&rid=10787&#5)

2.4.2. *siRNA design and synthesis*

Three siRNA duplexes were designed and synthesised by Eurogentec (Southampton, UK) based on the SKP2 cDNA sequence (Table 2.2) and their efficacy evaluated against a universal negative control (cat no. SR-CL000-005, Eurogentec), hereafter referred to as the negative control siRNA (NCS). p27 siRNAs were designed and functionally verified by Qiagen using RT-PCR (Qiagen, Manchester, UK), and compared to AllStars negative controls (Qiagen, cat no. 1027280). All siRNAs were designed using siRNA design software based on published methods (Elbashir *et al.*, 2001a; Elbashir *et al.*, 2001b; Krueger *et al.*, 2007).

siRNA Target	siRNA sequence (sense)
SKP2 siRNA 1	5'GUG-AUA-GUG-UCA-UGC-UAA-A3'
SKP2 siRNA 2	5'GGC-CAA-CUA-UUG-GCA-ACA-A3'
SKP2 siRNA 3	5'UCA-UUC-UUU-AGC-AUG-ACA-C3'

Table 2.2 siRNA sequences targeting SKP2

2.4.3. *siRNA Transfection*

Cells were seeded at 4 x 10^5 cells/well into 6-well plates in RPMI 1640 medium containing 10% (v/v) FBS, 24 hrs prior to transfection. siRNA was transfected into cells using lipofectamine® 2000 in Opti-MEM® reduced serum medium (Invitrogen, Life Technologies, Paisley, UK). siRNA was stored at stock concentrations of 20 µM and the following calculations used to determine the total volume of siRNA and Opti-MEM (400 µl/well) required:

siRNA volume: N x 0.12 x nM

Opti-MEM volume: 400 µl x N

N = no. wells, nM = final siRNA concentration

Separately, Lipofectamine 2000 was diluted in Opti-MEM as below to give a final ratio of DNA : Liofectamine of 1 : 1.25

Lipofectamine volume: N x 0.15 x nM

Opti-MEM volume: 400 µl x N

The two solutions were gently mixed and incubated at room temperature for 10 minutes after which an equal volume of each solution was gently mixed together and incubated for a further 30 minutes again at room temperature to allow siRNA containing liposomes to form. Meanwhile, the medium was removed from the wells, the cells washed with 1 ml of Opti-MEM to remove any remaining FBS and 1.6 ml of fresh Opti-MEM added to each well. Following the 30 minutes incubation, 0.8 ml of the DNA-liposome solution was added to each well and incubated at 37°C, 5% CO_2. After 24 hrs the DNA-liposome solution was removed and the cells either harvested, or Opti-MEM replaced with 2 ml RPMI 1640 containing 10% (v/v) FBS for collection at later time points.

2.5. Protein Expression

Protein expression was measured using western blotting. A widely used technique, it allows the protein expression levels of specific proteins to be identified in whole cell lysates or tissue samples. There are 3 stages to western blotting; proteins are first denatured by boiling with the reducing agent β-

mercaptoethanol to break disulphide bonds within the protein, and the anionic detergent sodium, dodecyl sulphate (SDS), which uniformly covers the protein with a negative charge. This creates a homogenous mass to charge ratio and allows for separation according to molecular weight by sodium dodecyl sulphate gel electrophoresis (SDS-PAGE). The proteins are then transferred to a nitrocellulose membrane, and finally visualised and detected by the use of specific antibodies, conjugated to horseradish peroxide (HRP), and chemiluminescence.

2.5.1. *Harvesting and preparation of cell lysates*

For the collection of adherent cells from a 6-well plate, medium was removed, the cells washed with PBS and 20 µl of Laemmli lysis buffer (2% (w/v) SDS, 10% (v/v) glycerol, 62.5 mM Tris pH 6.8) added. Cells were harvested using a cell scraper, lysates collected in a 1.5 ml eppendorf and then sonicated for 10 seconds (MSE Soniprep 150 Plus, Wolf Laboratories, UK) to fragment the viscous DNA. After a 10 minute centrifugation at 8000 x g the supernatant was transferred to a fresh Eppendorf and the lysates stored at -20^{0}C.

2.5.2. *Pierce® Protein Estimation*

To determine the total protein concentration in each sample the Pierce® BCA protein assay kit was used. When in an alkaline medium peptide bonds reduce Cu^{2+} ions to Cu^{1+}. This assay utilises the colourimetric reaction seen when bicinchoninic acid (BCA) reacts with Cu^{1+}. Measurable at 570 nm, the amount of Cu^{2+}reduced is proportional to the protein content of the solution allowing protein concentrations to be determined based on a calibration curve of albumin protein standards.

Lysates were vortexed and diluted 1:10 in sterile water to a total volume of 50 µl. Albumin protein standards at 0.2, 0.4, 0.6, 0.8, 1.0 and 1.2 µg/ml were prepared from the provided 200 µg/ml stock and 10 µl pipetted into 4 consecutive wells of a 96 well plate, followed by the samples (Figure 2.6). Sterile water was used as the negative control. Reagent A and B of the Pierce® BCA protein assay kit were mixed at a ratio of 50:1 and 190 µl added to each well. After a 30 minute incubation at 37°C the optical densities of the samples were measured on a

spectrophotometric plate reader (Model 680 Microplate Reader, Bio-Rad Laboratories, CA, USA) at 570 nm. After subtracting the average negative control, a standard curve was generated and the samples' protein content determined from the equation describing the line. All values were multiplied by 10 to account for the 1:10 dilution factor and the volume of each sample containing 25 µg of protein calculated.

Standards				Samples							
water	0.2	0.6	1.0	S1	S3	S5	S7	S9	S11	S13	S15
water	0.2	0.6	1.0	S1	S3	S5	S7	S9	S11	S13	S15
water	0.2	0.6	1.0	S1	S3	S5	S7	S9	S11	S13	S15
water	0.2	0.6	1.0	S1	S3	S5	S7	S9	S11	S13	S15
water	0.4	0.8	1.2	S2	S4	S6	S8	S10	S12	S14	S16
water	0.4	0.8	1.2	S2	S4	S6	S8	S10	S12	S14	S16
water	0.4	0.8	1.2	S2	S4	S6	S8	S10	S12	S14	S16
water	0.4	0.8	1.2	S2	S4	S6	S8	S10	S12	S14	S16

Figure 2.6 Pierce assay set up in a 96-well plate. Sterile water was aliquoted into the first row as the negative control, followed by 4 wells of 10 µl of each prepared standard and then 4 wells of 10 µl of each sample to be measured.

2.5.3. *SDS-PAGE and membrane transfer*

After determination of the protein content, the appropriate volume of lysate was added to 5 µl loading buffer (Laemmli lysis buffer with 5% (v/v) β-mercaptoethanol and 0.0025% (w/v) bromophenol blue) and denatured at 100°C. Samples (containing 25 µg of protein) were resoled on Novex® 4-20% Tris-glycine polyacrylamide gels (Invitrogen) at 150 V in 1 x electrode buffer (Appendix I) using SeeBlue® Plus2 pre-stained protein standard (Invitrogen) for the molecular weight markers. Proteins from the polyacrylamide gel were transferred to Hybond™-C nitrocellulose membrane (GE Healthcare, Life Sciences, Buckinghamshire, UK) using a 1 x transfer buffer (Appendix I) at 30 V overnight or 60 V for 2 hrs.

2.5.4. *Protein detection*

After protein transfer, the membrane was blocked in 5% (w/v) milk powder in 0.1% (v/v) Tween 20 in TBS (TBST, Appendix I) for 1 hr and then incubated

overnight with the chosen primary antibody at 5°C. All primary antibodies used are listed in Table 2.3 and were diluted in 5% (w/v) milk powder in TBST (Table 2.3).

Protein	Antibody	Dilution	Antibody Type	Manufacturer
GAPDH	SC-25778	1:1000	Rabbit PC	Santa-Cruz
MDM2	OP46	1:100	Mouse MAb	Calbiochem
MYCN	SC-53993	1:500	Mouse MAb	Santa-Cruz
$p27^{KIP1}$	SC-528	1:200	Rabbit PC	Santa-Cruz
$p21^{WAF1}$	OP64	1:200	Mouse MAb	Calbiochem
p53	DO-7	1:1000	Mouse MAb	Novocastra
SKP2	32-300	1:1000	Mouse MAb	Invitrogen

Table 2.3 Primary antibodies used in this study.
PC: Polyclonal, **MAb:** Monoclonal

After exposure to a primary antibody the blot was washed with TBST and incubated for 1 hour at room temperature with a stabilised peroxide conjugated goat anti-mouse (Dako) or goat anti-rabbit (Dako) antibody, diluted 1:1000 in 5% milk powder (w/v). Following 4 independent 10 minute washes with TBST the blots were treated with chemiluminescence reagents (ECL) (GE Healthcare) and exposed onto film (Kodak).

2.5.5. *Densitometry*

Densitometry was performed to semi-quantitatively measure protein expression levels compared to the GAPDH loading control. The Fuji-Las Pro (FUJIFILM Life Science, Stamford, CA, USA) scanner was used to capture the image of the bands from the x-ray film, and the AIDA image analyser (Raytest, Straubenhardt, Germany) was used to estimate size and density of the bands. The densitometry values for each band were first corrected for the background and then normalised to the GAPDH control.

2.6. Cell cycle analysis

The ‘replication state’ of cell populations was analysed using fluorescence activated flow cytometry (FACS). In FACS analysis a sample of suspended cells which are fluorescently labelled are hydrodynamically focused into a single stream to run pass a laser light source one cell at a time. A number of detectors then detect the scattered light which helps to identify particular cell populations within the sample. The detector in front of the light beam collects forward scatter (FSC) which is related to the cell size, while the detectors perpendicular to the incident light (FL1, FL2 and FL3) collect side scatter (SSC), which is often split into defined wavelengths by a set of filters or mirrors and identifies the cell granularity.

Propidium Iodide (PI) is a fluorescent DNA intercalating agent which binds to the DNA of the cell. When excited by an argon-laser DNA-bound PI emits an orange fluorescence which is detected by the FL2 detector and the photon energy converted into an electrical signal. PI binds stoichiometrically to DNA allowing the proportion of DNA in the cell to be measured. In this way the stage of the cell cycle can be determined. Cells going through S phase will have more DNA than those in G_1, due to DNA replication, and will therefore take up proportionally more PI and fluoresce more brightly. This trend will continue until G_2 phase where cells will have twice the amount of DNA and hence fluorescence than in G_1, until they undergo mitosis.

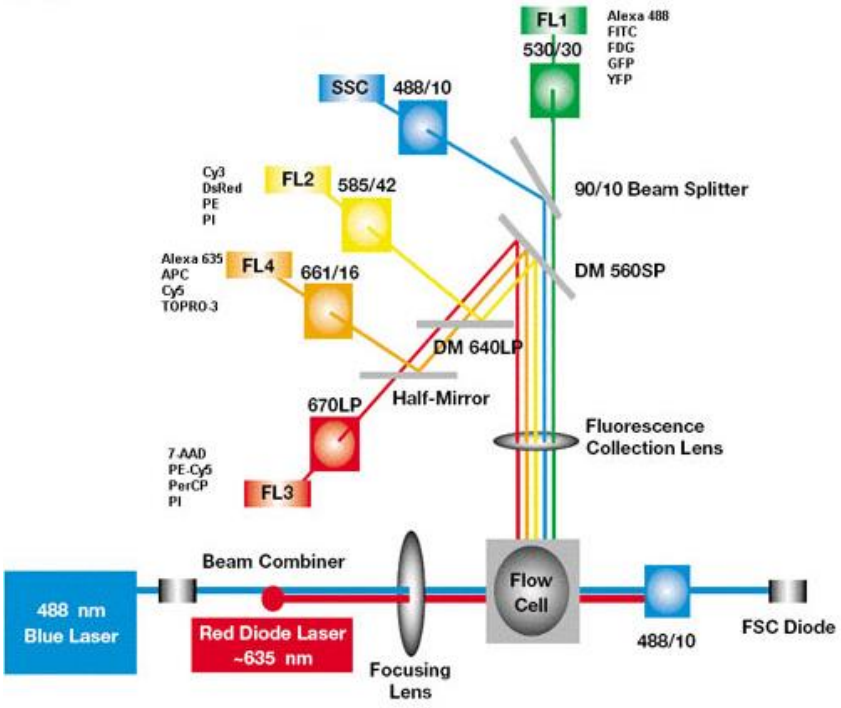

Figure 2.7 FACSCalibur optical layout (www.bdbiosciences.com).

2.6.1. *Preparation of samples*

Cells were seeded at 4 x 10^5 cells/well into 6-well plates in RPMI 1640 containing 10% (v/v) FBS and left overnight. After treatment cells were harvested, washed in ice cold PBS, centrifuged at 500 x g for 5 minutes and then fixed in 70% (v/v) ethanol and stored at 4°C. Cells were then rehydrated, washed twice with PBS, treated with RNase H (0.1 mg/ml, Sigma) and stained with propidium iodide (40 µg/ml, Sigma), and finally incubated under light-protected conditions at 37°C for 30 minutes.

2.6.2. *FACSCalibur flow cytometer*

Before running the samples through the flow cytometer, they were passed through a syringe to separate clumped cells. Samples were measured and the data acquired using the FACSCalibur™ (Becton Dickinson, Franklin Lakes, NJ, USA), and CellQuest software (Becton Dickinson). To optimise instrument settings a dot plot of FL2-Area vs. FL2-Width was set up using untreated control cells and a gate set around the G0/G_1/G_2/M population to exclude cell aggregates and doublet particles. The gated population was also represented in a histogram graph of cell counts vs. FL2-Area and the G_1 peak adjusted to 200 on the linear axis. For each sample, 1000 events were collected and saved.

2.6.3. *Analysis*

Cells were analysed using Cyflogic analysis software (Cyflo Ltd, Finland). FL2-W vs. FL2-A scatter plots were generated and the cells gated to exclude doublets/aggregates. Using the gated data, FL2-A histograms were generated and the proportion of cells in G_1, S, G_2 and sub-G_1 determined by marking the various phases of the cell cycle as shown in Figure 2.8. A table of statistics identifying the percentage of cells in each phase was generated from the histogram and recalculated from the total cells gated for that sample to correct for variation in phase size.

a)

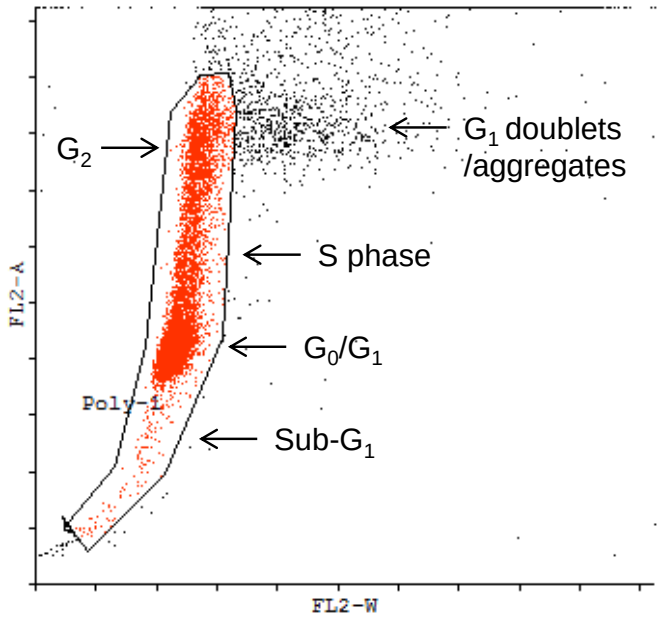

b)

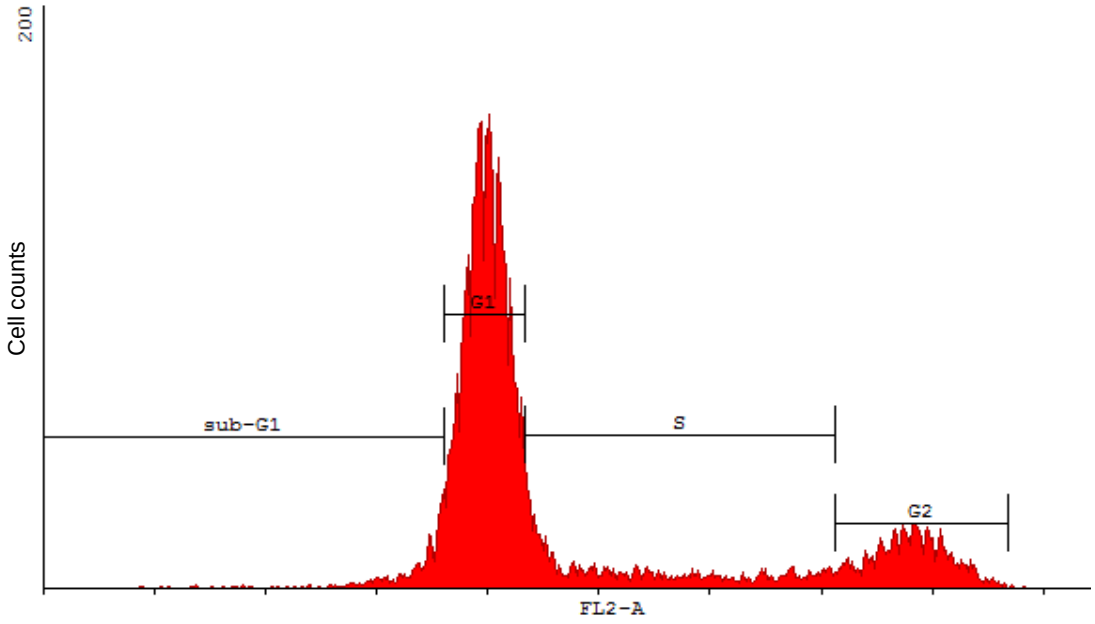

Figure 2.8 FL2-W vs. FL2-A scatter plots and corresponding histogram of gated population. a) Dot plot of FL2-Width (FL2-W) vs. FL2-Area (FL2-A) allowing discrimination between G_1 doublet and G_2 /M single cell. **b)** Histogram analysis of the percentage of cells in each phase of the cell cycle determined from the events gated in the dot plot.

2.7. Caspase 3/7 activity assay

The Caspase-Glo® 3/7 assay (Promega, Southampton, UK) measures apoptosis by providing a luminogenic caspase-3/7 substrate which contains the amino acid sequence DEVD based on the caspase-3 and 7 consensus cleavage site. Once added to the cells, cell lysis releases the caspase enzymes which by cleaving the DVED sequence, release the luciferase substrate (aminoluciferin) resulting in the emission of light. Luminescence is proportional to the amount of caspase-3/7 activity.

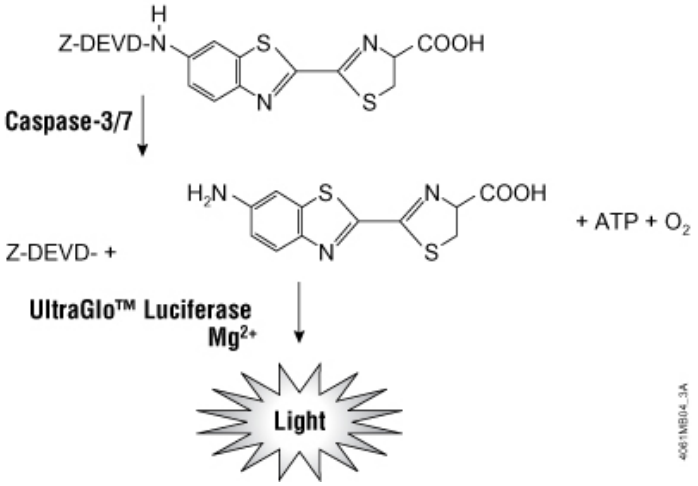

Figure 2.9 Detection of caspase 3/7 activity by the Caspase-Glo® assay
www.promega.co.uk

2.7.1. *Caspase-Glo® 3/7 assay protocol*

Cells were seeded at 5000 cells/well in a 96-well white plate in a final volume of 50 µl prior to caspase reagent addition. Once at room temperature, 50 µl of the caspase reagent was added to each well. The plate was put in light protected conditions and incubated for 1 hr at room temperature after which it was analysed on a microplate luminometer (Berthold Technologies, Herefordshire, UK). Luminescence readings were corrected for background (medium only), normalised to the untreated control and plotted relative to negative control (non-coding siRNA). Results are the average of 3 independent wells.

2.8. mRNA extraction and determination of concentration

Extraction and purification of mRNA was performed using the RNeasy® Mini kit (Qiagen, Venlo, Limburg, Netherlands) according to the manufacturer's protocol for the purification of total RNA from animal cells using spin technology. Centrifuged samples were homogenised by the addition of Buffer RLT and moved through a syringe 3 times. An equal volume of 70% (v/v) ethanol was then added to the lysate, gently pipetted to mix the sample and immediately applied to the RNeasy Mini spin column. Total RNA binds to the column membranes, allowing contaminants to be washed away by the flow-through of the washing buffers RW1 followed by RPE. RNA was then eluted from the membrane in 40 µl of RNase-free water, and the RNA concentration and quality determined using the NanoDrop™ ND-1000 Spectrophotometer (NanoDrop Technologies, INC., Wilmington, DE, USA). Absorbance was measured at 260 and 280 nm, and the purity of the RNA determined by the 260/280 ratio, which should be ~2.0 for good quality RNA.

2.9. Generation of cDNA by reverse transcription

The synthesis of cDNA was carried out using the iScript™ cDNA synthesis kit (BioRad). RNA (1 µg), was added to 4 µl of 5x iScript reagent, containing oligo(dT) and reaction hexamer primers, and 1 µl of the iScript reverse transcriptase, RNase H+. The oligo d(T) primers bind to the poly-A tail of the mRNA ensuring RNA transcription, preventing genomic DNA contamination, whilst RNase H+ degrades the RNA template after cDNA synthesis. The thermal reaction conditions were:

5 minutes at 25 °C
30 minutes at 42 °C
5 minutes at 85 °C
Hold at 4 °C (optional)

2.10. Quantitative reverse-transcription polymerase chain reaction

Quantitative reverse-transcription polymerase chain reaction (qRT-PCR) is a technique which adopts the amplification techniques of PCR to identify a specific DNA sequence, with either fluorescent dyes or fluorescently-tagged probes to

determine the amount of DNA formed during each cycle. As the PCR reaction progresses the amplification of the PCR product (amplicon) is detected and quantified. As the amount of fluorescence measured is proportional to the total amount of the amplicon, by monitoring the changes in fluorescence the amount produced in each cycle can be calculated. Based on this relationship the initial number of copies of template DNA can be determined as the higher the starting level of the target sequence, the fewer the PCR cycles required to generate the final level of DNA.

There are 3 steps to the PCR reaction:

1. Denaturation at 95°C, which disrupts the hydrogen bonds between the complementary DNA bases yielding single stranded DNA.

2. Primer annealing at 50-68°C, which allows the hybridisation of primers onto the single stranded DNA promoting the attachment of the DNA polymerase.

3. Elongation at the optimum temperature for the DNA polymerase, which synthesizes a new strand of DNA complementary to the DNA template.

Two types of fluorescence detection method are used in qRT-PCR. SYBR-based chemistry uses non-specific fluorescent dyes or flurophores which intercalate within the DNA helix and rely on DNA primers for their sensitivity and specificity. Probe-based chemistry, such as the hydrolysis Taqman® probe (Applied Biosystems, Life Technologies, Carlsbad, CA, USA) uses fluorescently-tagged oligonucleotide probes which are specifically designed to target a particular DNA sequence. In this study Taqman chemistry was employed.

2.10.1. *Taqman® gene expression assay*

Taqman® probes (Applied Biosystems) utilise energy transfer from a high to a low energy state, termed fluorescence resonance energy transfer (FRET). The 5' end of the probe is labelled with a high energy fluorophore (e.g. 6-carboxyfluorescein: FAM) which upon excitation by a light source transfers energy to the low energy quencher (e.g. tetramethylrhodamine: TAMRA) on the

3’ end supressing the FAM fluorescence. Specific for a particular cDNA sequence, the probe binds to the specific amplicon during the annealing step of the PCR, and is then cleaved by the 5’ to 3’ endonuclease activity of the *Taq* polymerase during the elongation phase. The release of the fluorophore from the quencher stops the transfer of energy between the two resulting in an increase in fluorescence from the fluorophore reflecting the amplification of the specific target sequence (Figure 2.10).

Once the fluorescence signal is strong enough to be detected it is captured and displayed in an amplification plot where ΔRn is plotted against the PCR cycle number (Figure 2.11). Rn is the signal from the fluorophore normalised to the fluorescence intensity of a passive reference dye e.g. ROX. By subtracting the baseline emission, where the signal is not yet strong enough to be detected, ΔRn can be calculated. The amplification plot has 2 phases, an exponential phase and a plateau phase. During the exponential phase the amount of PCR product approximately doubles until the reagents begin to become limiting which slows the reaction down. By setting the threshold level (the point at which a reaction reaches a fluorescent intensity above background) in the exponential phase of amplification the most accurate reading can be made. The cycle number at which the fluorescent signal of a reaction crosses the threshold is called the threshold cycle (C_t). Inversely proportional to the amount of the target sequence, it allows for the initial amount of target DNA to be determined, which is directly proportional to the level of mRNA in the original sample.

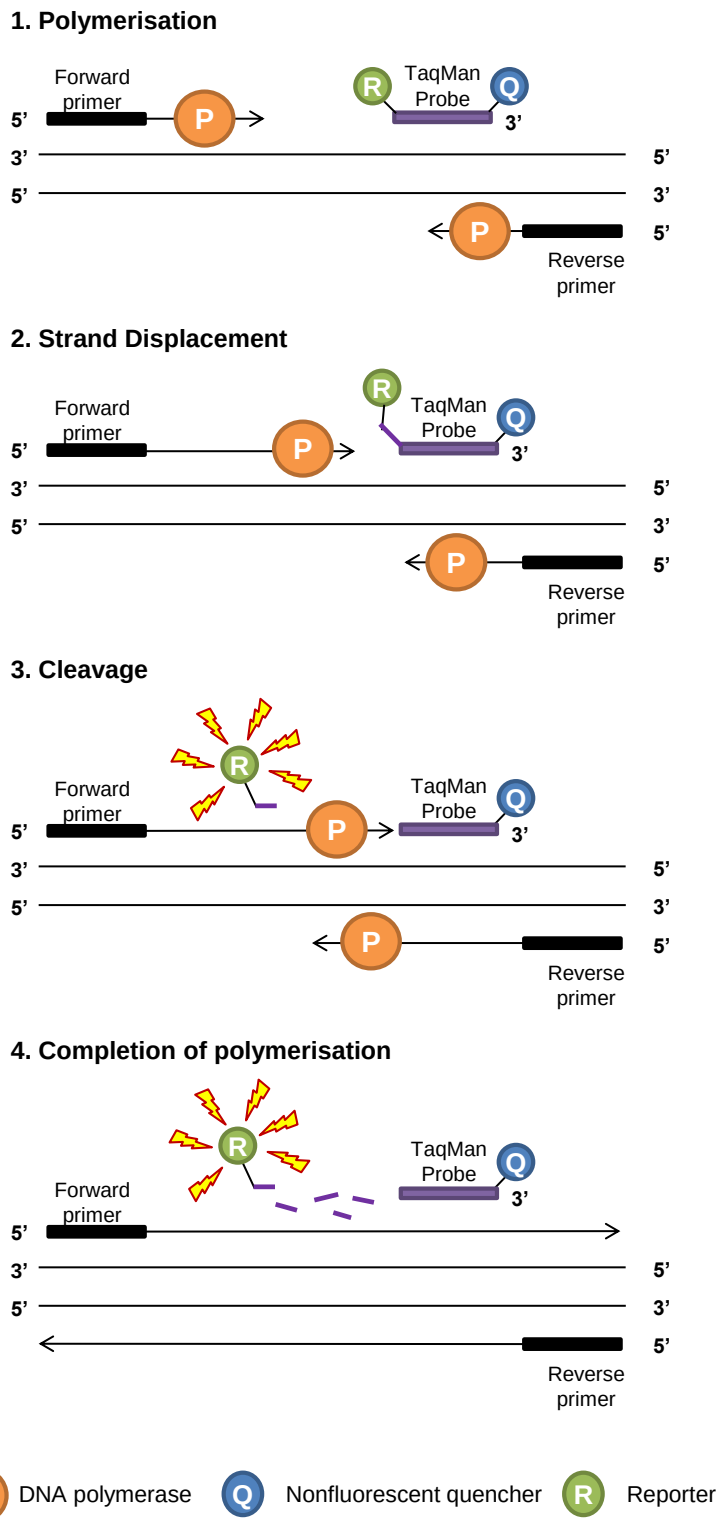

Figure 2.10 Taqman probe-based assay. During PCR the Taqman probe anneals specifically to a complementary sequence between the forward and reverse primer sites. With the probe intact the reporter fluorescence is quenched until the polymerase cleaves the probe hybridised to the target. This separates the reporter from the quencher resulting in a fluorescent signal which is detected. Polymerisation then continues yet is not extended along the probe due to the 3' end being blocked. Figure adapted from Taqman protocol (https://tools.lifetechnologies.com/content/sfs/manuals/).

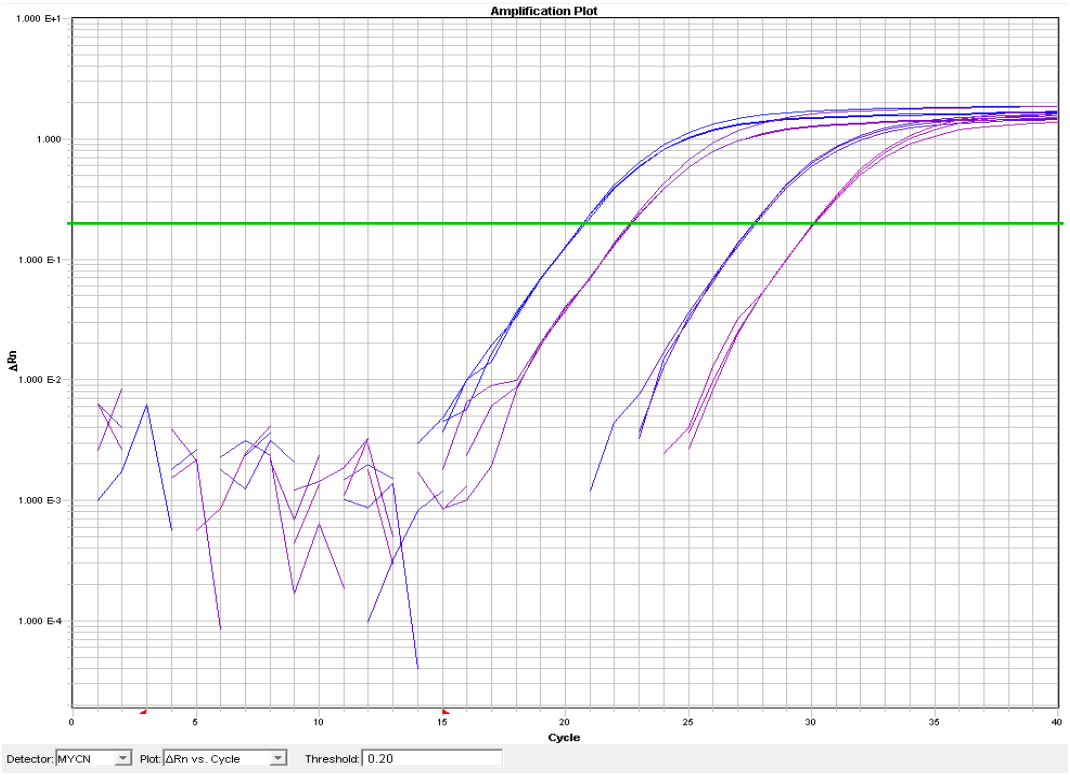

Figure 2.11 An example of an amplification plot for MYCN in the Tet21N MYCN regulatable cell lines after increasing exposure to tetracycline. Each curve represents readings from 3 replica wells and were generated by SDS software, threshold levels indicated in green.

2.10.2. *qRT-PCR Protocol*

qRT-PCR was carried out according to the Taqman® gene expression assay protocol (Applied Biosystems). Each cDNA sample was diluted 1 in 10 with nuclease-free water before being run in triplicate with each of the individual probes (Table 2.4). The total reaction volume was 10 µl: 7.5 µl of the reaction mix and 2.5 µl of diluted cDNA (Table 2.5).

Gene Name	Assay Reference
MYCN	Hs00232074_m1
SKP2	Hs00180634_m1
ODC1	Hs-00159739_m1
p27	Hs-00153277_m1
p21	Hs00355782_m1
GAPDH	Hs03929097_g1

Table 2.4 List of Taqman® Probes (www.appliedbiosystmes.com).

Reaction components	Per well
2x Taqman® master mix	5 µl
20x Taqman® Primer and Probe	0.5 µl
Nuclease-free water	2 µl
1 in 10 diluted cDNA	2.5 µl

Table 2.5 qRT-PCR reaction composition

The Taqman® gene expression master mix contains the chemically modified form of AmpliTaq Gold® DNA polymerase called Ultra Pure (UP). Activated only at high temperatures, i.e. once the DNA is fully denatured, the UP enzyme promotes primer extension and elongation resulting in the cleavage of the probe and generation of the fluorescent signal. The master mix also contains the pre-mixed passive reference dye (ROX) which is used to normalise the fluorescence emission from the Taqman® probe. The qRT-PCR reactions were run on the 7900HT Fast Real-Time PCR system (Applied Biosystems) in a 384-well plate format using the thermal cycling conditions shown in Figure 2.12. Fluorescence emissions in the range 500-600 nm wavelength were detected.

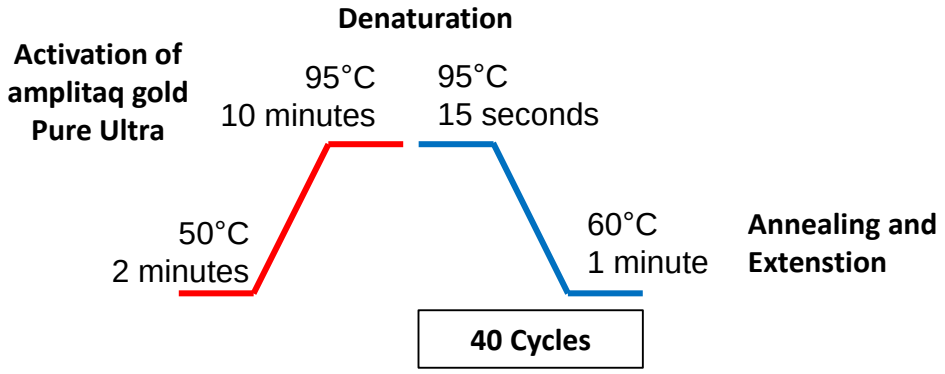

Figure 2.12 Thermal cycling programmed for quantitative real-time PCR

2.10.3. *Analysis of qRT-PCR results*

SDS 2.2 software (Applied Biosystems) was used to analyse the qRT-PCR results. Amplification plots were generated for each cDNA sample and the threshold automatically set (Figure 2.11). All Ct values were first normalised to GAPDH (ΔCt) and then analysed using the comparative Ct method where the ΔCt values of each sample were compared to the ΔCt value of a reference sample or

non-treated control. The normalised target gene expression level could then be determined by the equation:

$$\Delta Ct = Ct\ (Sample) – Ct\ (Housekeeping\ gene)$$

$$\Delta\Delta Ct = \Delta Ct(Sample) - \Delta CT(reference)$$

$$Sample\ Gene\ expression = 2^{\Delta\Delta Ct}$$

2.11. Plasmid purification and amplification

2.11.1. *Transformation of competent cells*

Plasmid DNA was transformed into DH5α™ chemically competent *E-coli* bacterial cells for replication of plasmid DNA. Approximately 50 pg (1 µl) of DNA was added to 30 µl of freshly defrosted competent cells (Invitrogen) and incubated on ice for 30 minutes. The competent cells/DNA mixture was heat shocked for 45 seconds at 42°C and immediately placed on ice for 2 minutes. Lysogeny broth (LB, 250 µl) was added to the competent cells/DNA mixture and incubated at 37°C with shaking at 180 rpm for 1 hr. After incubation 100 µl was spread onto LB-agar plates containing 100 µg/ml ampicillin (Sigma), and incubated at 37°C overnight. Single colonies were selected and inoculated in 5 ml of LB broth containing 100 µg/ml ampicillin and grown for 8 hours at 37°C, with shaking at 200 rpm. When competent, 500 µl of the starter culture was used to inoculate 500 ml LB-broth containing 100 µg/ml ampicillin, grown overnight at 37°C, with shaking at 200 rpm and used in plasmid extraction as described in section 2.12.2. The remaining culture was centrifuged at 1500 x g for 15 minutes, the supernatant removed and the cell pellet used for plasmid extraction and sequencing.

2.11.2. *Plasmid extraction*

Extraction of plasmid DNA was performed using a HiSpeed™ Plasmid Maxi Kit (Qiagen) according to the manufacturer's protocol. Briefly, the overnight culture prepared as described in Section 2.12.1 was collected by centrifugation at 5000 x g for 30 minutes at 4°C and the bacterial cells lysed by resuspending the pellet in 10 ml of Buffer P1 containing RNase A (100 µg/ml) and LyseBlue reagent (1:1000). Once fully resuspended 10 ml of Buffer P2 was added causing a colour change to blue as the LyseBlue precipitate dissolves in Buffer P1. The sample

was gently inverted to create a homogenously coloured solution and incubated for 5 minutes at room temperature. To precipitate genomic DNA, proteins and cell debris, 10 ml of pre-chilled Buffer P3 was added to the lysate and mixed immediately by gently inverting 4-6 times. Upon addition of the neutralisation buffer the LyseBlue turns colourless indicating that all SDS from the lysis buffer has been effectively precipitated. The lysate was immediately poured into a QIAfilter cartridge and incubated for 10 minutes to allow separation of the solution containing the plasmid DNA and the precipitate. During this latter incubation a HiSpeed Maxi tip was equilibrated by passing through 10 ml of Buffer QBT, after which the lysate was added from the QIAfilter. Once the lysate had entered the resin, the HiSpeed tip was washed with 60 ml of Buffer QC which passed through the tip by gravity flow. Plasmid DNA was eluted into a fresh 50 ml falcon tube using 15 ml of Buffer QF and precipitated by mixing with 10.5 ml of 70% (v/v) isopropanol at room-temperature for 5 minutes.

2.12. Reporter Gene Assay

Reporter genes are used to study the regulation of gene expression by cis-acting (e.g. regulatory DNA sequences) or trans-acting (e.g. transcription factors) elements by attaching a DNA sequence of interest upstream of a reporter which is not naturally expressed in the cells being transfected, e.g. luciferase. The presence of the reporter gene products or, if appropriate, their enzymatic activity can then be quantitatively measured to determine the functional status of the DNA sequence of interest.

2.12.1. *SKP2-promoter luciferase reporter assay*

pGL3-Basic luciferase plasmids containing a 1148bp fragment of the *SKP2* promoter were kindly donated by Professor Javier Léon (University of Cantabria, Spain) and have been previously described by Huang *et al* (Huang and Hung, 2006; Bretones *et al.*, 2011). An extremely sensitive system, the luciferase reporter gene produces an optical signal by catalysing the bioluminescent oxidation of luciferin to oxyluciferin in the presence of ATP, Mg^{2+} and O_2 (Figure 2.14).

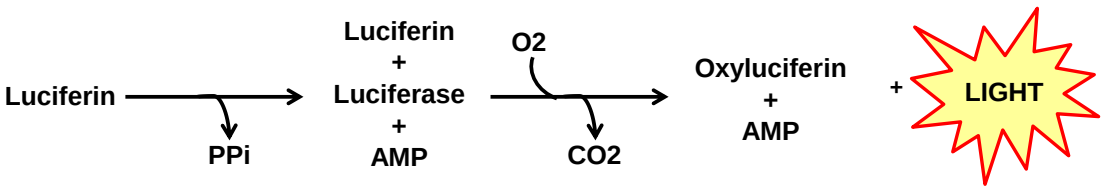

Figure 2.13 Oxidation reaction of luciferin by luciferase. Figure adapted from www.piercenet.com

To account for variability in the transfection efficiency the control reporter construct β-galactosidase was co-transfected with the reporter construct. Driven by the constitutively active cytomegalovirus (CMV) promoter, the control reporter was measured by the expression of β-galactosidase. The activity of the luciferase reporter was then normalised to β-galactosidase expression, measured colorimetrically using the substrate ONPG, to account for variability.

2.12.2. *Luciferase reporter gene assay protocol*

Cells were seeded at 1 x 10^5 (SHSY5Y and IMR32) or 5 x 10^4 (Tet21N) cells/well into 24-well plates in RPMI 1640 medium containing 10% (v/v) FBS, 24 hrs prior to transfection. pGL3-Basic, pGL3-SKP2 and pGL3-SKP2-MutEB were transfected into cells using Lipofectamine® 2000 in Opti-MEM® reduced serum medium (Invitrogen) together with β-galactosidase as a transfection control. Plasmids were stored at -20°C in stock concentrations of 0.2 µg/µl and the transfection mixture made as shown in Table 2.6.

Reaction components	Per well	Final Concentration/well
Plasmid DNA (0.2 µg/µl)	4 µl	0.8 µg/µl
β-Gal (0.2 µg/µl)	0.5 µl	0.1 µg/µl
Lipofectamine® 2000	2 µl	
Opti-MEM®	43.5 µl	

Table 2.6 Luciferase reporter gene transfection mixture

Plasmid DNA was first added to the Opti-MEM® media, mixed thoroughly and incubated at room temperature for 15 minutes. Following incubation, Lipofectamine® 2000 was added directly to the DNA/serum free media mixture, mixed thoroughly and incubated for a further 40 minutes at room temperature. The RPMI medium was removed from the wells, the cells rinsed with Opti-MEM®

to remove any remaining FBS, and then replaced with 500 µl of Opti-MEM® medium. After the incubation, 50 µl of the transfection mixture was added to each well, plates were shaken, and then incubated at 37°C for 24 hrs prior to cell lysis.

Reporter lysis 5x buffer (Promega, Madison, WI, USA) was first diluted 1 in 5 with sterile water and after the cells were washed with PBS, lysis buffer (500 µl) was added directly to each well and the plate incubated at 37°C for 10 minutes. The cell lysates were then stored at -20°C overnight after which the luciferase and β-galactosidase activity was measured using the Luciferase Assay System (Promega) and Ortho-nitrophenyl-β-D-galactopyranoside (ONPG) assay (Thermo Scientific, Waltham, MA, USA), respectively.

Luciferase activity was measured using the BMG LABTECH FLUOstar Omega microplate reader (BMG LABTECH, Germany). Cell lysates (100 µl) were transferred in triplicate to a microplate, placed onto the plate reader and, using automated injectors, 50 µl of luciferase reagent was added to each well, plates were shaken for 5 seconds and luminescence immediately read. β-Galactosidase activity was measured separately using the colorimetric ONPG reagent (Thermo Scientific). ONPG solution (150 µl) was added to 10 µl of cell lysate in a 96 well plate, in triplicate, and incubated at 37°C for 15 minutes. Following the colour change, 5 µl of sodium carbonate was added to each well to stop the reaction and the plate read at 415 nm on a spectrophotometric plate reader (Model 680 Microplate Reader, Bio-Rad Laboratories, CA, USA).

Luciferase activity was normalised to the β-galactosidase activity to control for transfection efficiency and the data analysed using Prism Version 6.0. Results are the average of 3 independent wells.

2.13. Generation of pGL3-*SKP2*-MutEB construct

2.13.1. *Site directed mutagenesis*

Site directed mutagenesis allows specific, targeted changes to be made in double stranded plasmid DNA either by the insertion, deletion or substitutions of bases. It is a technique that is used to investigate the structure and biological activity of DNA, RNA and proteins, especially enzymes and receptors. The technique uses a synthetic DNA primer which contains the desired mutation surrounded by

sequences complementary to the template DNA called flanking sequences. These sequences hybridise to the plasmid DNA and are then extended during the thermal cycle incorporating the mutation into the newly synthesised plasmid DNA. Following a PCR reaction, the product is digested with the restriction endonuclease DpnI, which recognises and cleaves only at the methylated adenine in the GATC recognition sequence. Most template plasmids are from *E.coli* strains which contain site-specific DNA methylases, such as DNA adenine methylase (DAM) and DNA cytosine methylase (DCM), which transfer methyl-groups to specific sites after replication. As the newly synthesised mutant DNA will not be methylated, digestion by DpnI will therefore isolate the mutant product from the original plasmid, which can then be transformed into competent bacteria as described in section 2.12 (Figure 2.15).

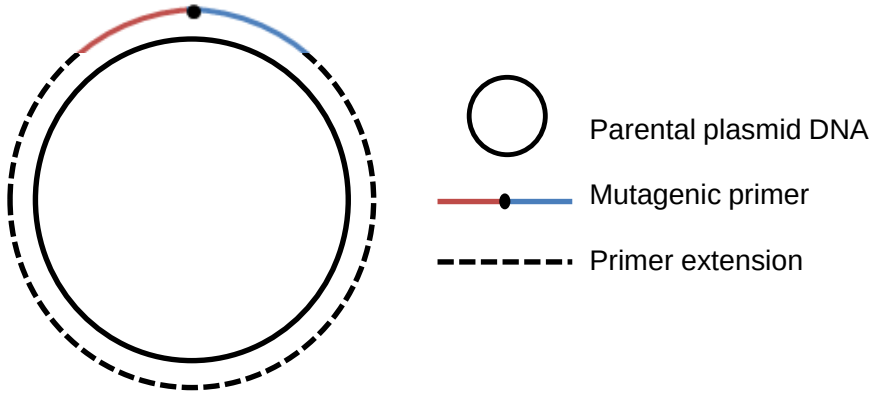

Figure 2.14 Schematic representation of single-primer site-directed mutagenesis.

2.13.2. *Generation of* pGL3-*SKP2*-MutEB

The two E-box motifs (CCCGTG) and (CACCTG) were identified within the -1148bp *SKP2* promoter construct, mutated and replaced with the PstI restriction site CTGCAG. Using the specific primers listed in Table 2.7 plasmid DNA was amplified using PCR with 5x Phusion® High-Fidelity DNA polymerase (New England Biolabs, Ipswich, MA, USA) as indicated in Tables 2.8 and 2.9. The PCR products were incubated for 1 hour at 37°C with DpnI (New England Biolabs) to digest the parental DNA and run on a 1% agrose gel to determine whether the PCR was successful. Once confirmed, the remaining PCR products were purified using a QIAquick PCR puritifcation Kit (Qiagen) according to the manufacturer's protocol and transformed into competent cells as described in Section 2.12.

E-box	Sense (SN) or Antisense (ASN)
CACCTG	SN: 5'-CAGTTCGCAGCCTCT**CTGCAG**GCCGGCGGGCTGGGC-3'
	ASN: 5'-GCCCAGCCCGCCGGC**CTGCAG**AGAGGCTGCGAACTG-3'
CCCGTG	SN: 5'-CCGCCTCCCGCCTAC**CTGCAG**GGCCGACCAGTCCCG-3'
	ASN: 5'-CGCCTCCCCGCCTAC**CTGCAG**GTAGGCGGGGAGGCG-3'

Table 2.7 Primers used to generate pGL3-*SKP2*-MutEB

Component	1x 50µl Reaction	Final Concentration
Plasmid DNA	1 µl	~100 ng/µl
DNA polymerase (5x solution)	10 µl	1x
Deoxynucleotide (dNTP) solution mix	1 µl	200 µM
Primer Stock *	1 µl	0.5 µM
Nuclease free Water	37 µl	

Table 2.8 Reaction mixture for site-directed mutagenesis PCR. * Primer stock contains 2 µl of SN and ASN primers in sterile water at a total volume of 100 µl

Step	Temperature	Time
Initial Denaturation	98°C	30 seconds
25 cycles	98°C	10 seconds
	55°C	30 seconds
	72°C	30 seconds per kb
Final Extension	72°C	7 minutes
Hold	4°C	

Table 2.9 Thermocycling conditions for PCR

2.13.3. *Restriction enzyme digestion*

To confirm the presence of the mutated E-Box sequence CTGCAG, PGL3-*SKP2*-MutEB was digested with PstI (New England Biolabs) using the reagents shown in Table 2.10. The plasmid was incubated with PstI for 1 hour at 37°C, and the products separated using 1% agarose gel electrophoresis, visualised under UV and the images captured by the BioRad Molecular Imager Gel Doc XR system (Figure 2.8). The presence of the mutation was confirmed by sequencing (Source BioScience, LifeSciences, Nottingham, UK). Following sequence confirmation, the plasmid DNA was diluted into 0.2 µg/µl stocks in sterile distilled water and stored at -20°C.

Component	1x 50 µl Reaction	Final Concentration
Plasmid DNA	2 µg	2 µg
4x NEBuffer 3.1	5 µl	1x
PstI	1 µl	20 units
Sterile Water	*	

Table 2.10 Restriction endonuclease reaction mixtures for digestion of E box motifs

2.14. Cell proliferation assay

Cell proliferation was measured using the sodium 3'-{1-(phenylaminocarbonyl)-3,4-tetrazolim]-bis(4-methoxy-6-nitro)benzene sulfonic acid hydrate (XTT) assay (Roche applied Science, West Sussex, UK). A colorimetric assay, it determines the number of viable cells based on the cleavage of the tetrazolium salt (XTT) to the soluble formazan salt, in the presence of an electron-coupling reagent. Indicated by a colour change with an absorbance measured at 450 nm, this conversion can only occur within functioning mitochondria which reflects the number of viable cells. Before use, the reagents are equilibrated at room temperature and mixed together by adding 50 µl of XTT labelling reagent to 1 µl electron-coupling reagent for each individual well. The 50 µl of mixed XTT reagent is then added to each well containing 100 µl of medium. Wells containing growth medium only are also analysed to act as a negative control.

2.14.1. *Determining optimal cell density*

The optimal number of cells was determined by generating 5 day growth curves. In 96-well plates, cell were seeded in intervals of 1000 cells up to 5000 cells/well and the cell proliferation determined each day using the XTT assay. A seeding density was chosen such that cells were in the exponential growth phase throughout the experiment and not in the plateau or lag phase of growth, illustrated in Figure 2.16

2.14.2. *XTT assay*

Cells were seeded at their optimal density and incubated at 37°C, 5% CO_2 overnight to allow attachment. Following treatment and incubation for the time period indicated, 50 µl of XTT reagent was added and the cells incubated for a further 6 hours at 37°C, before the optical density was measured at 450 nm using a microplate reader (Model 680 Microplate Reader, Bio-Rad Laboratories, CA, USA).

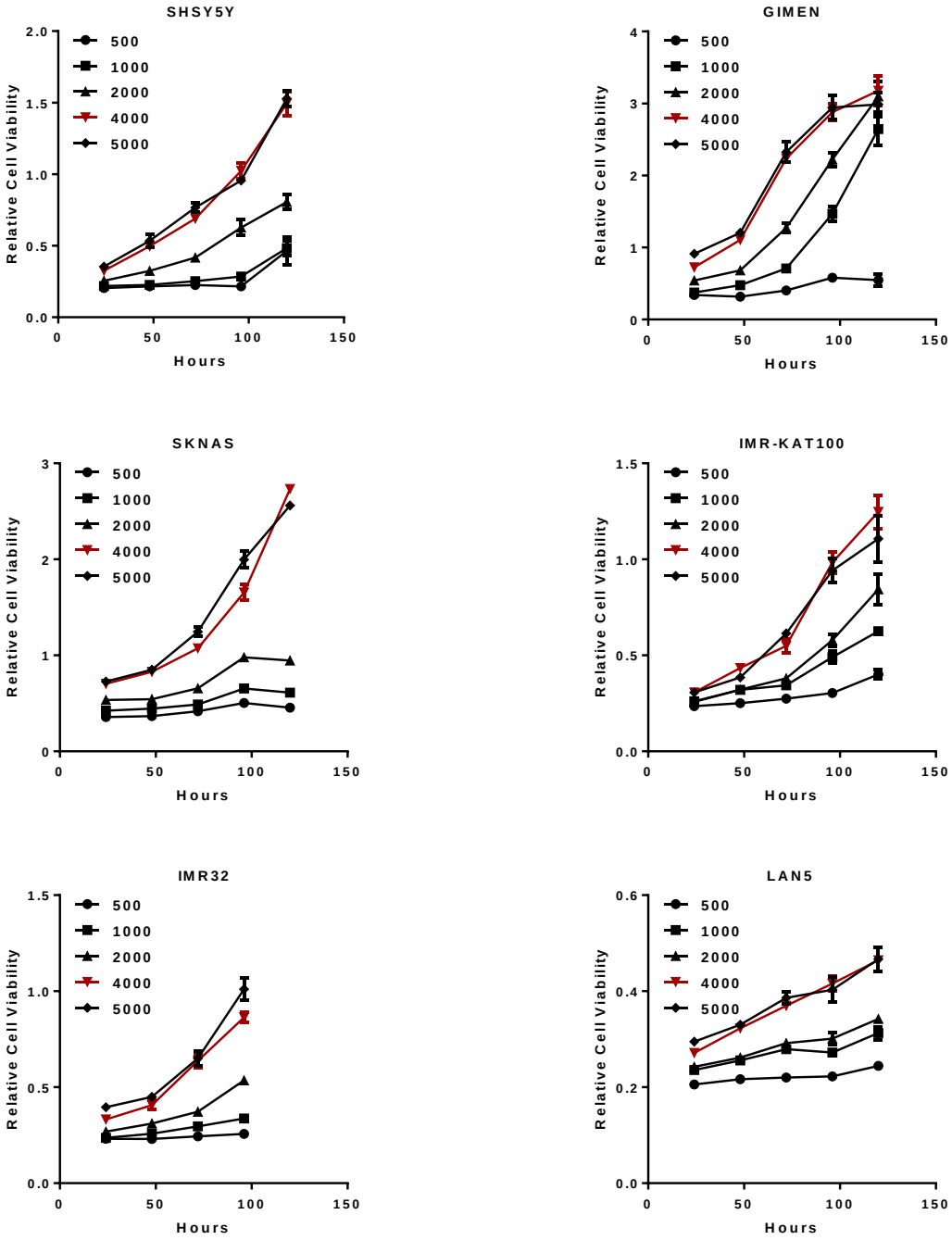

Figure 2.15 Five day growth curves for 6 neuroblastoma cell lines measured by the XTT assay to determine seeding densities for growth inhibition assay.

2.15. Compound Screening

Compounds were screened in HeLa cells to determine a GI_{50} value, i.e. the concentration at which the compound inhibits growth to 50% of the untreated cell population. All compounds were screened at a range of concentrations between 0.1 and 100 µM. Compounds were suspended in 100% DMSO at 100mM, when solubility allowed, and stored at -20°C. Final drug concentrations added to each well were in 100 µl full medium, containing 0.5% (v/v) DMSO.

2.15.1. *Growth Inhibition Assays*

Growth inhibition was measured using the sulforhodamine B (SRB) dye method which binds to basic amino acid residues in proteins allowing cell proliferation to be measured based on the protein content of each well (Skehan *et al.*, 1990). The optimal cell density for HeLa cells was determined by using the SRB assay as described in section 2.16.2.

2.15.2. *SRB Assay*

HeLa cells were seeded at 2 x 10^3 cells/well in 96-well plates and given 24 hrs to attach. Cells were then treated with a range of compound concentrations and incubated for 72 hrs. A day 0 control was plated and fixed on the day of drug treatment to provide a pre-treatment measure of cell number. Cells were fixed by adding 25µl of 50% (w/v) cold aqueous trichloroacetic Acid (TCA) to each well containing 100 µl of culture medium. After 1 hr at 4°C plates were washed with deionised water and stained with 0.4% (w/v) SRB in 1% (v/v) acetic acid for 30 minutes at room temperature. Unbound dye was removed with 1% (v/v) acetic acid and plates left overnight to air dry. Bound dye was solubilised by the addition of 100µl 10 mM Tris pH 9.5 and the optical density measured using a spectrophotometric plate reader (Model 680 Microplate Reader, Bio-Rad Laboratories, CA, USA) at 570 nm.

2.15.3. *Analysis*

GI_{50} values were calculated using GraphPad Prism Version 6.0 software (GraphPad Software Inc). Following corrections for the pre-treatment cell number, the percentage cell number relative to the control (DMSO only treated)

was calculated for each concentration, data were plotted and GI_{50} values determined based on a standard point to point curve with 1000 segments using GraphPad Prism statistical software.

2.16. Statistical Analyses

All statistical tests were performed using GraphPad Prism Version 6.0 software (GrpahPad Software Inc). Significance differences were determined by the tests stated and indicated as follows: * $p \geq 0.05$, ** $p \geq 0.01$, *** $p \geq 0.001$.

Chapter 3.
The relationship between MYCN and SKP2 expression in neuroblastoma cell lines

3.1. Introduction

3.1.1. *MYCN and neuroblastoma*

Amplification of the *MYCN* oncogene, first identified by Schwab *et al* (Schwab *et al.*, 1983), occurs in 20 to 25% of neuroblastoma and is a well-established prognostic indicator associated with rapid tumour progression and a poor outcome. There is strong experimental evidence that MYCN initiates and promotes neuroblastoma tumorigenesis evident by the dose-dependent tumour formation upon targeted *MYCN* expression in the neuroectoderm in transgenic mouse models (Weiss *et al.*, 1997). Functioning as a heterodimer with MAX, MYCN forms a functional transcriptional activator which exerts activity by directly binding to E-box motifs (CACA/GTG) located within the promoter regions of target genes. Implicated in multiple aspects of malignancy including the promotion of proliferation and metastasis and the suppression of apoptosis and differentiation, the diverse role of MYCN in neuroblastoma development continues to be investigated by attempting to identify the particular MYCN-driven genes which contribute to the aggressive phenotype of *MYCN*-amplified disease.

3.1.2. *The MYC family interchange*

The *MYC* family of oncoproteins have been implicated in the transcriptional regulation of genes involved in cellular proliferation, differentiation and apoptosis (Henriksson and Luscher, 1996). Sharing protein structural features and DNA consensus core binding sites (E-Box), evidence indicates a functional interchangeability within the family. *MYCN* and *c-MYC* are reported to display homologous coding regions and show similar oncogenic potential in *in vitro* transformation assays. Along with the ability of *MYCN* to replace *c-MYC* functions in embryonic development, it is often assumed that the molecular mechanisms known for c-MYC can be extrapolated to MYCN (Schwab *et al.*, 1985b; Kohl *et al.*, 1986; Malynn *et al.*, 2000).

Although greater progress has been made in the identification of c-MYC target genes, (http://www.myccancergene.org/site/about.asp) (Zeller *et al.*, 2003), known MYCN downstream targets, including indirect and putative direct MYCN targets, have been summarised in an attempt to clarify the current knowledge on MYCN activity (http://medgen.ugent.be/MYCNot) (Kumps *et al.*, 2013). In neuroblastoma there is an assumed redundancy between the two family members with functional interchange between c-MYC and MYCN in the regulation of tumorigenesis being well documented. Whilst deregulated MYCN expression identifies with an aggressive subtype in *MYCN* amplified neuroblastoma, the presence of MYCN in single-copy tumours correlates with a favourable clinical outcome (Tang *et al.*, 2006a). In neuroblastoma derived cell lines, c-MYC is often expressed in favour of MYCN in the absence of *MYCN* amplification due to each repressing the other at defined promoter sites, indicating a regulatory interaction (Breit and Schwab, 1989; Tang *et al.*, 2006a). Conversely, a subset of MYCN/c-MYC target genes have been identified which define malignant neuroblastoma progression independent of other established risk markers such as disease stage or *MYCN* amplification (Westermann *et al.*, 2008).

As a result of the homology between *MYC* family members a candidate gene approach can be used to identify MYCN target genes by investigating those previously identified as c-MYC transcriptional targets. This approach can also be adopted to investigate genes involved in the known biological functions of MYCN such as cell cycle progression. However, while there is considerable overlap in function between the *MYC* family members, they do maintain a distinct expression pattern in normal tissue with c-MYC expression correlating with high proliferative activity and MYCN and L-MYC playing a more dominant role in the differentiation of postmitotic cells (Hirvonen *et al.*, 1990). Therefore, while c-MYC is a useful candidate gene for the exploration of MYCN driven tumorigenesis, it is important to note that the two are not completely interchangeable.

Alternatively a whole genome approach can be utilised to investigate target genes differentially expressed in the presence and absence of MYCN, for example; studies in *MYCN* amplified vs. non-*MYCN* amplified cell lines or tumour cohorts, siRNA targeted MYCN knock down and MYCN regulatable cell lines. This

approach often uses microarray analysis or serial analysis of gene expression (SAGE) and identifies a broad spectrum of genes associated with *MYCN* amplification and expression which require further investigation to distinguish whether they are directly or indirectly regulated (reviewed by (Bell *et al.*, 2010)).

A direct target gene is one where MYCN drives transcription by binding to an E-box motif within close proximity of the transcriptional start site of the gene. An indirect target gene is one which shows no evidence of MYCN binding yet whose RNA or protein expression is altered as a result of MYCN driven mechanisms or pathways. Ultimately the identification of MYCN regulated genes allows for a further understanding of the biological role of MYCN in driving the tumorigenesis of neuroblastoma. As there is currently no inhibitor directly blocking MYCN, these downstream target genes may also provide potential therapeutic options in treating *MYCN* driven neuroblastoma.

3.1.3. *Identification of direct targets of MYCN*

For gene expression to be identified as a direct transcriptional target of MYCN a combination of ChIP and reporter gene assays are used to determine whether MYCN directly binds to the gene promoter region and functionally activates gene expression.

Principles of chromatin immunoprecipitation analysis

Chromatin immunoprecipitation (ChIP) is a technique which allows for analysis of DNA sequences that are bound by a given protein in living cells. A well-established technique it can be used to map the localisation of post-translationally modified histones, histone variants, transcription factors or chromatin modifying enzymes (Collas, 2010). Cells are first exposed to a crosslinking agent, such as formaldehyde, which covalently links nuclear proteins to the DNA sequences they are bound to at the moment of treatment, thereby creating stabilised DNA-protein complexes. The cells are then lysed and the nuclear material extracted and fragmented by sonication or enzymatic digestion *via* micrococcal nuclease. Using an appropriate antibody the protein of interest is immunoprecipitated and isolated from the remaining nuclear components creating an enriched pool of the specific DNA-protein complexes. To identify the bound DNA sequence, the crosslinking

is first reversed often by heat incubations or enzymatic digestion of the protein component by proteinase K. The purified DNA is then quantified using qRT-PCR as described in Section 2.10 to determine if the DNA from a specific promoter is present and whether a direct correlation exists between the amount of immunoprecipitated complex and bound DNA. While this technique determines whether a transcription factor can bind to a promoter, DNA ChIP-seq combines ChIP with DNA sequencing to identify the DNA binding sites of the immunoprecipitated proteins. Additionally ChIP-chip examines the DNA binding on a genome wide basis by utilising microarray analysis as described below, to identify further direct gene targets of the investigated DNA binding protein.

Reporter gene activation

A reporter gene, for example firefly luciferase as described in Section 2.12 is placed under the control of the particular promoter of interest. The reporter gene product activity can then be quantitatively measured in the presence or absence of MYCN expression using a MYCN regulatable expression system.

3.1.4. *Identification of indirect targets of MYCN*

An indirect gene target is one where mRNA or protein expression is altered in the presence of MYCN, but there is no evidence of MYCN binding. Instead, indirect target gene expression may be affected by downstream mechanisms or pathways initiated by MYCN expression. One such method of analysis is transcriptome profiling. Representing the transcripts present in a given cell i.e. mRNA, the transcriptome reflects the genes activated at a given time. Two methodologies are currently used, DNA microarray and RNA-seq.

Microarray analysis

DNA microarray technology measures the expression levels of thousands of genes simultaneously. A genome-wide analysis, it allows expression patterns of genes to be observed in response to a change in environmental conditions. To determine which genes are switched on or off in response to MYCN in a given cell, the mRNA is first collected and reverse transcribed into cDNA during which fluorescent nucleotides are incorporated labelling the treated and untreated cell

cDNA with different fluorescent dyes. The cDNA is then applied to a microarray chip which contains tens of thousands of pre-programmed probes, each with multiple single-stranded pieces of DNA attached to it which represent a specific gene sequence. The labelled cDNA is applied and hybridises to any complementary strands on the chip generating a fluorescent signal. After washing to remove sequences that are not specifically bound, the chip is imaged to detect which genes are expressed and at what level, based on the intensity of the signal which reflects the relative abundance of each mRNA transcript.

RNA-Seq

More recently RNA-Seq technology is being favoured. Using the same premise as microarray analysis, RNA-Seq utilises next-generation sequencing to identify and characterise gene expression. By the addition of sequencing adaptors onto the RNA-derived cDNA fragments, short sequence reads are determined which can be aligned with the reference genome or transcriptome (Wang *et al.*, 2009b). This technique carries an advantage over hybridisation-based techniques as it does not rely on a pool of previously collated DNA probes, allowing for identification of both known and novel genomic sequences. RNA-Seq has also been shown to have lower background noise and a greater dynamic range of expression levels over DNA microarray resulting in greater sensitivity and a more precise assessment of the gene expression profile.

These techniques have been used to identify MYCN target genes by observing their differential expression after MYCN induction, knockdown or manipulation in MYCN regulatable cell lines (Bell *et al.*, 2007; Schramm *et al.*, 2013). A whole genome approach, regulated genes identified using microarray analysis or RNA-Seq often require further investigation, for example to determine whether the mRNAs are translated into a protein product which contribute to the oncogenic behaviour of MYCN, and if so, whether they directly or indirectly target genes.

3.2. Aims

Taking into consideration the correlation between MYCN and SKP2 expression in neuroblastoma as well as the recognition of SKP2 as a direct c-MYC target gene, the overall aim of the work presented in this chapter was to further characterise the relationship between MYCN and SKP2 in neuroblastoma cell lines and establish whether *SKP2* is a direct transcriptional target gene of MYCN. These aims were addressed with the following specific objectives:

- To investigate the relationship between MYCN and SKP2 expression in the conditional MYCN expression systems SHEP Tet21N and SKNAS-Nmyc-ER.

- To clarify the impact of SKP2 on the expression of the CDK inhibitors p27 and p21, and cell cycle progression in the SHEP Tet21N conditional MYCN expression system.

- To evaluate the relationship between MYCN and SKP2 expression in a panel of *MYCN* amplified and non-amplified neuroblastoma cell lines.

- To determine whether SKP2 is a direct target of MYCN using chromatin immunoprecipitation (ChIP) analysis and a *SKP2* promoter reporter gene assay

3.3. Chapter specific material and methods

3.3.1. *Chromatin immunoprecipitation (ChIP)*

Chromatin Immunoprecipitation was kindly performed by Prof. Giovanni Perini, Giorgio Milazzo and Dr. Samuele Gherardi (University of Bologna, Italy) as previously described (Chen *et al.*, 2010b). The antibodies employed were: MYCN (Santa Cruz, B8.4.B, C-22), c-MYC (Santa Cruz N-262) and MAX (Santa Cruz C-17). Mapping of the transcription factor binding was determined on the *SKP2* promoter (-3000/+2000 bp) by SYBER green qRT-PCR using the six different pairs of primers listed in Table 3.1. DNA primers were designed in the proximity of canonical and non-canonical E-boxes of the *SKP2* promoter region centred round the transcriptional start site. The known MYCN target gene ornithine decarboxylase (ODC1) was used as a positive control using forward primer 5'-ATCACTTCCAGGTCCCTTGC-3' and reverse primer 5'-GAGAGCGGAAAAGGGAAATC-3'. All experiments were performed in triplicate.

E Box	Forward/Reverse	Sequence	Amplicon Size
A1	Forward Reverse	5'-GGCTTAGCCTAGGATTCTGCA-3' 5'-AAACCTCCCTTGTGCAGGTA-3'	184 bp
A	Forward Reverse	5'-CGTGTTTAGCTGTTGTGCGT-3' 5'-CGCACCTGTTCGTCCTTTTG-3'	124 bp
B	Forward Reverse	5'-GTGGGGATGGAACGTTGCTA-3' 5'-TTACCTGTGCATAGCGTCCG-3'	163 bp
C	Forward Reverse	5'-CGGGGGTATTGTGCACTTCT-3' 5'-TCCTGGGGGATGTTCTCACT-3	177 bp
D	Forward Reverse	5'-AGGAGTGGGCACAACAAACA-3' 5'-ACAAGCCAAGAGGGAATGCA-3'	152 bp
E	Forward Reverse	5'-AGGGTGGTCAGATTCCGGAT-3' 5'-TCTTCTTCGCCATCATCCCC-3'	128 bp
Dist	Forward Reverse	5'-CCGTTTGTTCTTGCCCCAAG-3' 5'-CCCTTGAACAGAGCTCACCA-3'	139 bp

Table 3.1 Primer sequences for MYCN ChIP analysis of *SKP2* promoter

3.4. Results

3.4.1. *Switching MYCN expression off in the Tet21N cell line influences SKP2 mRNA and protein expression*

Tet21N MYCN regulatable cells were treated with tetracycline (1 µg/ml) over 5 days and MYCN and SKP2 expression monitored by qRT-PCR and western blotting. After 24 hr exposure to tetracycline the Tet21N MYCN- cells showed a significant reduction in both *MYCN* and *SKP2* mRNA expression (Figure 3.1, p = 0.009 and 0.04, respectively, paired *t* test).

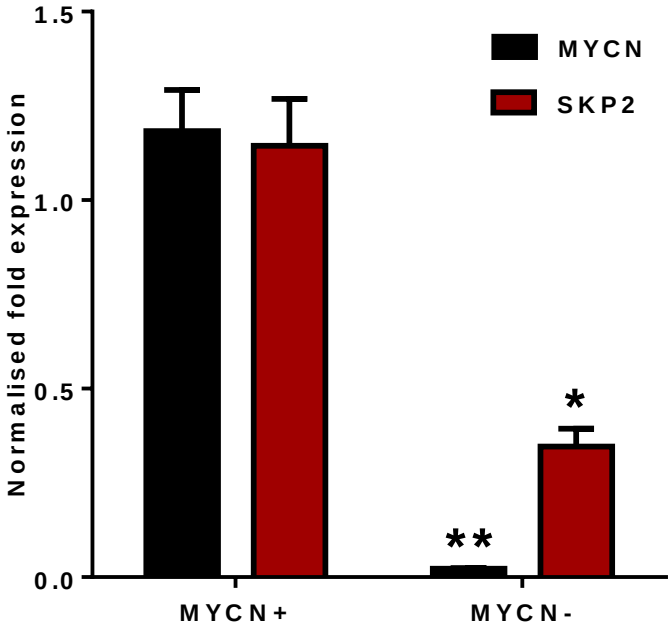

Figure 3.1 qRT-PCR analysis analysis of MYCN and SKP2 mRNA expression in the Tet21N cell line in the presence and absence of tetracycline. mRNA expression was normalised to the housekeeping gene GAPDH and expressed relative to the Tet21N-MYCN+ cells at day 1 of growth. Data are the mean and error bars represent the SEM of n=3 experiments. * and ** correspond to a p value of <0.05 and <0.01, respectively.

The decrease at transcript level translated to a complete loss of MYCN protein expression within 24 hr tetracycline exposure (Figure 3.2, day 3) with SKP2 protein expression gradually decreasing over the 5 days in line with the hypothesis that *SKP2* is a direct MYCN target gene. The loss of both MYCN and SKP2 expression was associated with an increase in protein levels of the SKP2 targets p27 and p21, in addition to an increase in the G_1 fraction of the cell cycle phase distribution (Figure 3.3a) and separation of the growth curves (Figure 3.3b). Taken together these data suggest that the G_1 arrest induced by switching off MYCN expression is in part due to stabilisation of the CDK inhibitors p27 and p21 resulting from the loss of SKP2.

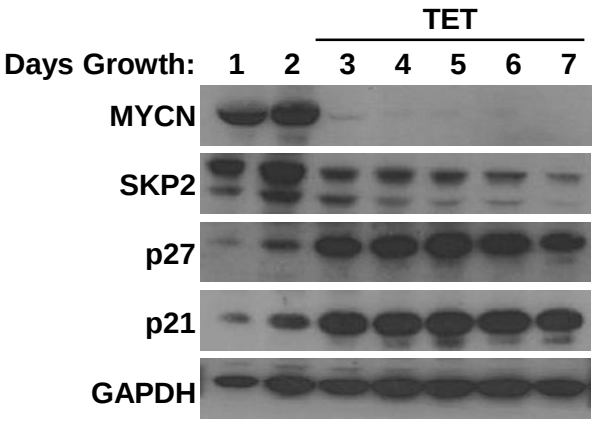

Figure 3.2 Western blot showing the effect of tetracycline on MYCN, SKP2, p27 and p21 expression in the Tet21N cell line. Cell lysates were collected at the time points stated. The western blot shown is a representative of 3 independent repeats.

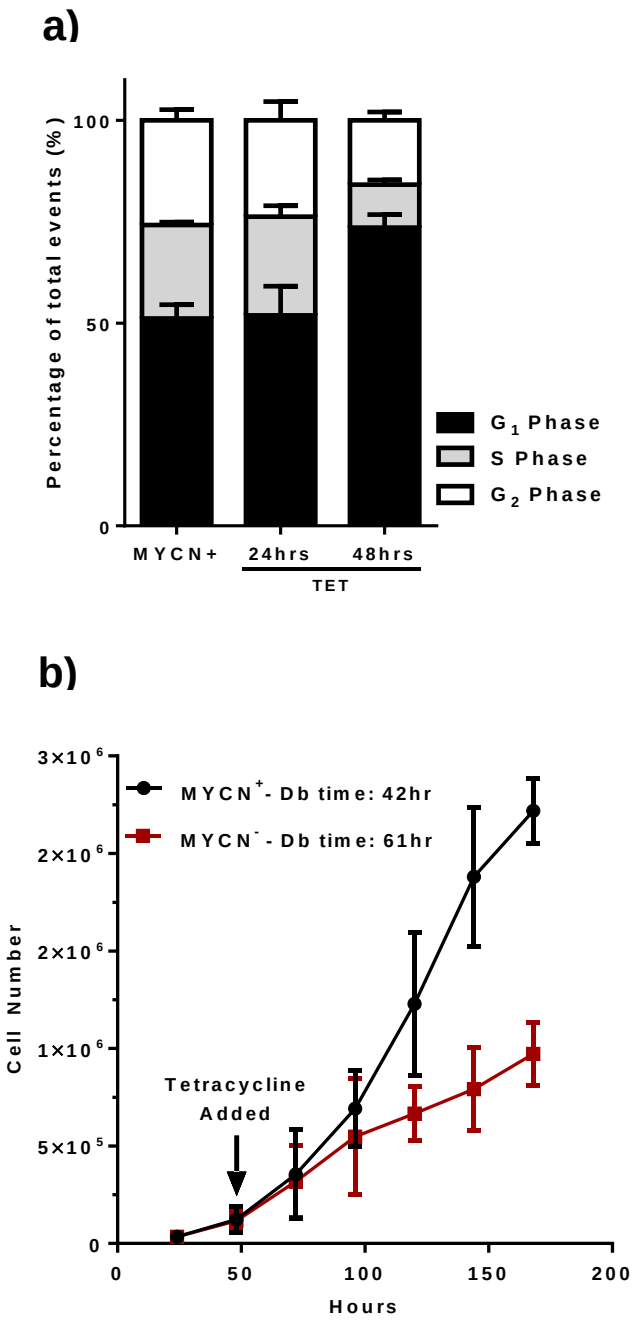

Figure 3.3 Cell cycle analysis and proliferation of Tet21N cells grown in the presence and absence of tetracycline. a) Percentage distribution of cell cycle phase populations measured by flow cytometry **b)** Growth curves of Tet21N MYCN+ and MYCN-. Cell number was determined by a Coulter counter. Data are the mean and error bars represent the SEM of n=3 experiments. Db = doubling time.

3.4.2. *Reduction of SKP2 protein expression stabilises p27 protein expression in the Tet21N cell line*

As MYCN overexpression promotes S phase entry, the transcript levels of p27 and p21 were measured by qRT-PCR to determine whether the increased expression of the CDK inhibitors was from enhanced transcription (Figure 3.4). Given that the mRNA expression of p27 and p21 were found to increase substantially following the removal of MYCN, Tet21N cells were treated with a combination of tetracycline and the mRNA translation inhibitor cycloheximide (25 µmol/L), to determine the contribution of SKP2 loss (Figure 3.5). Cycloheximide treatment decreased MYCN and SKP2 protein expression (lanes 3 and 4), mirroring the effect of tetracycline only (lanes 5-7), and reduced the level of p27 and p21. Only p27 protein was still present, although at a reduced level, after combination treatment (lanes 8 and 9). Combined with the findings from the qRT-PCR, these results suggest that the loss of SKP2 in the Tet21N MYCN- cells resulted in post-translational stabilisation of p27 but not p21.

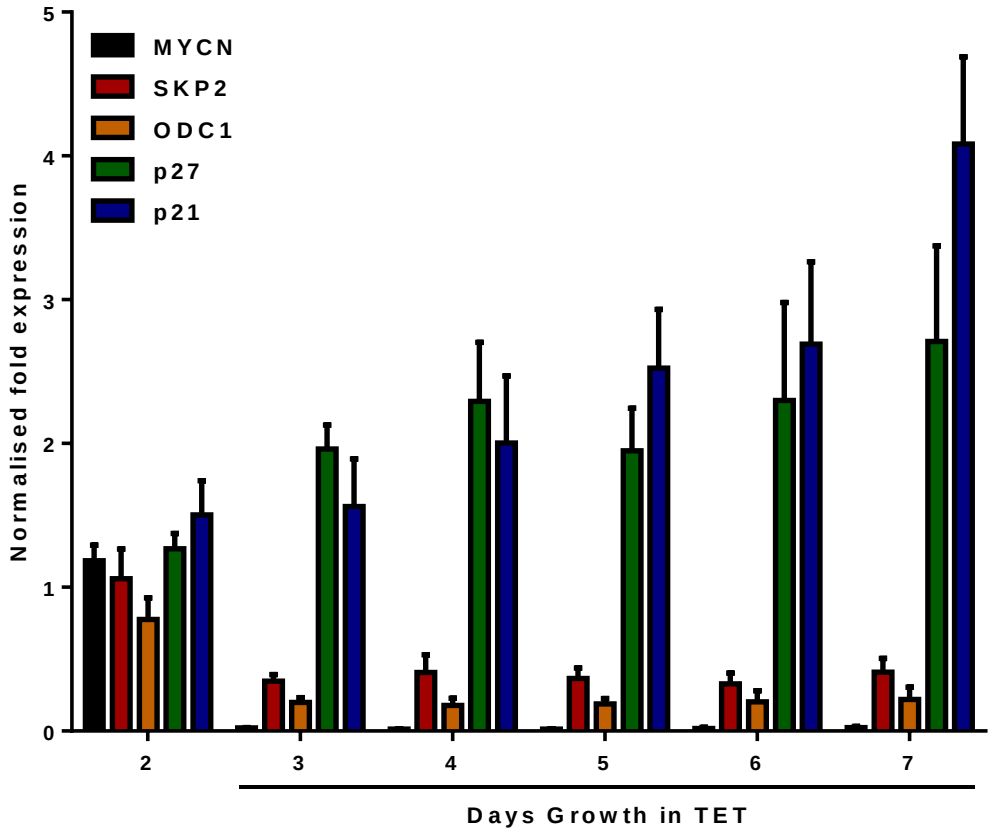

Figure 3.4 qRT-PCR analysis of MYCN, SKP2, p27 and p21 mRNA expression in the Tet21N cell line in the presence and absence of tetracycline. mRNA expression was normalised to the housekeeping gene GAPDH and expressed relative to Tet21N-MYCN+ cells at day 1 of growth.

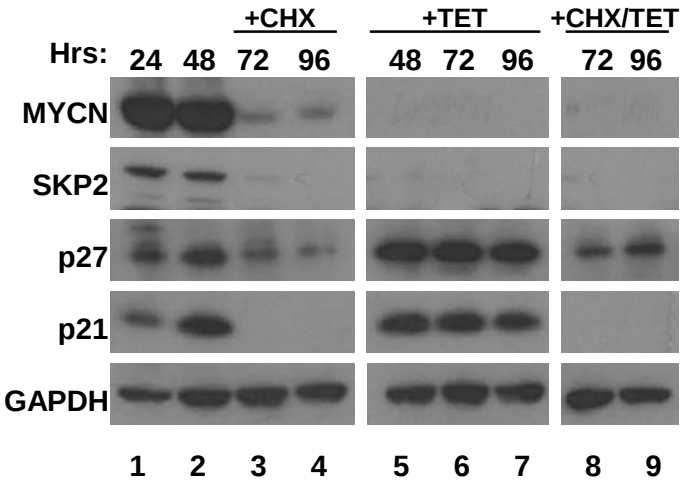

Figure 3.5 Western blot of the effect of tetracycline (TET) and cycloheximide (CHX) treatment on the expression of MYCN, SKP2, p27 and p21 in the Tet21N cell line. Cell lysates were collected at timepoints stated. The western blot shown is a representative of 3 independent repeats

3.4.3. *Activation of MYCN transcriptional activity only influences SKP2 at the* transcript *level in the SKNAS-Nmyc-ER cell line*

The involvement of MYCN in the regulation of SKP2 expression was further demonstrated in the SKNAS-Nmyc-ER cell line. Expressing a hybrid N-*myc*-oestrogen receptor protein (Nmyc-ER), the construct is only active when the ER domain is bound to 4-hydroxytamoxifen (4-OHT), due to the point mutation (G525R) in the receptor domain as discussed in Section 2.2.5. As shown in Figure 3.6a, after 48 hrs exposure to 4-OHT (100 ng/ml) *SKP2* mRNA expression increased significantly ($p = 0.02$, paired t-test); however, this did not translate to an increase in SKP2 protein expression (Figure 3.6b), suggesting that MYCN only plays a partial role in regulating SKP2. Interestingly, as shown in Figure 3.7, the addition of 4-OHT caused a significant growth suppression of the SKNAS-Nmyc-ER cell line ($p = 0.001$, paired t test) as measured by the XTT assay described in Section 2.15.2. This effect is consistent with recent reports where enhanced *MYCN* expression in a non-*MYCN* amplified setting was shown to reduce the viability of neuroblastoma cells through the induction of apoptosis and promotion of expression of favourable genes (i.e. genes whose high expression levels predict a favourable clinical outcome) (Tang *et al.*, 2006b; Valentijn *et al.*, 2012). The SKNAS-Nmyc-ER cell line, prior to 4-OHT treatment also had a slower doubling time than the SKNAS parental cell line, suggesting the vector was affecting the cell cycle, independent of 4-OHT treatment (Figure 3.7, black line on both graphs)

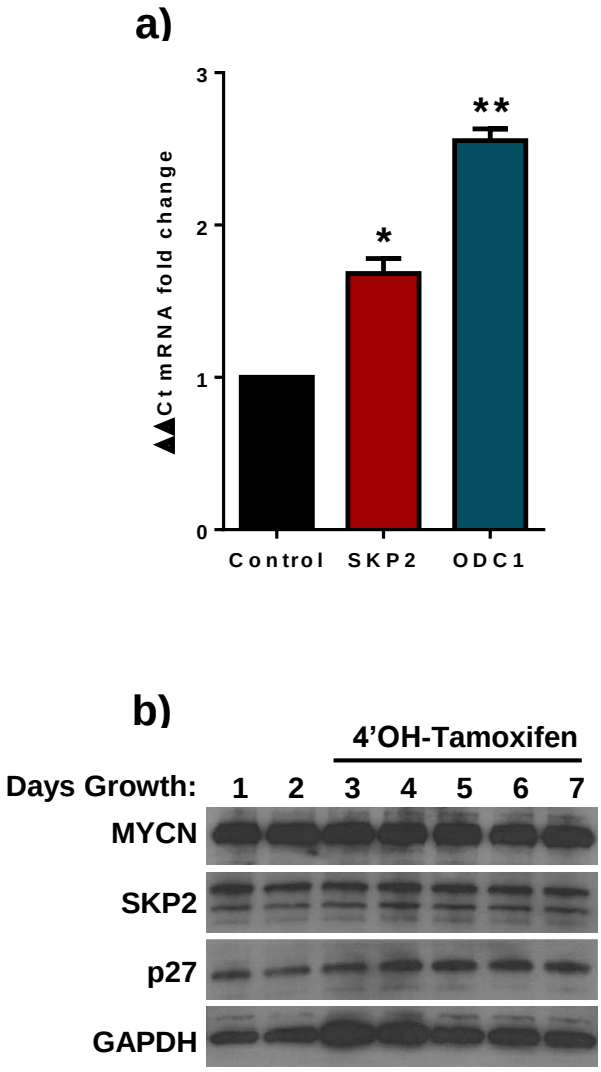

Figure 3.6 qRT-PCR and protein analysis of MYCN activation in the SKNAS-Nmyc-ER cell line. a) Fold change of mRNA level of *SKP2* and *ODC1* after 48 hr exposure to 4-OHT. mRNA was normalised to the housekeeping gene GAPDH and expressed relative to the UT control. Data are the mean and error bars represent the SEM of n=3 experiments. * and ** correspond to a p value of <0.05 and <0.01, respectively. **b)** Western blot showing the effect of 4'OHT on the expression of MYCN, SKP2, p27 and p21. Cell lysates were collected at timepoints stated. The western blot shown is a representative of 3 independent repeats.

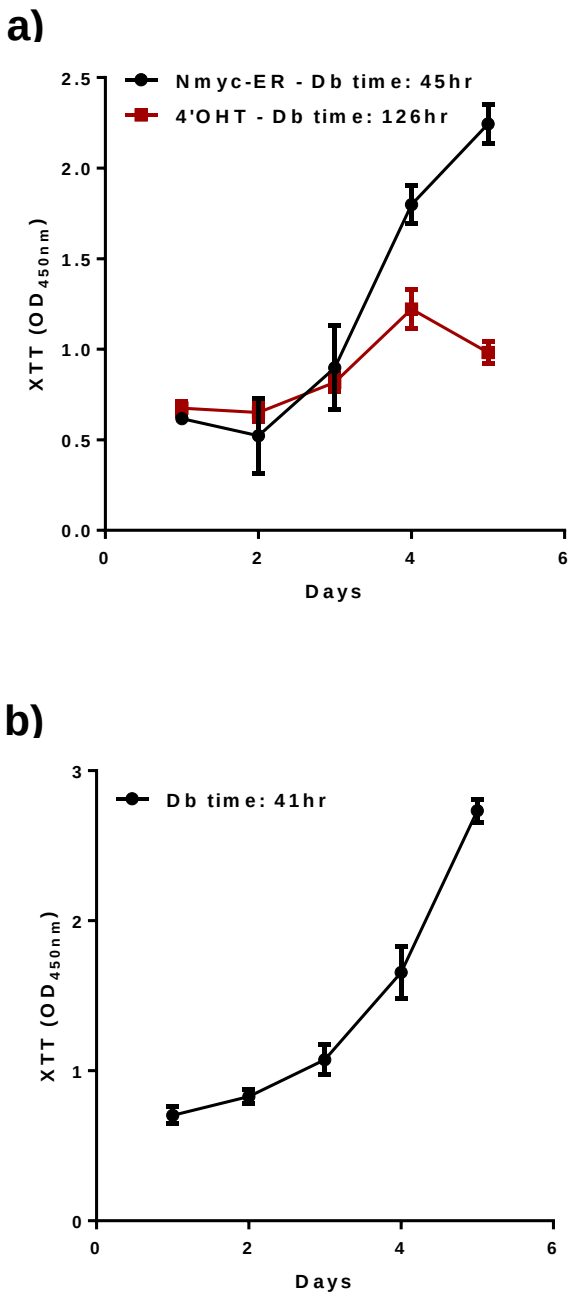

Figure 3.7 Rate of proliferation of the SKNAS and SKNAS-Nmyc-ER cell line analysed by XTT assay. a) Growth curve for the SKNAS-Nmyc-ER cell line in the presence and absence of 4'OHT**.** Data are the mean and error bars represent the SEM of n=3 experiments. **b)** Growth curve for the SKNAS cell line. Data are the mean and error bars represent the SEM of 5 individual wells on a 96 well plate. Both SKNAS-Nmyc-ER and SKNAS cell lines were seeded at 4000 cells/well. Db = doubling time.

3.4.4. *The relationship between MYCN, SKP2, p27 and p21 expression in neuroblastoma cell lines*

To further investigate the relationship between MYCN and SKP2, mRNA expression was analysed by qRT-PCR and protein levels by densitometry in a panel of *MYCN* amplified (*MNA*) and non-*MYCN* amplified (non-*MNA*) neuroblastoma cell lines (Figure 3.8). A significant correlation was observed between MYCN protein and *SKP2* mRNA expression (Pearsons correlation, r = 0.92, p = 0.01, Figure 3.9) but not with SKP2 protein levels at the 95% level (Pearsons correlation, r = 0.77, p = 0.07, Figure 3.10). The relationship between MYCN protein and *SKP2* mRNA is consistent with the hypothesis that MYCN regulates SKP2 at the transcript level, and is further supported by the significant Spearman correlation between MYCN and SKP2 protein levels (Spearman correlation, r = 1, p = 0.003, Figure 3.10) when a rank order correlation analysis was performed. These cell line data are consistent with the previous report that SKP2 is a prognostic indicator in neuroblastoma independent of MYCN, yet is often found at its highest level in *MYCN*-amplified tumours (Westermann *et al.*, 2007).

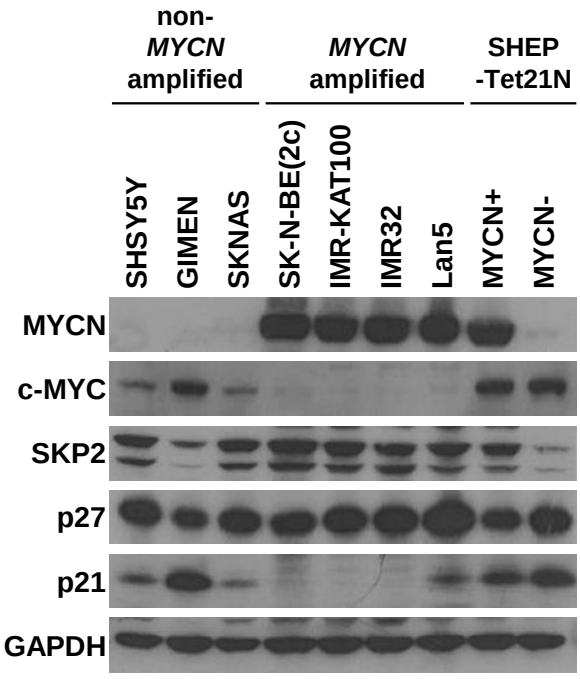

Figure 3.8 Western blot showing the basal level of MYCN, c-MYC and SKP2 in a panel of neuroblastoma cell lines. The western blot shown is a representative of 2 independent repeats.

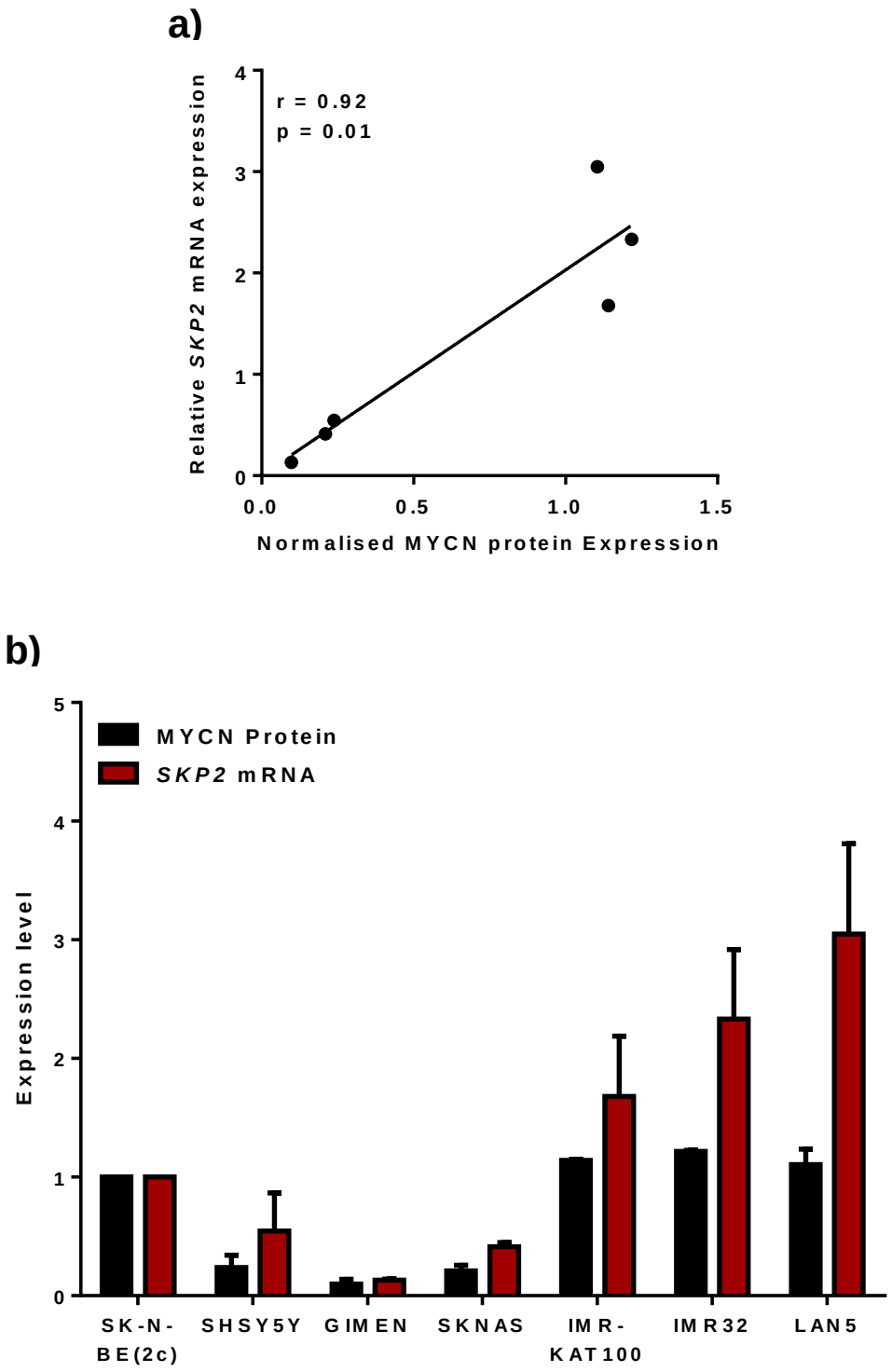

Figure 3.9 Comparison of MYCN protein and *SKP2* transcript levels in a panel of neuroblastoma cell lines. a) Linear regression analysis. Each point is a separate cell line, r the Pearson correlation coefficient and p the significance. **b)** MYCN protein and *SKP2* transcript level in each cell line. mRNA expression was determined by qRT-PCR and protein expression by densitometry. Both sets of data were first normalised to GAPDH and expressed relative to the *MYCN* amplified SK-N-BE(2c) cell line. Data are the mean and error bars represent the SEM of n=2 experiments.

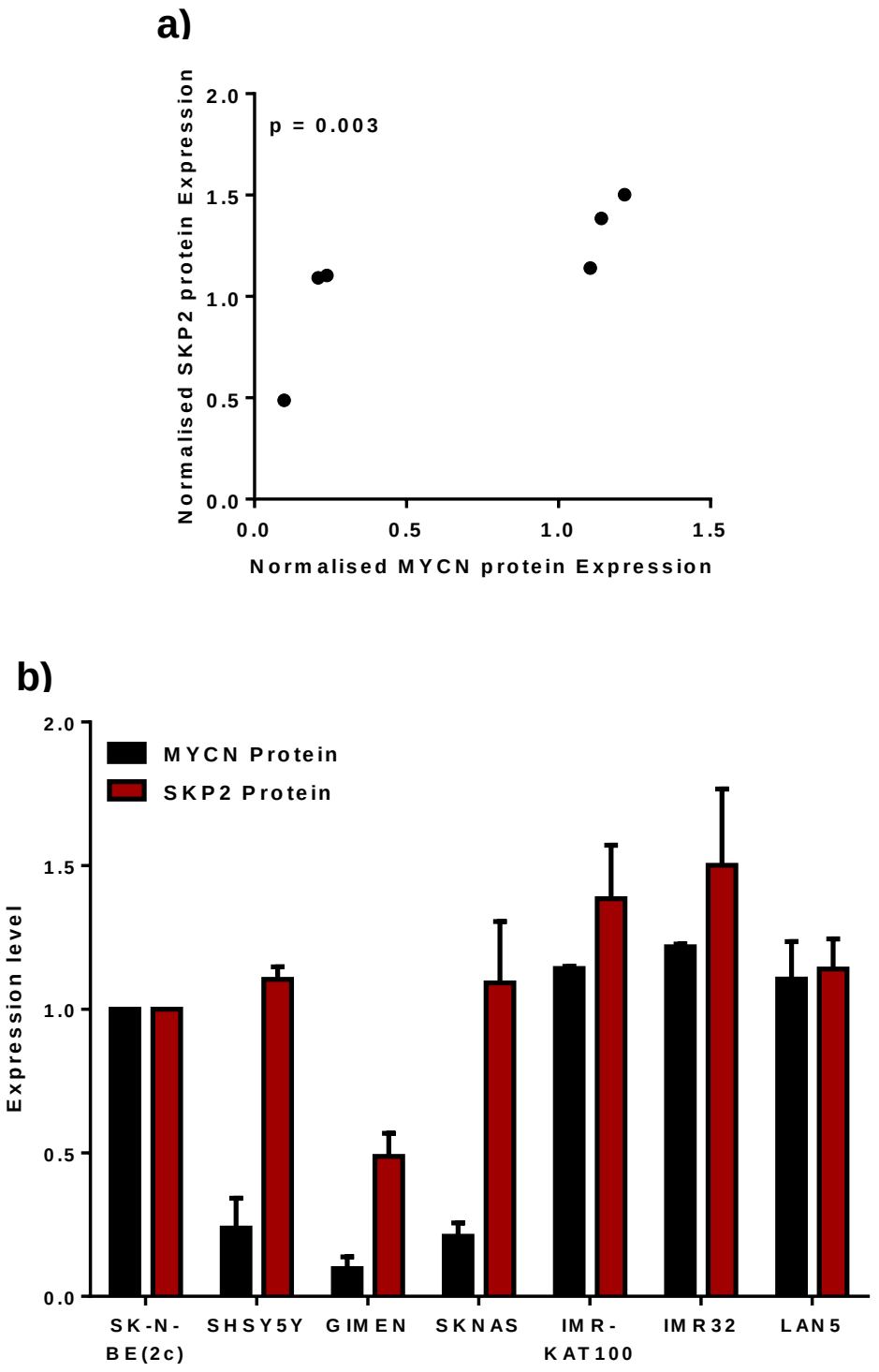

Figure 3.10 Comparison of MYCN and SKP2 protein level in a panel of neuroblastoma cell lines. a) Linear regression analysis. Each point is a separate cell line and p the significance **b)** MYCN and SKP2 protein level in each cell line. Protein expression was determined by densitometry, normalised to GAPDH and expressed relative to the *MYCN* amplified SK-N-BE(2c) cell line. Data are the mean and error bars represent the SEM of n=2 experiments.

3.4.5. *MYCN expression sensitises Tet21N cells to cell cycle arrest.*

To further characterise the role of SKP2 and its relationship with MYCN in the Tet21N model, SKP2 protein was successfully knocked down using siRNA (Figure 3.11a). SKP2 loss resulted in a clear increase in p21 protein levels independent of MYCN and yet only influenced p27 levels in the Tet21N-MYCN+ cells, although this may be due to the higher basal expression of p27 in the Tet21N-MYCN- cells masking the influence of SKP2 inhibition.

The presence or absence of MYCN did not influence the effect of SKP2 knockdown on cell proliferation (Figure 3.11b) as significant growth inhibition, compared to the negative control siRNA (NCS), was observed after 72 hr treatment with the siRNA regardless of MYCN status ($p \leq 0.01$, paired t test). However cell cycle arrest, measured by an increase in the G_1:S ratio after 24 hr SKP2 siRNA exposure, was only induced in the Tet21N MYCN+ cells ($p = 0.01$, paired t test) and not in the Tet21N MYCN- cells (Figure 3.12a).

Although the different effects on cell cycle could be the result of the enhanced stability of p27 and p21, as suggested by the western blot (Figure 3.11a), it may also reflect the role of MYCN in cell cycle regulation. Tet21N MYCN- cells have a markedly higher proportion of cells in G_1 compared to Tet21N MYCN+ cells, which have a larger percentage of cells in S phase consistent with the role of MYCN in regulating proliferation (Figure 3.12b). The effect on the G_1:S ratio in Tet21N MYCN+ cells may therefore reflect, in part, the lower baseline G_1 population of 50% as opposed to the Tet21N MYCN- cells where the baseline G_1 population may already be maximal at 80%.

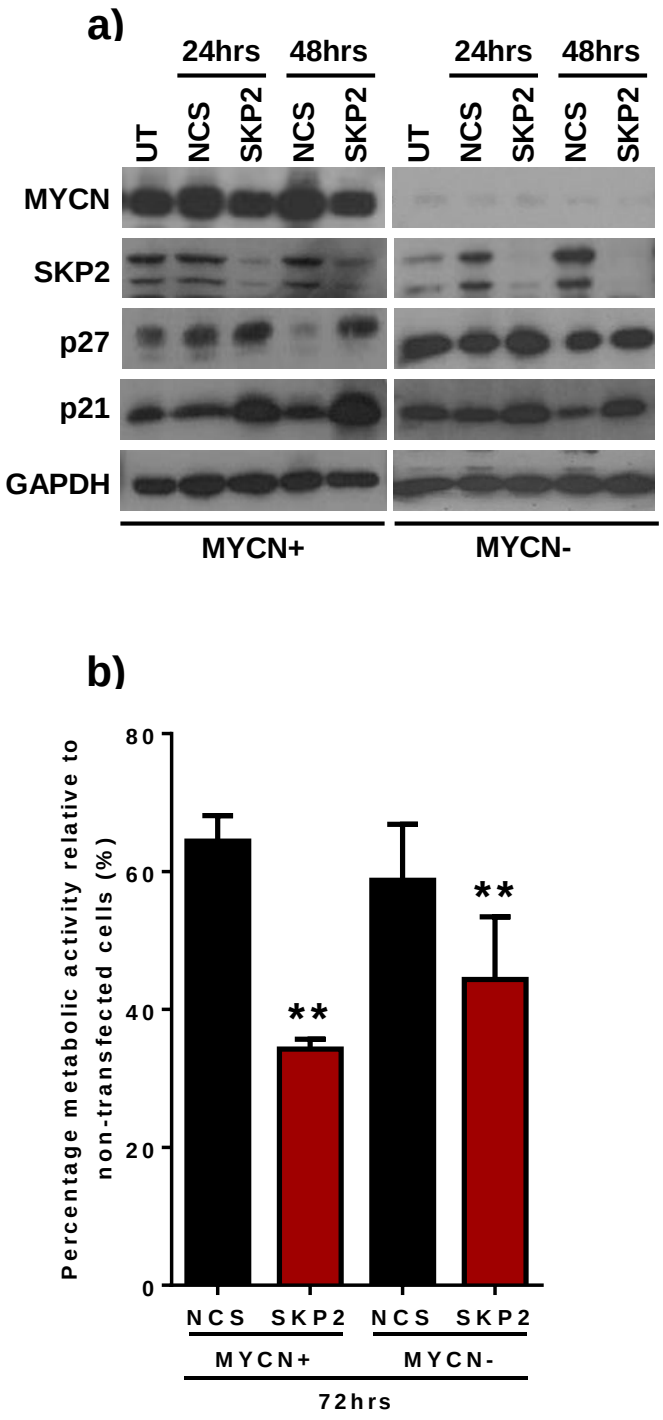

Figure 3.11 The effect of SKP2 siRNA transfection on p27 and p21 protein expression and cell proliferation in the Tet21N cell line. a) Western blot showing the effect of SKP2 knockdown (SKP2) on p27 and p21 protein level. Knockdown is compared to negative control siRNA (NCS) and cell lysates collected at time points indicated. The western blot shown is a representative of 3 independent repeats. **b)** Cell proliferation: An XTT assay was performed after 72 hr exposure to siRNA. Data are normalised to non-transfected cells. Data are the mean and error bars represent the SEM of n=3 experiments. * and ** correspond to a p value of <0.05 and <0.01, respectively.

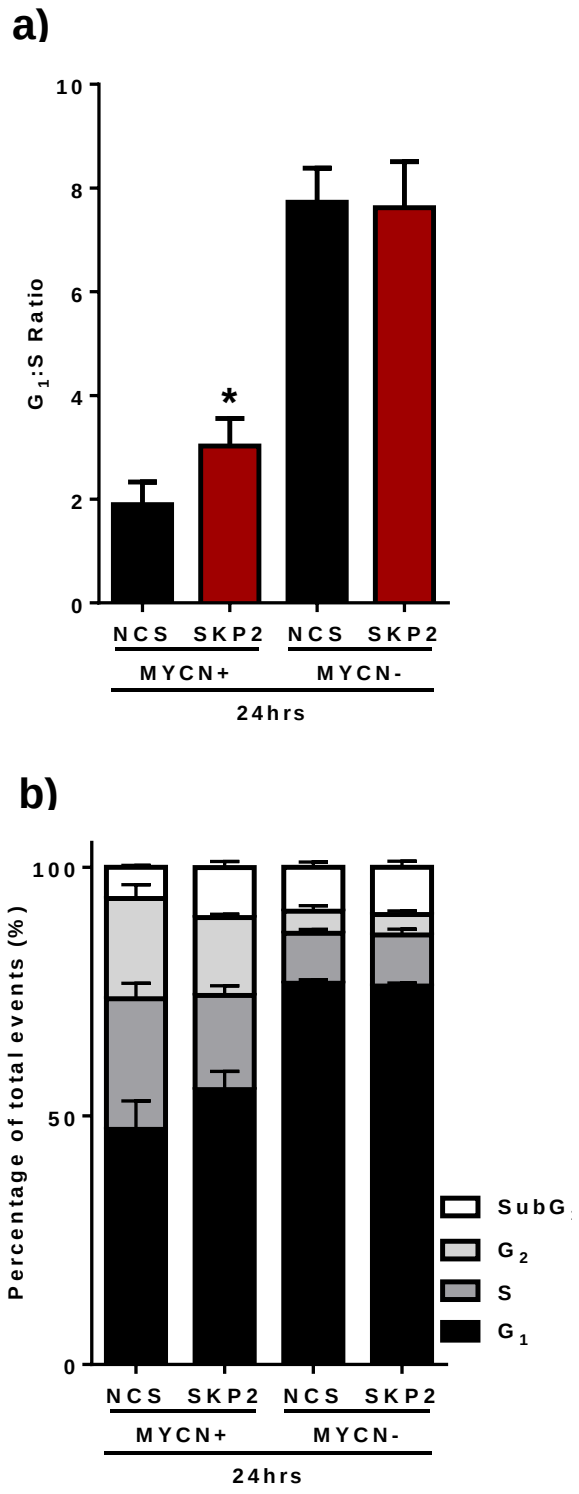

Figure 3.12 The effect of SKP2 siRNA transfection on the G_1/S ratio and cell cycle phase distribution in the Tet21N cell line. a) G_1/S ratio measured by flow cytometry after a 24 hr exposure to siRNA. **b)** Cell cycle phase distribution after 24 hr exposure to SKP2 siRNA compared to negative control siRNA (NCS). Data are the mean and error bars represent the SEM of n=3 experiments.

3.4.6. *SKP2 knockdown induces apoptosis independently of MYCN expression in the Tet21N cell line*

Two techniques were used to investigate the levels of apoptosis following SKP2 knockdown; the induction of a population of cells with a sub-G_1 DNA content and activation of caspase-3/7. There was a significant increase in the sub-G_1 population following 48 hrs SKP2 siRNA treatment independent of the presence of MYCN (Figure 3.13a); however, the increase was greater in Tet21N MYCN+ ($p = 0.007$ paired t test) than in Tet21N MYCN- cells ($p = 0.02$ paired t test). This difference was confirmed by analysing caspase 3/7 activity (Figure 3.13b). Consistent with the sub-G_1 fraction from the flow cytometry data, the Tet21N cells showed an increase in caspase 3/7 activity 24 hrs after exposure to SKP2 siRNA compared to the negative control siRNA (NCS). However, the response was only statistically significant in the Tet21N MYCN+ cells ($p = 0.05$, paired t test).

A reduction in the G_1 fraction was observed in both Tet21N MYCN+ and MYCN- cells following SKP2 knockdown, yet only reached significance in the Tet21N MYCN+ cells (Figure 3.14a, $p = 0.03$, paired t test). As there was no change in either the S phase or G_2 phase population following a 48 hr exposure to SKP2 siRNA (Figure 3.14b), the apoptotic response to SKP2 knockdown may be a result of replication stress.

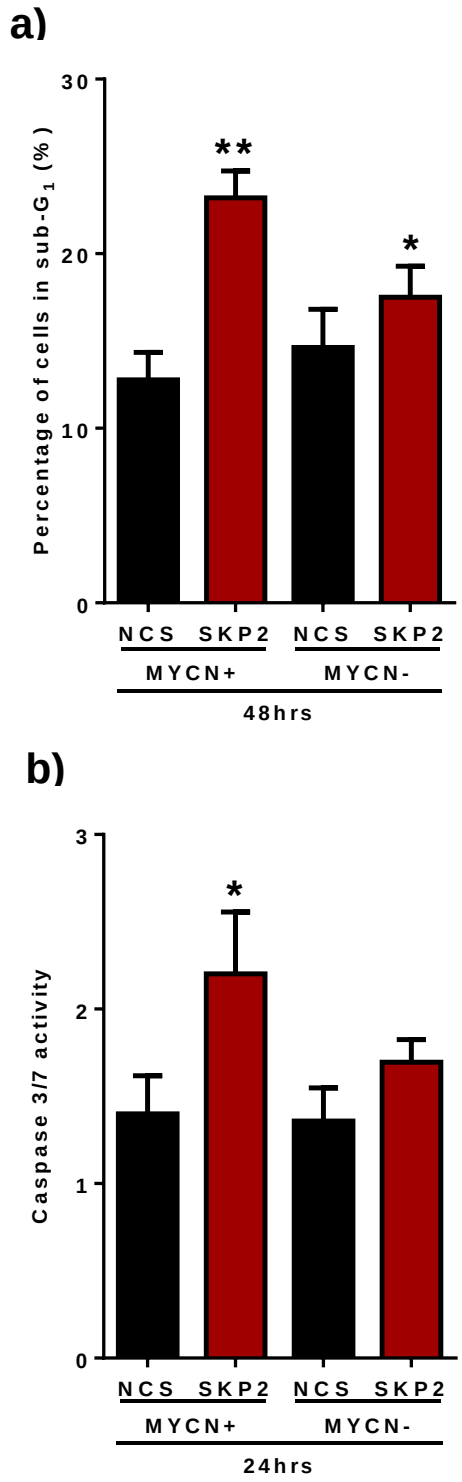

Figure 3.13 The effect of SKP2 siRNA transfection on apoptosis in the Tet21N cell line. a) Percentage of cells in sub-G_1 DNA fraction of the cell cycle measured by flow cytometry after 48 hr exposure to SKP2 siRNA. **b)** Caspase-3/7 activity after 24 hr exposure to SKP2 siRNA. Data are normalised to the non-transfected (NT) control and compared to negative control siRNA (NCS). Data are the mean and error bars represent the SEM of n=3 experiments. * and ** correspond to a p value of <0.05 and <0.01, respectively.

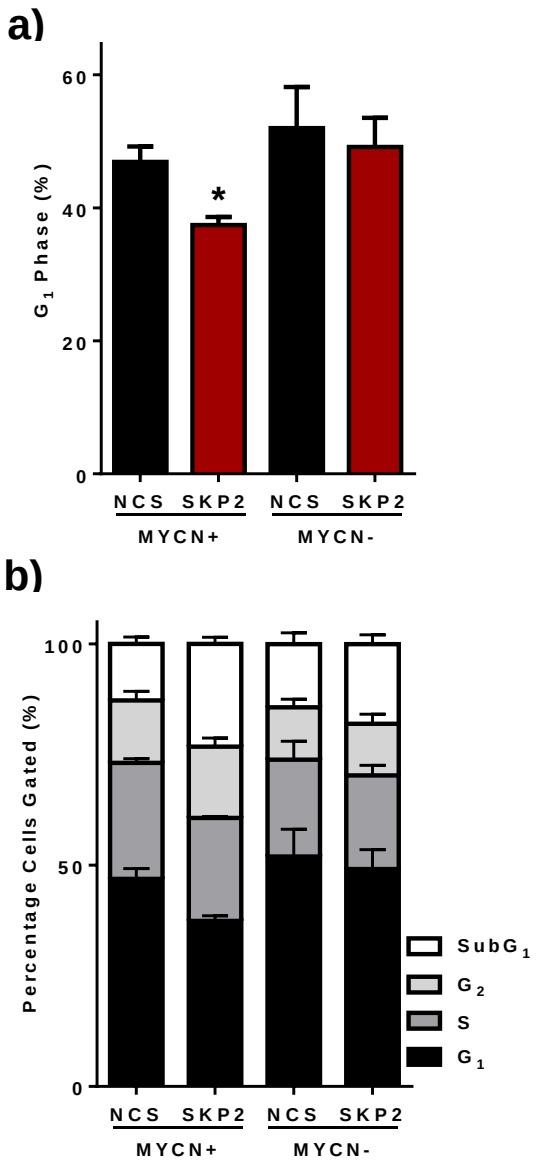

	Tet21N MYCN+		Tet21N MYCN-	
	NSC	**SKP2**	**NCS**	**SKP2**
G_1 Phase	47 ± 4	37 ± 2	52 ± 11	49 ± 8
S Phase	26 ± 2	23 ± 1	22 ± 7	21 ± 4
G_2 Phase	14 ± 4	16 ± 3	12 ± 3	12 ± 4
Sub-G_1 Phase	13 ± 3	23 ± 3	14 ± 4	18 ± 4

Figure 3.14 The effects of a 48 hr exposure to SKP2 siRNA on the cell cycle in the Tet21N cell line. a) G1 cell cycle phase distribution **b)** Cell cycle phase distribution. Data were analysed by flow cytometry after 48 hr exposure to SKP2 siRNA and compared to negative control siRNA (NCS). Data are the mean and error bars represent the SEM of n=3 experiments. * and ** correspond to a p value of <0.05 and <0.01, respectively.

3.4.7. *The role of the SKP2/p27 axis in cell cycle arrest and apoptosis induced by Skp2 knockdown in Tet21N MYCN+ cells*

To establish the extent to which p27 stabilisation contributed to the G_1 arrest in Tet21N MYCN+ cells, dual knockdown of p27 and SKP2 was investigated. Preventing p27 expression attenuated the cell cycle arrest induced by SKP2 knockdown, implying that SKP2/p27 relationship plays a key role in the regulation of the G_1/S transition by SKP2 in Tet21N MYCN+ cells ($p = 0.04$ paired t test, Figure 3.15a).

Unexpectedly, a larger sub-G_1 fraction, indicative of apoptotic cell death, was observed following the 48 hr exposure to p27 siRNA than following the 48 hr exposure to SKP2 siRNA ($p = 0.02$ paired t test, Figure 3.15b). The sub-G_1 population was reduced ($p = 0.02$ paired t test) following the dual knockdown suggesting that the accumulation of p27 plays a role in the apoptotic cell death induced by SKP2 knockdown.

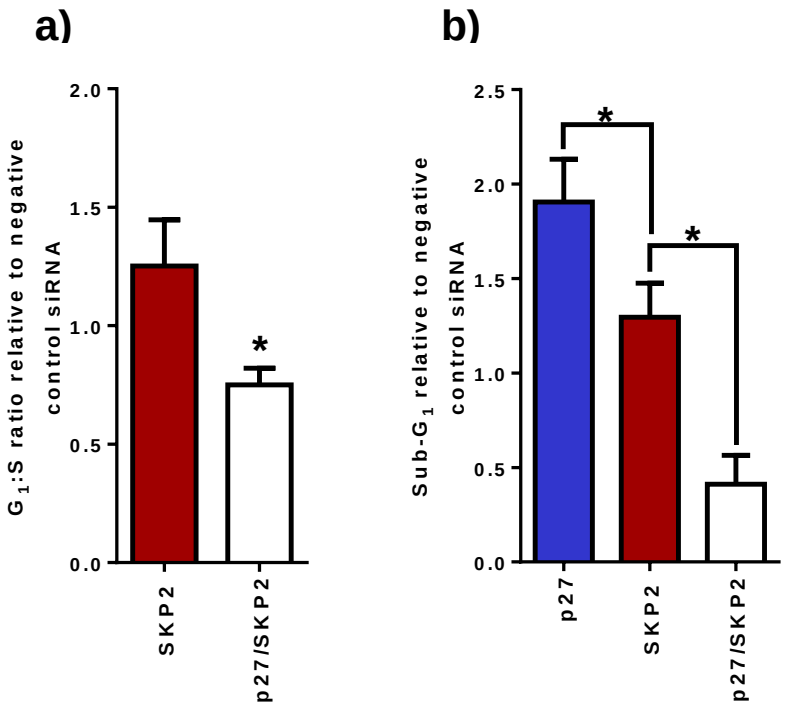

Figure 3.15 The effect of dual knockdown of SKP2 and p27 on G_1 arrest and apoptosis in the Tet21N MYCN+ cells. The effect of dual knockdown on **a)** G_1:S ratio and **b)** Sub-G_1 fraction. Data was normalised to the negative control siRNA and the mean plotted. Error bars represent the SEM of n=3 experiments. * corresponds to a p value of < 0.05.

3.4.8. *MYCN directly binds to and activates the human SKP2 promoter*

MYCN ChIP was performed in the SHEP-Tet21N MYCN regulatable cells, *MYCN* amplified IMR32 and non-amplified SHSY5Y cell lines using the established MYCN target gene *ODC1* as the positive control. MYCN was observed to bind to several non-canonical E-boxes in both TET21N MYCN+ (Figure 3.16, maroon bar) and IMR32 cells (Figure 3.17), as well as a canonical E-Box downstream of the transcriptional start site (TSS). The highest MYCN binding was observed at the TSS level (amplicon B), and was reduced to an un-detectable level after a week of tetracycline treatment in the Tet21N cell line (Figure 3.15, pink bar). No MYCN binding was observed in the SHSY5Y cells (Figure 3.18), as predicted, although a high intensity of c-MYC binding was observed which mirrored that of MYCN in the IMR32 cell line. The binding of MYCN to the *SKP2* promoter was confirmed by ChIP-chip arrays in a second MYCN-inducible system and in the *MYCN*-amplified Kelly cell line (Figure 3.19) performed by Ray Stallings (Royal College of Surgeons in Ireland, Dublin, Ireland). Significant MYCN binding was seen in the 5' region of the *SKP2* gene in SHEP cells (MYCN high expression) which was abrogated when the cells were treated with DOX to produce low MYCN expression. A high level of MYCN binding to the *SKP2* promoter was also observed in *MYCN* amplified Kelly cells.

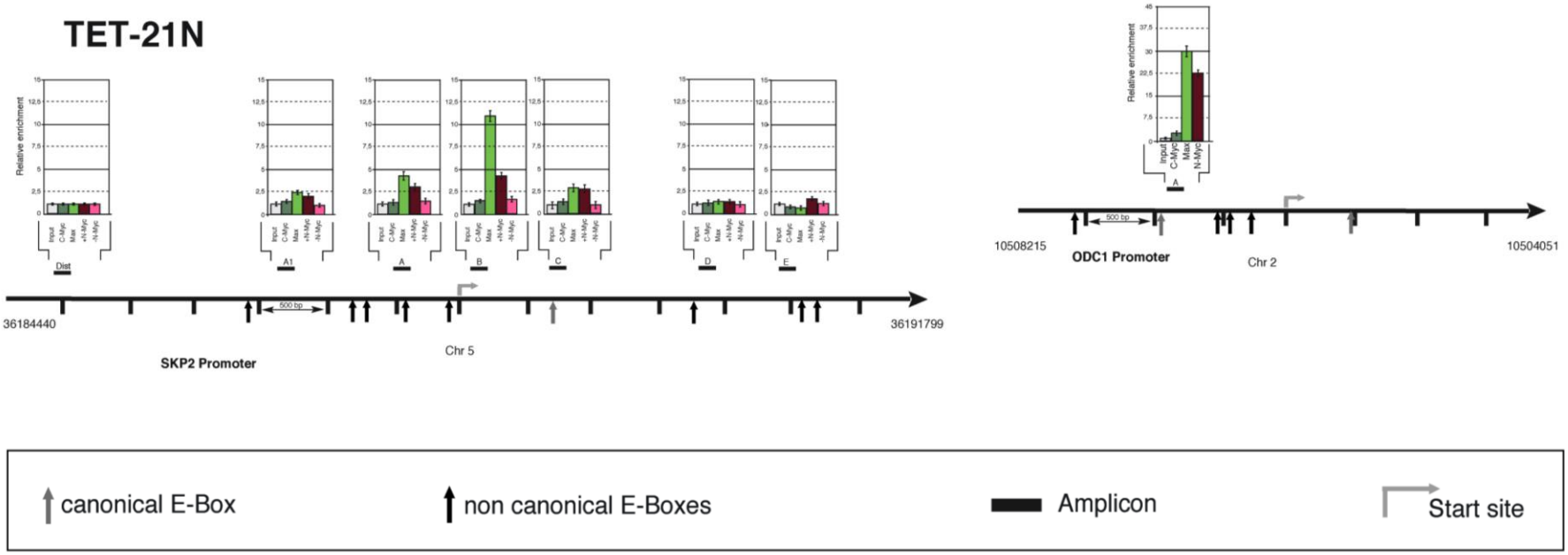

Figure 3.16 Binding of MYCN, MAX and c-MYC to the *SKP2* promoter in SHEP-Tet21N MYCN regulatable cells as determined by quantitative ChIP. Fold enrichment is relative to INPUT-DNA. Maroon bar represents cells in the absence of tetracycline (MYCN+) and pink bar represents MYCN binding following a week exposure to tetracycline (MYCN-). The *ODC*1 promoter was used as a positive control. Bent arrow, transcription start site; grey arrow, canonical E-box; black arrow, non-canonical E-box; black boxes, amplicons indicated with a capital letter. Chromosome coordinates (bp) of the human *SKP2* promoter are also given. Data are the mean and error bars represent the SEM of n=3 experiments. Experiments were performed by G. Perini and co-workers, University of Bologna, Italy.

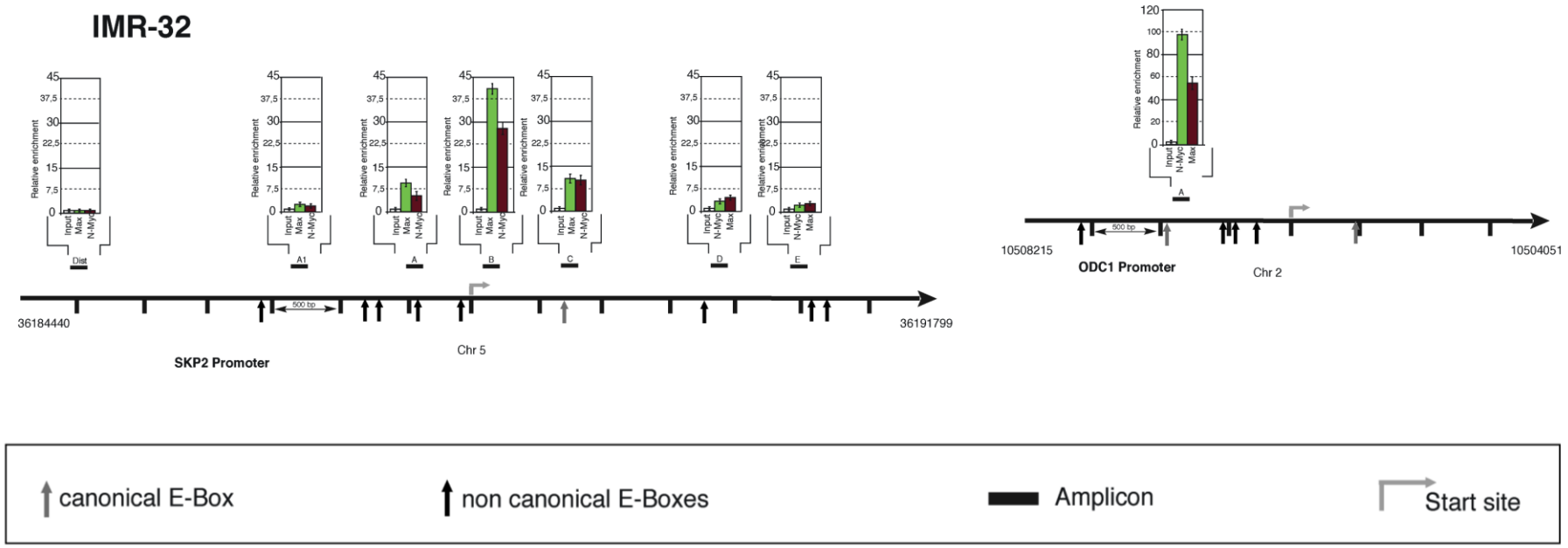

Figure 3.17 Binding of MYCN, MAX and c-MYC to the *SKP2* promoter in *MYCN* amplified IMR32 cells as determined by quantitative ChIP. Fold enrichment is relative to INPUT-DNA. The *ODC1* promoter was used as a positive control. Bent arrow, transcription start site; grey arrow, canonical E-box; black arrow, non-canonical E-box; black boxes, amplicons indicated with a capital letter. Chromosome coordinates (bp) of the human *SKP2* promoter are also given. Data are the mean and error bars represent the SEM of n=3 experiments. Experiments were performed by G. Perini and co-workers, University of Bologna, Italy.

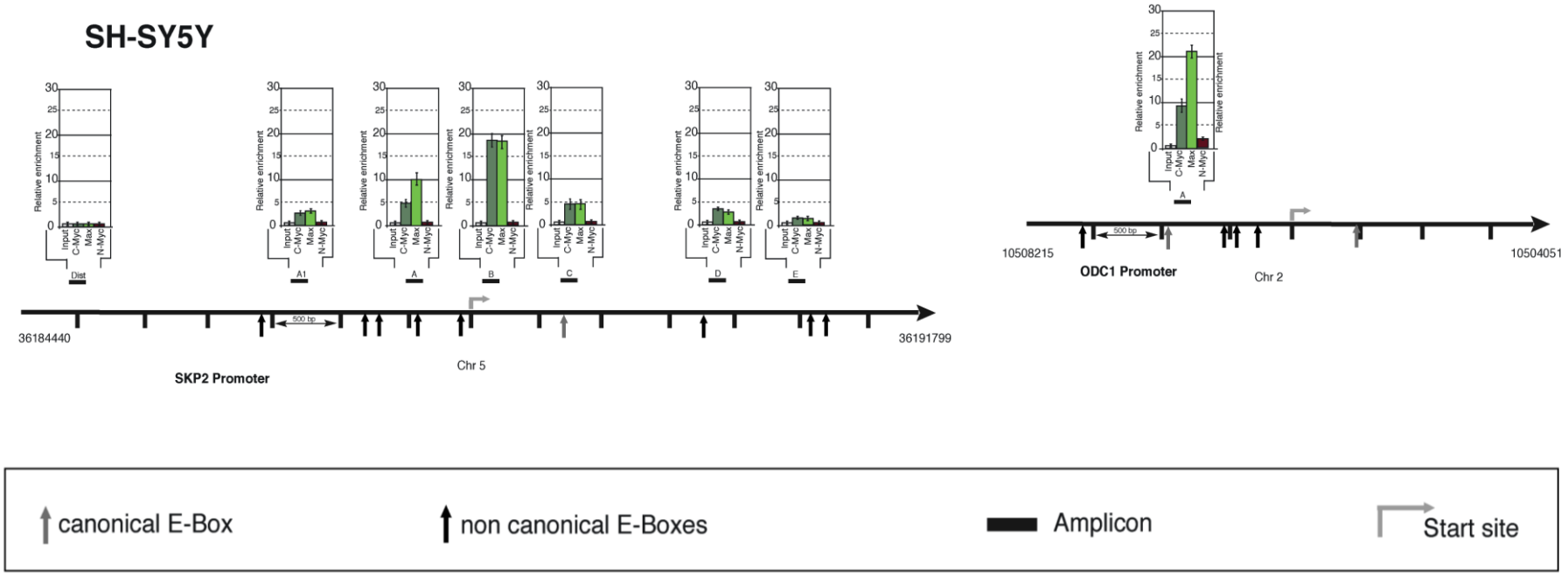

Figure 3.18 Binding of MYCN, MAX and c-MYC to the *SKP2* promoter in non-*MYCN* amplified SHSY5Y cells as determined by quantitative ChIP. Fold enrichment is relative to INPUT-DNA. The *ODC1* promoter was used as a positive control. Bent arrow, transcription start site; grey arrow, canonical E-box; black arrow, non-canonical E-box; black boxes, amplicons indicated with a capital letter. Chromosome coordinates (bp) of the human *SKP2* promoter are also given. Data are the mean and error bars represent the SEM of n=3 experiments. Experiments were performed by G. Perini and co-workers, University of Bologna, Italy**.**

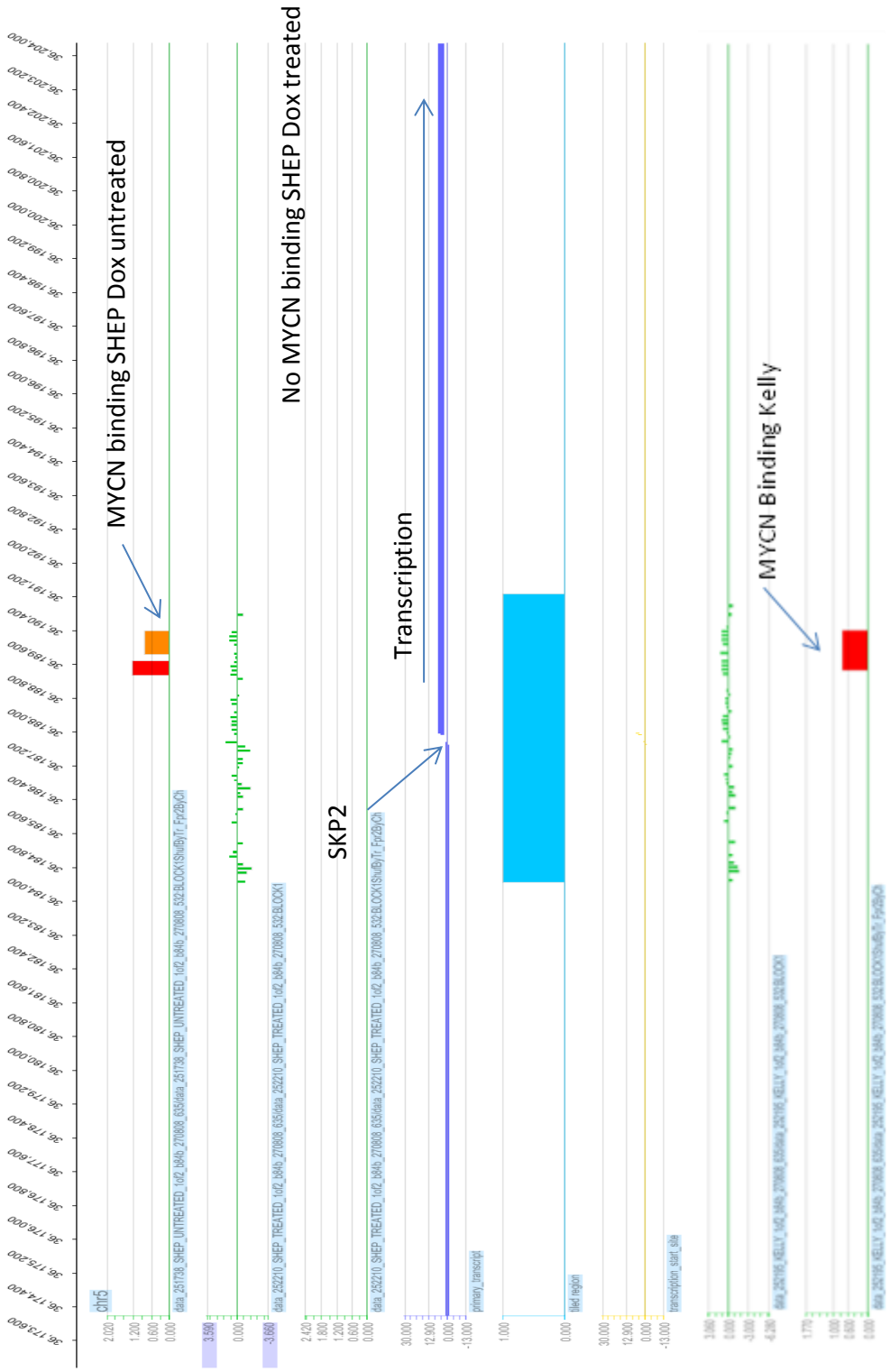

Figure 3.19 ChIP-chip microarray data for the *SKP2* gene in the SHEP-MYCN regulatable cell line and *MYCN* amplified Kelly cells. Identification of MYCN binding in 5' region of *SKP2* promoter in SHEP-MYCN regulatable cells and *MYCN* amplified Kelly cells. Scale across the top of the panel indicates the base pair position on chromosome 5. Fluorescent intensity of probes are expressed as log2 ratios (green bars) and high confidence MYCN peaks (red bars) as identified by the NimbleScan peak finding algorithm, Position of the *SKP2* transcript and the region tiled on the array are indicated by the two middle panels. Data provided by R. Stallings, Royal College of Surgeons, Dublin.

3.4.9. *MYCN functionally activates the human SKP2 promoter*

To confirm the functional regulation of the *SKP2* promoter by MYCN, a *SKP2* reporter construct incorporating the 1148/+20 region from the translational start site was employed (Huang and Hung, 2006). Previously used to assess the functional regulation of the *SKP2* promoter by c-MYC (Bretones *et al.*, 2011), the sequence matched that used for the ChIP assay covering the oligonucleotide sequences for amplicon A and B. Two E-boxes were identified within the construct (CACCTG and CCCGTG) and targeted by site-directed mutagenesis. The constructs were transfected into Tet21N MYCN+/MYCN- cells (Figure 3.20a), *MYCN* amplified IMR32 cells and non-*MYCN* amplified SHSY5Y cells (Figure 3.20b) and the highest promoter activity observed when MYCN was present; Tet21N MYCN+ ($p = 0.05$, paired t test) and IMR32 ($p = 0.002$, unpaired t test). Mutation of the E-box motifs significantly reduced promoter activity, to a level similar to that observed when MYCN was absent/not amplified ($p < 0.05$, paired t test), implying that MYCN directly activates the *SKP2* promoter. Mutation of the two E-boxes reduced promoter activity in the Tet21N MYCN- and non-*MYCN* amplified SHSY5Y cells. While this finding is consistent with the findings that other E-box binding factors, e.g. c-MYC, can influence *SKP2* promoter activity (Bretones *et al.*, 2011), it may also demonstrate *SKP2* promoter regulation by the basal level of MYCN present in a non-amplified setting.

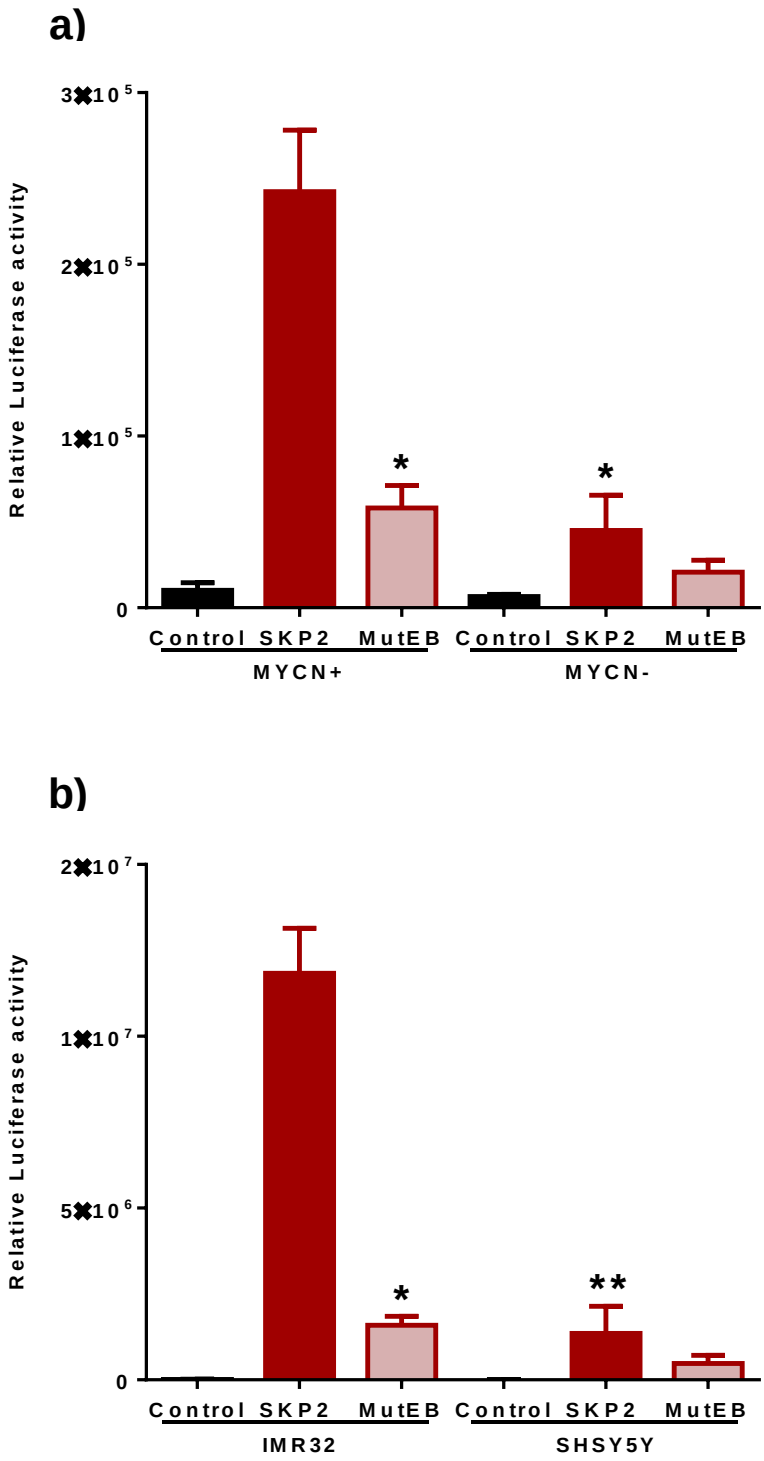

Figure 3.20 The effect of MYCN on *SKP2* promoter activity analysed by a luciferase reporter construct. Relative luciferase activity of the *SKP2* promoter constructs pGL3-SKP2 and pGL3-MutEB transfected into **a)** Tet21N-MYCN+/MYCN cells and **b)** *MYCN* amplified IMR32 cells and non-amplified SHSY5Y cells. Luciferase activity was normalised to β-galactosidase activity to control for transfection efficiency Data are the mean and error bars represent the SEM of n=3 experiments. * and ** correspond to a p value of <0.05 and <0.01, respectively.

3.5. Discussion

MYCN has a paradoxical role in neuroblastoma as it is able to both drive proliferation (Lutz *et al.*, 1996) and sensitise cells to apoptosis (van Noesel *et al.*, 2003). The net effect of *MYCN* amplification is therefore dependent on the interplay between these two responses. As the molecular mechanisms of MYCN-driven neuroblastoma are not fully understood, the identification of MYCN target genes may help in the understanding of the mechanisms and pathways MYCN uses to drive tumorigenesis.

SKP2 has been previously identified as a potential MYCN target in neuroblastoma (Bell *et al.*, 2007), with *SKP2* transcript levels shown to significantly correlate with *MYCN* amplification (Figure 3.20, http://r2.amc.nl), in addition to independently indicating a poor outcome in primary neuroblastoma tumours (Westermann *et al.*, 2007). The high levels of *SKP2* core promoter activity in *MYCN* amplified cells has been associated with high E2F1 activity combined with low abundance of repressive pRB-E2F1 complexes bound to the *SKP2* promoter (Muth *et al.*, 2010). SKP2 has also been shown to play a role in both the ubiquitin-mediated destruction of c-MYC as well as act as a transcriptional co-activator, a role further complicated by the identification of SKP2 as a direct c-MYC target gene (Kim *et al.*, 2003; Bretones *et al.*, 2011). Together, these data, in addition to the homology between *MYC* family members suggest that *MYCN* amplification promotes SKP2 protein expression which enhances neuroblastoma proliferation and aggressiveness.

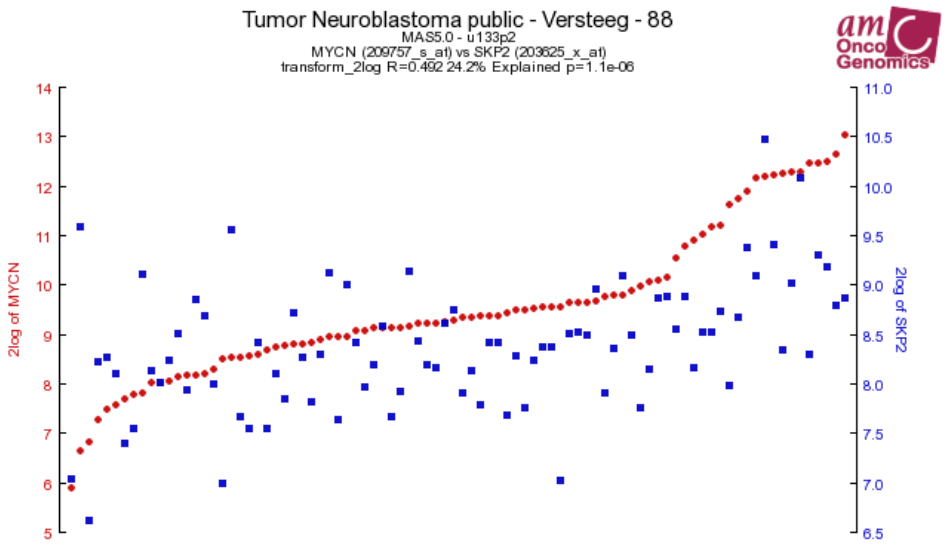

Figure 3.21 Gene expression data from the R2 microarray analysis and visualisation platform (http://r2.amc.nl) showing the correlation between *MYCN* and *SKP2* expression in dataset of 88 neuroblastoma tumours.

3.5.1. *The interplay between MYCN and SKP2 in regulatable MYCN expression systems*

Switching off MYCN expression in the SHEP-Tet21N MYCN regulatable cell line reduced SKP2 expression at the transcript and protein level (Figure 3.1). The gradual decline of SKP2 protein levels over 5 days of tetracycline treatment (Figure 3.2), correlated with a reduction in growth in Tet21N MYCN- cells (Figure 3.3b) and an accumulation of the CDK inhibitors p27 and p21, suggesting that p27/p21 stabilisation induced the observed growth inhibition. MYCN alters the expression of several cell cycle related targets to override the G_1 checkpoint and has been reported to repress the expression of p21 (Iraci *et al.*, 2011). Following the removal of MYCN the mRNA levels of both CDK inhibitors substantially increased (Figure 3.4), suggesting that the enhanced protein expression of p27 and p21 was due to the loss of MYCN and increased transcription instead of enhanced stabilisation through loss of SKP2-mediated degradation. To determine the contribution of SKP2 loss, Tet21N cell were treated with cycloheximide and tetracycline which resulted in p27 stabilisation only (Figure 3.5), suggesting that the increased p21 protein level in the Tet21N MYCN- cell line was controlled at the transcript level and in neuroblastoma cell lines MYCN regulates the SKP2/p27 axis. Previous reports show Tet21N MYCN- cells to have higher baseline hypo-phosphorylated pRB than the Tet21N MYCN+ cells, which

in association with *SKP2* being recognised as a direct E2F1 target gene may explain the lower SKP2 expression in the Tet21N MYCN- cells as the promoter activity is reduced by both the lack of E2F1 activity and by hypo-pRB repression at the promoter level (Bell *et al.*, 2006; Muth *et al.*, 2010).

Although there was an increase in *SKP2* mRNA levels upon MYCN induction in the *p53* mutant SKNAS-Nmyc-ER cell line (Figure 3.6a) increased expression was not reflected at the protein level (Figure 3.6b). MYCN gene overexpression in SKNAS cells has been shown to restore the ability to undergo retinoic acid activated differentiation by downregulating the expression levels of the microRNAs *miR-20a*, *miR-9* and *miR-92a* (Guglielmi *et al.*, 2014). Interestingly *miR-20a* negatively regulates *E2F* genes which may explain the increase in *SKP2* transcript levels in SKNAS-Nmyc-ER cells as the induction of MYCN transcriptional activity leads to a decrease in *miR-20a* activity which corresponds to an increase in E2F activity (Guglielmi *et al.*, 2014). Conversely *miR-20a*, *miR-9* and *miR-92a* have all been previously reported to positively correlate with MYCN. Nonetheless a growing body of evidence suggests that MYCN has a predominantly repressive role in the overall miRNA signature with the downregulation of miRNA being the result of the deregulation of key enzymes in the miRNA-processing pathway (Lin *et al.*, 2010b; Buechner and Einvik, 2012). Additionally, Guglielmi *et al* presented the downregulation of *miR-20a*, *miR-9* and *miR-92a* as a mechanism in which MYCN could trigger the early phases of differentiation (Guglielmi *et al.*, 2014). As miRNA expression patterns are known to correlate with neuroblastoma prognosis, differentiation and apoptosis (Chen and Stallings, 2007), the relationship between MYCN and a particular miRNA may therefore be dependent on the stage of the differentiation pathway.

Exposure to 4'OH-Tamoxifen (4-OHT) also suppressed cell growth (Figure 3.7a) consistent with the literature which associates favourable prognostic characteristics upon forced MYCN expression in an non-amplified setting (Tang *et al.*, 2006a). It would have therefore been interesting to monitor apoptotic and differentiation markers, in addition to genes associated with a favourable clinical prognosis e.g. *TrkA*, to confirm this. In relation to the suppression of growth, further investigation into cell cycle phase distribution would be of interest to determine whether the growth inhibition was a result of a G_1 arrest, an increase

in the sub-G_1 fraction indicating apoptosis, or a combination of the two. Treatment of the parental SKNAS cell line with 4-OHT would also be required to establish whether inhibition of growth was through mechanisms independent of activation of the Nmyc-ER vector.

The discrepancies between data from the SHEP-Tet21N and SKNAS Nmyc-ER models at the SKP2 protein level reflects the limitations of gene expression systems as well as highlights differences between completely switching off the gene, and consequently protein expression, and manipulation of the transcriptional activity of MYCN. Nonetheless, the higher *SKP2* transcript level in both the Tet21N and SKNAS-Nmyc-ER cell lines, when MYCN is present/active, implies that *SKP2* is regulated by MYCN.

3.5.2. *SKP2 and the functional MYCN signature*

The relationship between the expression of MYCN and SKP2 both at the transcript and protein level was reiterated in the panel of neuroblastoma cell lines (Figure 3.8). A significant linear relationship was seen between MYCN protein expression and *SKP2* mRNA level, ($r = 0.92$, Pearsons coefficient, Figure 3.9a), but not with the SKP2 protein level at 95% significance level ($r = 0.77$, Pearsons coefficient, Figure 3.10a). While this followed the pattern reported by Bell *et al* (Bell *et al.*, 2007), further statistical analysis demonstrated that there was a rank order relationship generated by the two oncogenes which was perfectly positively monotonic ($r_s = 1$, Spearman coefficient, Figure 3.10a). This nonparametric measure indicates that the expression level of MYCN and SKP2 are functions of one another, that is any increase in one will always be paired with an increase in the other. These data indicates that while SKP2 expression is a shared feature in *MYCN* amplified and non-amplified neuroblastoma cell lines the level of expression is in part dependent on the level of MYCN expression, as previously reported (Westermann *et al.*, 2007; Muth *et al.*, 2010).

The functional MYCN gene signature in neuroblastoma is constantly being redefined. The ability of MYCN to both promote and repress gene expression, along with its interactions with microRNAs, adds another level of complexity to its role in tumour progression. While many investigations into MYCN-regulated

genes identify sets of genes which share common cellular roles e.g. DNA repair, cell cycle and differentiation pathways, they do not often yield overlapping prognostic signatures. Some of the discrepancies from these mRNA expression based screens can be linked to these studies only accounting for *MYCN* mRNA levels and not protein levels as often mRNA and protein expression does not correlate (Ohira *et al.*, 2005; Vermeulen *et al.*, 2010; Valentijn *et al.*, 2012). This lack of correlation between mRNA and protein expression, as demonstrated by SKP2 in the panel of neuroblastoma cell lines (Figure 3.8) is often observed with potential MYCN transcriptional targets. While on one hand this may reflect the complexity of the proteome, as a diverse multitude of post-transcriptional modifications alter both mRNA and protein expression and stability, it also reiterates the importance of identifying the functional MYCN signature. That is, genes where elevated mRNA expression in the presence of MYCN relates to protein levels and clinical outcome, in an attempt to identify MYCN gene targets which contribute to oncogenicity.

As SKP2 has been identified as a direct c-MYC target gene (Bretones *et al.*, 2011), the significant homology within the *Myc* family may play a role in its expression profile in neuroblastoma. Non-*MYCN* amplified tumours generally express higher levels of c-MYC expression than MYCN and vice versa in a *MYCN* amplified setting. This inverse correlation is due to repression at the MYCN promoter by c-MYC and may explain the high SKP2 protein expression in the *NMA* cell lines (Breit and Schwab, 1989; Westermann *et al.*, 2008). However, the highest c-MYC expression in the panel of neuroblastoma cell lines investigated was in the non-*MNA* GIMEN and Tet21N MYCN- cells which expressed the lowest levels of SKP2 (Figure 3.8). The presence of c-MYC also failed to influence the *SKP2* transcript levels, suggesting that post-translational mechanisms which regulate SKP2 protein stability are responsible for the high expression in the absence of MYCN. Lower levels of p21 were seen in the *MYCN* amplified cell lines in line with the suppression of p21 transcription by MYCN (Iraci *et al.*, 2011). Interestingly, the highest levels of p21 expression were associated with the lowest SKP2 expression suggesting that the SKP2/p21 axis may be dominant over the regulation of p27 by SKP2 in neuroblastoma cell lines. However, given the presence of *MYCN* amplified and *p53* mutant cell lines, both of which have less p21 transcriptional activity, a larger panel of non-*MYCN*

amplified cell lines would have to be investigated to confirm this hypothesis (Figure 3.8). Contrary to the inverse relationship observed in primary tumour samples (Westermann *et al.*, 2007), no clear relationship was seen between the protein expression of SKP2 and p27, suggesting that additional events associated with either SKP2 expression or p27 proteolysis may be operating in these cell lines.

3.5.3. *MYCN expression influences the effect of SKP2 knockdown on cell proliferation and cell cycle progression in the Tet21N cell line*

Although SKP2 siRNA treatment significantly inhibited proliferation independent of MYCN expression (Figure 3.11b), a G_1 arrest and increase in p27 protein level was only observed in Tet21N MYCN+ cells (Figure 3.12a and Figure 3.11a respectively). As both Tet21N MYCN+ and MYCN- cells showed an increase in p21 stabilisation following SKP2 knockdown, these data suggest that the SKP2/p27 axis plays an important role in the G_1:S transition in neuroblastoma cell lines and that MYCN expression sensitises cells to a G_1 arrest following SKP2 inhibition. This hypothesis was supported by p27 siRNA treatment rescuing the cells from the cell cycle arrest induced by SKP2 inhibition (Figure 3.15a).

Under normal growth conditions, both a higher G_1:S ratio and basal levels of p27 were observed in the Tet21N MYCN- cells in comparison to Tet21N MYCN+ cells (Figure 3.12b and Figure 3.11a, repectively). MYCN plays an instrumental role in the length of the G_1 phase (Lutz *et al.*, 1996), and as discussed in Section 3.4.2, when switched off in the Tet21N cell line increases the half-life of p27 (Figure 3.5). The lack of G_1 arrest following SKP2 knockdown in the Tet21N MYCN- cells may therefore be due to the higher proportion of cells already in G_1 phase, as a consequence of MYCN removal, masking the effect of SKP2 inhibition. This observation demonstrates the dominant role of MYCN on cell cycle progression and questions the contribution of SKP2 to cell cycle progression in neuroblastoma, emphasizing the need for further investigation in a panel of non-isogenic cell lines of differing *MYCN* status.

SKP2 knockdown increased p21 levels irrespective of the presence of MYCN in the Tet21N cell line, although a greater effect was observed in the Tet21N MYCN+ cells. An increase in p21 expression has previously been identified as a

mechanism of inducing G_1 arrest upon MYCN inhibition in neuroblastoma, attributing a decrease in SKP2 expression to be in part responsible for the stabilised expression (Bell *et al.*, 2007). Furthermore, p21 is a well-established downstream effector of p53 which in turn is a known direct MYCN target gene (Chen *et al.*, 2010b). As p27 stabilisation and a G_1 arrest was only observed in the Tet21N MYCN+ cells, yet an increase in p21 expression and suppression of growth was induced independent of MYCN, the growth inhibition following SKP2 knockdown may be a consequence of apoptotic cell death (Figure 3.11).

3.5.4. *MYCN expression sensitises Tet21N cells to apoptosis induced by SKP2 knockdown*

Forty eight hour treatment with SKP2 siRNA increased the sub-G_1 fraction in the Tet21N MYCN+ and MYCN- cells, indicating apoptotic cell death (Figure 3.13a). This effect was confirmed by the increase in caspase 3/7 activity compared to the negative control siRNA after a 24 hr siRNA exposure (Figure 3.13b). As discussed in Section 3.4.2, dual treatment of the Tet21N cells with tetracycline and cycloheximide had no effect on the half-life of p21 (Figure 3.5) implying that protein synthesis must be in part responsible for the increase in p21 protein expression following SKP2 knockdown (Figure 3.11a). Although qRT-PCR would have to be performed to confirm this assumption, taken together with the greater induction of caspase 3/7 activity observed in the Tet21N MYCN+ cells it is probable that SKP2 inhibition is inducing a p53 response. Both MYCN and SKP2 have been implicated in the regulation of the p53 pathway. A recognised direct MYCN target gene, *MYCN* amplified neuroblastoma cells are reported to have higher basal levels of transcriptionally active p53 sensitising them to apoptosis (Chen *et al.*, 2010b). In contrast, SKP2 is known to suppress p53-dependent apoptosis by interacting with the p53-cofactor p300, antagonizing its ability to acetylate and consequently activate p53 (Kitagawa *et al.*, 2008).

Although MYCN is reported to stimulate the transcription of p53, the MYCN-dependent sensitisation to apoptosis would still require p53 activation. Both Tet21N MYCN+ and MYCN- cells undergo a prolonged period in G_1 arrest be it due to SKP2 inhibition (MYCN+) or the loss of MYCN (MYCN-) and experience a shift of cells from G_1 to sub-G_1 at the 48 hr time-point suggesting replicative stress activates the p53 pathway (Figure 3.14). The higher sensitivity of the Tet21N

MYCN+ cells to SKP2 knockdown (Figure 3.13), albeit minor, may therefore be due to the higher levels of available p53. These observations on one hand may implicate the overexpression of SKP2 as a mechanism to evade chemosensitivity, while on the other identify a novel mechanism to trigger p53-mediated apoptotic cell death in *MYCN* amplified neuroblastoma.

Alternatively the difference in caspase-3/7 induction between the Tet21N MYCN+ and MYCN- cells may be a consequence of the level of p27 accumulation. The dual knockdown of SKP2 and p27 significantly reduced the sub-G_1 fraction induced from SKP2 siRNA treatment alone (Figure 3.15b), suggesting that the p27 accumulation in Tet21N MYCN+ cells had a role in the apoptotic response from SKP2 inhibition. This assumption was supported by the significant reduction in the sub-G_1 population following the dual knockdown of SKP2 and p27. Overexpression of p27 has shown to induce apoptosis in several cancer models (Katayose *et al.*, 1997). Although the mechanism is not fully understood it is thought to be in-part associated with the p53-dependent apoptotic response, specifically the elevation of the BCL-2 negative regulator BAX (Fujieda *et al.*, 1999). Conversely knockdown of p27 alone induced the highest sub-G_1 fraction (Figure 3.15b) implying that the stabilisation of p27 through SKP2 inhibition may not be beneficial for treatment of *MYCN* amplified neuroblastoma. However, further investigation into non-isogenic neuroblastoma cell lines of differing *MYCN* and *p53* status would be required to further investigate the role of the SKP2/p27 axis in cell survival.

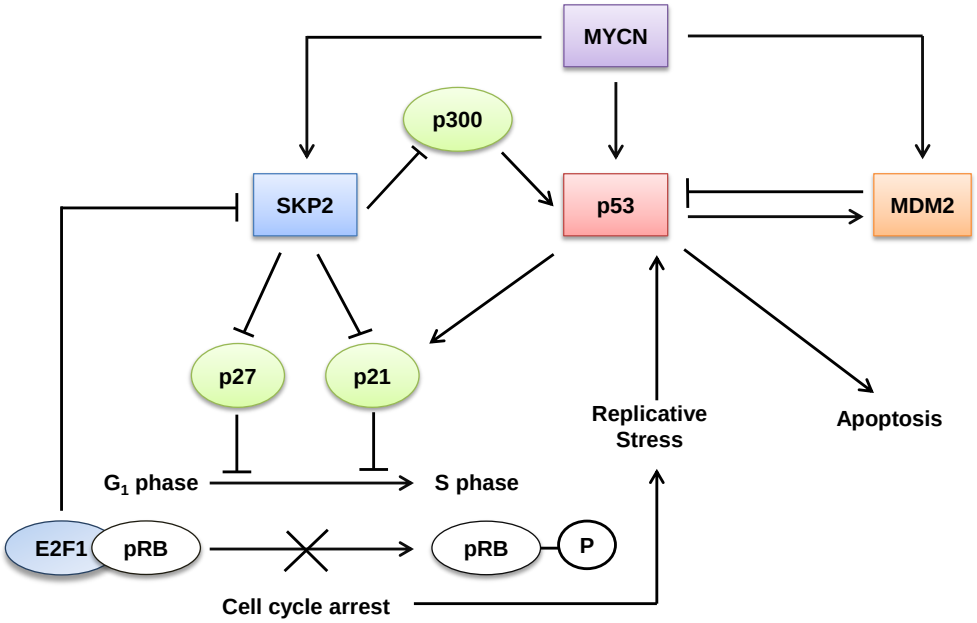

Figure 3.22 Proposed interactions between MYCN, SKP2 and p53 in the regulation of apoptosis. In response to SKP2 inhibition, p27 and p21 accumulate initiating a G1 arrest which induces replicative stress activating a p53 response. The loss of SKP2 releases p300 inhibition allowing activation of p53, while the pRb-E2F1 complexes repress SKP2 transcription**.** *SKP2* and *p53* are direct target genes of MYCN resulting in higher levels in Tet21N MYCN+ cells increasing the sensitivity of a G_1 cell cycle arrest and consequent apoptosis activated by replicative stress, following SKP2 inhibition.

3.5.5. *MYCN directly binds to, and activates, the human SKP2 promoter*

SKP2 is a recognised direct target gene of c-MYC which binds to non-cannonical E-boxes on the *SKP2* promoter (Bretones *et al.*, 2011). Given the conserved nature of E-boxes and homology of binding between *MYC* family members, there is great potential for an interaction between MYCN and the *SKP2* promoter. Quantitative MYCN ChIP identified a direct interaction between MYCN and non-canonical E-box motifs within the *SKP2* promoter, which correlated with ChIP-chip array data identifying MYCN binding to the *SKP2* promoter in a second MYCN-inducible and *MYCN* amplified cell line (Figure 3.19). Together these data provide strong evidence that SKP2 is a direct transcriptional target of MYCN.

As already discussed c-MYC is often expressed in neuroblastoma in favour of MYCN in the absence of *MYCN* amplification. It is therefore of interest to note that the intensity of c-MYC binding to the promoter of the non-*MYCN* amplified SHSY5Y cell line is comparable to that of MYCN in the *MYCN* amplified IMR32 cell line (Figure 3.17 and 3.18). As both cell lines have been shown to express a

similar level of SKP2 protein (Figure 3.8), this observation suggests that *SKP2* is a dual MYCN/c-MYC target gene (Westermann *et al.*, 2008) while again emphasising the role of SKP2 in neuroblastoma independent of MYCN status (Westermann *et al.*, 2007).

3.5.6. *MYCN expression activates the SKP2 promoter*

To confirm the functional regulation of the *SKP2* promoter by MYCN, a *SKP2* luciferase reporter construct incorporating the -1148/+20 region from the translational start site was employed (Bretones *et al.*, 2011). The construct sequence matched that used for the ChIP assay, covering the oligonucleotide sequences for amplicons A and B, and two E-boxes were identified (CACCTG and CCCGTG) and targeted by site-directed mutagenesis. The highest promoter activity was recorded in the presence of MYCN and was significantly decreased when MYCN expression was switched off/not amplified (Figure 3.20). This result implicates a functional role for MYCN expression in *SKP2* promoter activity and supports the relationship between MYCN protein and *SKP2* transcript level observed in the panel of neuroblastoma cell lines (Figure 3.9). Furthermore, mutation of the E-boxes significantly reduced promoter activity to a level similar to that seen when MYCN was not induced or amplified, suggesting that SKP2 is a direct MYCN target gene.

The *SKP2* promoter is regulated by a network of molecular mechanisms. Numerous pathways have been shown to promote *SKP2* transcriptional activity either through direct interaction such as c-MYC (Bretones *et al.*, 2011) and the IKKα subunit of the NF-κB pathway (Schneider *et al.*, 2006), or by integrating signalling through the E2F1 binding sites (Zhang and Wang, 2006) e.g. PI3K/AKT (Reichert *et al.*, 2007). Conversely *SKP2* transcription is also suppressed by repressive units directly binding to the promoter, for example pRB-E2F1 complexes in *MYCN* amplified neuroblastoma cells (Muth *et al.*, 2010), FOXP3 binding in breast cancer (Zuo *et al.*, 2007) and STAT1 which inhibits SKP2 expression to induce an anti-tumour function in Ras-transformed cells (Wang *et al.*, 2010b).

These different regulatory mechanisms may explain the discrepancies observed between the Tet21N MYCN+ cells and *MYCN* amplified IMR32 cells as although this study shows the MYCN protein level to be comparable between the two cell lines (Figure 3.8), the IMR32 cells showed ~50 fold higher luciferase activity (Figure 3.20b). The amplicon which includes the *MYCN* gene is reported to vary in size and has been shown to vary from 100 kb to 1 Mb long. Given that the *MYCN* gene only spans ~7 kb, additional genes are often co-amplified and contribute to the malignant behaviour of *MYCN* amplified disease (Amler and Schwab, 1989; Scott *et al.*, 2003). The fold difference in *SKP2* promoter activity between Tet21N MYCN+ and IMR32 cells could therefore potentially be through mechanisms regulated by the genes co-amplified with *MYCN*. Importantly, the difference between the two cell lines highlights the potential limitations of comparing MYCN-regulatable systems with amplified/non-amplified cell lines.

3.6. Conclusions

The results discussed in this chapter provide strong evidence that *SKP2* is a direct transcriptional target of MYCN in neuroblastoma. MYCN has been shown to: a.) upregulate *SKP2* mRNA level in two independent MYCN regulatable expression systems, b.) bind to non-canonical E-box motifs within the human *SKP2* promoter in ChIP assays and c.) functionally activate a *SKP2* promoter, luciferase-reporter construct. Furthermore functional studies of SKP2 have confirmed a correlation between MYCN protein and *SKP2* mRNA in a panel of neuroblastoma cell lines with the presence of MYCN sensitising the Tet21N cells to a G_1 arrest and apoptosis after treatment with SKP2 siRNA.

Taken together this data suggests that the MYCN/SKP2 relationship plays an important role in the perpetual cell cycle entry in *MYCN* amplified neuroblastoma, and identifies a potential downstream effector of MYCN for pharmacological inhibition. However further investigation is required into the role of SKP2 in non-isogenic *MYCN* amplified and non-amplified neuroblastoma cell lines.

Chapter 4.

Target validation of SKP2 in neuroblastoma cell lines

4.1. Introduction

4.1.1. *SKP2 expression in neuroblastoma*

SKP2 has been hypothesised to play a key role in the progression of neuroblastoma due to its association with MYCN expression, as discussed in Chapter 3, in addition to its overexpression predicting a poor clinical outcome in primary tumours (Bell *et al.*, 2007; Westermann *et al.*, 2007). These reports are supported by the Kaplan-Meier survival curves and correlation analyses from the R2 microarray analysis and visualisation platform (http://r2.amc.nl) which show a strong correlation between *MYCN* and *SKP2* expression ($r = 0.4924$, $p = 1.1x10^{-6}$, Figure 4.1a) and high levels of *SKP2* relating to poor overall survival (Figure 4.1b). The oncogenic functions of SKP2 are often related to its ability to target the CDK inhibitor p27 for degradation. Although SKP2 is the rate-limiting factor within the SCF^{SKP2} complex, the interaction between the E3 ligase and its primary target is dependent on the phosphorylation of a p27 threonine reside (Thr187) by the cyclin E-CDK2 complex (Montagnoli *et al.*, 1999b) and formation of a trimeric complex between SKP2-cyclinA/CDK2 and the SKP2 accessory protein CKS1 (Hao *et al.*, 2005; Ungermannova *et al.*, 2005; Xu *et al.*, 2007).

c-MYC has been shown to be promote CKS1 activity by indirect mechanisms which up-regulate *CKS1* mRNA (Keller *et al.*, 2007). While this observation does open the possibility for the regulation of CKS1 expression by MYCN due to the homology within the MYC family of oncoproteins, the R2 database identified no correlation between *MYCN* and *CKS1B* (CKS1) expression (Figure 4.2a). CKS1 has been shown to have oncogenic roles outside of its regulation of p27 stability in other tumours and high levels of CKS1 were found to associate with a poor overall survival in neuroblastoma (Figure 4.2b). However as low levels of p27 are associated with the high expression of SKP2 seen in *MYCN* amplified tumours (Westermann *et al.*, 2007), and this relationship is dependent on CKS1 activity, the oncogenic role of CKS1 in neuroblastoma may be primarily through its regulation of CDK inhibitors.

One transcription factor which has recently been demonstrated to regulate both SKP2 and CKS1 expression is the Forkhead Box M1 (FOXM1). A key modulator of the G_1/S transition and mitotic progression, siRNA knockdown of FoxM1 expression has been shown to significantly reduce *SKP2* and *CKS1* mRNA levels as it diminished the binding of FOXM1 to the endogenous *SKP2* and *CKS1B* promoter regions (Wang *et al.*, 2005; Kim *et al.*, 2014). Interestingly, the R2 database identified a strong correlation between *MYCN* and *FOXM1* ($r = 0.401$, $p = 1.1x10^{-4}$, Figure 4.3) which could contribute both to the high levels of SKP2 in *MYCN* amplified tumours and the inverse relationship with p27 as both high levels of SKP2 and CKS1 would be present in the *MYCN* amplified setting.

Although SKP2 targets numerous proteins for degradation, the studies described in this chapter concentrate on the regulation of the CDK inhibitors p27 and p21. High levels of p27 protein expression have been shown to act as a good prognostic indicator, independent of *MYCN* amplification (Bergmann *et al.*, 2001), with its accumulation contributing to a G_1 arrest (Matsuo *et al.*, 2001) and acting as a key mediator of neuronal differentiation in neuroblastoma cell lines (Borriello *et al.*, 2000; Munoz *et al.*, 2003; Nakamura *et al.*, 2003). Unlike p27, p21 expression in *MYCN* amplified neuroblastoma is also regulated at the transcript level by p53 which itself is a direct MYCN target gene. The failure of *MYCN* amplified neuroblastoma cell lines to undergo a G_1 arrest following DNA damage has been in part associated with lower levels of p21 induction (Bell *et al.*, 2006). As SKP2 has been implicated in the suppression of p53 activity (Kitagawa *et al.*, 2008) the high levels of SKP2 seen in *MYCN* amplified neuroblastoma may contribute to the lack of a G_1 arrest.

In summary, the high expression of SKP2 observed in neuroblastoma is associated with a poor outcome and could potentially be a contributing factor in the aggressive behaviour of *MYCN* amplified neuroblastoma. Given the challenges in targeting MYCN, it is therefore of interest to understand further the role of SKP2 in neuroblastoma and its potential as a therapeutic target.

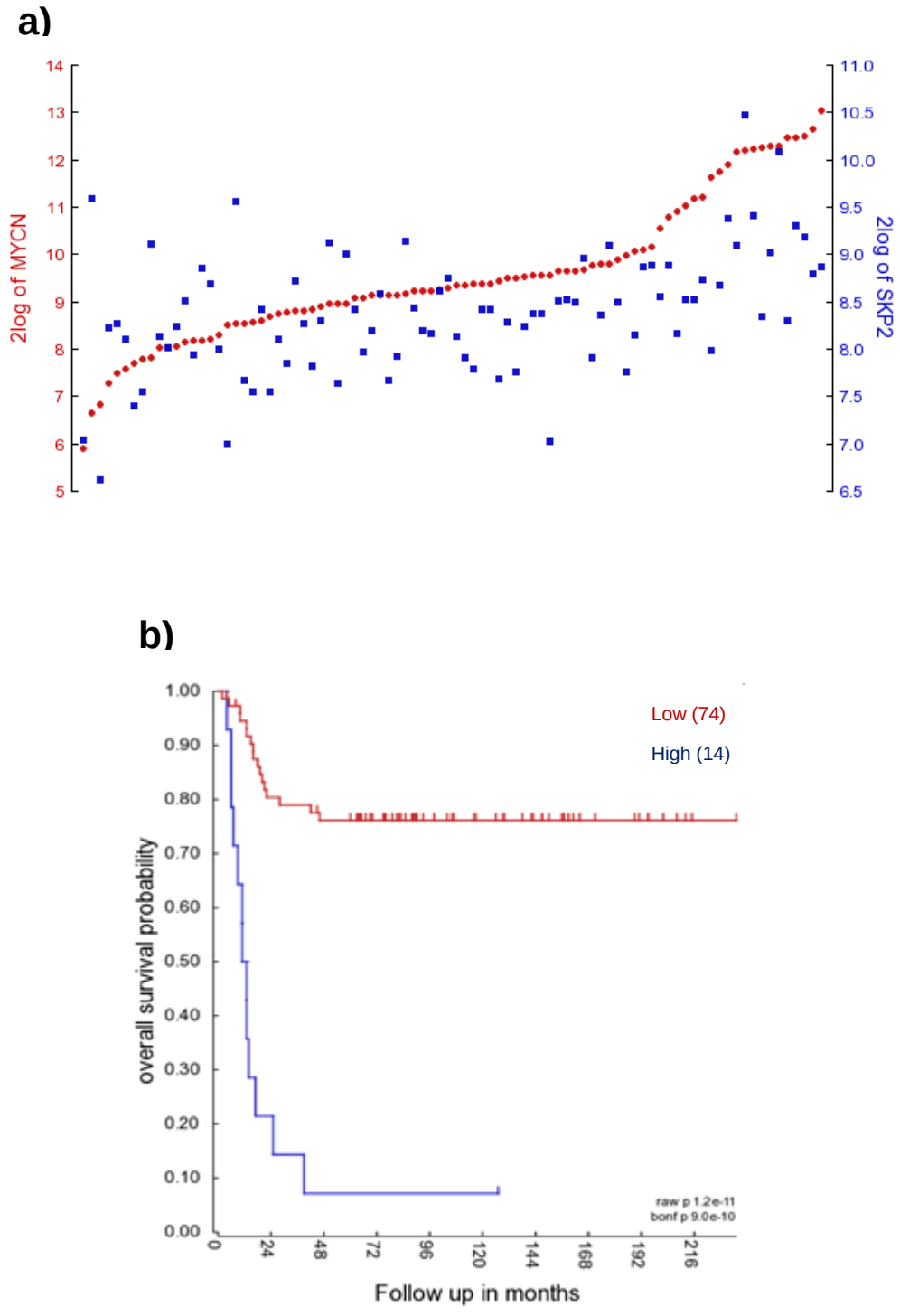

Figure 4.1 Gene expression data from the R2 microarray analysis and visualisation platform (http://r2.amc.nl) showing analysis from the Versteeg dataset of 88 neuroblastoma tumours. a) Relationship between *MYCN* and *SKP2*. **b)** Kaplan-Meier analysis for overall survival according to *SKP2* expression. Patients with *SKP2* expression greater than 511.2 (n=14) had shorter survival than those with lower expression (n=74). Following probes were chosen for analysis, *MYCN* : 209757_s_at and *SKP2* : 203625_x_at

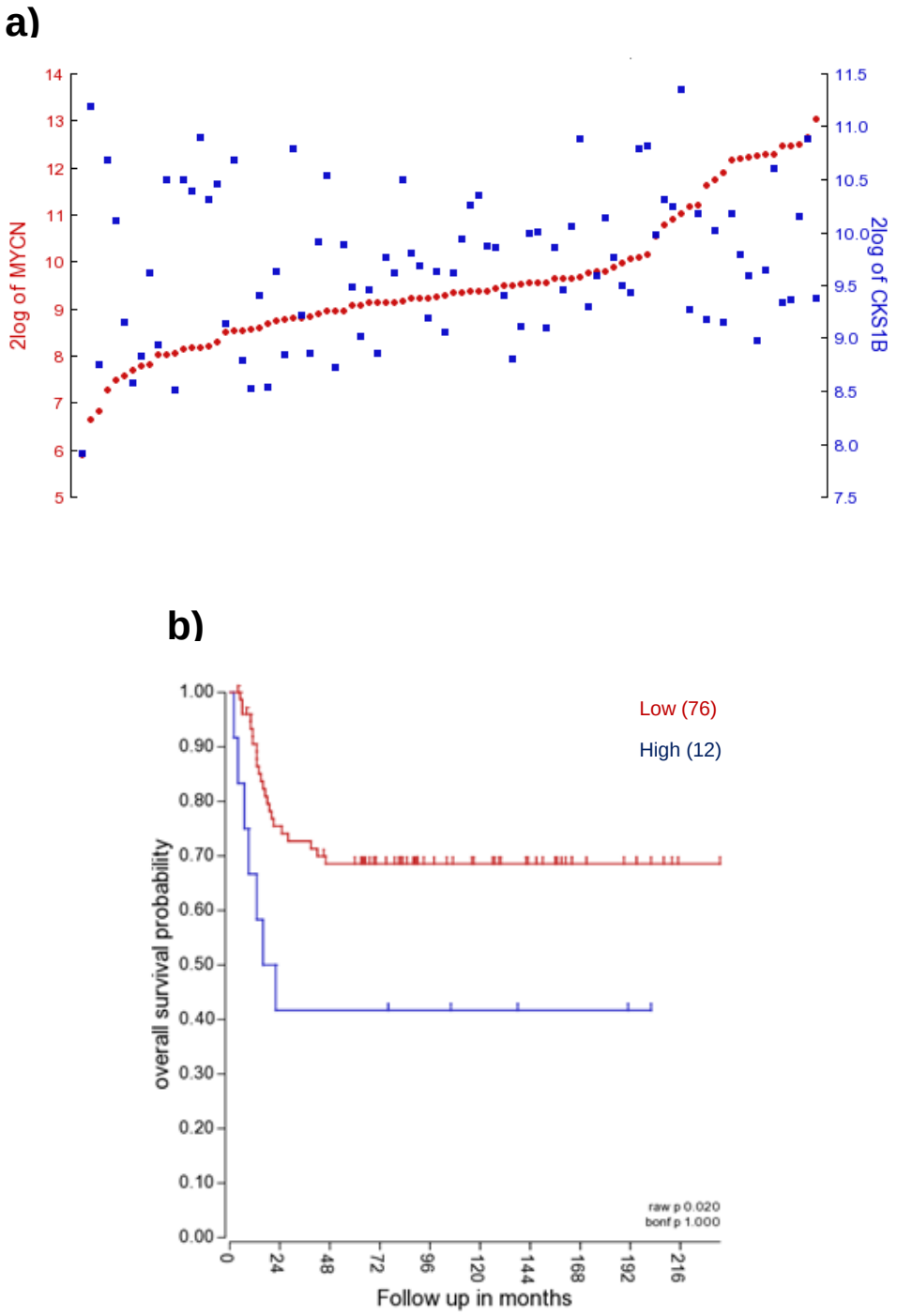

Figure 4.2 Gene expression data from the R2 microarray analysis and visualisation platform (http://r2.amc.nl) showing analysis from the Versteeg dataset of 88 neuroblastoma tumours. a) Relationship between *MYCN* and *CKS1B.* **b)** Kaplan-Meier analysis for overall survival according to *CKS1B* expression. Patients with *CKS1B* expression greater than 1450.8 (n=12) had shorter survival than those with lower expression (n=76). Following probes were chosen for analysis, *CKS1B* : 201897_s_and *MYCN* : 209757_s_at

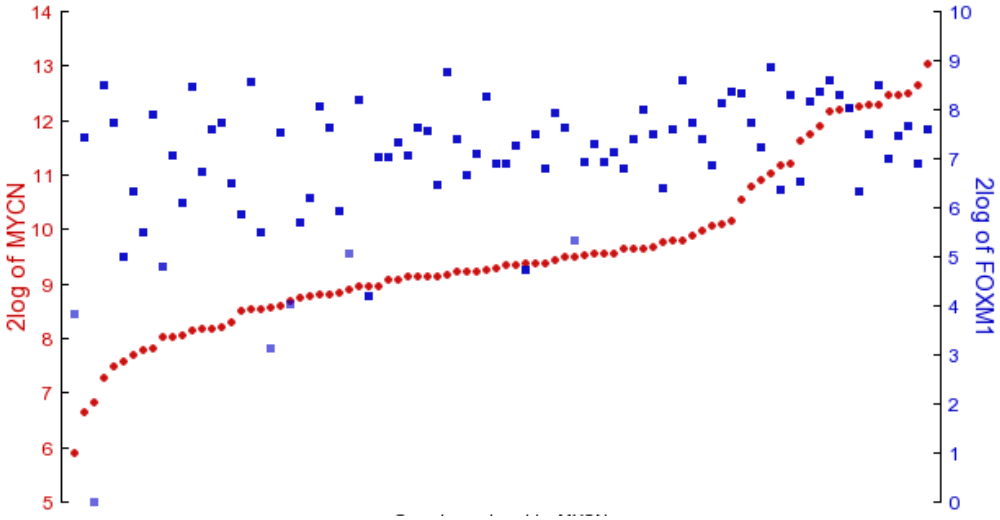

Figure 4.3 Gene expression data from the R2 microarray analysis and visualisation platform (http://r2.amc.nl) showing analysis from the Versteeg dataset of 88 neuroblastoma tumours. Relationship between *MYCN* and *FOXM1.* Following probes were chosen for analysis, *MYCN* : 209757_s_at and *FOXM1* : 202580_x_at

4.1.2. *Functional studies into the role of SKP2 in oncogenesis*

Investigations into the oncogenic role of SKP2 have largely involved the removal of gene function using either siRNA targeted knockdown or gene knockout mice. Both powerful tools, although one more absolute than the other, the removal of the protein provides information of the molecular function through the resultant phenotypic changes observed. Identification of p27 as the primary target of SKP2 was in part through observations of SKP2 knockout mice (*SKP2*$^{-/-}$). Although viable, *SKP2*$^{-/-}$ mice were smaller than their *SKP2*$^{+/+}$ littermates and showed characteristics of polyploidy and multiple centrosomes, much of which was corrected by the additional knockout of p27 (Nakayama *et al.*, 2000). Thus the ability of *SKP2*$^{-/-}$ mice to grow to adulthood indicates that the accumulation of p27 is not sufficient on its own to arrest cell proliferation completely. This observation that *SKP2* knockout was not embryonically lethal nor promoted any predisposition to cancer supported reports that SKP2 is a proto-oncogene reliant on additional oncogenic events to promote tumorigenesis (Nakayama *et al.*, 2000). In the studies described in this chapter, siRNA was employed which, although a more transient technique, provides a better representation of the effects of therapeutically inhibiting SKP2 than permanent gene deletion. Ideally both a small molecular inhibitors and SKP2 targeting siRNA would be used to investigate the functional role of the oncoprotein; however, no small molecule

SKP2 inhibitors which produce the same level of target-specific inhibition of SKP2 function are currently available. As it is the overexpression of SKP2 which is associated with a poor prognosis, SKP2 siRNA knockdown in cancer cell lines will help validate any potential therapeutic benefit of targeting the oncoprotein. Conversely expression vectors can be employed to exogenously overexpress SKP2 in low level expressing cells, which may identify molecular mechanisms undetected in the loss-of-function analysis. The parallel approach allows clarification of whether SKP2 overexpression is a driving force in neuroblastoma or simply a bi-product of *MYCN* amplification. Taken together these experiments provide important evidence on the potential benefit of therapeutically targeting SKP2 in neuroblastoma.

4.2. Aims

Having identified *SKP2* as a direct MYCN target gene as described in Chapter 3, the overall aim of the work presented in this chapter was to investigate SKP2 as a potential therapeutic target in neuroblastoma using cell lines and determine whether *MYCN* amplification or *p53* status influenced sensitivity to SKP2 knockdown. These aims were addressed with the following specific objectives:

- To examine the effect of SKP2 siRNA treatment on the expression of the CDK inhibitors p27 and p21, cell cycle progression and cell survival in *MYCN* amplified and non-amplified neuroblastoma cell lines.

- To clarify the relationship between SKP2 and p27 in the G_1/S checkpoint in neuroblastoma cell lines.

- To investigate the relationship between SKP2 and the p53 pathway by monitoring the effects of SKP2 siRNA knockdown on cell cycle arrest, apoptotic cell death and the p53 response following ionising radiation treatment.

- To determine the role of the overexpression of SKP2 in driving cellular proliferation in the SHEP neuroblastoma cell line by transfection with a pcDNA-*SKP2* expression vector.

4.3. Chapter specific material and methods

4.3.1. *SKP2 siRNA optimisation*

MYCN amplified IMR32 cells and non-*MYCN* amplified SHSY5Y cells were treated with 20, 40 and 60 nM siRNA targeting SKP2 for 24 hrs, as described in Section 2.5.3. Knockdown efficiency was analysed in comparison to a negative control siRNA (NCS) by western blotting as described in Section 2.5, and the optimum concentration of 40 nM chosen and subsequently applied to each cell line unless stated otherwise.

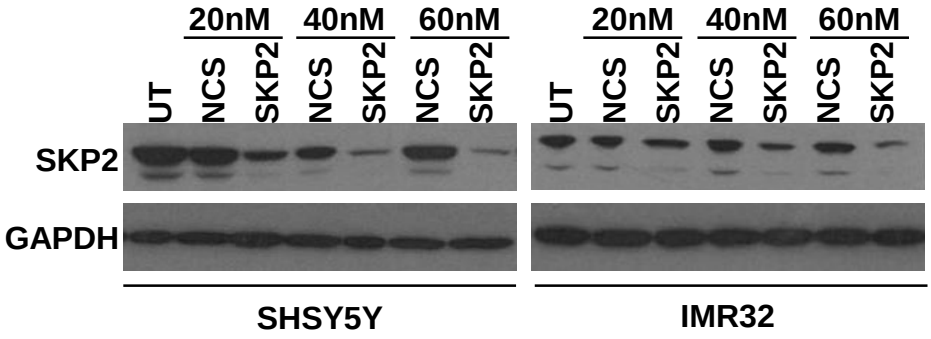

Figure 4.4 Optimisation of a 24 hr exposure to SKP2 siRNA in non-*MYCN* amplified SHSY5Y and *MYCN* amplified IMR32 cells.

4.3.2. *Transfection and optimisation of the pcDNA-SKP2 expression plasmid*

The parental cells for the Tet21N cell line, SHEP cells, were chosen for transfection with the pcDNA-*SKP2* expression vector (kindly donated by Professor Neil Perkins, Newcastle University) due to their recognised tolerance to stable transfections and low levels of endogenous SKP2 (Figure 4.5). A range of plasmid concentrations were evaluated to determine an optimum level of plasmid. Cells were seeded at 4 x 10^5 cells/well into 6-well plates in RPMI 1640 (10% (v/v) FBS), 24 hrs prior to transfection. The pcDNA-*SKP2* plasmid was transfected into cells using Lipofectamine® 2000, in Opti-MEM® reduced serum medium (Invitrogen, Life Technologies, Paisley, UK). Plasmids were stored at -20°C in stock concentrations of 0.2µg/µl, and the transfection mixture used as shown in Table 4.1.

Final concentration/well	Volume of 0. 2 µg/µl stock/well	Volume of Lipofectamine® 2000/well
0.5 µg	2.5 µl	1 µl
0.8 µg	4 µl	1.6 µl
1 µg	5 µl	2 µl
2 µg	10 µl	4 µl
Volume of Opti-MEM®	250 µl	250 µl

Table 4.1 pcDNA-*SKP2* plasmid transfection mixture

DNA and Lipofectamine were diluted separately in Opti-MEM® media as shown in Table 4.1 and incubated for 10 minutes at room temperature. Following incubation, the two solutions were then mixed at a 1:1 ratio, gently inverted and incubated for a further 30 minutes at room temperature. The RPMI medium was removed from the wells, the cells rinsed with Opti-MEM® to remove any remaining FBS and replaced with 1.6 ml of the serum free medium. After the incubation, 400 µl of the transfection mixture was added to each well, briefly shaken, and the plate incubated at 37°C for 24 hrs. Lysates were collected and analysed using western blotting as describe in Section 2.5. Based on Figure 4.5 a concentration of 0.8 µg/well was chosen for the subsequent transfections

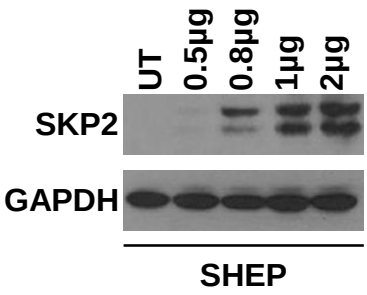

Figure 4.5 Optimisation of a 24 hr pcDNA-*SKP2* plasmid transfection in SHEP cells

4.3.3. *SKP2 knockdown and DNA damage induction by γ-irradiation*

Cells were seeded at 4 x 10^5 cells/well into 6-well plates in RPMI 1640 (10% (v/v) FBS), 24 hrs prior to transfection with SKP2 siRNA as described in Section 2.4.3. After a 24 hr exposure to siRNA the OptiMEM serum free medium was replaced with 2 ml RPMI 1640 medium and the plate irradiated with 4 Gy 2103 kV X-rays from a RS320 irradiation system (Gulmay Medical, Surrey UK). The irradiation (IR) dose had been previously optimised (Bell *et al.*, 2006). Cells were harvested at 6 and 24 hrs post irradiation for western blotting and 24 hrs post irradiation for cell cycle and caspase-3/7 analysis. Control lysates were prepared from cells treated in parallel to the IR treated samples and collected following a 48 hrs exposure to SKP2 siRNA to match the siRNA exposure length of the irradiated lysates

4.4. Results

4.4.1. *SKP2 knockdown inhibits cell growth independent of MYCN and p53 status*

Based on the findings in the Tet21N cell line that MYCN sensitised cells to a G_1 arrest following SKP2 knockdown (Section 3.4.5), the functional role of SKP2 in the G_1/S transition was examined in a panel of neuroblastoma cell lines varying in *MYCN* and *p53* status. An XTT assay, performed after a 72 hr exposure to SKP2 siRNA showed significant growth inhibition in all cell lines compared to negative control siRNA (NCS), with the exception of *MYCN* amplified, *p53* mutant, IMR-KAT100 cells (Figure 4.6). Selected as a result of repeated-3 day exposure of the parental *MYCN* amplified IMR32 cell line to potassium antimony tartrate (KAT), a point mutation was identified within the DNA-binding domain of p53, at codon 135. This same mutation has previously been reported in the SK-N-BE(2c) cell line which was established from a patient with relapsed disease; however, this cell line underwent a significant growth inhibition following SKP2 knockdown ($p < 0.01$) (Goldschneider *et al.*, 2006b; Xue *et al.*, 2007).

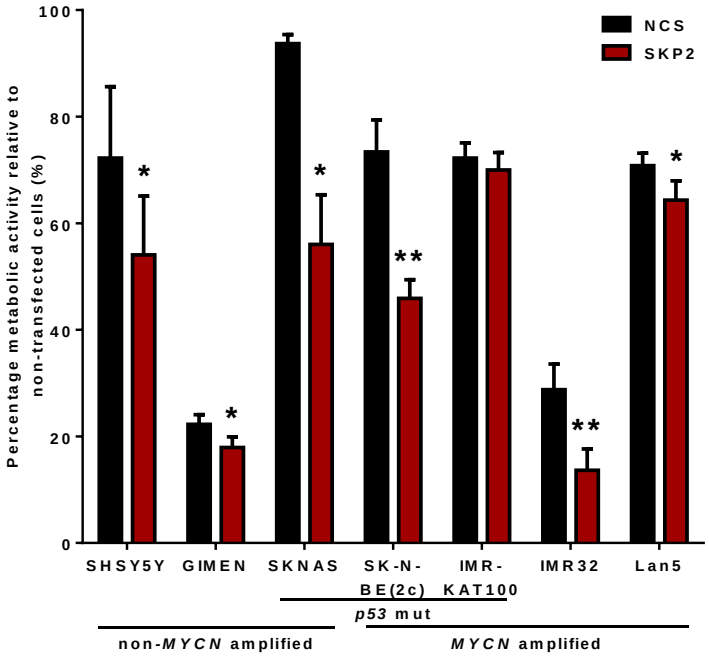

Figure 4.6 The effect of SKP2 siRNA transfection on cell proliferation. An XTT assay was performed after 72 hr exposure to siRNA. Data are normalised to non-transfected cells and compared to the negative control siRNA (NCS). Data are the mean and the error bars represent SEM of n=3. * and ** correspond to a p value of <0.05 and <0.01, respectively.

4.4.2. *SKP2 knockdown induces G_1 arrest and apoptosis in non-MYCN amplified neuroblastoma cells independently of the p53 pathway*

Contrary to what was observed in the MYCN regulatable Tet21N cells, only the non-*MYCN* amplified cell lines showed an increase in the G_1/S ratio after a 24 hr SKP2 siRNA exposure, (Figure 4.7), implying that the inhibition of proliferation seen in the SK-N-BE(2c) cells was not a result of a G_1 arrest. The non-*MYCN* amplified, *p53* mutant, SKNAS cells are known to only express the C-terminal truncated isoform of p53 (p53β), which is reported to be unable to induce p21 protein accumulation. Although p21 stabilisation was seen across the whole panel of *p53* wild-type cell lines (Figure 4.8), p27 protein levels only consistently increased in the non-*MYCN* amplified cells at the 24 hr time-point (Figure 4.8a), suggesting that the SKP2/p27 axis plays an important role in the G_1/S transition in non-*MYCN* amplified neuroblastoma cells. This lateral observation reinforces the findings of the protein stability experiments in Tet21N cells where only p27 was found to be stabilised after switching off MYCN expression, as discussed in Section 3.4.2.

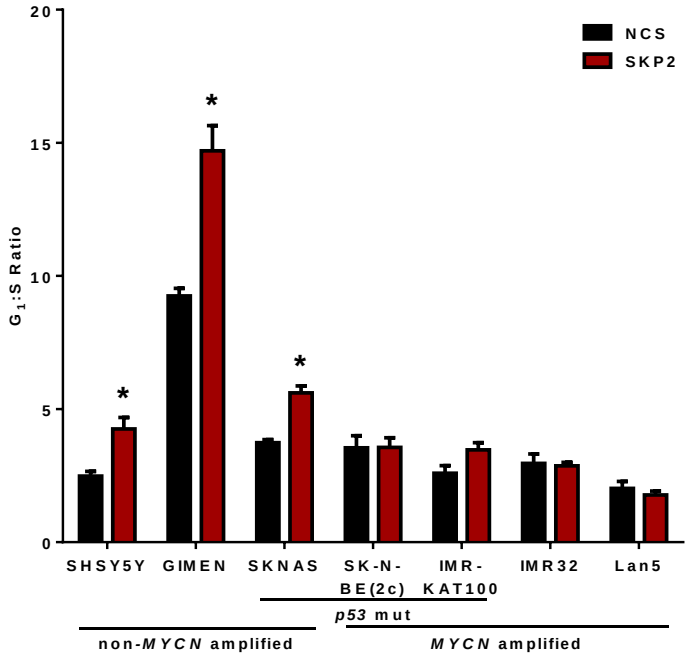

Figure 4.7 The effect of SKP2 siRNA transfection on the G_1/S ratio in a panel of neuroblastoma cell lines. G_1:S ratio measured by flow cytometry after a 24hr exposure to siRNA. Data are normalised to non-transfected cells and compared to the negative control siRNA (NCS). Data are the mean and the error bars represent SEM of n=3. * and ** correspond to a p value of <0.05 and <0.01, respectively.

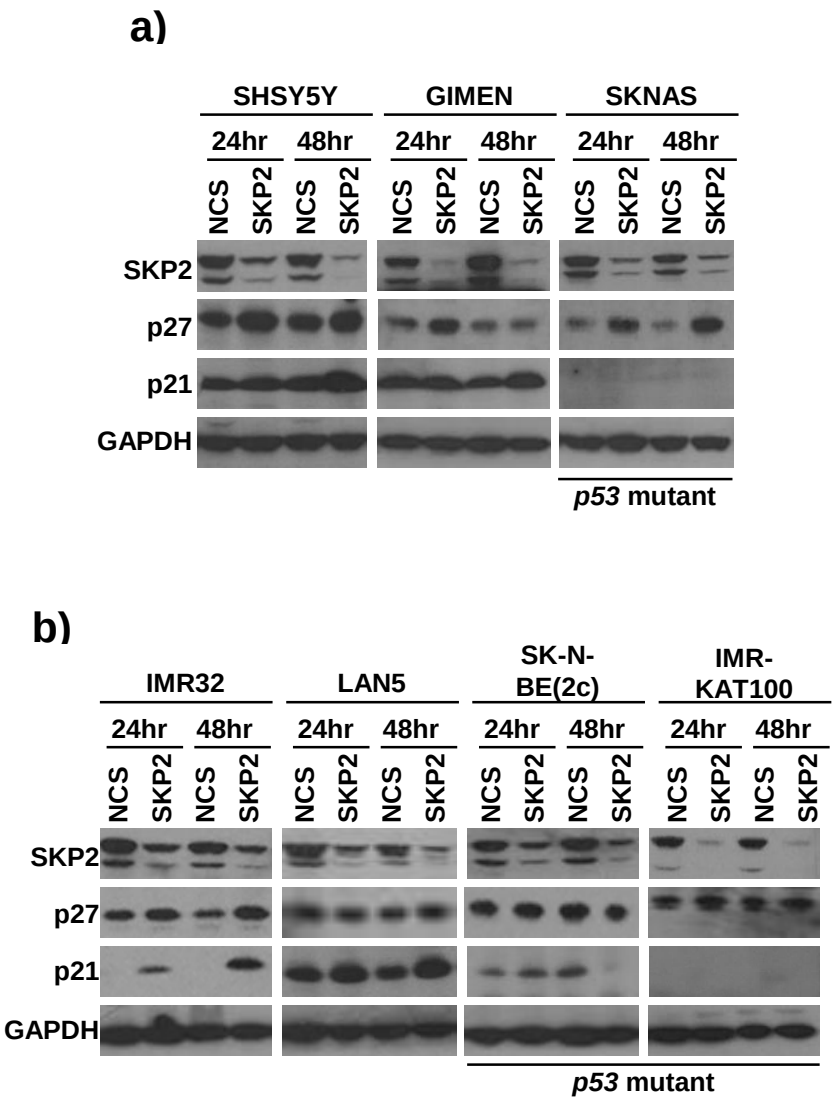

Figure 4.8 Western blot showing the effect of SKP2 knockdown on p27 and p21 protein expression in a panel of neuroblastoma cell lines. a) non- *MYCN* amplified cell lines **b)** *MYCN* amplified cell lines. Cell lysates were collected at the time-points stated. The western blot shown is representative of 3 independent repeats.

A significant increase in the sub-G_1 fraction, indicative of apoptotic cell death, was observed in non-*MYCN* amplified cell lines following a 48 hr SKP2 siRNA exposure (Figure 4.9a) and confirmed by the induction of caspase-3/7 activity 24hrs after siRNA treatment (Figure 4.9b). As SKNAS cells harbour an inactive form of p53 (p53β) these results suggest that SKP2 knockdown initiates caspase-dependent apoptosis, independent of the p53 pathway, but only in non-*MYCN* amplified cells.

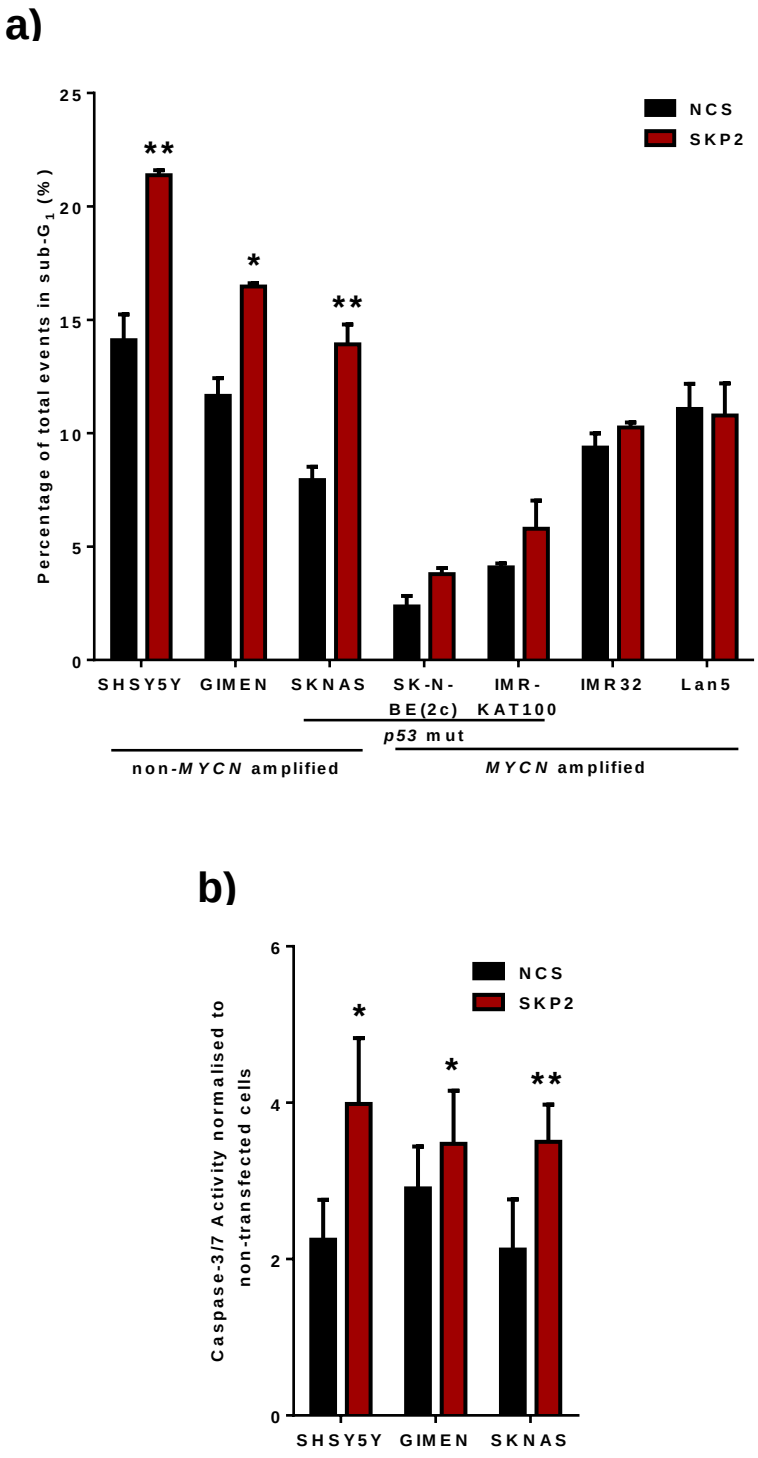

Figure 4.9 The effect of SKP2 siRNA transfection on apoptosis in a panel of neuroblastoma cell lines. a) Percentage of cells in the sub-G_1 DNA fraction of cell cycle measured by flow cytometry after 48 hr exposure to SKP2 siRNA. **b)** Caspase-3/7 activity after 24 hr exposure to SKP2 siRNA in non-*MYCN* amplified cell lines. All data are normalised to the non-transfected controls and compared to the negative control siRNA (NCS). Data are the mean and error bars represent the SEM of n=3 experiments, * and ** correspond to a p value of <0.05 and <0.01, respectively.

4.4.3. *Depletion of p27 prevents the effects of SKP2 knockdown on the cell cycle*

To establish the extent to which p27 accumulation was responsible for the induction of the G_1 arrest, dual knockdown of p27 and SKP2 was investigated in the non-*MYCN* amplified cell lines (Figure 4.10a). Preventing the increase of p27 following SKP2 knockdown attenuated the cell cycle arrest significantly in all cell lines investigated ($p \leq 0.05$, paired t test) implying that p27 accumulation is a key step in the G_1 arrest induced by SKP2 depletion. The importance of the SKP2/p27 axis in the regulation of the G_1/S transition in neuroblastoma is supported by the lack of a G_1 arrest in the *MYCN* amplified cell lines (Figure 4.7), where the effect of SKP2 knockdown on p27 stabilisation was not as pronounced (Figure 4.8b). Alternatively, deregulated MYCN may be influencing the SKP2-independent degradation of p27 such as the activity of the E3 ligase KIP1 ubiquitination-promoting complex (KPC) which promotes the degradation of cytoplasmic p27 exported during the G_0 - G_1 transition (Kamura *et al.*, 2004).

Interestingly, preventing p27 stabilisation in GIMEN and SKNAS cell lines significantly decreased the apoptotic cell death induced by SKP2 knockdown in all cell lines investigated suggesting that p27 contributes to the apoptotic response from SKP2 inhibition. This effect was not observed in the SHSY5Y cells where the p27 knockdown alone induced a greater increase in the sub-G_1 population which was reduced upon SKP2 knockdown (Figure 4.10b).

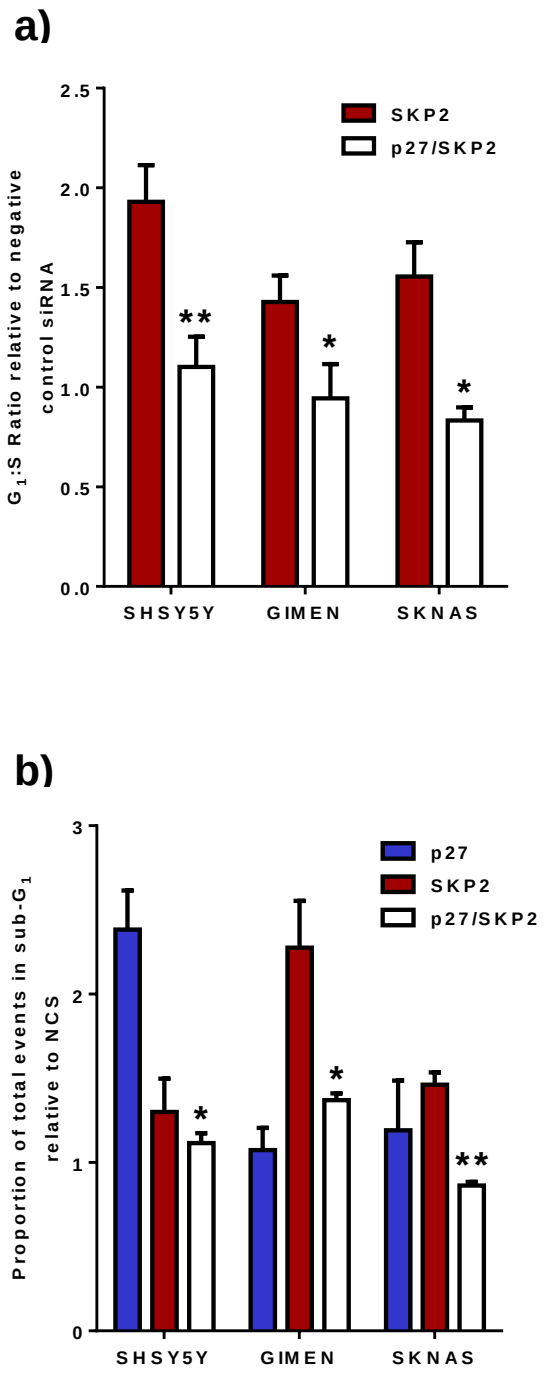

Figure 4.10 The effect of dual knockdown of SKP2 and p27 on G_1 arrest and the sub-G_1 fraction in a panel of neuroblastoma cell lines. a) G_1:S ratio and **b)** Sub-G_1 fraction measured by flow cytometry after exposure to siRNA. Data was normalised to the negative control siRNA and the mean plotted. Error bars represent the SEM of n=3 experiments, * and ** corresponds to a p value of <0.05 and < 0.01, respectively.

4.4.4. *SKP2 knockdown induces a p53 apoptotic response to DNA damage*

MYCN amplification is associated both with the activation and suppression of the MDM2-p53 apoptotic pathway. As *SKP2* is a direct MYCN target gene and is reported to suppress p53 dependent apoptosis through inhibition of the p53 co-factor p300 (Kitagawa *et al.*, 2008), experiments were performed to determine whether SKP2 inhibition could enhance the p53 response to DNA damage induced by ionising radiation (IR). Cells were treated with SKP2 siRNA for 24 hr prior to exposure to 4Gy IR and lysates collected 24 hrs post irradiation.

The proportion of cells in the sub-G_1 population significantly increased in non-*MYCN* amplified SHSY5Y cells, and *MYCN* amplified *p53* mutant SK-N-BE(2c) cells, 24 hrs after DNA damage (Figure 4.11). A 24 hr treatment with SKP2 siRNA increased the sub-G_1 fraction in the non *MYCN* amplified cell lines, as previously shown in Figure 4.9, and the response was increased in SHSY5Y cells following exposure to 4Gy ionising radiation (Figure 4.12a). Dual treatment with SKP2 siRNA and IR increased the sub-G_1 population in the *MYCN* amplified IMR32 and IMR-KAT100 cell lines compared to SKP2 knockdown alone, suggesting that SKP2 knockdown sensitises the cell lines to DNA damage (Figure 4.12b). This pattern of induction of apoptotic cell death was confirmed by the significant induction of caspase-3/7 activity (Figure 4.13), although the increase following dual treatment in the *MYCN* amplified, *p53* mutant IMR-KAT100 cells did not reach significance at the 95% level ($p = 0.06$, paired t test, Figure 4.13b)

The p53 functional response to DNA damage was investigated using western blotting for p53, MDM2 and p21 in the *p53* wt cell lines (Figure 4.14a). Lower levels of MDM2 induction were seen in the *MYCN* amplified IMR32 cells, which returned to basal levels by the 24 hr time point. Both SHSY5Y and IMR32 cell lines demonstrated induction of p53 and p21; however, SKP2 knockdown maintained the p21 stability in the IMR32 cell line 24 hrs post irradiation. SKP2 siRNA exposure had no effect on the level of p53 expression although a slight increase in MDM2 levels was observed in the SHSY5Y cells, which was associated with an increase in p21 expression 6 hrs post IR treatment. Neither MDM2 nor p21 induction was observed in the *p53* mutant cell lines although combined treatment of SKP2 siRNA and 4Gy IR was associated with an increase

in p27 protein levels (Figure 4.14b), implying that p27 accumulation may play a role in the apoptotic cell death induced by combined ionising radiation treatment and SKP2 depletion.

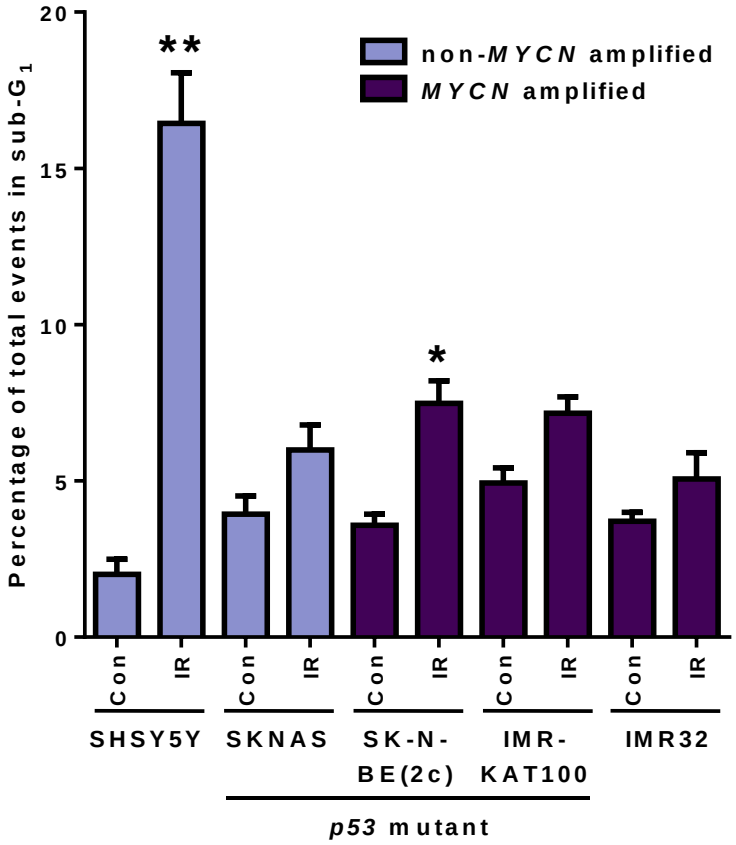

Figure 4.11 The effect of ionising radiation on sub-G_1 population in a panel of neuroblastoma cell lines. Percentage of cells in the sub-G_1 DNA fraction of the cell cycle measured by flow cytometry 24 hr after exposure to 4Gy irradiation. Data are the mean and error bars represent the SEM of n=3 experiments, * and ** correspond to a p value of <0.05 and <0.01, respectively.

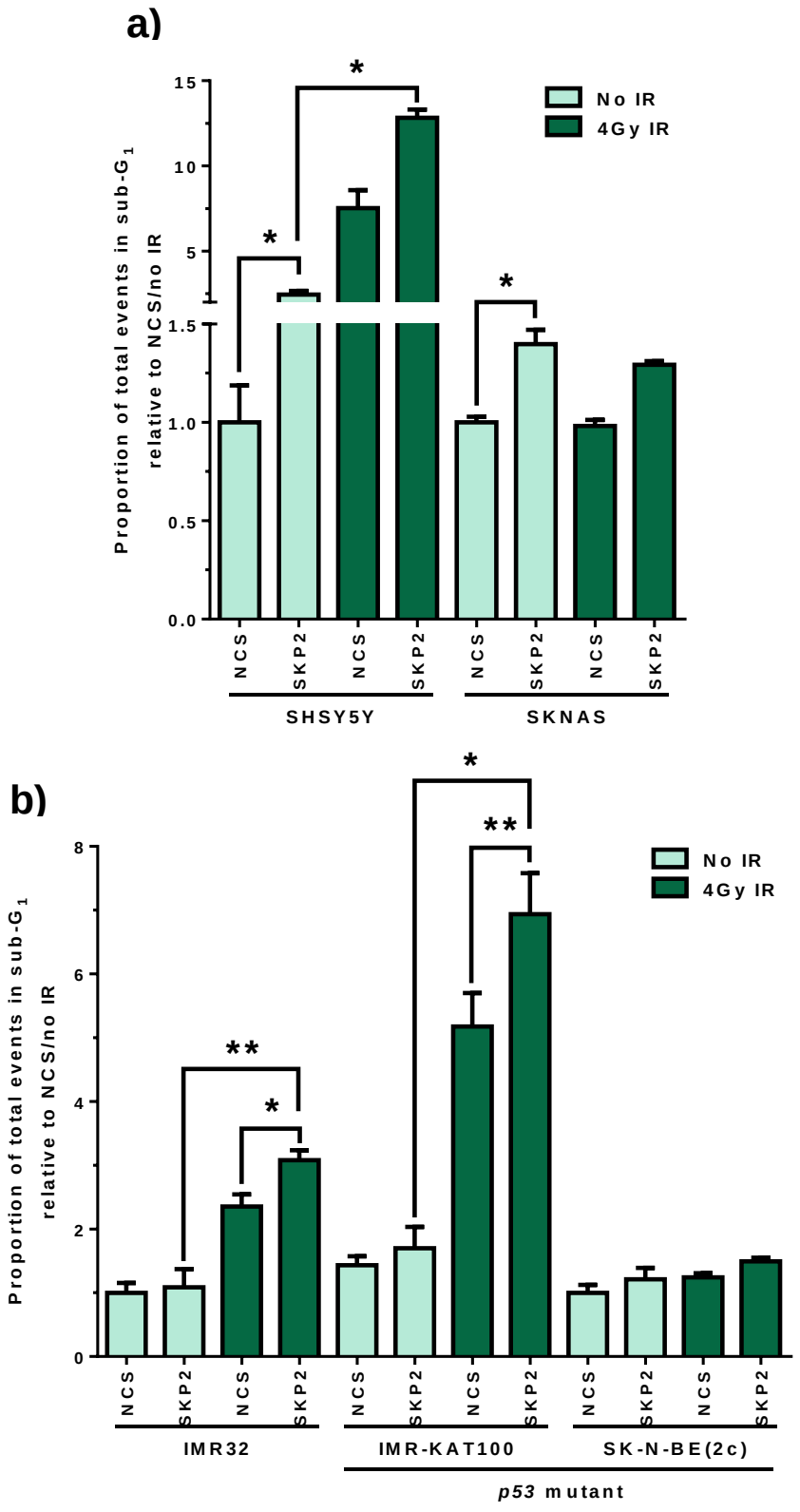

Figure 4.12 The effect of dual treatment with SKP2 siRNA and IR on the sub-G_1 population in a panel of neuroblastoma cell lines. Sub-G_1 population 48 hr post SKP2 siRNA treatment and 24 hr post 4Gy IR treatment. **a)** p53 wildtype cell lines**. b)** *p53* mutant cell lines. Data are normalised to the non-irradiated negative control siRNA (NCS). All data are the mean and error bars represent the SEM of n=3 experiments, * and ** correspond to a p value of <0.05 and <0.01, respectively.

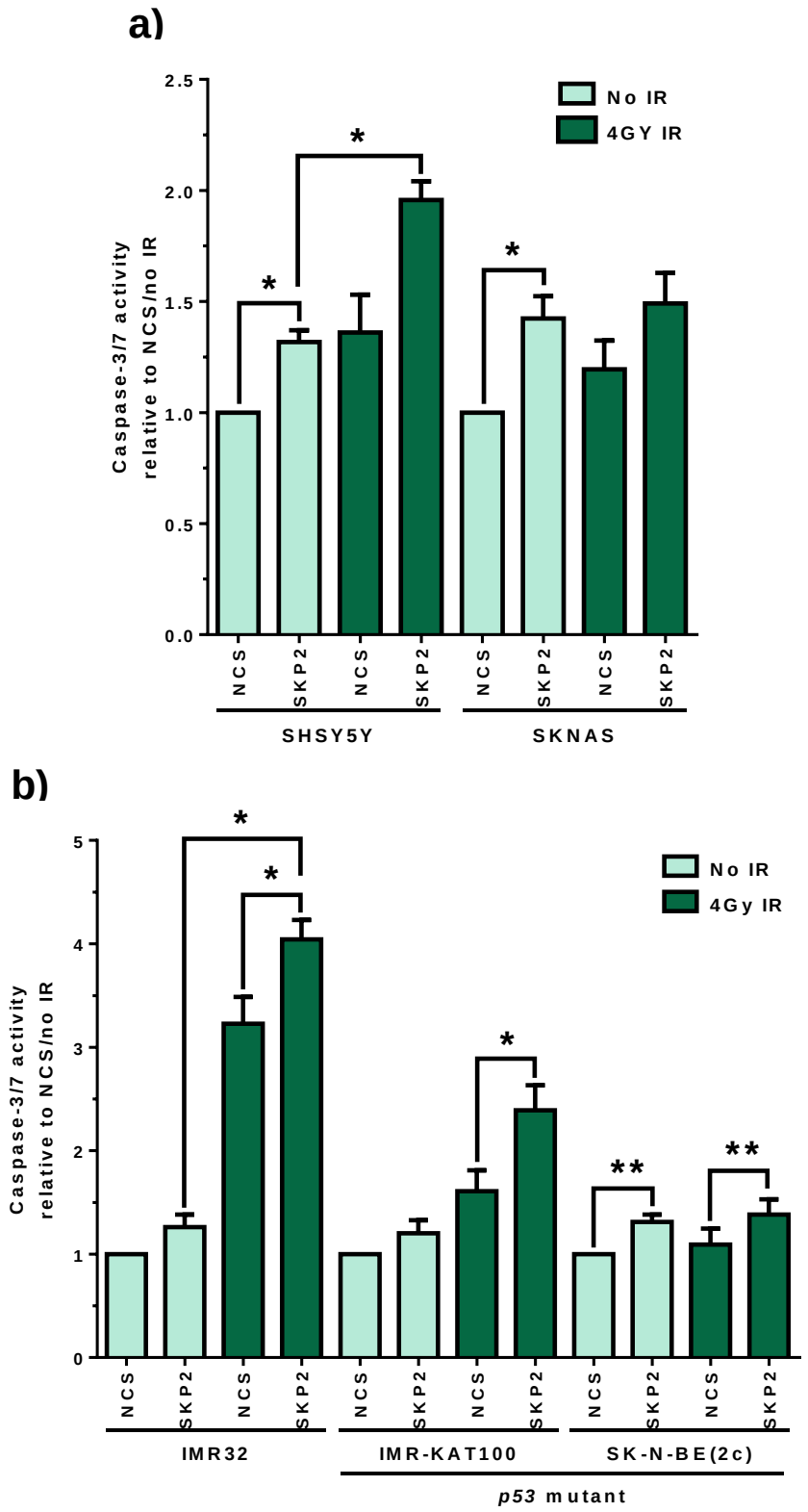

Figure 4.13 The effect of dual treatment with SKP2 siRNA and IR on caspase-3/7 activity in a panel of neuroblastoma cell lines. Caspase-3/7 activity 48 hr post SKP2 siRNA and 24 hr post 4Gy IR treatment. **a)** p53 wildtype cell lines. **b)** *p53* mutant cell lines**.** Data are normalised to the non-irradiated negative control siRNA (NCS). All data are the mean and error bars represent the SEM of n=3 experiments, * and ** correspond to a p value of <0.05 and <0.01, respectively.

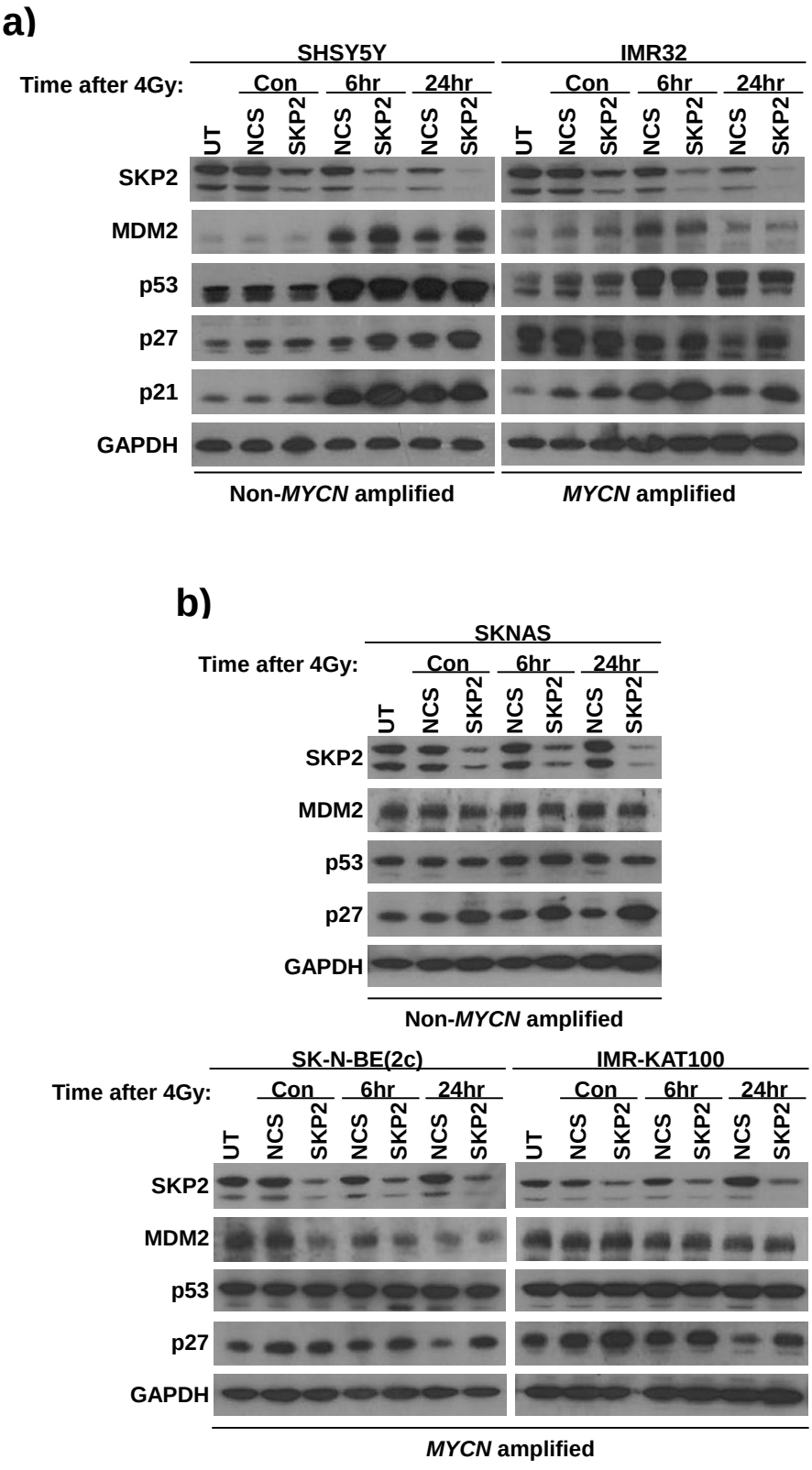

Figure 4.14 Western blot showing the effect of SKP2 knocdown and 4Gy ioninsing radiation on SKP2, p53, MDM2, p27 and p21 expression in a panel of neuroblastoma cell lines. Cell lysates were collected at the time points stated. **a)** p53 wildtype cell lines. **b)** *p53* mutant cell lines**.** The western blot shown is a representative of 3 independent repeats.

4.4.5. *Exogenous overexpression of SKP2 induces a G2 arrest in the SHEP neuroblastoma cell line*

To investigate the dependence of cell cycle progression on SKP2, SHEP cells, which have low endogenous levels of SKP2 protein, were transfected with a cDNA-*SKP2* expression plasmid. A transient transfection, the expression level of SKP2 returned back to its basal level by the 72 hr time-point indicative of the short half-life of the protein (Figure 4.15). The exogenous expression of SKP2 had no effect on the levels of p27 or p21, suggesting that other factors contribute to the expression profile of the CDK inhibitors. Forced expression of SKP2 significantly increased the G_2 population at the 48 hr time point compared to the empty vector control suggesting a G_2 arrest (Figure 4.16). Cell cycle arrest at the G_2 checkpoint is often associated with the p53 pathway; however, although SHEP cells do not harbour a *p53* mutation they do have a homozygous deletion of the MDM2 antagonist $p14^{ARF}$ (Carr-Wilkinson *et al.*, 2010b). As the lack of p14 expression results in suppression of p53 activity, the observed G_2 arrest from SKP2 induction may be through a p53-independent pathway. The accumulation of cells in G_2 was associated with a decrease in the G_1 population rather than S phase (Figure 4.16b), suggesting accelerated passage through the cell cycle as seen when MYCN is exogenously expressed in Tet21N MYCN+ cells (Figure 4.17). These data support the hypothesis that SKP2 contributes to the oncogenic behaviour of *MYCN* amplification.

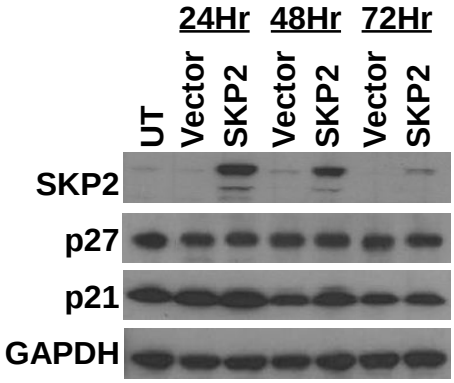

Figure 4.15 Western blot showing the effect of pcDNA-*SKP2* transfection on p27 and p21 expression in SHEP cells. Cell lysates were collected at the time points stated following transfection with the cDNA-*SKP2* or empty vector. The western blot shown is representative of 3 independent repeats.

a)

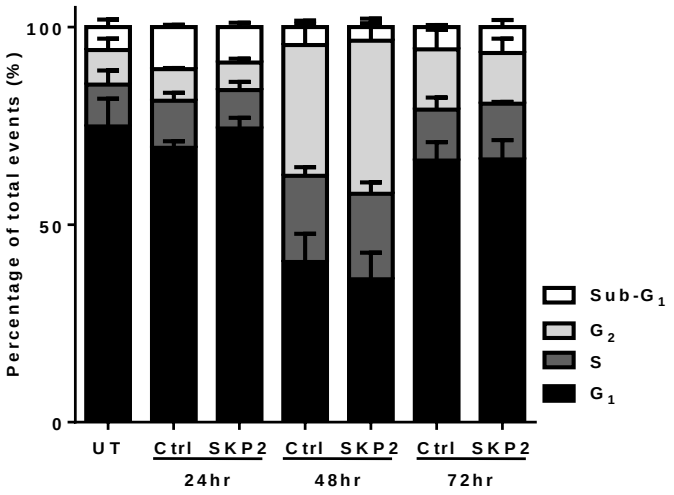

	24hr		48hr		72hr	
% Total events	**Ctrl**	**SKP2**	**Ctrl**	**SKP2**	**Ctrl**	**SKP2**
G1 Phase	69 ± 2	74 ± 3	41 ± 7	35 ± 7	66 ± 5	66 ± 5
S Phase	12 ± 2	10 ± 2	22 ± 2	22 ± 3	13 ± 3	14 ± 0.5
G2 Phase	8 ± 1	7 ± 1	33 ± 5	38 ± 5	15 ± 5	13 ± 4
Sub-G1 Phase	11 ± 1	9 ± 1	5 ± 2	3 ± 1	6 ± 0.5	7 ± 2

b)

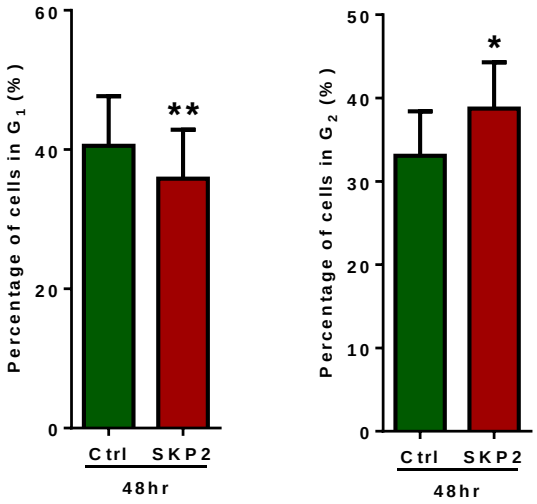

Figure 4.16 The effect of pcDNA-*SKP2* transfection on cell cycle distribution in SHEP cells measured by flow cytometry. a). Cell cycle phase distribution across all time points. **b)** Percentage of cells in G_1 and G_2 after a 48 hr exposure to the pcDNA-*SKP2* plasmid. Data are the mean and the error bars represent SEM of n=3, * and ** correspond to a p value of <0.05 and <0.01, respectively.

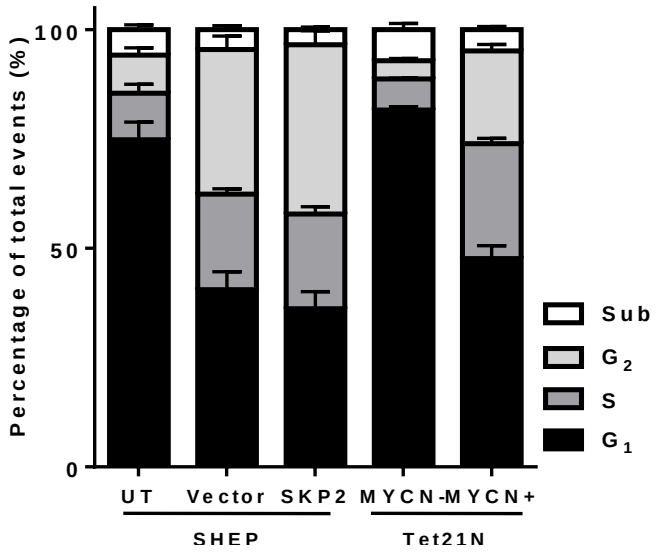

Figure 4.17 The effect of a 48 hr transfection with pcDNA-*SKP2* on cell cycle distribution in SHEP cells compared to Tet21N MYCN+/MYCN- cells. Data are the mean and the error bars represent SEM of n=3, * and ** correspond to a p value of <0.05 and <0.01, respectively.

4.5. Discussion

Identified as an oncoprotein, the role of SKP2 in tumour progression is predominantly characterised by its ability to modulate the G_1/S transition by targeting numerous regulatory proteins/tumour suppressors for proteasomal degradation. SKP2 over-expression often correlates with reduced levels of p27 and a poor prognosis (Bloom and Pagano, 2003), with p27 knockout in *SKP2*$^{-/-}$ mice reversing many of the unfavourable phenotypes seen from SKP2 loss (Nakayama *et al.*, 2004). However, while SKP2 is often identified as the rate limiting factor in the degradation of the target proteins, additional factors are required, namely, phosphorylation and, especially in the cases of p27 and p21, the presence of the SKP2 accessory protein CKS1. When analysing the role of SKP2 in accelerating cell proliferation and promoting tumorigeneis it is therefore necessary to consider these contributing factors.

CKS1 has been identified as a potential oncogene in an array of cancers, often associated with the amplification of the *CKS1B* gene and the ability of CKS1 to contribute to tumour progression both dependent and independently of the SCF^{SKP2} complex (Tsai *et al.*, 2005; Zhan *et al.*, 2007; Wang *et al.*, 2009a). Situated on chromosome 1q21.2, gains at 1q21-q25 have been linked to drug-resistant phenotypes and aggressive growth in stage 4 neuroblastoma (Hirai *et al.*, 1999), although there are currently no reports associating these gains with increased *CKS1B* expression. Alternatively the ability of MYC to induce *CKS1B* transcription (Keller *et al.*, 2007) raises the possibility that CKS1 expression is regulated by MYCN, which would be an additional aspect of SKP2 biology in *MYCN* amplified neuroblastoma. Additionally, SKP2 levels fluctuate during the cell cycle, and SKP2 itself targeted for degradation by the anaphase promoting complex/cyclosome (APC/C) E3 ligase when bound to the activator CDH1 (Wei *et al.*, 2004). The proteolysis of p27 is also regulated by the KIP1 ubiquitination-promoting complex (KPC) at the G_0-G_1 transition, a process dependent on the export of p27 into the cytoplasm independent of SKP2 (Kamura *et al.*, 2004). The precise role of SKP2 therefore varies depending on the phase of the cell cycle.

In addition to its role as an E3 ligase, the oncogenic behaviour of SKP2 has been linked to roles independent of its F-box and interaction with the SCF complex.

The contribution of SKP2 to tumour progression often depends on the cancer type and oncogenic driver which determines initial pathway activation and how SKP2 participates. In neuroblastoma the role of SKP2 in tumour progression is mainly focussed on its relationship with p27. As shown in Chapter 3, *SKP2* is a direct MYCN target gene and inhibition of SKP2 could potentially influence this aggressive oncogene by preventing MYCN-driven proliferation, tipping the balance towards MYCN-driven apoptosis.

4.5.1. *Non-MYCN amplified cell lines are more sensitive to SKP2 knockdown*

SKP2 siRNA treatment reduced cell proliferation across the panel of neuroblastoma cell lines, excluding the *MYCN* amplified *p53* mutant IMR-KAT100 cells (Figure 4.6), indicating a dependence on SKP2 for cell viability in neuroblastoma. However, only the non-*MYCN* amplified cell lines underwent a G_1 arrest (Figure 4.7), which was associated with the stabilisation, albeit modest, of p27 at the same time point. No effect of SKP2 knockdown on p27 was observed in the *MYCN* amplified cell lines (Figure 4.8), and the absence of p27 stabilisation may therefore explain the lack of a G_1 arrest. The requirement for p27 accumulation was confirmed when cell cycle arrest was reversed by additional p27 knockdown, demonstrating the SKP2-p27 interaction plays a key role in the G_1/S transition in non-*MYCN* amplified neuroblastoma (Figure 4.10a). Interestingly this conflicted with the effect of SKP2 knockdown in the MYCN regulatable Tet21N cells where a G_1 arrest (Figure 3.12a) and p27 stabilisation (Figure 3.11a) was only observed in the presence of MYCN. However as discussed in Section 3.5.3 this may reflect the lower baseline G_1 population in the Tet21N MYCN+ cells compared to Tet21N MYCN- cells. This discrepancy between *MYCN* amplification and MYCN overexpression is discussed further in the final discussion (Section 6.3.2).

MYCN amplification is characterised by deregulated cell proliferation and the shortening of G_1 phase, due to the increased activity of CDK4 and CDK2. The impact of SKP2-p27 on the G_1/S transition may therefore not be as significant as in the non-MYCN driven cell lines. Although SKP2-mediated proteolysis of p27 is the best characterised, a multitude of pathways have been reported to regulate p27 degradation depending on the cell cycle phase and p27 localisation

(reviewed by (Chu *et al.*, 2008)). The lack of p27 stabilisation following SKP2 knockdown in the *MYCN* amplified cell lines could for instance be the result of degradation by the cytoplasmic KPC E3 ligase in early G_1 promoted by the MYCN driven progression through the cell cycle (Kamura *et al.*, 2004). Alternatively, p27 may be protected from degradation by being sequestered into cyclin D-CDK4/6 complexes. Implicated in the assembly and nuclear import of cyclin D-CDK4, the ability of p27 to inhibit the kinase activity is thought to be dependent on the growth-state of the cell although it is also argued that p27 has a non-inhibitory role in proliferating/cycling cells which is regulated by the phosphorylation of two tyrosine residues (Y88 and Y89) in p27's CDK interaction domain (James *et al.*, 2008). Supported further by reports that p27 levels are prognostic indicators independent of MYCN amplification (Bergmann *et al.*, 2001), the lack of p27 stabilisation in the *MYCN* amplified cell lines exposed to SKP2 siRNA emphasizes the dominant role played by MYCN in tumour progression.

SKP2 targets numerous tumour suppressor proteins for degradation which could potentially contribute to the suppression of growth observed in the absence of a G_1 arrest. All the *p53* wt cell lines elicited an increase in p21 expression following SKP2 knockdown (Figure 4.8), potentially indicating increased p53-mediated induction of p21 in addition to the increased stabilisation. Although the p53-p21 axis regulates the G_1/S transition, growth inhibition in the *MYCN* amplified cell lines could potentially be due to a G_2/M block or increased apoptosis. Further investigation into the transcript and protein levels of p53 effectors, e.g. p21, 14-3-3σ and BAX, would therefore be of interest. This hypothesis is supported by the ability of SKP2 to suppress p53 activity (Kitagawa *et al.*, 2008) and the lack of growth inhibition in the IMR-KAT100 cells compared to the parental IMR32 cells. Although a G_1 arrest was not induced in the *MYCN* amplified cell lines used in this current study, this could be due to the increase in p21 levels only being high enough to slow proliferation but not cause cell cycle arrest (Bell *et al.*, 2006). Nevertheless, taken together these data support the role of SKP2 in MYCN driven tumorigenesis whilst again reinforcing the dominance of the MYCN oncogene in an amplified setting.

A significant reduction in cell proliferation was observed following SKP2 knockdown in the *p53* mutant SK-N-BE(2c) and SKNAS cell lines in the absence

of p21 accumulation (Figure 4.6). Although for the non-*MYCN* amplified SKNAS cells inhibition of proliferation can be attributed to p27 accumulation and a G_1 arrest, this observation does not explain the suppression of growth in the *MYCN* amplified SK-N-BE(2c) cells. IMR-KAT100 and SK-N-BE(2c) are both *MYCN* amplified and harbour the same *p53* mutation which confers loss of function (Xue *et al.*, 2007), yet only SK-N-BE(2c) cells undergo growth inhibition. This difference may be a reflection of cellular morphology as the parental IMR32 cells are N-type while the SK-N-BE(2c) cells are I-type. An intermediate between the neuroblastic N-type and non-neuronal, substrate adherent S-type, I-type neuroblastoma cells are reported to carry both N and S-type characteristics as well as show the greatest malignant potential (Ross *et al.*, 2003). As SKP2 siRNA exposure induced growth inhibition in the S-type SKNAS cells it may be that in response to SKP2 knockdown SK-N-BE(2c) cells act more like S-type cells. Alternatively as IMR-KAT100 cells were developed to have a multidrug resistance (MDR) profile by the repeated exposure to the heavy metal compound potassium antimony tartrate (KAT), they could be resistant to SKP2 inhibition due to more general mechanisms (Xue *et al.*, 2007). However, further investigations into possible mechanisms associated with the resistant phenotype compared to the parental IMR32 cell line would be required to confirm the reasons for resistance to SKP2 knockdown.

SKP2 has been shown to regulate glycolysis in cancer cells by modulating the function of GLUT1 (glucose transporter type 1) through non-proteolytic ubiquitination and subsequent activation of AKT by phosphorylation (Chan *et al.*, 2012). The AKT pathway is a key driver in the up-regulation of aerobic glycolysis in tumour cells (Warburg effect) and its activation is a common event in human cancers, including neuroblastoma. A poor prognostic indicator, activation of the PI3K/AKT pathway is reported to promote chemotherapeutic resistance in neuroblastoma cell lines and maintain MYCN stability through the inhibition of GSK3β which, when active, destabilises MYCN by phosphorylation on residue Thr50 (Kenney *et al.*, 2004; Chesler *et al.*, 2006; Opel *et al.*, 2007). Consequently, *MYCN* amplified neuroblastomas are more sensitive to therapeutic intervention of the AKT pathway with small molecule inhibitors shown to downregulate cyclin D1 and MYCN expression, which suppresses cell growth and induces apoptosis (Segerstrom *et al.*, 2011).

Recent findings have shown that the AKT pathway can influence SKP2 activity by both direct and indirect mechanisms (Figure 4.18). The phosphorylation of SKP2 on Ser72 by AKT both promotes the formation of the SCF^{SKP2} complex and primes SKP2 for further phosphorylation on Ser75 by casein kinase 1 (CK1). Dual phosphorylation protects SKP2 from degradation by the APC^{CDH1} complex (Gao *et al.*, 2009; Lin *et al.*, 2009), potentially creating a positive feedback loop as SKP2 can then target AKT for ubiquitination and activation. Alternatively, the AKT-mediated phosphorylation, and inactivation, of the FOXO transcription factor FOXO3a could influence SKP2 activity. High FOXO3a expression has been shown to correlate with a good prognosis in neuroblasotoma, and is able to drive apoptotic cell death following its re-activation by treatment with PI3K/AKT inhibitors (Santo *et al.*, 2013). FOXO3a has also been identified as a negative regulator of SKP2 activity both at the transcript level, by directly binding and repressing the *SKP2* promoter, and in a transcription-independent manner by disrupting the formation of the SCF^{SKP2} complex (Wu *et al.*, 2013).

As the XTT assay measures cell proliferation indirectly as reflected by total glycolytic activity (i.e. NADH production, Section 2.14) the reduction in cell proliferation seen in *MYCN* amplified cell lines following a 72 hr exposure to SKP2 siRNA could potentially reflect their sensitivity to the inhibition of AKT regulated glycolysis. It would therefore be of interest to probe for MYCN protein, cyclin D1 and phosphorylated AKT (pAKT(T308) and pAKT(S473)) to determine the effect of SKP2 inhibition on the AKT pathway. It would also be useful to employ a second cell proliferation assay to confirm the XTT assay data.

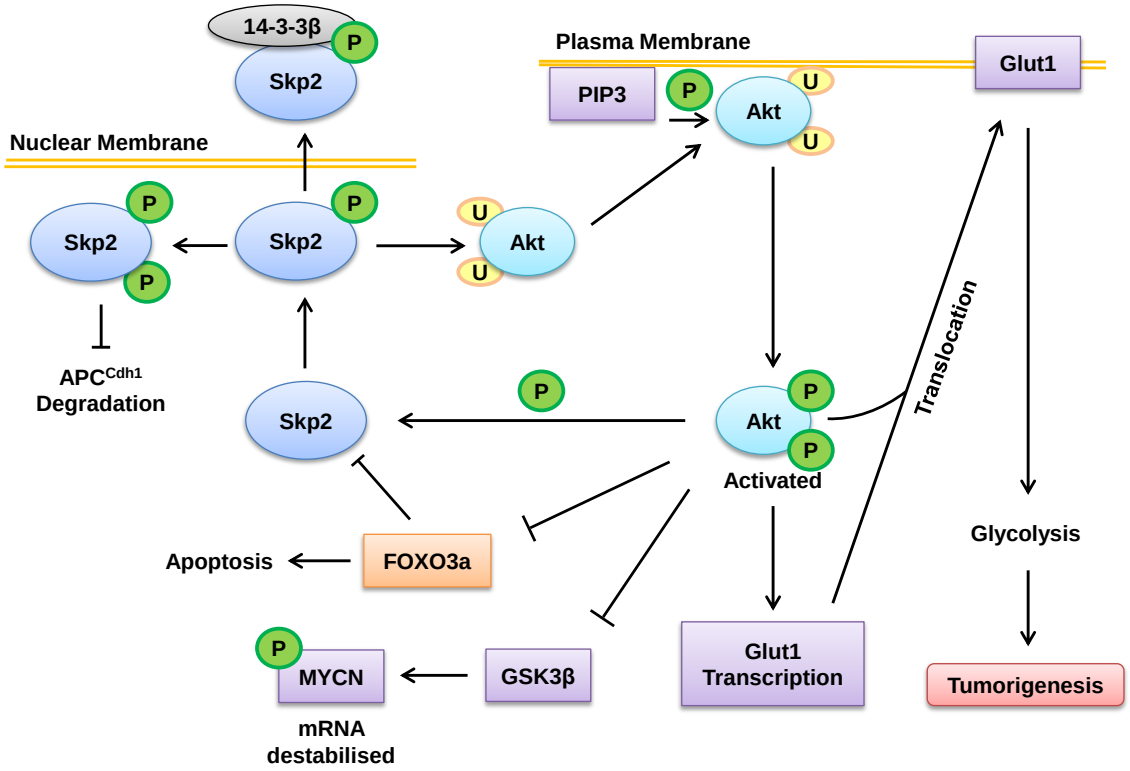

Figure 4.18 Interplay between SKP2 and the PI3K/AKT pathway. AKT phosphorylates SKP2 at Ser72 leading to cytoplasmic retention by binding to 14-3-3β and inhibiting binding to nuclear import receptors. Ser72 phosphorylation enhances the formation and activation of the SCF^{SKP2} complex, as well as promotes Ser75 phosphorylation which stabilises SKP2 by disrupting the interaction with CDH1. The SCF^{SKP2} complex ubiquitinates AKT at K8 and K14 residues promoting its membrane recruitment and EGF-triggered AKT phosphorylation and activation. Activated AKT: 1. Induces GLUT1 transcription and protein expression promoting the glycolytic phenotype and tumour development, 2. Phosphorylates GSK3β preventing its phosphorylation of MYCN on Thr50 resulting in increased MYCN stabilisation and 3. Inactivates FOXO3a preventing apoptotic cell death and the negative regulation *SKP2* expression.

4.5.2. *SKP2 and apoptotic cell death in neuroblastoma cell lines*

SKP2 inhibition has been shown to induce apoptotic cell death in a range of cancer models (Gstaiger *et al.*, 2001), and the reduced proliferation of *MYCN* amplified cell lines following SKP2 knockdown, independent of a G_1 arrest, could potentially be a result of apoptosis. However, as observed for the G_1/S transition, the induction of apoptosis, represented by an increase in the sub-G_1 population and induction of caspase-3/7 activity (Figure 4.9), was only significantly enhanced in the non-*MYCN* amplified cell lines including the *p53* mutant SKNAS cells, suggesting that a p53-independent pathway is responsible.

Apoptotic cell death involves two main pathways dependent on the type of cellular stress and the action of p53 co-activators. The extrinsic network involves the activation of death receptors to trigger a caspase cascade and the intrinsic mitochondrial pathway the activation of pro-apoptotic BCL-2 family members to form the apoptosome, ultimately initiating caspase-mediated apoptosis. The two pathways are also linked having been shown to in turn activate each other (Fulda and Debatin, 2006). SKNAS cells have been reported to show increased expression of the pro-apoptotic BH3-only protein BAD after inhibition of glycolysis (Chuang *et al.*, 2013), a process SKP2 inhibition could attenuate via PI3K/AKT inhibition as discussed in Section 4.5.1. As both pathways culminate with the activation of the executioner caspases such as caspase 3 and 7, the methods used in this study to determine apoptosis does not distinguish between the two pathways. The apoptotic cell death induced by SKP2 knockdown in the *p53* mutant SKNAS cells may therefore involve the intrinsic mitochondrial pathway.

The accumulation of p27, observed in all cells which underwent apoptosis, may potentially play a role in the apoptotic response. The expression of p27 has been shown to correlate with the pro-apoptotic regulator BAX in oropharyngeal carcinoma (Fujieda *et al.*, 1999), and act as a predictor of sensitivity to apoptotic cell death induced by proteasome inhibitors (Drexler and Pebler, 2003) and chemotherapy (Taguchi *et al.*, 2004). This role of p27 accumulation as a predictor of cell death is supported by the reduction in the sub-G_1 population following the dual knockdown of SKP2 and p27 in all 3 non-*MYCN* amplified cell lines (Figure 4.10b). Interestingly knockdown of p27 in SHSY5Y cells induced a greater

increase in sub-G_1 than that observed following SKP2 siRNA treatment suggesting that promoting p27 stability in this cell line would be unfavourable for the promotion of cell death, although a second assay is required to confirm that apoptosis is being induced. As SHSY5Y cells did undergo apoptosis following SKP2 knockdown this observation suggests that p27 accumulation did not promote cell death in this cell line, and could potentially induce resistance to cell death from further therapeutic intervention.

4.5.3. *SKP2 and p53*

A growing body of data has demonstrated the ability of SKP2 to alter p53 function. Alongside the inhibition of the p300 cofactor (Kitagawa *et al.*, 2008), the SKP2 isoform, SKP2B, has been observed to prevent p53-mediated apoptosis and transcriptional activity by promoting the degradation of the prohibitin (Chander *et al.*, 2010). In addition to the ability of *SKP2* deficiency to initiate oncogenic-stress driven senescence independent of the $p19^{ARF}$-p53 pathway (Lin *et al.*, 2010a), targeting SKP2 may provide a strategy to reactivate p53 or trigger cellular senescence.

SKP2 is reported to promote homologous recombination by aiding Mre11-Rad50-Nbs1 (MRN) complex-mediated recruitment and activation of the checkpoint kinase ATM in response to double strand DNA breaks (Wu *et al.*, 2012a). Recent reports have also associated the over-expression of SKP2 with resistance to ionising radiation through its manipulation of the rad51 pathway (Wang *et al.*, 2012b). The DNA damage response in p53-wild type neuroblastoma is in part determined by the MYCN expression level due to the dual role of MYCN in regulating cellular proliferation and sensitising cells to apoptosis. Although failure to undergo a G_1 arrest after irradiation is characteristic of *MYCN* amplified neuroblastoma, this has been shown to be associated with a lower induction of p21 and hypo-pRB accumulation, and a proposed switch from cell cycle arrest to a higher sensitivity to apoptotic cell death (Bell *et al.*, 2006). MYCN has also been shown to sensitises cells to apoptosis by inducing p53 transcription (Chen *et al.*, 2010b) and activating the pro-apoptotic activator HIPK2, which phosphorylates p53 on Ser46 directing the cell towards apoptosis (Petroni *et al.*, 2011).

In the current study SKP2 siRNA treatment caused a pronounced accumulation of p21 in all the p53 wild type cell lines independent of MYCN expression (Figure 4.8) implying a p53 response. Although no G_1 arrest or apoptosis was observed in the *MYCN* amplified cell lines, due to the involvement of SKP2 in p53 activity and the DNA damage response, it was of interest to investigate whether SKP2 inhibition could strengthen the response to irradiation-induced DNA damage.

Ionising radiation (IR) at 4Gy increased the sub-G_1 fraction in non-*MYCN* amplified SHSY5Y cells and in *MYCN* amplified *p53* mutant SK-N-BE(2c) cells (Figure 4.11). Interestingly, SKP2 siRNA treatment followed by 4Gy IR significantly increased apoptotic cell death compared to SKP2 knockdown alone in the SHSY5Y cells, as well as in *MYCN* amplified *p53* mutant IMR-KAT100 cells and parental IMR32 cells. No further increase in apoptosis was seen in the SK-N-BE(2c) cell line (Figure 4.12 and 4.13). Both SHSY5Y and IMR32 cells underwent a p53 response following ɣ-irradiation, as indicated by the increase in p53 and MDM2 expression (Figure 4.14). Although the response was maximal at 6 hrs post-irradiation for the *MYCN* amplified IMR32 cells, SKP2 siRNA treatment maintained p21 stability up to 24 hrs. A slight increase in MDM2 expression following combined treatment was observed in SHSY5Y cells but not in IMR32 cells. As MYCN directly regulates both *SKP2* (Chapter 3) and *p53* expression (Chen *et al.*, 2010b) a greater induction of MDM2 was expected for the IMR32 cells due to the larger pools of p53 being activated by the release of SKP2-mediated inhibition of the p300 cofactor (Kitagawa *et al.*, 2008). However, as an increase in cell death was also observed in the *p53* mutant IMR-KAT100 cell line, it may be that the sensitisation to irradiation induced cell death by SKP2 knockdown is independent of the p53 pathway.

SKP2 knockdown was shown to induce apoptosis in the non-*MYCN* amplified *p53* mutant SKNAS cell line (Figure 4.9). This apoptotic response was observed in the absence of p21 stabilisation yet was associated with an increase in p27 levels (Figure 4.8). This relationship between increased p27 expression and apoptotic cell death was also observed in the SHSY5Y, IMR32 and IMR-KAT100 cell lines following SKP2 siRNA/4Gy treatment, suggesting that p27 plays a role in the regulation of cell survival in neuroblastoma cell lines (Figure 4.14). The role of p27 in the regulation of apoptosis is conflicting with some reports suggesting

p27 overexpression protects from apoptosis (Masuda *et al.*, 2001) whilst others show it induces it (Katayose *et al.*, 1997). Although p27 knockout mice retain their ability to undergo a G_1 arrest they do display organ hyperplasia. It is therefore possible that the ability of p27 to induce apoptosis plays an important role in its ability to maintain correct organ size (Nakayama *et al.*, 1996). As p27 stabilisation was only present in IMR32 and IMR-KAT100 cells following the combination of SKP2 siRNA and 4Gy IR treatment (Figure 4.14), these data suggests that SKP2 inhibition could potentially be a mechanism for promoting cell death in *MYCN* amplified neuroblastoma. However, further investigation would be required to confirm this using a larger panel of cell lines as well as a second mechanism of DNA damage, e.g. doxorubicin.

An alternative role for p27 could involve suppression of centrosome amplification in *MYCN* amplified neuroblastoma, thereby preventing further tumour development and promoting stress-induced apoptosis. Centrosome duplication begins during the G_1/S transition and although a tightly regulated aspect of the DNA replication cycle, these regulatory mechanisms are often abrogated in aggressive tumours such as *MYCN* amplified neuroblastoma resulting in amplified centrosomes and chromosomal instability. The enhanced expression of MYCN has been shown to lead to centrosome amplification following DNA damage in neuroblastoma cell lines through a mechanism involving suppression of p27 expression via the up-regulation of SKP2 (Sugihara *et al.*, 2004). The accumulation of p27 following SKP2 siRNA could therefore trigger stress-induced apoptosis through a mitotic block (Sugihara *et al.*, 2006).

Alternatively, the increase in apoptosis observed following SKP2 knockdown in cells lacking a functional p53 pathway could be the result of p73 stabilisation. A close relative of p53, p73 is thought to mediate apoptosis in an E2F1- dependent manner (Irwin *et al.*, 2000), and to rely on acetylation by the p300 co-factor for transcriptional activation following DNA damage (Costanzo *et al.*, 2002). As with p53, SKP2 siRNA treatment could potentially promote p73-driven apoptosis by releasing the inhibition on the p300 co-activator.

In the above setting, the increased p73 activity could potentiate the apoptotic response through the up-regulation of tumour protein p53-inducible nuclear

protein 1 (TP53INP1) expression. A MYCN transcriptional (Bell *et al.*, 2007) target, TP53INP1 has been shown to promote apoptosis in p53-deficient cells by increasing the transactivation capacity of p73 (Tomasini *et al.*, 2005). The increase in apoptosis following the dual treatment of SKP2 siRNA and IR in the *p53* mutant *MYCN* amplified cell lines (Figure 4.12b and 4.13b), could therefore be though the formation of a self-amplifying loop, where SKP2 inhibition and IR promotes p73 activity which transactivates *TP53INIP1* which, in turn, modifies p73 activity to stimulate pro-apoptotic functions.

4.5.4. *Forced expression of exogenous SKP2*

The oncogenic role of SKP2 is primarily attributed to it targeting p27 for degradation, consequently promoting the G_1/S transition. However in this study the overexpression of SKP2 in SHEP cells increased the G_2 population suggesting cells were unable to enter mitosis. The G_2 checkpoint is associated with DNA damage repair and progression into mitosis, and requires the accumulation and activation of CDK1 by its binding to cyclin B1. In the SKP2/p27 relationship, p27 accumulation is often associated with the inhibition of CDK2 (bound to either cyclin A or E) and potential effects on CDK1 are often overlooked (Toyoshima and Hunter, 1994). Alternatively, the G_2/M transition is controlled by a p53-dependent pathway which inhibits CDK1 by the direct transcriptional regulation of p21, Gadd45 and 14-3-3σ (Taylor and Stark, 2001). However, as SHEP cells are homozygously deleted for the MDM2 suppressor $p14^{ARF}$, the G_2 arrest is unlikely to be through p53-regulated pathways.

Surprisingly, the transient overexpression of SKP2 had no effect on the protein levels of p27 or p21 compared to the control vector (Figure 4.15). While this suggests that the exogenously expressed protein is non-functional, the ability of SKP2 to target p27 and p21 for degradation also requires substrate phosphorylation and the formation of a trimeric complex between SKP2, CKS1 and the cyclin A/E-CDK2 (Sitry *et al.*, 2002; Bornstein *et al.*, 2003). As SHEP cells are reported to express neither MYCN nor c-MYC (Chen *et al.*, 1994) and CKS1 has been identified as a MYC target gene (Keller *et al.*, 2007), there is potential for the lack of p27/p21 degradation being due to lack of CKS1 to compensate for the increased levels of SKP2. It would therefore be of interest to investigate the

expression levels of CKS1, phosphorylated p27 and p21, as well as CDK1 and p53 downstream activators in this setting of SKP2 overexpression.

Although forced expression of SKP2 did not have the anticipated effect on p27 and p21 protein levels (Figure 4.15), it did cause a redistribution of the cells throughout the cell cycle, suggesting increased proliferative activity (Figure 4.16). Despite the minimal effects on cell cycle compared to the empty vector control, the enhanced G_2 fraction following the transient SKP2 overexpression was matched by a decrease in the G_1 population as expected, consistent with high levels of SKP2 accelerating S phase entry (Figure 4.16). Unfortunately, due to the transient nature of the transfection used the effect of SKP2 expression on overall proliferation rates could not be monitored. It would therefore be of interest to form stable transfectants and investigate the effects of SKP2 overexpression on S phase entry, via BrdU-incorporation and long term proliferation.

Despite the lack of enhanced p27 and p21 degradation following forced SKP2 expression, the changes to cell cycle phase distribution may still be a result of increased cyclin A-CDK2 activity. SKP2 is reported to compete with p27 and p21 for binding to cyclin A in a regulatory mechanism which protects cyclin A-CDK2 from inhibition (Ji *et al.*, 2006). Although the authors did recognise that the molar concentration of SKP2 must be ~2 over that of p27 and p21, the forced expression of SKP2 may be physiologically relevant in the current study. Conversely Poon *et al* demonstrated that the interaction between SKP2 and cyclin A-CDK2 inhibited CDK2 activity (Yam *et al.*, 1999), preventing cell cycle progression upon SKP2 overexpression.

Interestingly, the 48 hr cDNA-*SKP2* transfection produced a similar cell cycle phase distribution as the SHEP-Tet21N MYCN+ cells (Figure 4.17). As this study has identified *SKP2* as a direct MYCN target gene (Chapter 3) this observation is consistent with the hypothesis that the accelerated proliferation seen in *MYCN* amplified neuroblastoma is in part due to increased SKP2 protein expression. It would therefore be of interest to develop stable SHEP-SKP2 transfectants for use in comparison with the SHEP-Tet21N MYCN+ cells to determine to what extent the MYCN/SKP2 relationship controls proliferation in neuroblastoma.

4.6. Conclusions

The results discussed in this chapter provide strong evidence that the inhibition of SKP2 would be of therapeutic benefit in non-*MYCN* amplified neuroblastoma. SKP2 siRNA treatment was shown to a.) induce a G_1 arrest by stabilising the expression of p27 and b.) promote apoptotic cell death independent of the p53-pathway in non-*MYCN* amplified cell lines. Functional studies of SKP2 have also identified a potential synergistic interaction between SKP2 knockdown and ɣ-irradiation, at the level of apoptosis independent of both *MYCN* status and the p53-pathway. Lastly, the overexpression of SKP2 was found to promote accumulation of the G_2 fraction indicative of accelerated proliferation.

Taken together these data suggest that although the SKP2/p27 axis contributes to the proliferation of neuroblastoma cell lines, *MYCN* amplification does not increase sensitivity to SKP2 inhibition, yet is instead able to compensate for the loss of SKP2 activity. Nevertheless, targeting SKP2 may be of therapeutic benefit in the treatment of non-*MYCN* amplified disease. However given that the phenotypes following siRNA knockdown of a gene are not always comparable to those induced by small-molecule inhibition, further investigation into pharmacological inhibition of SKP2 in neuroblastoma is required.

Chapter 5.
Pharmacological targeting of SKP2 using small molecule inhibitors

5.1. Introduction

5.1.1. *SKP2 as a therapeutic target*

The initial concept of targeting SKP2 therapeutically was as a mechanism to stabilise the expression of p27 levels, which are often found to be reduced in aggressive tumours and to correlate with a poor prognosis (Philipp-Staheli *et al.*, 2001). However, further insights into the functional role of SKP2 have resulted in additional protein targets being identified, and SKP2 has also been shown to contribute to tumorigenesis by mechanisms independent of its E3 ligase activity. Furthermore, SKP2 is recognised as an oncogene, and has been shown to be capable of promoting malignant transformation through cooperation with Ras (Gstaiger *et al.*, 2001), AKT (Chan *et al.*, 2012) and c-MYC (Bretones *et al.*, 2011), amongst other signalling pathways that are often deregulated during tumour progression. This diversity of roles results in SKP2 overexpression influencing a variety of cellular processes such as proliferation, apoptosis (Kitagawa *et al.*, 2008) and differentiation (Pirity *et al.*, 2006), and as a result the biological effects of SKP2 inhibition often depend on tumour cell-type and cellular biochemistry, as well as the specific activated oncogenic pathways. The complex biology of SKP2 was reflected in the responses of neuroblastoma cell lines to SKP2 siRNA knockdown, where non-*MYCN* amplified cell lines showed both a G_1 arrest and apoptotic cell death independent of the p53 pathway, identifying SKP2 as a potential drug candidate in non-*MYCN* amplified disease in particular (Chapter 4).

The premise of targeting SKP2 with small molecule inhibitors is strengthened by the observation that *SKP2*$^{-/-}$ mice are viable, suggesting a therapeutic window. Additionally the crystallographic 3D structures available of SKP2 and its SCF components, including CKS1 (Cardozo and Abagyan, 2005; Hao *et al.*, 2005), have identified potential targetable pockets for small molecule inhibitors. Taken together these data support SKP2 as a potential cancer drug target.

5.1.2. *Targeting the SCF E3 Ubiqutin Ligases*

SKP2 is a member of the largest family of E3 ubiquitin protein ligases, and a range of options are available to indirectly inhibit SCF^{SKP2} activity. Bortezomib (Velcade®, Millennium Pharmaceuticals) was the first proteasome inhibitor to be registered as a drug, identifying a new approach to targeting the ubiquitin proteasome system (UPS). However, the 26S proteasome is an essential part of protein homeostasis responsible for the degradation of an extensive range of proteins involved in various intracellular regulatory roles. As a consequence, although bortezomib has been shown to improve the clinical outcome for some haematological malignancies, multiple myeloma in particular, severe side effects and dose-limiting toxicities restrict its effectiveness and utility (Chen *et al.*, 2011). Attempts to increase the therapeutic index of proteasome inhibitors are ongoing with the production of second generation compounds, as reviewed by (Mattern *et al.*, 2012). However, an alternative approach to enhance specificity and therefore reduce potential side effects is to target the proteins upstream of the proteasome, such as the E3 ligases, in an attempt to increase selectivity for the effector proteins being stabilised.

SCF complexes are attractive anticancer targets due to their involvement in the regulation of tumour suppressor proteins and the deregulation found in several human malignancies (Nakayama and Nakayama, 2006b). Approaches to inhibit the activity of SCF complexes are summarised in Figure 5.1 and include; (1) Inhibition of substrate specific kinases, although not directly related to the E3 ligase *per se*, SCF substrates require phosphorylation to be recognised by the F-box proteins and hence, kinase inhibition will prevent substrate degradation, (2) Disruption of the interaction between the RBX1 RING protein and E3 ubiquitin conjugation enzyme (UBC), although no inhibitors have been reported (3) Disruption of the interaction between the SCF components such as between SKP2-CKS1 or SKP2-SKP1, as discussed in detail in Section 5.1.3, (4) Inhibition of CUL1 neddylation.

This last approach prevents the formation of the SCF complex by locking the CUL1 protein in an inactive state. Acting as the scaffold holding the SCF complex together, prior to complex formation CUL1 requires neddylation to remove the

cullin binding protein CAND1, which otherwise inhibits the interactions with RBX1 and SKP1. A pathway similar to ubiquitylation, the ubiquitin-like protein NEDD8 is first activated by the NEDD8-activating enzyme (NAE) and then attached to CUL1, inducing a conformational change which displaces CAND1 allowing SKP1-CUL1-RBX1 formation (Duda *et al.*, 2008). A rate limiting factor in the activity of SCF complexes, neddylation has been exploited by the development of MLN4924 (Millennium Pharmaceuticals), a potent selective inhibitor of NAE (Soucy *et al.*, 2009). Binding to the NAE active site, MLN4924 induces the accumulation of cullin-RING ligase (CRL) substrates including those of the SCF^{SKP2} complex (Soucy *et al.*, 2009). However, although more selective than bortezomib, MLN4924 still targets all CRLs in addition to other proteins reliant on the neddylation pathway, which potentially results in unfavourable side effects. Successfully increasing the therapeutic index of UPS inhibition is therefore dependent on the development of specific inhibitors which are highly selective towards a particular E3 ligase and its substrates, e.g. the F-box protein SKP2.

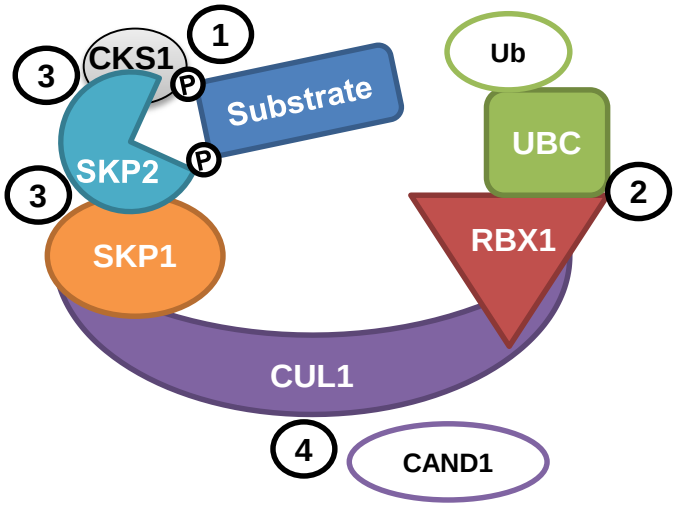

Figure 5.1 Graphical representation of mechanisms to potentially inhibit an SCF complex. (1) Inhibition of kinases which phosphorylate F-Box substrates. **(2)** Disruption of the interaction between the RBX1 RING protein and E3 ubiquitin conjugation enzyme (UBC). **(3)** Disruption of the interaction between the SCF components. **(4)** Inhibition of CUL1 neddylation.

5.1.3. *Direct targeting of SKP2 with small molecule inhibitors*

A primary objective in the development of small molecule inhibitors of SKP2 is to prevent the ubiquitylation and consequent degradation of p27. A measurable endpoint, this has led to the development of high-throughput screening methods for SCF^{SKP2} complex activity. One such screen led to the identification of a compound which was shown to inhibit p27 ubiquitylation by disrupting the SKP1-SKP2 interaction, inducing a G_1 arrest and cell death *via* autophagy in myeloma cell lines (Chen *et al.*, 2008a). 'Compound A' (**I**), was identified using an *in vitro* screen which was based on the radioactive labelling of *in vitro*-transcribed and -translated p27. Although compound A did not directly inhibit the E3 ligase activity of SKP2, it did act as a 'proof of principle' tool molecule and supported further development of small molecule SKP2 inhibitors. Utilising a more direct approach, Wu *et al* (2012) used an *in silico* structure-based tool termed virtual ligand screening (VLS) to search for compounds that might target the p27-binding interface formed by the SKP2-CKS1 interaction. A structure based approach exploiting the published SKP2-CKS1-p27 crystal structure, the authors first identified 'hotspot' residues that are essential for p27 binding and/or ubiquitination. The sub-structures containing the hotspots were then screened using a database of potential ligands in order to identify potential inhibitors based on the binding score and physico-chemical properties. Using this approach, an inhibitor (CI, Figure 5.7) was identified which disrupted SKP2-p27 binding and induced cell cycle arrest in cancer cell lines (Wu *et al.*, 2012b), although as with the compound published by Chen *et al*, the anti-tumour activity of compound CI was not evaluated. Nevertheless, by disrupting the SKP2-p27 interface the authors increased the specificity of targeting SKP2 E3 ligase activity to the substrates that require CKS1 (i.e. p27, p21 and p57).

More recently Chan *et al* (2012) extended previous findings by using high-throughput *in silico* screening approaches to specifically target the SKP1-SKP2 interaction based on two pockets observed in the SCF-SKP2 crystal structure which contribute to the SKP1-SKP2 interaction. From the high-throughput virtual screen 25 hits were selected and validated in an *in vitro* glutathione *S*-transferase (GST) pull-down assay, and an *in vitro* SKP1-SKP2 binding assay, resulting in the identification of SZL-P1-41 which showed the highest potency and most

significant inhibition of the SKP1-SKP2 interaction. Following conformation that SZL-P1-41specifically stabilised SKP2 targets (p27, p21 and AKT) but not other F-box substrates (FBW7), the authors investigated the therapeutic potential of SZL-P1-41 in cancer cell lines, identifying a potent suppressive effect on cell viability which was associated with the upregulation of p27 and p21 and the downregulation of AKT and GLUT1, presumably by the mechanism previously discussed in Chapter 4. Notably Chan *et al* also investigated the *in vivo* anti-tumour activity of SZL-P1-41, showing that it restricted tumour growth in a dose-dependent manner (Chan *et al.*, 2012). Although further validation is required to determine the effects of SZL-P1-41 on other F-box complexes, and potential effects on SKP2 that are independent of its E3 ligase activity (Chan *et al.*, 2013), the development of these small molecule inhibitors illustrates the potential of targeting SKP2 pharmacologically.

5.1.4. *Indirect targeting of SKP2 with small molecule inhibitors*

An alternative approach to inhibiting SKP2 activity is to target its transcription or stability. Although the underlying mechanisms of SKP2 overexpression are not fully understood, *SKP2* gene expression and protein stability have been shown to be upregulated by numerous signalling pathways, including those driven by oncoproteins, e.g. c-MYC/BCR-ABL. The inhibition of these pathways, for which small molecules have been developed, therefore offers an indirect approach to targeting SKP2 activity.

SKP2 protein stability is positively regulated by several post-translational modifications. AKT and CDK2 have been shown to interfere with the destruction of SKP2 by the APC^{CDH1} complex, through phosphorylation of Ser72 and Ser64. AKT-mediated Ser72 phosphorylation has also been shown to promote SCF^{SKP2} complex formation by stimulating subsequent phosphorylation at Ser75 by casein kinase I (Rodier *et al.*, 2008; Lin *et al.*, 2009). In addition to the Ser72 and Ser64 phosphorylation sites, a third site at Thr417 is targeted by Pim-1 protein kinase, which is often driven by c-MYC and AKT activity (Cen *et al.*, 2010). Small molecule inhibition of these SKP2 modulators may promote SKP2 degradation thereby reducing its activity. Alternatively, the APC^{CDH1} complex can be manipulated, for example with retinoic acid, which is currently used to treat high

risk neuroblastoma. Retinoic acid promotes SKP2 degradation by downregulating the nuclear export factor Rae1, resulting in the nuclear accumulation of CDH1 and hence SKP2 destabilisation and p27 accumulation (Pirity *et al.*, 2006).

Consistent with its key role in cell cycle progression, SKP2 interacts with numerous cell cycle proteins. First identified in transformed cells as a component of the cyclin A-CDK2 complex, SKP2 interacts stoichiometrically with cyclin A and SKP1, suggesting that its function when bound to cyclin A is of the same importance in tumour progression as its E3 ligase activity when bound to SKP1 in the SCF^{SKP2} complex. (Zhang *et al.*, 1995). SKP2 has been found to interact with cyclin A through an alternative binding motif to the RXL-HP interaction observed between cyclin A and p27. Instead the direct interaction between SKP2 and cyclin A has been found to be through a novel binding motif in the SKP2 N-terminal domain and is therefore independent of the ability of SKP2 to mediate p27 ubiquitination and degradation. The literature on the effects of the SKP2-cyclin A-CDK2 interaction on CDK2 kinase activity are conflicting, with one report stating the interaction is non-functional (Zhang *et al.*, 1995) and another that SKP2 inhibits cyclin A-CDK2 kinase activity (Yam *et al.*, 1999). However, by comparing SKP2/cyclin A and p27/cyclin A molar ratios throughout the cell cycle in HeLa cells with those required to reach an IC_{50} in an *in vitro* kinase assays, an inhibitory role has been argued to be impossible at physiological SKP2 concentrations. Alternatively it has been suggested that when SKP2 is in excess over p27, it plays a protective role, preventing the p27-mediated inhibition of cyclin A (Ji *et al.*, 2006). Given that the interaction of SKP2 with cyclin A-CDK2 was found to be specific for cyclin A, and independent of the E3 ligase activity of SKP2, the disruption of the complex identifies an alternative route to inhibiting cyclin A-CDK2 activity. This hypothesis was confirmed by the introduction of a SKP2-cyclin A blocking peptide which facilitated the inhibition of cyclin A-CDK2 by p27 and induced cell death specifically in cancer cells. Interestingly the disruption of this protective role of SKP2 induced a greater effect on cell proliferation and survival than SKP2 knockdown in the four cancer cell lines analysed (Ji *et al.*, 2007), suggesting that targeting a specific role of SKP2 may be a more effective therapeutic intervention than targeting overall SKP2 activity.

The observations discussed above highlight the importance of investigating all of the biological roles of SKP2 when determining its therapeutic potential. The contribution of SKP2 to malignancy has been reported to be tumour specific and the biological effects of SKP2 knockdown shown to depend on tumour type and genotypic features, e.g. *MYCN* amplification status as discussed in Chapter 4. The majority of studies of SKP2 inhibition have focused on supressing SKP2 E3 ligase activity, and the mechanisms of cancer cell death associated with the loss of SKP2 activity, range from apoptosis to autophagy and the induction of cellular senescence, depending on the method of SKP2 inhibition and cell type studied. Overall, when establishing the rationale for the development of SKP2 inhibitors it is important to acknowledge the difference between preventing protein expression and inhibiting its function.

5.2. Aims

The overall aim of the work presented in this chapter was to identify potential SKP2 inhibitors through an analogue based approach. This aim was addressed by the following specific objectives:

- To analyse the structure-growth inhibition relationships for compound A (**I**) analogues by determining their GI_{50} concentrations in HeLa cells.

- To examine the impact of selected **I** analogues on SKP2-mediated p27 degradation compared to commercially available ubiquitination pathway inhibitors using the p27 degradation Redistribution® assay.

- To investigate whether MYCN sensitises the Tet21N MYCN regulatable neuroblastoma cell line to small molecule inhibition of SCF^{SKP2} activity.

5.3. Chapter specific materials and methods

5.3.1. *SCF-Skp2 E3 Ligase: p27 degradation Redistribution® assay*

This HeLa cell-based assay, developed by BioImage, Thermo Scientific (R04-052-01, Thermo Scientific, Fisher Scientific, Waltham, MA, USA) uses Redistribution® technology to monitor a stably expressed GFP-tagged human p27 which contains a T187D mutation to imitate the phosphorylated state. The p27 protein is fused to the N-terminus of the GFP protein, and the continuous expression of the $p27^{KIP1}$(T187D)-EGFP controlled by a standard CMV promoter expression of which is maintained by G418 selection.

Due to the T187D mutation, the GFP-tagged p27 is constantly targeted for degradation by the SCF^{SKP2} complex allowing it to be used as a reporter for SKP2 E3 ligase activity. Inhibition of SKP2 activity therefore leads to the stabilisation of p27 and an increase in green fluorescence which can be quantified fluorometrically (Figure 5.2).

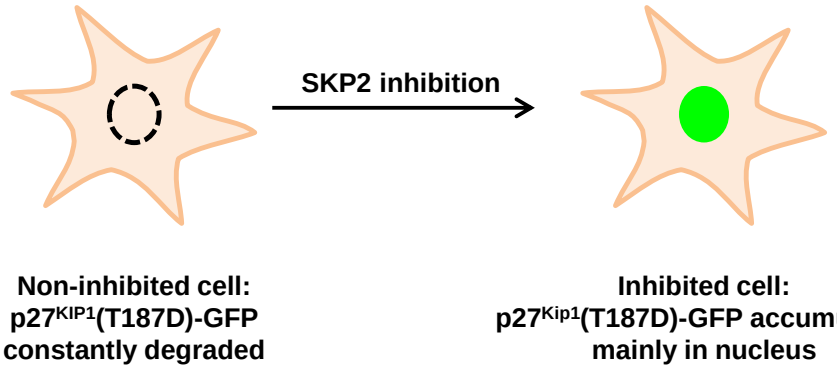

Figure 5.2 Schematic representation of the SCF^{SKP2}: $p27^{KIP1}$ degradation assay (Thermo Scientific)

5.3.1.1. Propagation of the HeLa-$p27^{KIP1}$(T187D)-EGFP cell line

The HeLa-$p27^{KIP1}$(T187D)-EGFP cell line was grown in DMEM growth medium, high glucose, without L-glutamine or sodium pyruvate (Thermo Scientific, Fisher Scientific cat.#SH30081) supplemented with 10% (v/v) FBS (Sigma), 2mM (v/v) L-glutamine (Sigma), 1% (v/v) penicillin-streptomycin (Sigma) and 0.5 mg/ml G418 w/v (Calbiochem). Cells were grown at 37°C in 5% CO_2 in a humidified incubator and passaged once 60-70% confluent.

5.3.1.2. HeLa-p27^{KIP1}(T187D)-EGFP assay protocol

Cells were seeded at 8000 cells/well in a 96-well microplate (Thermo Scientific cat.#165306), 24 hrs prior to treatment, and incubated at 37°C in 5% CO_2 overnight to allow attachment. Cells were treated with the putative inhibitors dissolved in DMSO and diluted to 0.5% (v/v) DMSO in assay medium (culture medium without G418 sulphate) at concentrations ranging from 0.01 – 100 µM, and incubated for a further 24 hrs. After inhibitor treatment, cells were fixed by replacing the assay buffer with 100 µl 10% (v/v) formalin, neutral-buffered solution (approximately 4% (v/v) formaldehyde) and incubated for 20 minutes at room temperature. Cells were then washed 4 times with 200 µl PBS and incubated at room temperature for 30 minutes under light restricted conditions with 100 µl 1 µM Hoechst staining solution (1 µM Hoechst in PBS containing 0.5% (v/v) Triton x-100). The cells were imaged using the BMG LABTECH FLUOstar Omega plate reader (BMG LABTECH, Germany) with filters set at 355/460 nm for Hoechst and 385/520 nm for EGFP (wavelength for excitation and emission, respectively). The proteasome inhibitor MG132 was used to validate the assay and a concentration of 5 µM chosen as the positive control in each assay. For all compounds the GFP intensity was corrected for background fluorescence, normalised to Hoechst 33342 fluorescence to correct for the cell number per well, and the level of GFP expressed as the percentage activity relative to the 5 µM MG132 positive control which was defined as being 100%.

5.3.1.3. Analysis

GFP fluorescence intensity (% of the 5 µM MG132 positive control) was plotted using Graphpad Prism Version 6.0 (GraphPad Software Inc.) and the mean EC_{50} values determined using Prism statistical software based on a standard point to point curve with 1000 segments.

5.4. Results

5.4.1. *Structure-growth inhibition relationship analysis of compound A (I)*

Based on the previously published compound A (**I**) (Chen *et al.*, 2008a), a compound library was synthesised by Andrew Shouksmith (NICR, School of Chemistry, Newcastle) by systematically modifying the chemical structure of **I** (Figure 5.3a). The GI_{50} values of the analogues were determined in HeLa cells as described in Section 2.15 (Figure 5.3b/c) and ranged from 5.8 µM (**Id**) to >100 µM (**Ik**), the maximum concentration investigated, indicating structure-growth inhibition relationships (Figure 5.3c). Importantly, a significant relationship was observed between the GI_{50} and cLogP values (Figure 5.3d), indicating that the lipophilicity of the compounds may play a significant role in their cellular toxicity (Spearman correlation, $r_s = -0.76$, $p < 0.0001$, Figure 5.3d).

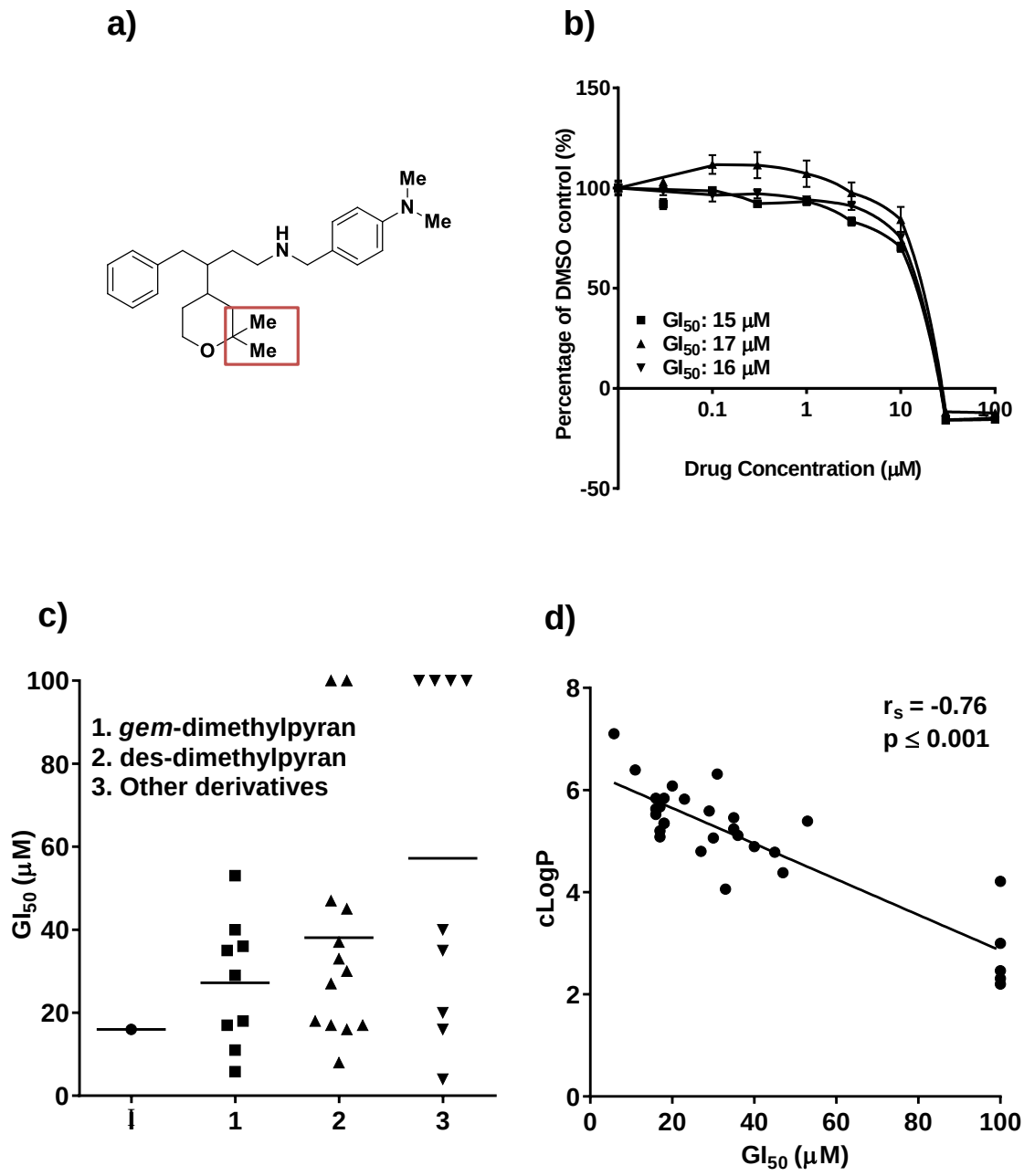

Figure 5.3 Growth inhibition induced by compound I and its analogues in HeLa cells analysed by SRB assay a) Structure of compound **I** and the dimethyl group removed for the *des*-dimethylpryan substituents. Other derivatives included replacement of the tetrahydropyran with a methyl group **b)** Representative graph of the growth inhibition curves generated for each analogue. HeLa cells were treated with indicated concentrations for 72 hrs and analysed using an SRB assay. Data are the mean and error bars represent the SEM of individual wells. **c)** GI_{50} values of analogues of compound **I** grouped according to the structural modification. Each point is the mean GI_{50}. **d)** Relationship between the mean GI_{50} value and cLogP value for each compound. Each point is the mean GI_{50} for a separate analogue and cLogP values were calculated using ChemDraw, ACS format.

Modification or removal of the 4-dimethyl amino group from the benzylamino ring had no effect on compound potency suggesting it was not required for growth inhibition (Figure 5.4, **Ia, Ib** and **Ic**). Furthermore, replacement of the 4-NMe_2 with a N-isopropyl group resulted in the most potent compound, as well as the most lipophilic (**Id**) suggesting the increased toxicity may have been a result of enhanced membrane permeability.

Removal of the dimethyl group from the tetrahydropyran ring (**Ie**) reduced potency compared to the gem-dimethyl analogue (**I**), although this was associated with a decrease in lipophilicity. In the des-dimethyl series, growth inhibitory activity was improved following the substitution of the 4-NMe_2 with 4-chloro (**If**), 4-methylthio (**Ig**) or 4-trifluoromethyl groups (**Ih**), with the most potent of this series being the 4-pyrolidinyl derivative (**Ii**), which again had a low cLogP value. Replacement of the tetrahydropyran ring in **If** with a methyl group (**Ij**) had no effect on the GI_{50} concentration, although additional removal of the phenyl ring inactivated the structure (**Ik**), implying that while the tetrahydropyran ring is not required for growth inhibitory activity, the phenyl ring is (Figure 5.4).

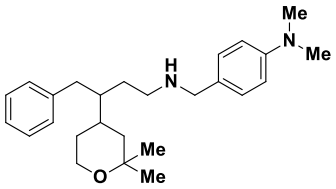

I
Mwt: 394.59
cLogP = 5.84
GI_{50} = 16 ± 1 µM

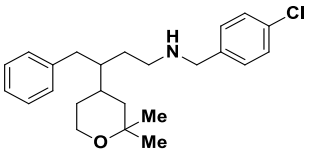

Ia
Mwt: 385.97
cLogP = 6.39
GI_{50} = 11 ± 4 µM

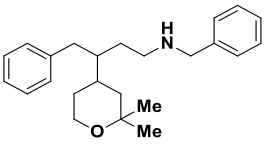

Ib
Mwt: 351.52
cLogP = 5.67
GI_{50} = 17 ± 3 µM

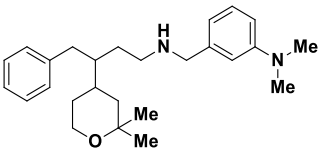

Ic
Mwt: 394.59
cLogP = 5.84
GI_{50} = 18 ± 2 µM

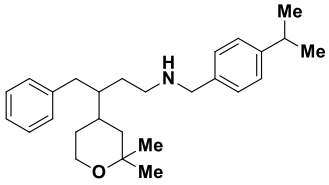

Id
Mwt: 393.60
cLogP = 7.10
GI_{50} = 5.8 ± 1.1 µM

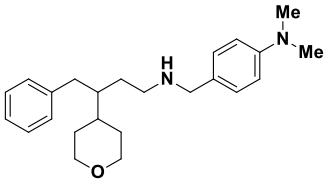

Ie
Mwt: 366.54
cLogP = 4.80
GI_{50} = 27 ± 4 µM

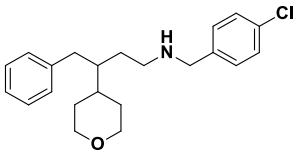

If
Mwt: 357.92
cLogP = 5.35
GI_{50} = 18 ± 1 µM

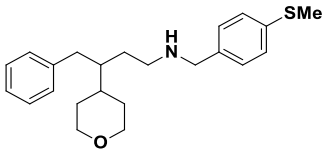

Ig
Mwt: 369.56
cLogP = 5.20
GI_{50} = 17 ± 1 µM

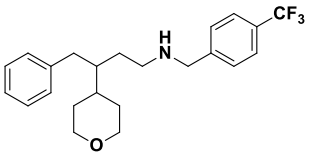

Ih
Mwt: 391.47
cLogP = 5.52
GI_{50} = 16 ± 1 µM

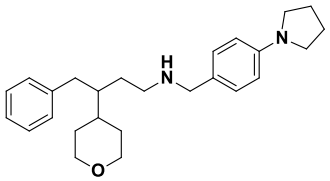

Ii
Mwt: 392.58
cLogP = 4.92
GI_{50} = 7 ± 1 µM

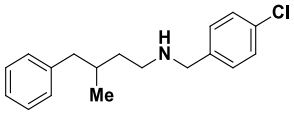

Ij
Mwt: 287.83
cLogP = 5.63
GI_{50} = 16 ± 1 µM

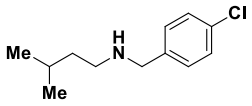

Ik
Mwt: 211.73
cLogP = 4.21
GI_{50} = ≥ 100 µM

Figure 5.4 Structures of compound A (I) analogues, cLogP and HeLa cell GI_{50} values. GI_{50} data are the mean of 3 individual repeats ± standard deviation. Compounds were drawn and the cLogP values calculated using ChemDraw (ACS format).

5.4.2. *Impact of compounds I and Id on p27 stability in HeLa cells*

Based on their growth inhibitory activity, the effect of **I** and **Id** on SKP2 activity as measured by p27 levels was investigated using western blotting. Both compounds were shown to induce a rapid cellular response, inducing cell death after 30 minutes exposure. Neither **I** nor **Id** influenced SKP2 protein levels (Figure 5.5), consistent with the findings of Chen *et al* and the predicted mechanism of action, namely disruption of the SKP1-SKP2 interaction (Chen *et al.*, 2008a). However, an increase in p27 protein level was observed after 24 hr exposure to either compound at their GI_{50} concentrations, suggesting that SKP2-mediated p27 degradation was inhibited (Figure 5.5). Due to the cytotoxic nature of the compounds longer time points could not be investigated.

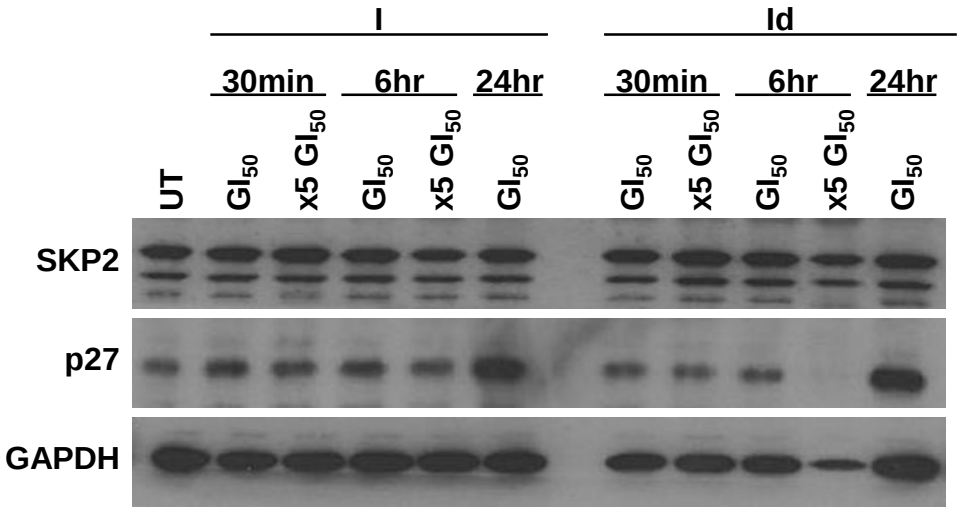

Figure 5.5 Western blot showing the effect of I and Id on SKP2 and p27 levels in HeLa cells. Cell lysates were collected at time points stated. The western blot shown is a representative of 2 independent repeats. Uneven protein loading was observed at the 6 hr timepoint for x5 GI_{50} compound Id in both repeats.

5.5. Impact of compound I and structural analogues on p27 stability in the HeLa-p27(T187D)-EGFP cell line

To confirm the accumulation of p27 following treatment with **I** and **Id**, presumed to be due to the inhibition of the SCF^{SKP2} complex, the compounds were investigated using the HeLa-p27(T187D)-EGFP cell line. Due to limited compound supply no further studies could be carried out on **Id** which was replaced with a compound with similar potency (**Ii**, GI_{50} 8 ± 1 μM), a des-methyl derivative with the benzyl 4-NMe2 substituent replaced with a 4-pyrolidinyl group. Additional analogues were selected including the 2 enantiomers of **Ie**, **Ie-(S)** and **Ie-(R)** (Figure 5.6). The proteasome inhibitor bortezomib (Velcade®), the NAE inhibitor MLN4924 (both Millennium Pharmaceuticals) and the Merck Millipore SKP2 inhibitor (CI) were all also studied (Figure 5.7).

Due to the genetic modifications made to the HeLa-p27 cells the GI_{50} values of the selected compounds were re-assessed using the SRB assay. Interestingly, the *gem*-dimethyl analogues (**I** and **II**) were less toxic compared to the unmodified HeLa cells, suggesting that the constitutively degraded GFP-tagged mutant of p27 (p27T187D), the transfection process or G418 selection influenced drug potency. However, the enantiomers **Ie-(S)** and **Ie-(R)** which are *des*-dimethyl analogues, were found to induce greater growth inhibition than in the unmodified HeLa cells, while no change in potency was observed for **Ij**. Overall these data are consistent with the previous structure-growth inhibition relationships, which showed the removal of the tetrahydropyran ring had little influence of potency (Table 5.1).

In this small series of compounds no relationship was observed between the GI_{50} and EC_{50} concentrations. The most toxic compound, **Ii,** showed similar potency for p27 accumulation to **I**, which had a ~6 fold greater GI_{50} concentration, suggesting that off-target effects may influence **Ii** induced growth inhibition. For the enantiomers of **Ie**, while equipotent in growth inhibition studies, the **(S)** configuration gave a 2-fold greater potency in the p27 accumulation assay. The most potent analogue in the p27 accumulation assay was **Ij**, indicating that the tetrahydropyran ring is not required for inhibition of SKP2-mediated p27 degradation.

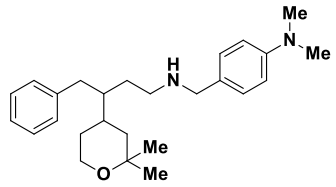

I
GI_{50} = 37 ± 0.6 µM
EC_{50} = 20 ± 5 µM
cLogP = 5.84

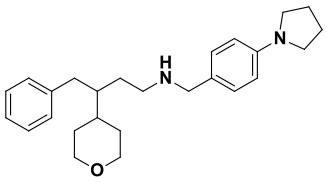

Ii
GI_{50} = 5.1 and 5.4 µM
EC_{50} = 21 ± 3 µM
cLogP = 4.92

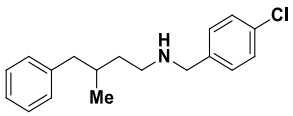

Ij
GI_{50} = 18 and 17 µM
EC_{50} = 15 ± 4 µM
cLogP = 5.63

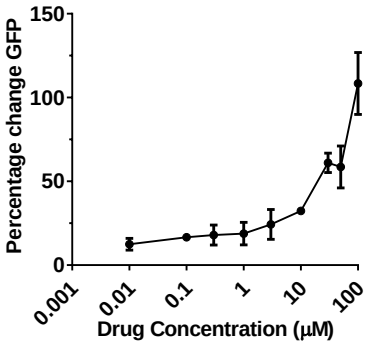

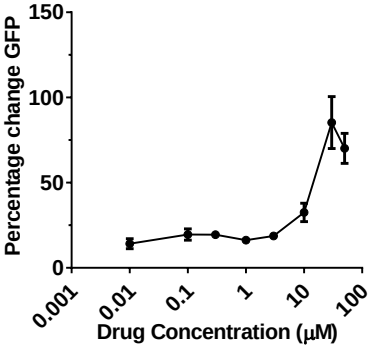

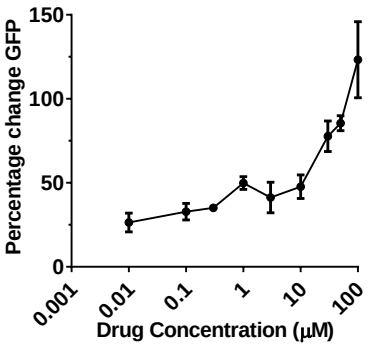

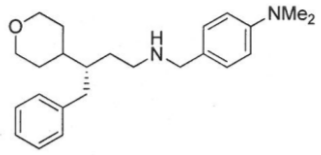

Ie-(S)
GI_{50} = 17 and 14 µM
EC_{50} = 36 ± 3 µM
cLogP = 4.8

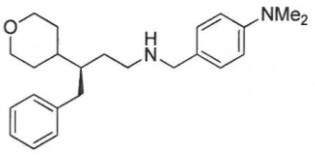

Ie-(R)
GI_{50} = 15 and 16 µM
EC_{50} = 61 ± 7 µM
cLogP = 4.8

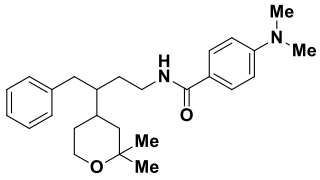

II
GI_{50} = 80 and 61 µM
EC_{50} = N/A
cLogP = 5.39

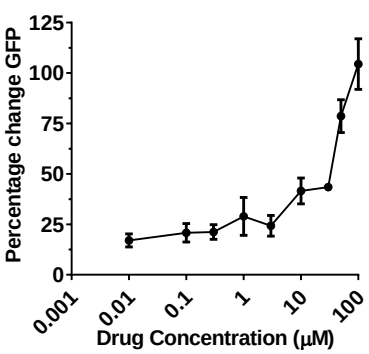

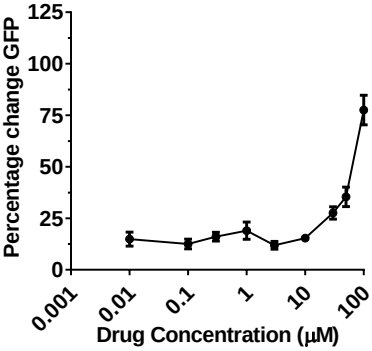

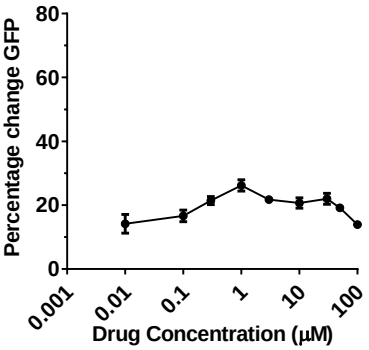

Figure 5.6 Structures, GI_{50} and EC_{50} values and concentration response curves for compound I and analogues in the HeLa-p27(T187)-EGFP cell line. GI_{50} data are the mean of 3 replica wells as determined using an SRB assay. EC_{50} data refers to the concentration at 50% GFP change and are the mean of 3 independent experiments ± standard deviation, excluding compound II which is n=2. Concentration-response curves shown are representative and data are the mean of 3 replica wells. cLogP values were determined using ChemDraw, ACS format.

A concentration response was observed for p27-GFP accumulation for all the analogues of **I**, excluding **II** (Figure 5.7). The least toxic compound (GI_{50} 71 ± 13 µM), **II** did not produce p27-GFP accumulation to 50% of the level induced by 5 µM MG132, suggesting that the growth inhibitory effect was not due to inhibition of the SCF^{SKP2} complex. However, unexpectedly, a similar observation was made for the NAE inhibitor MLN4924, although in contrast to **II** a concentration response was observed with the highest level of GFP-p27 being reached at 10 µM (Figure 5.7). As expected, the most effective compound was the proteasome inhibitor bortezomib (EC_{50} 200 ± 8 nM) followed by the Merck Millipore SKP2 inhibitor CI (SKPin), which is reported to disrupt specifically the SKP2-p27 interaction and hence is potentially the most selective small molecule assayed with regards to the inhibition of SKP2-mediated p27 degradation (Wu *et al.*, 2012b).

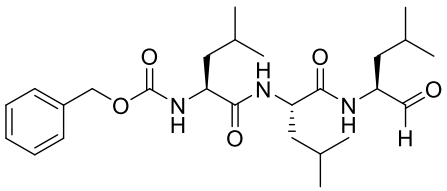

MG132
Mwt: 475.62
ECI_{50} = 1 ± 0.6 µM

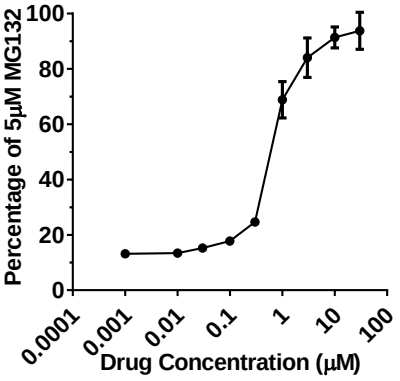

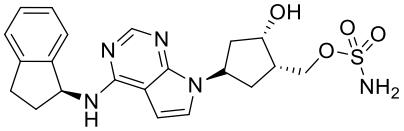

MLN4924
Mwt: 443.16
GI_{50} = 1.3 µm ± 0.6
Top % at 10 µM

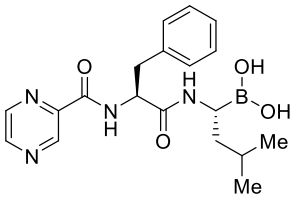

Bortezomib
Mwt: 384.24
GI_{50} = 20 nM ± 2
EC_{50} = 200 ± 8 nM

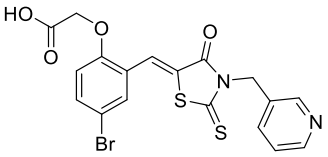

CI
Mwt: 205.30
GI_{50} = 22 µM ± 4
EC_{50} = 1.9 and 2.5 µM

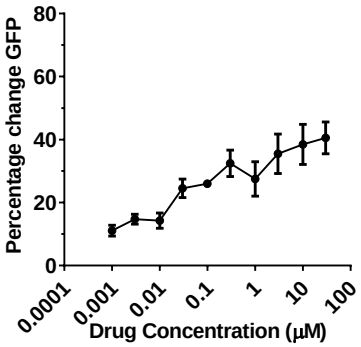

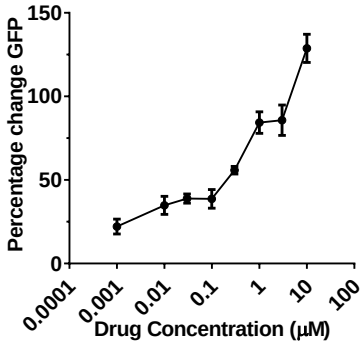

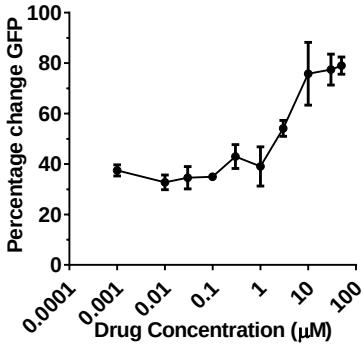

Figure 5.7 Structures, GI_{50} and EC_{50} values and concentration response curves of commercially available compounds in the HeLa-p27(T187)-EGFP cell line. GI_{50} data are the mean of 3 replica wells as determined using an SRB assay. EC_{50} data refers to the concentration at 50% GFP change and are the mean of 3 independent experiments ± standard deviation, excluding the EC_{50} data for CI which in n=2. Concentration-response curves shown are representative and data are the mean of 3 replica wells.

Inhibitor	Mechanism of Action	HeLa GI_{50}	HeLa-p27 GI_{50}	EC_{50}
Bortezomib	Proteasome Inhibitor	-	20 ± 2 nM	200 ± 2 nM
MLN4924	NAE Inhibitor	-	1.6 ± 0.3 µM	-
SKP2 E3 ligase Inhibitor I (CI)	SKP2-CKS1 mediated substrate recruitment inhibitor (SKPins)	-	22 ± 0.6 µM	1.9 and 2.5 µM
I	Putative SKP1/SKP2 inhibitor	16 ± 1 µM	37 ± 0.6 µM	20 ± 5 µM
Ii	Putative SKP1/SKP2 inhibitor	7 ± 1 µM	5.1 and 5.4 µM	21 ± 3 µM
Ij	Putative SKP1/SKP2 inhibitor	16 ± 1 µM	18 and 17 µM	15 ± 4 µM
Ie-(S)	Putative SKP1/SKP2 inhibitor	31 ± 3 µM	17 and 14 µM	61 ± 7 µM
Ie-(R)	Putative SKP1/SKP2 inhibitor	28 ± 4 µM	15 and 16 µM	36 ± 3 µM
II	Putative SKP1/SKP2 inhibitor	51 ± 10 µM	80 and 61 µM	-

Table 5.1 Mechanism of action, HeLa cell GI_{50} and HeLa-p27(T187D)-EGFP (HeLa-p27) cell GI_{50} and EC_{50} values for molecules targeting SKP2. GI_{50} concentration in unmodified HeLa cells and EC_{50} data in HeLa-p27 cells are the mean ± standard deviated of n=3 excluding EC_{50} data of CI and **II** which is n=2. GI_{50} concentrations in the HeLa-p27 cell line are the mean of 3 replica wells determined using the SRB assay.

5.5.1. *Pharmacological targeting of SKP2 in the SHEP-Tet21N cell line*

As SKP2 has been reported to be overexpressed in *MYCN* amplified neuroblastoma (Westermann *et al.*, 2007) and identified as a direct MYCN target gene (Chapter 3), the influence of MYCN expression on SKP2 inhibition was investigated using the Tet21N MYCN regulatable cell line. In addition to the putative SKP2 inhibitors investigated in the HeLa-p27(T187D)-EGFP cell assay, the BET bromodomain inhibitor JQ1 and all-trans retinoic acid (ATRA) were also investigated due to their reported effects on MYCN regulated transcription (Puissant *et al.*, 2013) and SKP2 degradation (Dow *et al.*, 2001), respectively. Although expression of MYCN sensitised the cells to all of the compounds investigated, a significant increase in sensitivity was only observed following treatment with MLN4924 and CI (Table 5.2, $p = 0.027$ and 0.037, respectively, paired t test).

Western blotting analysis demonstrated a MYCN-dependent increase in SKP2 expression following exposure of MLN4924 to Tet21N MYCN- cells. However, this was not associated with a decrease in p27 stabilisation. Interestingly MLN4924 was observed to have no effect on SKP2 levels in Tet21N MYCN+ cells. Conversely, JQ1 induced a loss of SKP2 protein independently of MYCN expression at both concentrations tested; however, this did not have a marked effect on p27 levels (Figure 5.9).

Inhibitor	Mechanism of Action	Tet21N MYCN+	Tet21N MYCN-
Bortezomib	Proteasome Inhibitor	7 ± 0.6 nM	13 ± 4 nM
MLN4924	NAE Inhibitor	9 ± 1nM *****	80 ± 20nM
CI	SKP2-CKS1 mediated substrate recruitment inhibitor (SKPins)	26 ± 2 µM *****	40 ± 4 µM
NCL-00018545	Putative SKP1/SKP2 inhibitor	21 ± 0.6 µM	24 ± 0.6 µM
NCL-00018645	Putative SKP1/SKP2 inhibitor	4.4 ± 0.5 µM	7.6 ± 0.3 µM
Roscovitine	CDK2, CDK7 and CDK9 inhibitor	14 ± 2 µM	18 ± 1 µM
NU6102	CDK2 inhibitor	8.6 ± 5 µM	12 ± 3 µM
ATRA	Promotes neuronal differentiation, represses MYCN expression	75 ± 0.5 µM	88 ± 11 µM
JQ1	BET bromodomain inhibitor, down-regulates *MYCN* mRNA	170 ± 70 nM	210 ± 60 nM

Table 5.2 GI_{50} concentrations of small molecule inhibitors analysed by the XTT assay in Tet21N neuroblastoma cell line. Data are the mean and standard deviation of n=3. ***** Corresponds to p values of ≤ 0.05 for GI_{50} values in the two cell lines. ATRA: All trans-retinoic acid

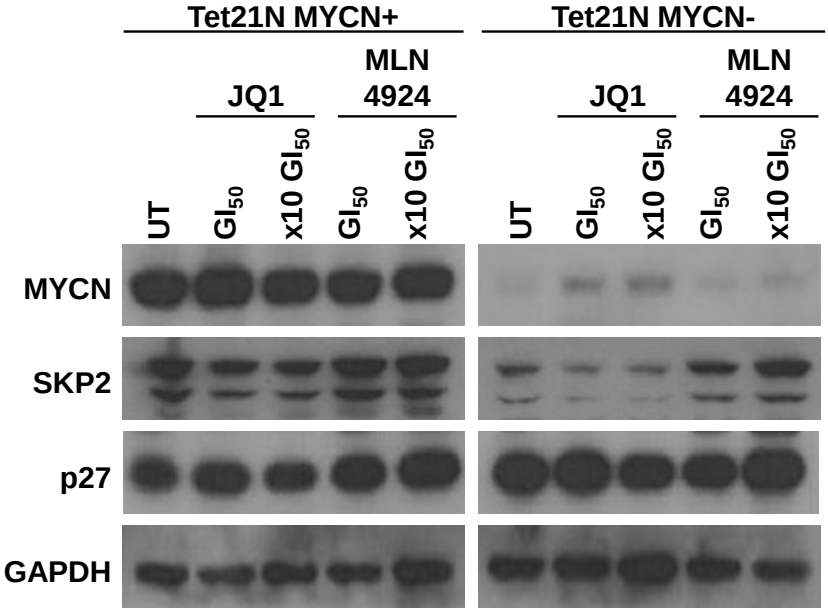

Figure 5.8 Western blot showing the effect of the BET inhibitor JQ1 and NAE inhibitor MLN4924 on SKP2 and p27 levels in the Tet21N neuroblastoma cell line. Cell lysates were collected following 24 hr treatment at the concentrations indicated. The western blot shown is a representative of 2 independent repeats.

5.6. Discussion

F-box proteins act as the substrate recognition subunits for the SCF E3 ligases and represent a class of potential therapeutic targets which would provide a higher selectivity, and less associated toxicity than proteasome inhibitors, as their inhibition should only stabilise a specific set of cellular proteins. However, unlike protein kinases where inhibitors can bind in the ATP catalytic pocket or peptide substrate binding sites, targeting E3 ubiquitin ligases is challenging as it requires the disruption of a protein-protein interaction. As a result it is only recently that compounds capable of directly targeting SKP2 have been described (Chen *et al.*, 2008a; Wu *et al.*, 2012b; Chan *et al.*, 2013).

Protein-protein interactions present a challenging target for pharmaceutical intervention as often lack the small pockets that accommodate natural substrates and ligands in enzymes and receptors. Additionally, binding sites on protein surfaces are often not conserved, although 'hot spot' residues can be identified, for example by alanine-scanning mutagenesis as reviewed by Moreira (Moreira *et al.*, 2007). Due to these challenges many of the small molecules targeting p27 degradation have been discovered using screening and end-point analysis (Chen *et al.*, 2008a), rather than rational design approaches. However, advances in computational methods, structural bioinformatics and fragment-based lead discovery have both increased the ability to predict binding pockets on a protein surface, and allowed for rapid probing of the surfaces for small molecule binding sites.

The studies described in chapter 4 investigated the potential of targeting SKP2 in neuroblastoma by using siRNA knockdown and in the current chapter small molecule inhibition of SKP2 activity was studied.

5.6.1. *Growth inhibition and physiochemical properties of analogues of compound I*

Based on the chemical structure of **I** (compound A), a putative inhibitor of the SKP1-SKP2 interaction (Chen *et al.*, 2008a), 32 analogues were synthesised and HeLa cell GI_{50} concentrations determined to explore structure-growth inhibition relationships. A strong relationship was observed between the GI_{50} and cLogP

values, with the more lipophilic compounds inducing greater toxicity (Figure 5.3d), suggesting that cell membrane permeability is a determining factor in the growth inhibitory response.

The cLogP or partition coefficient is related to the distribution of drugs within the body. Often measured by determining the ratio of the distribution of a compound between octanol and water, a higher value reflects preferential distribution to hydrophobic compartments such as lipid bilayers and a low value to more aqueous environments such as extracellular fluid. In designing small molecule drugs a clogP value no greater than 5 is often sought in accordance with Lipinski's rule of five (Lipinski *et al.*, 2001). A measure of the 'drug-like' qualities of a substance 4 parameters are associated with the solubility and permeability of orally active drugs, and the 'rule' states that poor absorption/permeation is more likely when: (1) there are more than 5 H-bond donors (expressed as the sum of OH and NH groups), (2) the molecular weight is over 500, (3) the LogP is over 5 and (4) there are more than 10 H-bond acceptors (expressed as the sum of N and O atoms) (Lipinski *et al.*, 2001).

For the putative SKP2 inhibitors, lipophilicity could theoretically result in increased binding to SKP1 improving disruption of the SKP1-SKP2 interaction. Alternatively, the hydrophobic nature of the compounds could result in non-specific disruption of membrane integrity which would induce cell death, as observed by compounds **I** and **Id**. Taken with the strong monotonic relationship between the partition coefficient and GI_{50} values it may be that the decrease in cell viability observed in HeLa cells is the result of non-specific cell death rather than selective growth inhibition.

Regardless of the mechanism of cellular toxicity, variations in GI_{50} concentrations were observed following the systematic alterations of the structure **I** (Figure 5.4). Modifications to the dimethyl amino group on the benzyl ring had little effect on toxicity, e.g. compounds **I**, **Ia** - **Id**, although alkylation of the aromatic ring led to the most toxic and lipophilic analogue **Id**. Removal of the dimethyl group from the tetrahydropyran ring increased the GI_{50} concentrations of the series, despite reducing the cLogP value to within Lipinski's 'rule of 5' (Lipinski *et al.*, 2001). Toxicity was maintained when the 4-NMe_2 on **Ie** was replaced with the 4-

pyrrolidinyl group (**Ii**) without increasing lipophilicity. Collectively these data suggest that the tetrahydropyran ring contributes to the lipophilic nature of the compound yet is not required for cellular toxicity. In contrast, both phenyl rings are required for activity and attachment of a *para* electron withdrawing group (propyl or pyrrolidinyl) increases toxicity which may be a product of the electron-withdrawing substituents stabilising the phenyl ring.

5.6.2. *Targeting SKP2-mediated degradation of p27*

Compounds **I** and **Id** induced rapid toxicity and cells began to display characteristics of cell death, such as detachment from the tissue culture flask and cell rupture, after a 30 minute exposure. Nevertheless, both compounds induced p27 accumulation following 24 hr exposure to the GI_{50} concentration, indicating that SKP2 activity had been inhibited (Figure 5.5).

For the limited number of compounds studied in the HeLa-p27(T187D)-EGFP cell-based assay there was no relationship between the GI_{50} concentration and that required to induce p27-GFP accumulation to 50% of the level observed with 5 µM MG132. Interestingly, a higher concentration of **I** was required to suppress growth in the HeLa-p27(T187D)-EGFP cell line compared to the unmodified HeLa cells, while the opposite was observed for the enantiomers **Ie-(S)** and **Ie-(R)**. Differing in the dimethyl group attached to the tetrahydropyran ring, this observation is consistent with the structure-growth inhibitory relationship observed in the unmodified HeLa cells.

As expected, the most effective small molecule in stabilising GFP-p27 was the proteasome inhibitor bortezomib (Velcade®, Millennium Pharmaceuticals), which along with MG132 validated the cell based assay. The 'SKPin' CI was the most specific compound investigated, and is reported to be highly selective in stabilising SKP2-CKS1 targets (i.e. p27, p21 and p57). As with bortezomib, a 10-fold difference was observed between the concentrations of CI required for growth inhibition (GI_{50} 22 µM ± 0.6) and GFP-p27 stabilisation (EC_{50} 2.2 µM ± 0.4). Initially this may suggest that p27 accumulation only partly contributes to the observed growth inhibition.

The lack of p27 accumulation in the HeLa-p27(T187D)-EGFP cell line following treatment with the NAE inhibitor MLN4924 was unexpected as the compound is a well-established inhibitor of SCF complex formation. However, unlike **II** which also failed to induce GFP-p27 accumulation to 50% of the level produced by 5 µM MG132, a concentration response effect was induced by MLN4924, indicating that SKP2-mediated degradation of p27 was being inhibited. However, p27 stabilisation was not to the level achieved by the proteasome inhibitor. Although the assay was optimised to analyse inhibition of SKP2 activity, low levels of GFP-p27 accumulation were also found following siRNA knockdown of the E3 ligase E6AP which can also target p27 for degradation (ThermoScientific, 2004; Mishra *et al.*, 2009). As MG132 prevents the turnover of all proteins reliant on the 26S proteasome, it may potentially be inhibiting alternative pathways which regulate p27 stability, including E6AP and the ubiquitin ligase KPC (Kamura *et al.*, 2004). The inability of MLN4924 to produce an EC_{50} value may therefore be a reflection of its higher specificity towards the SCF^{SKP2} complex compared to MG132.

MLN4924 is structurally related to adenosine 5'-monophosphate (AMP) and upon binding to the NEDD9-activating enzyme (NAE) forms a tight MLN4924-NEDD8 adduct which blocks the NAE active site (Soucy *et al.*, 2009). The HeLa-p27(T187D)-EGFP cell line has been modified to express a constitutively degraded mutant p27 protein and consequently the SCF pathway should be more active than in unmodified HeLa cells. Neddylation of CUL1 is regulated in part by the availability of the F-box protein and its substrate, i.e. SKP2 and p27, with increased levels of p27 being reported to lock the SCF^{SKP2} complex in the neddylated and assembled state by preventing deneddylation (Bornstein *et al.*, 2006). The CMV-driven p27 expression in the HeLa-p27(T187D)-EGFP cell line may therefore be reducing the contribution of the neddylation pathway towards the SKP2-p27 axis, and thereby abrogating the MLN4924 response. It would therefore be informative to determine the basal levels of the SCF^{SKP2} components (e.g. NAE, CUL1, SKP1-SKP2, CKS1, p27) in the HeLa-p27(T187D)-EGFP cell line compared to unmodified HeLa cells.

The HeLa-p27(T187D)-EGFP cell line was employed as a cell-based screen to evaluate the novel analogues of compound **I** studied, and validation by secondary assays would be required to confirm proposed mechanisms of action. For

example, given the unknown selectivity of the analogues, determination of the EC_{50} values in comparison to and after SKP2 siRNA knockdown would help determine the proportion of p27 stabilisation from SKP2-specific inhibition versus off-target effects. As **I** analogues are proposed to target the SKP1-SKP2 interaction, active compounds would be expected to stabilise all SKP2 substrates. Western analysis could therefore be performed to investigate the influence of the inhibitors on the accumulation of additional SKP2 targets, for example p21, E2F1 and c-MYC, followed by the analysis of substrate half-lives to confirm that any increase in protein level is due to stabilisation.

Although not all analogues synthesised were assessed in the HeLa-p27(T187D)-EGFP assay, for the sub-set that were tested a structure activity relationship was suggested. While the enantiomers of **Ie** were equipotent in the growth inhibition assay, **Ie-(S)** showed greater activity for SKP2 inhibition than **Ie-(R)**, demonstrating stereo-specificity for GFP-p27 stabilisation. Addition of the dimethyl substituent to the tetrahydropyran ring increased potency, decreasing the EC_{50} from 36 µM ± 3 (**Ie-(S)**) to 20 µM ± 5 (**I**); whereas in contrast the GI_{50} concentration increased ~2 fold suggesting that growth inhibition is not solely a function of p27 stabilisation. Similar p27 stabilisation was observed with compounds **I** and **Ii** (EC_{50}: 20 µM ± 5 and 21 µM ± 3, respectively), although **Ii** was ~7x more potent in the growth inhibition assay (**I** GI_{50}: 37 µM ± 0.6 and **Ii** GI_{50}: 5.1 and 5.4 µM). Overall, no relationship was identified between the GI_{50} concentrations and the EC_{50} values for GFP-p27 stabilisation; however, in both assays removal of the tetrahyropyran ring increased potency (**I** to **Ij**), suggesting that this moiety is not required for activity.

In extending these studies further analysis of the novel analogues is required. Firstly, all of the compounds synthesised should be tested using the HeLa-p27(T187D)-EGFP cell line, and any GFP-p27 stabilisation observed confirmed by western blotting. The relationship between growth inhibition and GFP-p27 accumulation should be further evaluated and additional mechanistic studies performed, such as co-immunoprecipitation or pull down assays, to establish whether the SKP1-SKP2 interaction has been disrupted. In addition, structural biology studies could be performed such as *in silico* analysis and experimental x-

ray crystallography to confirm compound binding and predict modifications which may increase SKP2-inhibtion potency and selectivity.

5.6.3. *Targeting SKP2 activity in neuroblastoma*

As demonstrated in Chapter 3, *SKP2* is a direct MYCN target gene and MYCN was shown to sensitise the Tet21N cell line to G_1 arrest and apoptotic cell death following SKP2 siRNA knockdown. Based on these findings a selection of small molecule inhibitors were investigated which are reported to target pathways associated with SKP2 activity and MYCN expression, in order to determine whether MYCN sensitises neuroblastoma cells to SKP2 inhibition. Although Tet21N MYCN+ cells were more sensitive to all of the inhibitors tested, a significant increase in growth inhibition compared to Tet21N MYCN- cells was only demonstrated for the NAE inhibitor MLN4924 and the SKPin CI (Table 5.2). Encouragingly, these two compounds are the more specific SKP2 inhibitors, in contrast to the CDK inhibitors, ATRA and compound **I** analogues, with the mechanism of activity yet to be established for the latter. Overall, the greater sensitivity of the Tet21N MYCN+ cells to MLN4924 and CI supports SKP2 inhibition as a potential therapeutic strategy in *MYCN* amplified neuroblastoma.

Analysis of the functional effects of MLN4924 on SKP2-mediated p27 degradation by western blotting (Figure 5.8), showed an increase in SKP2 protein expression in Tet21N MYCN- cells, although this had no influence on p27 levels most probably due to the SCF complex being inactive. All cullin RING ligases (CRLs) require neddylation for full activation and thus, as an inhibitor of NEDD8 modification, MLN4924 can influence the stability of a broad spectrum of substrates. SKP2 is targeted for degradation primarily though the APC/C^{CDH1} complex and although the APC2 protein, which forms the APC/C scaffold, is related to the cullin protein it does not require neddylation for activation (Tateishi *et al.*, 2001). Alternatively, SKP2 can undergo auto-ubiquitination when linked to the SCF complex in a mechanism that is dependent on the SKP2-binding of CUL1 (Galan and Peter, 1999; Wirbelauer *et al.*, 2000). The prevention of CUL1-RBX1-SKP1 complex formation, by locking CUL1 in its inactive conformation, could therefore prevent the auto-ubiquitination of SKP2 resulting in its stabilisation. As SKP2 is a direct MYCN transcriptional target, this effect may be masked by the higher basal levels of SKP2 in the Tet21N-MYCN+ cells. Interestingly MLN4924

induced no further increase in SKP2 protein expression most probably due to already high basal levels.

Bromodomain and extra-terminal (BET) proteins regulate gene expression by binding to ε-*N*-acetylated lysine residues in chromatin to promote gene expression. One BET family member, BRD4, has been identified as a crucial mediator of RNA polymerase II-driven transcription (Yang *et al.*, 2008) and has been identified as a promising therapeutic target in hematologic malignancies (Ott *et al.*, 2012; Stewart *et al.*, 2013). JQ1 is a selective and potent inhibitor which competitively binds to the acetyl-lysine recognition pockets in chromatin, displacing BRD4 (Filippakopoulos *et al.*, 2010). Recently *MYCN* amplification has been identified as a marker for sensitivity to JQ1 and has been shown to downregulate MYCN-dependent transcription in the *MYCN* amplified neuroblastoma cell lines SK-N-BE(2c) and Kelly by displacing BRD4 from the MYCN promoter (Puissant *et al.*, 2013). The decrease in SKP2 protein expression seen in Tet21N MYCN+ cells is consistent with this observation, and the direct regulation of *SKP2* by MYCN as discussed in Chapter 3. Interestingly JQ1 exposure decreased SKP2 protein levels in Tet21N MYCN- cells, although the effect was partly masked by the removal of MYCN. However, as *SKP2* is a c-MYC target gene (Bretones *et al.*, 2011), this loss of SKP2 protein may be due to the JQ1-downregulation of c-MYC transcription (Delmore *et al.*, 2011). No convincing increase in p27 expression stabilisation was observed following the decrease in SKP2 protein levels, although this may reflect the short time interval investigated.

The lack of marked effects on p27 protein levels questions the therapeutic potential of targeting the SKP2/p27 axis in neuroblastoma; however, MLN4924 and JQ1 are selective inhibitors of neddylation and bromodomains, respectively, and do not directly target the SKP2/p27 axis. SKP2 knockdown studies (Chapter 4) identified SKP2 targeting in non-*MYCN* amplified neuroblastoma cell lines as a therapeutic approach, and knockdown was associated with an increase in p27 protein expression, albeit modest. Given that MLN4924 also failed to induce GFP-p27 accumulation to 50% of the level produced by 5 μM MG132 (Figure 5.7) the lack of p27 stabilisation in the Tet21N cells following treatment with JQ1 and MLN4924 may be a reflection of their indirect targeting of the SKP2/p27 axis.

Apart from bortezomib, a non-specific proteasome inhibitor, the 'SKPin' CI was the most potent inhibitor of GFP-p27 degradation. The higher potency of CI in Tet21N MYCN+ cells is further evidence of the contribution of the SKP2/p27 axis in neuroblastoma and its upregulation in *MYCN* amplified tumours; further investigation of CI is therefore warranted.

5.7. Conclusions

This chapter describes the evaluation of a small compound library based on the published putative inhibitor, (**I**), of the SKP1-SKP2 interaction of the SCF^{SKP2} complex (Chen *et al.*, 2008a). For the analogues of **I** studied, there was a relationship between the GI_{50} concentration and lipophilicity, with the more lipophilic compounds being more potent. Some overlap was observed in the structural determinants of growth inhibition and GFP-p27 stabilisation; however, further studies are required to determine the contribution of p27 stabilisation to the growth inhibitory properties of **I** and its analogues. Investigation into the potential of inhibiting SKP2 in neuroblastoma suggested that MYCN expression sensitised the Tet21N MYCN regulatable cell line to growth inhibition induced by both direct and indirect inhibition of SKP2 activity. These observations are consistent with the previous finding that MYCN promotes *SKP2* expression (Chapter 3), and that SKP2 knockdown promotes a G_1 arrest and cell death (Chapter 4).

Chapter 6.
General Discussion

First identified ~30 years ago, *MYCN* amplification remains the best-characterised genetic marker of high risk neuroblastoma. A member of the MYC family of transcription factors, MYCN regulates a plethora of genes by forming heterodimers with MAX at consensus E-box sequences. The *MYCN* gene is amplified in 20-25% of cases and creates a stem-like state by driving the expression of genes involved in cellular proliferation (e.g. *CDK4*) (Westermann *et al.*, 2008) and apoptosis (e.g. *TP53*) (Chen *et al.*, 2010b), whilst supressing the activity of genes which promote differentiation (e.g. *TG2*) (Liu *et al.*, 2007). Given the frequency of *MYCN* amplification, and the resistance of high-risk relapsed neuroblastoma to conventional chemotherapeutic options, targeting MYCN therapeutically represents an important approach in the treatment of neuroblastoma. However, while advances are being made in the development of direct inhibitors, predominantly by targeting the MYC/MAX binding domain (reviewed by (Prochownik and Vogt, 2010)), inhibiting MYCN activity still represents a formidable challenge. Given that MYCN overexpression is associated with driving proliferation and sensitising cells to apoptosis, some studies have suggested an alternative approach of targeting downstream of MYCN, to tip the balance in favour of apoptosis (Bell *et al.*, 2010).

SKP2 has been previously identified as a MYCN candidate gene in neuroblastoma by gene expression microarray analysis where *SKP2* expression was downregulated following MYCN siRNA knockdown, and a relationship was observed between *SKP2* transcript levels and *MYCN* amplification in tumours (Bell *et al.*, 2007; Westermann *et al.*, 2007). Interestingly, although *SKP2* mRNA was found to correlate with aggressiveness of disease, there was no correlation with MYCN expression in non-amplified tumours. Accordingly, this pattern of expression was found at the protein level, where SKP2 was more prevalent in *MYCN* amplified tumours and inversely correlated with p27 protein levels (Westermann *et al.*, 2007). Nevertheless, the identification of E-box motifs within the *SKP2* promoter (Bretones *et al.*, 2011) strengthened the hypothesis that SKP2 is a direct MYCN transcriptional target, and may therefore contribute to the

enhanced proliferation and aggressiveness seen in *MYCN* amplified neuroblastoma.

6.1. *SKP2* is a direct transcriptional target of MYCN

This study confirmed the positive association between MYCN and SKP2 in investigations in neuroblastoma cell lines (Chapter 3). Switching off MYCN expression in the SHEP-Tet21N MYCN regulatable cell line, and activating MYCN activity in the SKNAS-NMyc-ER cell line, resulted in opposing effects on *SKP2* mRNA expression levels as expected for a MYCN candidate gene. The hypothesis of direct transcriptional regulation of *SKP2* by MYCN was also supported by the positive linear relationship observed between MYCN protein and *SKP2* mRNA expression in *MYCN* amplified and non-amplified cell lines. Prior to the studies described in this thesis the hypothesis was that low level of *SKP2* transcript in a cell with low MYCN levels is a combined effect of reduced E2F1 activity, due to the absence of MYCN driving the CDK4-mediated phosphorylation of pRB, and increased *SKP2* promoter repression, resultant from the direct binding of hypo-phosphorylated pRB complexes (Muth *et al.*, 2010). However, following the detection of E-box motifs within the *SKP2* promoter and demonstration of direct transcriptional regulation by c-MYC (Bretones *et al.*, 2011), ChIP and *SKP2*-reporter gene assays were performed to explore a more direct mechanism (Figure 3.16, 3.17, 3.18 and 3.20). MYCN was found to directly bind to non-canonical E-box motifs within the *SKP2* promoter and upregulate transcriptional activity, which was confirmed by the significant reduction in promoter activity following mutation of the E-boxes in the reporter construct. Taken together with the ChIP-chip array data (Figure 3.19) showing MYCN binding to the *SKP2* promoter in a second MYCN-inducible and *MYCN* amplified cell line, these results provide strong evidence that SKP2 is a direct transcriptional target of MYCN.

6.2. MYCN expression does not correlate with SKP2 protein level

Although SKP2 protein expression gradually decreased following the removal of MYCN in the Tet21N cell line, no association was observed between MYCN and SKP2 protein levels in SKNAS-Nmyc-ER cells or across the panel of *MYCN*

amplified and non-amplified cell lines, where high levels of SKP2 were observed in the absence of MYCN expression (Figure 3.6, 3.8, 3.9 and 3.10).

The inverse relationship between MYCN and c-MYC in neuroblastoma is well documented (Breit and Schwab, 1989), with c-MYC reported to drive malignancy in non *MYCN* amplified tumours (Westermann *et al.*, 2008). Downstream targets of c-MYC are grouped by their binding affinity, with the genes with lower affinity sites more likely to be influenced by MYCN expression (Fernandez *et al.*, 2003). As c-MYC was shown to bind to two high affinity E-boxes in the *SKP2* promoter (Bretones *et al.*, 2011), the interplay between MYCN and c-MYC could potentially play a significant role in driving *SKP2* gene expression. However, as higher c-MYC expression in the non-*MYCN* amplified cell lines did not alter the relationship between MYCN and *SKP2* mRNA levels (Figure 3.9), or explain the low levels of SKP2 protein in the non-*MYCN* amplified c-MYC expressing GIMEN cells (Figure 3.8), it is hypothesised that the high levels of SKP2 protein observed are the result of post-translational mechanisms that regulate SKP2 stability. One such mechanism is activation of the PI3K/AKT pathway which has been found to be a frequent event in neuroblastoma with activated AKT, i.e. phosphorylated in the regulatory (S473) and/or catalytic domains (T308), and identified as a prognostic indicator of poor outcome. An established regulating factor for SKP2 stability, as discussed in Section 1.9.6, activated AKT has been shown to be present in neuroblastoma cell lines independent of *MYCN* status (Opel *et al.*, 2007) and could therefore be contributing to the high levels of SKP2 protein in the absence of MYCN.

6.3. Induction of cell cycle arrest and apoptosis by SKP2 knockdown is dependent on the stabilisation of p27

6.3.1. *SHEP-Tet21N cell line data*

SKP2 protein expression gradually decreased in Tet21N MYCN- cells following treatment with tetracycline, and was associated with accumulation of the CDK inhibitors p27 and p21, and the suppression of cell proliferation (Figure 3.2 and 3.3). MYCN is closely associated with p21 expression and has been shown to regulate several components of the p53-p21 axis including the p53 inhibitor MDM2, resulting in the suppression of p21 transcription (Slack *et al.*, 2005; Bell *et al.*, 2007; Chen *et al.*, 2010b). Knockdown of MYCN has been shown to

promote the accumulation of p21 and increase the G_1 phase population, suggesting that the increased p21 expression in Tet21N MYCN- cells was a reflection of released transcriptional repression as opposed to p21 protein stabilisation (Bell *et al.*, 2006). This hypothesis was supported by the lack of p21 observed after dual treatment with tetracycline and the translation inhibitor cycloheximide. The persistence of p27 protein, although at a lower level, following dual MYCN suppression and cycloheximide treatment, supported the current view that the oncogenic role of SKP2 overexpression in neuroblastoma is associated with accelerated p27 proteolysis (Westermann *et al.*, 2007). However the difference in p27 protein level between tetracycline only and dual tetracycline/cycloheximide treatment suggests that MYCN is also regulating p27 expression by alternative mechanisms either at a transcriptional or post-translational level (Figure 3.5).

MYCN sensitised Tet21N cells to a G_1 arrest following SKP2 siRNA treatment (Figure 3.12), an effect which was reversed upon dual knockdown of p27 and SKP2 (Figure 3.15), emphasising further the role of the SKP2/p27 axis in neuroblastoma, and consistent with the lack of p27 stabilisation and cell cycle arrest in the Tet21N MYCN- cells. However, when MYCN expression is absent the effects of SKP2 inhibition may be masked by release from MYCN-induced shortening of the G_1 phase (Lutz *et al.*, 1996).

SKP2 knockdown had a greater effect on the level of p21 protein over p27 independent of MYCN expression, although a higher sensitivity was observed in Tet21N MYCN+ cells (Figure 3.11a). As SKP2 is reported to suppress p53 activity by sequestering the p53 acetyltransferase p300, SKP2 inhibition may potentially be influencing p21 protein expression by both increasing p53-mediated transcription and decreasing the SKP2-mediated degradation. As p53 (Chen *et al.*, 2010b) and SKP2 (Chapter 3) are direct MYCN transcriptional targets, the greater increase in p21 protein levels following SKP2 siRNA treatment in Tet21N MYCN+ cells, may therefore be the result of the higher basal levels of the p53 and SKP2.

The increase in p21 levels seen in Tet21N cells suggests that SKP2 inhibition induces a p53 response. However, SKP2 knockdown increased the sub-G_1 population independently of MYCN expression, whereas enhanced caspase-3/7

activity was only detected in Tet21N MYCN+ cells (Figure 3.13b). The lack of consistency between the two apoptosis assays may reflect the different endpoints. Caspase-3/7 cleavage is a sensitive measure of cells committed to apoptotic cell death, while the sub-G_1 fraction reflects fragmented DNA and thus gives no information on whether the cells are later stage apoptotic, necrotic or at an early stage of apoptosis from which they can recover. SKP2 inhibition has also been reported to induce caspase-independent cell death through the induction of autophagy (Chen *et al.*, 2008a), and autophagy may explain the SKP2 siRNA knockdown induced decrease in cell viability observed in the Tet21N cells. Further clarification of the mechanisms and pathways of cell death induced by SKP2 knockdown is required.

Overexpression of p27 has also been reported to cause apoptotic cell death (Wang *et al.*, 1997). Taken together, the data from the Tet21N MYCN regulatable cell line model emphasises the importance of the SKP2/p27 axis in neuroblastoma and suggests that MYCN expression sensitises cells to G_1 arrest and apoptotic cell death following SKP2 inhibition. However, when MYCN is expressed, the effects of SKP2 knockdown may still be dominated by MYCN and its paradoxical role in cell cycle progression and apoptosis.

6.3.2 MYCN amplified and non-MYCN amplified cell line data

In contrast to the effect of SKP2 siRNA treatment in Tet21N cells, MYCN amplification did not sensitise a panel of non-isogenic cell lines to the growth inhibitory effects of SKP2 knockdown. However, in non-*MYCN* amplified cells SKP2 knockdown did induce a G_1 arrest and apoptotic cell death (Figure 4.7 and 4.9). Importantly, following SKP2 knockdown, a significant reduction in cell viability was observed in all cell lines, with the exception of the *MYCN* amplified *p53* mutant IMR-KAT100 cells (Figure 4.6). This difference between Tet21N cells and non-isogenic neuroblastoma cell lines in the effect of MYCN on SKP2 knockdown-induced cell cycle phase distribution and apoptosis may reflect the difference between MYCN overexpression and amplification. Although the level of MYCN expression in Tet21N cells has been reported to be comparable to that in *MYCN* amplified cells, at both the mRNA and protein level (Bell *et al.*, 2006), the difference in response to SKP2 knockdown may reflect the higher *MYCN* copy number in the amplified setting. This hypothesis is supported by the greater level

of MYCN binding and SKP2 promoter activity seen in the ChIP and luciferase reporter assays in *MYCN* amplified IMR32 cells compared to Tet21N MYCN+ cells.

The structure and size of the amplicon that includes the *MYCN* gene can vary between 100 kb and 1 Mb, with *MYCN* occupying a central position yet only spanning 100-200 kb (Amler and Schwab, 1989; Scott *et al.*, 2003). Other genetic aberrations that can coexist with *MYCN* amplification, e.g. 1p loss and 17q gain, may therefore be responsible for the failure of cells to arrest in the G_1 phase and undergo apoptotic cell death following SKP2 inhibition. Alternatively, the co-amplification of genes on the MYCN amplicon in the *MYCN* amplified cell lines may influence the response to SKP2 knockdown. For example *NCYM*, the *cis*-antisense gene of MYCN, has been reported to be co-amplified with *MYCN* and to both stabilise MYCN protein and promote metastatic tumour development in *MYCN/NCYM* transgenic mice (Suenaga *et al.*, 2014). Comparison of the doubling times of Tet21N MYCN+ cells (42 hr, Figure 3.3) and IMR32 cells (20 hr, www.atcc.org), highlights further the non-*MYCN* amplified background of the Tet21N cell line, emphasizing again the importance of recognising the difference between MYCN overexpression and amplification, and how this can affect tumour cell biology.

As with Tet21N MYCN+ cells, the G_1 arrest observed in the non-*MYCN* amplified cell lines (Figure 4.7), was associated with an increase in p27 protein expression following a 24 hr exposure to SKP2 siRNA (Figure 4.8), an effect which was reversed by additional p27 knockdown (Figure 4.10a). These findings provide proof of principal data that targeting the SKP2/p27 axis has potential therapeutic benefits in neuroblastoma, and are consistent with previous reports of high levels of p27 expression being associated with a favourable outcome independent of *MYCN* status (Bergmann *et al.*, 2001).

Although p21 stabilisation was observed in all of the *p53* wild-type cells (Figure 4.8), the G_1 arrest and apoptosis induced by SKP2 loss in *p53* mutant SKNAS cells (Figure 4.7 and 4.9), independent of p21 expression, suggests that p27 accumulation is the primary factor in coordinating apoptotic cell death (Wang *et al.*, 1997). This suggestion is supported by the observation that the sub-G_1 population in neuroblastoma cells is reduced following dual p27/SKP2

knockdown. However, a greater response was observed following knockdown of p27 as opposed to SKP2 in SHSY5Y cells, suggesting that the apoptotic response observed in this cell line involves mechanisms that are independent of the E3 ligase activity of SKP2 (Figure 4.10b). The potential pro-apoptotic role of p27 accumulation in neuroblastoma cells was emphasised by the increased sensitivity of *MYCN* amplified cells to irradiation following SKP2 knockdown and associated p27 accumulation.

Based on the SKP2 knockdown studies, the data presented in this thesis suggest that although *MYCN* amplification does not sensitise neuroblastoma cells to the effects of SKP2 knockdown as first hypothesised, the SKP2/p27 axis does nevertheless play an important role in regulating the G_1/S cell cycle transition, and potentially in cell survival in a non-*MYCN* amplified setting.

6.4. Novel small molecules show potential as SKP2 inhibitors

Putative SKP2 inhibitors were synthesised based on a published structure (compound A, (**I**), (Chen *et al.*, 2008a)), and a strong association was observed between the lipophilicity of the novel compounds and their GI_{50} concentrations in HeLa cells (Figure 5.3d), implying that membrane permeability may be a contributing factor to their toxicity. Systematic alterations of **I**, identified a structure-growth inhibition relationship suggesting that while the tetrahydropyran ring was not required for growth inhibition both phenyl rings were, with toxicity being increased by substitution with electron-withdrawing groups at the benzylamine *para* position (Figure 5.4).

No relationship was observed between growth inhibition (GI_{50}) and p27 stabilisation (EC_{50}) across a sub-set of compounds assayed in the HeLa-p27(T187D)-EGFP cell line (Figure 5.6, Table 5.1). Enantiomers of **Ie**, i.e. **Ie-R and Ie-S**, demonstrated that p27 stabilisation was greater for the compound with an (R) configuration, whilst the (S) and (R) enantiomers were equipotent in the growth inhibition assay. The most active compound tested lacked the tetryhydropyran ring suggesting that this group does not contribute to the activity of the compound as inhibitors of SKP2-mediated p27 degradation.

Although MYCN expression did not sensitise Tet21N cells to growth inhibitory activity of the **I** derivatives, MYCN expression did increase sensitivity to the NAE

inhibitor MLN4924 and the SKPin CI, consistent with the rational of targeting the SKP2/p27 axis in *MYCN* overexpressing neuroblastoma (Table 5.2). However, due to the differences between amplification and overexpression as discussed previously, and the functional studies showing that non-*MYCN* amplified cell lines are in fact more responsive towards SKP2 knockdown, further analysis in a larger panel of neuroblastoma cell lines is required.

6.5. Final Conclusions

In conclusion, the data presented in this thesis demonstrates that *SKP2* is a direct transcriptional target of MYCN in neuroblastoma and is likely to contribute to perpetual cell cycle entry in *MYCN*-amplified cells. Based on the siRNA knockdown studies, SKP2 is a potential therapeutic target in neuroblastoma with the response to SKP2 inhibition primarily involving the SKP2/p27 axis, independent of the p53 pathway. Although MYCN was found able to compensate for the loss of SKP2, Tet21N MYCN+ cells showed a greater sensitivity towards both direct and indirect inhibition of SKP2-mediated p27 degradation, suggesting that pharmacological inhibition of SKP2 may be beneficial in neuroblastoma; both *p53* wt and mutant disease.

6.6. Further Directions

Although SKP2 knockdown was consistent throughout the study and produces repeatable biological effects, it would be beneficial to confirm this data using a second method of protein inhibition such as a different siRNA olig sequence or shRNA constructs. This would highlight any off target effects and verify the observed phenotypes.

The effects of SKP2 knockdown and of putative SKP2 inhibitors e.g. CI, in neuroblastoma cell lines confirm SKP2 as a potential therapeutic target in neuroblastoma, although further investigation of the effects of SKP2 siRNA knockdown and inhibition are warranted. Additionally, given the involvement of SKP2 in AKT activation and glycolysis, it would be of interest to determine whether SKP2 inhibition acts synergistically with AKT and glycolysis inhibitors.

With regards to the novel inhibitors, additional systematic structure-activity analysis is required to identify drug candidates with mechanism of action studies

in both cell-free assays and a panel of neuroblastoma cell lines. Such studies would also benefit from structural biology insights.

SKP2-mediated p27 degradation is dependent on phosphorylation and presentation of p27 by cyclin E-CDK2, in addition to the formation of the binding pocket between SKP2 and CKS1. Elevated CDK4 expression is a common characteristic of *MYCN* amplified disease and CDK4 inhibition has been shown to partly restore G_1 arrest and reduce SKP2 activity (Muth *et al.*, 2010; Gogolin *et al.*, 2013). CDK4 inactivates p27 and p21 by sequestering the CDK inhibitors, lowering the inhibitory threshold and activating the cyclin E-CDK2 complexes, while CDK2 inhibition has been shown to be a potential MYCN disease-selective therapy in neuroblastoma (Molenaar *et al.*, 2009). It would therefore be of interest to evaluate the effects of inhibiting both SKP2 and cyclin E-CDK2 in *MYCN* amplified neuroblastoma. Furthermore, CKS1 has been identified as a c-MYC transcriptional target (Keller *et al.*, 2007), which has p27-independent oncogenic roles, and hence further investigations are warranted into the contribution of CKS1 to neuroblastoma malignancy.

References

Adams, J.M., Harris, A.W., Pinkert, C.A., Corcoran, L.M., Alexander, W.S., Cory, S., Palmiter, R.D. and Brinster, R.L. (1985) 'The c-myc oncogene driven by immunoglobulin enhancers induces lymphoid malignancy in transgenic mice', *Nature*, 318(6046), pp. 533-8.

Adhikary, S. and Eilers, M. (2005) 'Transcriptional regulation and transformation by Myc proteins', *Nat Rev Mol Cell Biol*, 6(8), pp. 635-45.

Ambros, I.M., Zellner, A., Roald, B., Amann, G., Ladenstein, R., Printz, D., Gadner, H. and Ambros, P.F. (1996) 'Role of Ploidy, Chromosome 1p, and Schwann Cells in the Maturation of Neuroblastoma', *New England Journal of Medicine*, 334(23), pp. 1505-1511.

Amente, S., Gargano, B., Diolaiti, D., Della Valle, G., Lania, L. and Majello, B. (2007) 'p14ARF interacts with N-Myc and inhibits its transcriptional activity', *FEBS Letters*, 581(5), pp. 821-825.

Amler, L.C. and Schwab, M. (1989) 'Amplified N-myc in human neuroblastoma cells is often arranged as clustered tandem repeats of differently recombined DNA', *Mol Cell Biol*, 9(11), pp. 4903-13.

Andreu, E.J., Lledo, E., Poch, E., Ivorra, C., Albero, M.P., Martinez-Climent, J.A., Montiel-Duarte, C., Rifon, J., Perez-Calvo, J., Arbona, C., Prosper, F. and Perez-Roger, I. (2005) 'BCR-ABL induces the expression of Skp2 through the PI3K pathway to promote p27Kip1 degradation and proliferation of chronic myelogenous leukemia cells', *Cancer Res*, 65(8), pp. 3264-72.

Appleman, L.J., Chernova, I., Li, L. and Boussiotis, V.A. (2006) 'CD28 Costimulation Mediates Transcription of SKP2 and CKS1, the Substrate Recognition Components of SCFSkp2 Ubiquitin Ligase That Leads p27kip1 to Degradation', *Cell Cycle*, 5(18), pp. 2123-2129.

Auld, C.A., Caccia, C.D. and Morrison, R.F. (2007) 'Hormonal induction of adipogenesis induces Skp2 expression through PI3K and MAPK pathways', *J Cell Biochem*, 100(1), pp. 204-16.

Baek, D., Villén, J., Shin, C., Camargo, F.D., Gygi, S.P. and Bartel, D.P. (2008) 'The impact of microRNAs on protein output', *Nature*, 455(7209), pp. 64-71.

Bagatell, R., London, W.B., Wagner, L.M., Voss, S.D., Stewart, C.F., Maris, J.M., Kretschmar, C. and Cohn, S.L. (2011) 'Phase II study of irinotecan and temozolomide in children with relapsed or refractory neuroblastoma: a Children's Oncology Group study', *J Clin Oncol*, 29(2), pp. 208-13.

Bai, C., Sen, P., Hofmann, K., Ma, L., Goebl, M., Harper, J.W. and Elledge, S.J. (1996) 'SKP1 connects cell cycle regulators to the ubiquitin proteolysis machinery through a novel motif, the F-box', *Cell*, 86(2), pp. 263-74.

Barford, D. (2011) 'Structure, function and mechanism of the anaphase promoting complex (APC/C)', *Q Rev Biophys*, 44(2), pp. 153-90.

Barre, B. and Perkins, N.D. (2007) 'A cell cycle regulatory network controlling NF-kappaB subunit activity and function', *EMBO J*, 26(23), pp. 4841-55.

Barrett, J.F., Lee, L.A. and Dang, C.V. (2005) 'Stimulation of Myc transactivation by the TATA binding protein in promoter-reporter assays', *BMC Biochem*, 6, p. 7.

Bashir, T., Dorrello, N.V., Amador, V., Guardavaccaro, D. and Pagano, M. (2004) 'Control of the SCFSkp2-Cks1 ubiquitin ligase by the APC/CCdh1 ubiquitin ligase', *Nature*, 428(6979), pp. 190-193.

Bassermann, F., Eichner, R. and Pagano, M. (2014) 'The ubiquitin proteasome system - implications for cell cycle control and the targeted treatment of cancer', *Biochim Biophys Acta*, 1843(1), pp. 150-62.

Bell, E., Chen, L., Liu, T., Marshall, G.M., Lunec, J. and Tweddle, D.A. (2010) 'MYCN oncoprotein targets and their therapeutic potential', *Cancer Lett*, 293(2), pp. 144-57.

Bell, E., Lunec, J. and Tweddle, D.A. (2007) 'Cell cycle regulation targets of MYCN identified by gene expression microarrays', *Cell Cycle*, 6(10), pp. 1249-56.

Bell, E., Premkumar, R., Carr, J., Lu, X., Lovat, P.E., Kees, U.R., Lunec, J. and Tweddle, D.A. (2006) 'The role of MYCN in the failure of MYCN amplified neuroblastoma cell lines to G1 arrest after DNA damage', *Cell Cycle*, 5(22), pp. 2639-47.

Bergmann, E., Wanzel, M., Weber, A., Shin, I., Christiansen, H. and Eilers, M. (2001) 'Expression of P27(KIP1) is prognostic and independent of MYCN amplification in human neuroblastoma', *Int J Cancer*, 95(3), pp. 176-83.

Bertoli, C., Skotheim, J.M. and de Bruin, R.A. (2013) 'Control of cell cycle transcription during G1 and S phases', *Nat Rev Mol Cell Biol*, 14(8), pp. 518-28.

Berwanger, B., Hartmann, O., Bergmann, E., Bernard, S., Nielsen, D., Krause, M., Kartal, A., Flynn, D., Wiedemeyer, R., Schwab, M., Schafer, H., Christiansen, H. and Eilers, M. (2002) 'Loss of a FYN-regulated differentiation and growth arrest pathway in advanced stage neuroblastoma', *Cancer Cell*, 2(5), pp. 377-86.

Besson, A., Gurian-West, M., Schmidt, A., Hall, A. and Roberts, J.M. (2004) 'p27Kip1 modulates cell migration through the regulation of RhoA activation', *Genes Dev*, 18(8), pp. 862-76.

Betters, E., Liu, Y., Kjaeldgaard, A., Sundstrom, E. and Garcia-Castro, M.I. (2010) 'Analysis of early human neural crest development', *Dev Biol*, 344(2), pp. 578-92.

Bhattacharya, S., Garriga, J., Calbo, J., Yong, T., Haines, D.S. and Grana, X. (2003) 'SKP2 associates with p130 and accelerates p130 ubiquitylation and degradation in human cells', *Oncogene*, 22(16), pp. 2443-51.

Biedler, J.L., Helson, L. and Spengler, B.A. (1973) 'Morphology and growth, tumorigenicity, and cytogenetics of human neuroblastoma cells in continuous culture', *Cancer Res*, 33(11), pp. 2643-52.

Biedler, J.L., Roffler-Tarlov, S., Schachner, M. and Freedman, L.S. (1978) 'Multiple Neurotransmitter Synthesis by Human Neuroblastoma Cell Lines and Clones', *Cancer Research*, 38(11 Part 1), pp. 3751-3757.

Biegalke, B.J., Heaney, M.L., Bouton, A., Parsons, J.T. and Linial, M. (1987) 'MC29 deletion mutants which fail to transform chicken macrophages are competent for transformation of quail macrophages', *Journal of Virology*, 61(7), pp. 2138-2142.

Binne, U.K., Classon, M.K., Dick, F.A., Wei, W., Rape, M., Kaelin, W.G., Naar, A.M. and Dyson, N.J. (2007) 'Retinoblastoma protein and anaphase-promoting complex physically interact and functionally cooperate during cell-cycle exit', *Nat Cell Biol*, 9(2), pp. 225-232.

Blain, S.W., Scher, H.I., Cordon-Cardo, C. and Koff, A. (2003) 'p27 as a target for cancer therapeutics', *Cancer Cell*, 3(2), pp. 111-5.

Bloom, J. and Pagano, M. (2003) 'Deregulated degradation of the cdk inhibitor p27 and malignant transformation', *Semin Cancer Biol*, 13(1), pp. 41-7.

Bornstein, G., Bloom, J., Sitry-Shevah, D., Nakayama, K., Pagano, M. and Hershko, A. (2003) 'Role of the SCFSkp2 ubiquitin ligase in the degradation of p21Cip1 in S phase', *J Biol Chem*, 278(28), pp. 25752-7.

Bornstein, G., Ganoth, D. and Hershko, A. (2006) 'Regulation of neddylation and deneddylation of cullin1 in SCFSkp2 ubiquitin ligase by F-box protein and substrate', *Proc Natl Acad Sci U S A*, 103(31), pp. 11515-20.

Borriello, A., Pietra, V.D., Criscuolo, M., Oliva, A., Tonini, G.P., Iolascon, A., Zappia, V. and Ragione, F.D. (2000) 'p27Kip1 accumulation is associated with retinoic-induced neuroblastoma differentiation: evidence of a decreased proteasome-dependent degradation', *Oncogene*, 19(1), pp. 51-60.

Bourne, Y., Watson, M.H., Hickey, M.J., Holmes, W., Rocque, W., Reed, S.I. and Tainer, J.A. (1996) 'Crystal Structure and Mutational Analysis of the Human CDK2 Kinase Complex with Cell Cycle–Regulatory Protein CksHs1', *Cell*, 84(6), pp. 863-874.

Bown, N. (2001) 'Neuroblastoma tumour genetics: clinical and biological aspects', *J Clin Pathol*, 54(12), pp. 897-910.

Bown, N., Lastowska, M., Cotterill, S., O'Neill, S., Ellershaw, C., Roberts, P., Lewis, I. and Pearson, A.D. (2001) '17q gain in neuroblastoma predicts adverse clinical outcome. U.K. Cancer Cytogenetics Group and the U.K. Children's Cancer Study Group', *Med Pediatr Oncol*, 36(1), pp. 14-9.

Breit, S. and Schwab, M. (1989) 'Suppression of MYC by high expression of NMYC in human neuroblastoma cells', *J Neurosci Res*, 24(1), pp. 21-8.

Brenner, D.W., Barranco, S.C., Winslow, B.H. and Shaeffer, J. (1989) 'Flow cytometric analysis of DNA content in children with neuroblastoma', *J Pediatr Surg*, 24(2), pp. 204-7.

Bretones, G., Acosta, J.C., Caraballo, J.M., Ferrandiz, N., Gomez-Casares, M.T., Albajar, M., Blanco, R., Ruiz, P., Hung, W.C., Albero, M.P., Perez-Roger, I. and Leon, J. (2011) 'SKP2 oncogene is a direct MYC target gene and MYC down-regulates p27(KIP1) through SKP2 in human leukemia cells', *J Biol Chem*, 286(11), pp. 9815-25.

Brodeur, G.M., Pritchard, J., Berthold, F., Carlsen, N.L., Castel, V., Castelberry, R.P., De Bernardi, B., Evans, A.E., Favrot, M., Hedborg, F. and et al. (1993) 'Revisions of the international criteria for neuroblastoma diagnosis, staging, and response to treatment', *J Clin Oncol*, 11(8), pp. 1466-77.

Brodeur, G.M., Seeger, R.C., Barrett, A., Berthold, F., Castleberry, R.P., D'Angio, G., De Bernardi, B., Evans, A.E., Favrot, M., Freeman, A.I. and et al. (1988) 'International criteria for diagnosis, staging, and response to treatment in patients with neuroblastoma', *J Clin Oncol*, 6(12), pp. 1874-81.

Brodeur, G.M., Seeger, R.C., Schwab, M., Varmus, H.E. and Bishop, J.M. (1984) 'Amplification of N-myc in untreated human neuroblastomas correlates with advanced disease stage', *Science*, 224(4653), pp. 1121-4.

Brzovic, P.S., Lissounov, A., Christensen, D.E., Hoyt, D.W. and Klevit, R.E. (2006) 'A UbcH5/ubiquitin noncovalent complex is required for processive BRCA1-directed ubiquitination', *Mol Cell*, 21(6), pp. 873-80.

Buechner, J. and Einvik, C. (2012) 'N-myc and noncoding RNAs in neuroblastoma', *Mol Cancer Res*, 10(10), pp. 1243-53.

Cardozo, T. and Abagyan, R. (2005) 'Druggability of SCF ubiquitin ligase-protein interfaces', *Methods Enzymol*, 399, pp. 634-53.

Caren, H., Erichsen, J., Olsson, L., Enerback, C., Sjoberg, R.M., Abrahamsson, J., Kogner, P. and Martinsson, T. (2008) 'High-resolution array copy

number analyses for detection of deletion, gain, amplification and copy-neutral LOH in primary neuroblastoma tumors: four cases of homozygous deletions of the CDKN2A gene', *BMC Genomics*, 9, p. 353.

Caron, H., van Sluis, P., de Kraker, J., Bokkerink, J., Egeler, M., Laureys, G., Slater, R., Westerveld, A., Voute, P.A. and Versteeg, R. (1996) 'Allelic loss of chromosome 1p as a predictor of unfavorable outcome in patients with neuroblastoma', *N Engl J Med*, 334(4), pp. 225-30.

Carr-Wilkinson, J., Griffiths, R., Elston, R., Gamble, L.D., Goranov, B., Redfern, C.P., Lunec, J. and Tweddle, D.A. (2011) 'Outcome of the p53-mediated DNA damage response in neuroblastoma is determined by morphological subtype and MYCN expression', *Cell Cycle*, 10(21), pp. 3778-87.

Carr-Wilkinson, J., O'Toole, K., Wood, K.M., Challen, C.C., Baker, A.G., Board, J.R., Evans, L., Cole, M., Cheung, N.K., Boos, J., Kohler, G., Leuschner, I., Pearson, A.D., Lunec, J. and Tweddle, D.A. (2010a) 'High Frequency of p53/MDM2/p14ARF Pathway Abnormalities in Relapsed Neuroblastoma', *Clin Cancer Res*, 16(4), pp. 1108-18.

Carr-Wilkinson, J., O'Toole, K., Wood, K.M., Challen, C.C., Baker, A.G., Board, J.R., Evans, L., Cole, M., Cheung, N.K.V., Boos, J., Kohler, G., Leuschner, I., Pearson, A.D.J., Lunec, J. and Tweddle, D.A. (2010b) 'High Frequency of p53/MDM2/p14(ARF) Pathway Abnormalities in Relapsed Neuroblastoma', *Clinical Cancer Research*, 16(4), pp. 1108-1118.

Carrano, A.C., Eytan, E., Hershko, A. and Pagano, M. (1999) 'SKP2 is required for ubiquitin-mediated degradation of the CDK inhibitor p27', *Nat Cell Biol*, 1(4), pp. 193-9.

Cen, B., Mahajan, S., Zemskova, M., Beharry, Z., Lin, Y.W., Cramer, S.D., Lilly, M.B. and Kraft, A.S. (2010) 'Regulation of Skp2 levels by the Pim-1 protein kinase', *J Biol Chem*, 285(38), pp. 29128-37.

Cenciarelli, C., Chiaur, D.S., Guardavaccaro, D., Parks, W., Vidal, M. and Pagano, M. (1999) 'Identification of a family of human F-box proteins', *Curr Biol*, 9(20), pp. 1177-9.

Chan, C.-H., Lee, S.-W., Li, C.-F., Wang, J., Yang, W.-L., Wu, C.-Y., Wu, J., Nakayama, K.I., Kang, H.-Y., Huang, H.-Y., Hung, M.-C., Pandolfi, P.P. and Lin, H.-K. (2010a) 'Deciphering the transcriptional complex critical for RhoA gene expression and cancer metastasis', *Nat Cell Biol*, 12(5), pp. 457-467.

Chan, C.-H., Li, C.-F., Yang, W.-L., Gao, Y., Lee, S.-W., Feng, Z., Huang, H.-Y., Tsai, Kelvin K.C., Flores, Leo G., Shao, Y., Hazle, John D., Yu, D., Wei, W., Sarbassov, D., Hung, M.-C., Nakayama, Keiichi I. and Lin, H.-K. (2012) 'The Skp2-SCF E3 Ligase Regulates Akt Ubiquitination, Glycolysis, Herceptin Sensitivity, and Tumorigenesis', *Cell*, 149(5), pp. 1098-1111.

Chan, C.H., Lee, S.W., Wang, J. and Lin, H.K. (2010b) 'Regulation of Skp2 expression and activity and its role in cancer progression', *ScientificWorldJournal*, 10, pp. 1001-15.

Chan, C.H., Morrow, J.K., Li, C.F., Gao, Y., Jin, G., Moten, A., Stagg, L.J., Ladbury, J.E., Cai, Z., Xu, D., Logothetis, C.J., Hung, M.C., Zhang, S. and Lin, H.K. (2013) 'Pharmacological inactivation of Skp2 SCF ubiquitin ligase restricts cancer stem cell traits and cancer progression', *Cell*, 154(3), pp. 556-68.

Chander, H., Halpern, M., Resnick-Silverman, L., Manfredi, J.J. and Germain, D. (2010) 'Skp2B attenuates p53 function by inhibiting prohibitin', *EMBO Rep*, 11(3), pp. 220-5.

Charron, J., Malynn, B.A., Fisher, P., Stewart, V., Jeannotte, L., Goff, S.P., Robertson, E.J. and Alt, F.W. (1992) 'Embryonic lethality in mice homozygous for a targeted disruption of the N-myc gene', *Genes Dev*, 6(12A), pp. 2248-57.

Chen, D., Frezza, M., Schmitt, S., Kanwar, J. and Dou, Q.P. (2011) 'Bortezomib as the first proteasome inhibitor anticancer drug: current status and future perspectives', *Curr Cancer Drug Targets*, 11(3), pp. 239-53.

Chen, G., Wang, Y., Garate, M., Zhou, J. and Li, G. (2010a) 'The tumor suppressor ING3 is degraded by SCF(Skp2)-mediated ubiquitin-proteasome system', *Oncogene*, 29(10), pp. 1498-508.

Chen, J., Liu, T. and Ross, A.H. (1994) 'Down-regulation of c-myc oncogene during NGF-induced differentiation of neuroblastoma cell lines', *Chin Med Sci J*, 9(3), pp. 152-6.

Chen, L.D., Iraci, N., Gherardi, S., Gamble, L.D., Wood, K.M., Perini, G., Lunec, J. and Tweddle, D.A. (2010b) 'p53 Is a Direct Transcriptional Target of MYCN in Neuroblastoma', *Cancer Research*, 70(4), pp. 1377-1388.

Chen, Q., Xie, W., Kuhn, D.J., Voorhees, P.M., Lopez-Girona, A., Mendy, D., Corral, L.G., Krenitsky, V.P., Xu, W., Moutouh-de Parseval, L., Webb, D.R., Mercurio, F., Nakayama, K.I., Nakayama, K. and Orlowski, R.Z. (2008a) 'Targeting the p27 E3 ligase SCF(Skp2) results in p27- and Skp2-mediated cell-cycle arrest and activation of autophagy', *Blood*, 111(9), pp. 4690-9.

Chen, Y. and Stallings, R.L. (2007) 'Differential patterns of microRNA expression in neuroblastoma are correlated with prognosis, differentiation, and apoptosis', *Cancer Res*, 67(3), pp. 976-83.

Chen, Y., Takita, J., Choi, Y.L., Kato, M., Ohira, M., Sanada, M., Wang, L., Soda, M., Kikuchi, A., Igarashi, T., Nakagawara, A., Hayashi, Y., Mano, H. and Ogawa, S. (2008b) 'Oncogenic mutations of ALK kinase in neuroblastoma', *Nature*, 455(7215), pp. 971-4.

Chen, Z.F. and Behringer, R.R. (1995) 'twist is required in head mesenchyme for cranial neural tube morphogenesis', *Genes Dev*, 9(6), pp. 686-99.

Cheng, M., Olivier, P., Diehl, J.A., Fero, M., Roussel, M.F., Roberts, J.M. and Sherr, C.J. (1999) 'The p21(Cip1) and p27(Kip1) CDK 'inhibitors' are essential activators of cyclin D-dependent kinases in murine fibroblasts', *EMBO J*, 18(6), pp. 1571-83.

Chesler, L., Schlieve, C., Goldenberg, D.D., Kenney, A., Kim, G., McMillan, A., Matthay, K.K., Rowitch, D. and Weiss, W.A. (2006) 'Inhibition of phosphatidylinositol 3-kinase destabilizes Mycn protein and blocks malignant progression in neuroblastoma', *Cancer Res*, 66(16), pp. 8139-46.

Cheung, N.K. and Dyer, M.A. (2013) 'Neuroblastoma: developmental biology, cancer genomics and immunotherapy', *Nat Rev Cancer*, 13(6), pp. 397-411.

Cheung, N.K., Zhang, J., Lu, C., Parker, M., Bahrami, A., Tickoo, S.K., Heguy, A., Pappo, A.S., Federico, S., Dalton, J., Cheung, I.Y., Ding, L., Fulton, R., Wang, J., Chen, X., Becksfort, J., Wu, J., Billups, C.A., Ellison, D., Mardis, E.R., Wilson, R.K., Downing, J.R. and Dyer, M.A. (2012) 'Association of age at diagnosis and genetic mutations in patients with neuroblastoma', *JAMA*, 307(10), pp. 1062-71.

Chi, Y., Welcker, M., Hizli, A.A., Posakony, J.J., Aebersold, R. and Clurman, B.E. (2008) 'Identification of CDK2 substrates in human cell lysates', *Genome Biol*, 9(10), p. R149.

Chipumuro, E., Marco, E., Christensen, C.L., Kwiatkowski, N., Zhang, T., Hatheway, C.M., Abraham, B.J., Sharma, B., Yeung, C., Altabef, A., Perez-Atayde, A., Wong, K.K., Yuan, G.C., Gray, N.S., Young, R.A. and George, R.E. (2014) 'CDK7 Inhibition Suppresses Super-Enhancer-Linked Oncogenic Transcription in MYCN-Driven Cancer', *Cell*, 159(5), pp. 1126-39.

Chong, J.-L., Wenzel, P.L., Saenz-Robles, M.T., Nair, V., Ferrey, A., Hagan, J.P., Gomez, Y.M., Sharma, N., Chen, H.-Z., Ouseph, M., Wang, S.-H., Trikha, P., Culp, B., Mezache, L., Winton, D.J., Sansom, O.J., Chen, D., Bremner, R., Cantalupo, P.G., Robinson, M.L., Pipas, J.M. and Leone, G. (2009) 'E2f1-3 switch from activators in progenitor cells to repressors in differentiating cells', *Nature*, 462(7275), pp. 930-934.

Chu, I.M., Hengst, L. and Slingerland, J.M. (2008) 'The Cdk inhibitor p27 in human cancer: prognostic potential and relevance to anticancer therapy', *Nat Rev Cancer*, 8(4), pp. 253-267.

Chuang, J.H., Chou, M.H., Tai, M.H., Lin, T.K., Liou, C.W., Chen, T., Hsu, W.M. and Wang, P.W. (2013) '2-Deoxyglucose treatment complements the cisplatin- or BH3-only mimetic-induced suppression of neuroblastoma cell growth', *Int J Biochem Cell Biol*, 45(5), pp. 944-51.

Clague, M.J. and Urbe, S. (2010) 'Ubiquitin: same molecule, different degradation pathways', *Cell*, 143(5), pp. 682-5.

Cobrinik, D. (2005) 'Pocket proteins and cell cycle control', 24(17), pp. 2796-2809.

Cohn, S.L., Look, A.T., Joshi, V.V., Holbrook, T., Salwen, H., Chagnovich, D., Chesler, L., Rowe, S.T., Valentine, M.B., Komuro, H. and et al. (1995) 'Lack of correlation of N-myc gene amplification with prognosis in localized neuroblastoma: a Pediatric Oncology Group study', *Cancer Res*, 55(4), pp. 721-6.

Cohn, S.L., Pearson, A.D., London, W.B., Monclair, T., Ambros, P.F., Brodeur, G.M., Faldum, A., Hero, B., Iehara, T., Machin, D., Mosseri, V., Simon, T., Garaventa, A., Castel, V. and Matthay, K.K. (2009) 'The International Neuroblastoma Risk Group (INRG) classification system: an INRG Task Force report', *J Clin Oncol*, 27(2), pp. 289-97.

Collas, P. (2010) 'The current state of chromatin immunoprecipitation', *Mol Biotechnol*, 45(1), pp. 87-100.

Cornaglia-Ferraris, P., Ponzoni, M., Montaldo, P., Mariottini, G.L., Donti, E., Di Martino, D. and Tonini, G.P. (1990) 'A new human highly tumorigenic neuroblastoma cell line with undetectable expression of N-myc', *Pediatr Res*, 27(1), pp. 1-6.

Corvetta, D., Chayka, O., Gherardi, S., D'Acunto, C.W., Cantilena, S., Valli, E., Piotrowska, I., Perini, G. and Sala, A. (2013) 'Physical interaction between MYCN oncogene and polycomb repressive complex 2 (PRC2) in neuroblastoma: functional and therapeutic implications', *J Biol Chem*, 288(12), pp. 8332-41.

Costanzo, A., Merlo, P., Pediconi, N., Fulco, M., Sartorelli, V., Cole, P.A., Fontemaggi, G., Fanciulli, M., Schiltz, L., Blandino, G., Balsano, C. and Levrero, M. (2002) 'DNA damage-dependent acetylation of p73 dictates the selective activation of apoptotic target genes', *Mol Cell*, 9(1), pp. 175-86.

Cotterman, R., Jin, V.X., Krig, S.R., Lemen, J.M., Wey, A., Farnham, P.J. and Knoepfler, P.S. (2008) 'N-Myc regulates a widespread euchromatic

program in the human genome partially independent of its role as a classical transcription factor', *Cancer Res*, 68(23), pp. 9654-62.
Davidoff, A.M. (2012) 'Neuroblastoma', *Seminars in Pediatric Surgery*, 21(1), pp. 2-14.
Davis, A.C., Wims, M., Spotts, G.D., Hann, S.R. and Bradley, A. (1993) 'A null c-myc mutation causes lethality before 10.5 days of gestation in homozygotes and reduced fertility in heterozygous female mice', *Genes Dev*, 7(4), pp. 671-82.
de Bie, P. and Ciechanover, A. (2011) 'Ubiquitination of E3 ligases: self-regulation of the ubiquitin system via proteolytic and non-proteolytic mechanisms', *Cell Death Differ*, 18(9), pp. 1393-1402.
De Brouwer, S., Mestdagh, P., Lambertz, I., Pattyn, F., De Paepe, A., Westermann, F., Schroeder, C., Schulte, J.H., Schramm, A., De Preter, K., Vandesompele, J. and Speleman, F. (2012) 'Dickkopf-3 is regulated by the MYCN-induced miR-17-92 cluster in neuroblastoma', *Int J Cancer*, 130(11), pp. 2591-8.
Dehay, C. and Kennedy, H. (2007) 'Cell-cycle control and cortical development', *Nat Rev Neurosci*, 8(6), pp. 438-450.
Delmore, J.E., Issa, G.C., Lemieux, M.E., Rahl, P.B., Shi, J., Jacobs, H.M., Kastritis, E., Gilpatrick, T., Paranal, R.M., Qi, J., Chesi, M., Schinzel, A.C., McKeown, M.R., Heffernan, T.P., Vakoc, C.R., Bergsagel, P.L., Ghobrial, I.M., Richardson, P.G., Young, R.A., Hahn, W.C., Anderson, K.C., Kung, A.L., Bradner, J.E. and Mitsiades, C.S. (2011) 'BET bromodomain inhibition as a therapeutic strategy to target c-Myc', *Cell*, 146(6), pp. 904-17.
Di Cristofano, A., De Acetis, M., Koff, A., Cordon-Cardo, C. and Pandolfi, P.P. (2001) 'Pten and p27KIP1 cooperate in prostate cancer tumor suppression in the mouse', *Nat Genet*, 27(2), pp. 222-4.
Diskin, S.J., Hou, C., Glessner, J.T., Attiyeh, E.F., Laudenslager, M., Bosse, K., Cole, K., Mosse, Y.P., Wood, A., Lynch, J.E., Pecor, K., Diamond, M., Winter, C., Wang, K., Kim, C., Geiger, E.A., McGrady, P.W., Blakemore, A.I., London, W.B., Shaikh, T.H., Bradfield, J., Grant, S.F., Li, H., Devoto, M., Rappaport, E.R., Hakonarson, H. and Maris, J.M. (2009) 'Copy number variation at 1q21.1 associated with neuroblastoma', *Nature*, 459(7249), pp. 987-91.
Dow, R., Hendley, J., Pirkmaier, A., Musgrove, E.A. and Germain, D. (2001) 'Retinoic acid-mediated growth arrest requires ubiquitylation and degradation of the F-box protein Skp2', *J Biol Chem*, 276(49), pp. 45945-51.
Dowen, S.E., Neutze, D.M., Pett, M.R., Cottage, A., Stern, P., Coleman, N. and Stanley, M.A. 'Amplification of chromosome 5p correlates with increased expression of Skp2 in HPV-immortalized keratinocytes', *Oncogene*, 22(16), pp. 2531-2540.
Dreidax, D., Gogolin, S., Schroeder, C., Muth, D., Brueckner, L.M., Hess, E.M., Zapatka, M., Theissen, J., Fischer, M., Ehemann, V., Schwab, M., Savelyeva, L. and Westermann, F. (2013) 'Low p14ARF expression in neuroblastoma cells is associated with repressed histone mark status, and enforced expression induces growth arrest and apoptosis', *Hum Mol Genet*, 22(9), pp. 1735-45.
Drexler, H.C. (2003) 'The role of p27Kip1 in proteasome inhibitor induced apoptosis', *Cell Cycle*, 2(5), pp. 438-41.

Drexler, H.C. and Pebler, S. (2003) 'Inducible p27(Kip1) expression inhibits proliferation of K562 cells and protects against apoptosis induction by proteasome inhibitors', *Cell Death Differ*, 10(3), pp. 290-301.

Drobnjak, M., Melamed, J., Taneja, S., Melzer, K., Wieczorek, R., Levinson, B., Zeleniuch-Jacquotte, A., Polsky, D., Ferrara, J., Perez-Soler, R., Cordon-Cardo, C., Pagano, M. and Osman, I. (2003) 'Altered expression of p27 and Skp2 proteins in prostate cancer of African-American patients', *Clin Cancer Res*, 9(7), pp. 2613-9.

Duda, D.M., Borg, L.A., Scott, D.C., Hunt, H.W., Hammel, M. and Schulman, B.A. (2008) 'Structural insights into NEDD8 activation of cullin-RING ligases: conformational control of conjugation', *Cell*, 134(6), pp. 995-1006.

Eberhardy, S.R. and Farnham, P.J. (2002) 'Myc recruits P-TEFb to mediate the final step in the transcriptional activation of the cad promoter', *J Biol Chem*, 277(42), pp. 40156-62.

Ecker, K. and Hengst, L. (2009) 'Skp2: caught in the Akt', *Nat Cell Biol*, 11(4), pp. 377-379.

Edsjo, A., Nilsson, H., Vandesompele, J., Karlsson, J., Pattyn, F., Culp, L.A., Speleman, F. and Pahlman, S. (2004) 'Neuroblastoma cells with overexpressed MYCN retain their capacity to undergo neuronal differentiation', *Lab Invest*, 84(4), pp. 406-17.

Elbashir, S.M., Harborth, J., Lendeckel, W., Yalcin, A., Weber, K. and Tuschl, T. (2001a) 'Duplexes of 21-nucleotide RNAs mediate RNA interference in cultured mammalian cells', *Nature*, 411(6836), pp. 494-8.

Elbashir, S.M., Lendeckel, W. and Tuschl, T. (2001b) 'RNA interference is mediated by 21- and 22-nucleotide RNAs', *Genes Dev*, 15(2), pp. 188-200.

Esteller, M. (2011) 'Non-coding RNAs in human disease', *Nat Rev Genet*, 12(12), pp. 861-874.

Ezhevsky, S.A., Ho, A., Becker-Hapak, M., Davis, P.K. and Dowdy, S.F. (2001) 'Differential regulation of retinoblastoma tumor suppressor protein by G(1) cyclin-dependent kinase complexes in vivo', *Mol Cell Biol*, 21(14), pp. 4773-84.

Fernandez, P.C., Frank, S.R., Wang, L., Schroeder, M., Liu, S., Greene, J., Cocito, A. and Amati, B. (2003) 'Genomic targets of the human c-Myc protein', *Genes Dev*, 17(9), pp. 1115-29.

Filippakopoulos, P., Qi, J., Picaud, S., Shen, Y., Smith, W.B., Fedorov, O., Morse, E.M., Keates, T., Hickman, T.T., Felletar, I., Philpott, M., Munro, S., McKeown, M.R., Wang, Y., Christie, A.L., West, N., Cameron, M.J., Schwartz, B., Heightman, T.D., La Thangue, N., French, C.A., Wiest, O., Kung, A.L., Knapp, S. and Bradner, J.E. (2010) 'Selective inhibition of BET bromodomains', *Nature*, 468(7327), pp. 1067-73.

Fong, C.T., Dracopoli, N.C., White, P.S., Merrill, P.T., Griffith, R.C., Housman, D.E. and Brodeur, G.M. (1989) 'Loss of heterozygosity for the short arm of chromosome 1 in human neuroblastomas: correlation with N-myc amplification', *Proc Natl Acad Sci U S A*, 86(10), pp. 3753-7.

French, S., DuBois, S.G., Horn, B., Granger, M., Hawkins, R., Pass, A., Plummer, E. and Matthay, K. (2013) '131I-MIBG followed by consolidation with busulfan, melphalan and autologous stem cell transplantation for refractory neuroblastoma', *Pediatr Blood Cancer*, 60(5), pp. 879-84.

Frescas, D. and Pagano, M. (2008) 'Deregulated proteolysis by the F-box proteins SKP2 and beta-TrCP: tipping the scales of cancer', *Nature Review: Cancer*, 8(6), p. 12.

Fujieda, S., Inuzuka, M., Tanaka, N., Sunaga, H., Fan, G.-K., Ito, T., Sugimoto, C., Tsuzuki, H. and Saito, H. (1999) 'Expression of p27 is associated with Bax expression and spontaneous apoptosis in oral and oropharyngeal carcinoma', *International Journal of Cancer*, 84(3), pp. 315-320.

Fulda, S. and Debatin, K.M. (2006) 'Extrinsic versus intrinsic apoptosis pathways in anticancer chemotherapy', *Oncogene*, 25(34), pp. 4798-811.

Fulda, S., Lutz, W., Schwab, M. and Debatin, K.M. (1999) 'MycN sensitizes neuroblastoma cells for drug-induced apoptosis', *Oncogene*, 18(7), pp. 1479-86.

Galan, J.M. and Peter, M. (1999) 'Ubiquitin-dependent degradation of multiple F-box proteins by an autocatalytic mechanism', *Proc Natl Acad Sci U S A*, 96(16), pp. 9124-9.

Galderisi, U., Di Bernardo, G., Cipollaro, M., Peluso, G., Cascino, A., Cotrufo, R. and Melone, M.A. (1999) 'Differentiation and apoptosis of neuroblastoma cells: role of N-myc gene product', *J Cell Biochem*, 73(1), pp. 97-105.

Gamble, L.D., Kees, U.R., Tweddle, D.A. and Lunec, J. (2012) 'MYCN sensitizes neuroblastoma to the MDM2-p53 antagonists Nutlin-3 and MI-63', *Oncogene*, 31(6), pp. 752-63.

Ganoth, D., Bornstein, G., Ko, T.K., Larsen, B., Tyers, M., Pagano, M. and Hershko, A. (2001) 'The cell-cycle regulatory protein Cks1 is required for SCF(Skp2)-mediated ubiquitinylation of p27', *Nat Cell Biol*, 3(3), pp. 321-4.

Gansler, T., Chatten, J., Varello, M., Bunin, G.R. and Atkinson, B. (1986) 'Flow cytometric DNA analysis of neuroblastoma. Correlation with histology and clinical outcome', *Cancer*, 58(11), pp. 2453-8.

Gao, D., Inuzuka, H., Tseng, A., Chin, R.Y., Toker, A. and Wei, W. (2009) 'Phosphorylation by Akt1 promotes cytoplasmic localization of Skp2 and impairs APCCdh1-mediated Skp2 destruction', *Nat Cell Biol*, 11(4), pp. 397-408.

Gargano, B., Amente, S., Majello, B. and Lania, L. (2007) 'P-TEFb is a crucial co-factor for Myc transactivation', *Cell Cycle*, 6(16), pp. 2031-7.

George, R.E., Sanda, T., Hanna, M., Frohling, S., Luther, W., 2nd, Zhang, J., Ahn, Y., Zhou, W., London, W.B., McGrady, P., Xue, L., Zozulya, S., Gregor, V.E., Webb, T.R., Gray, N.S., Gilliland, D.G., Diller, L., Greulich, H., Morris, S.W., Meyerson, M. and Look, A.T. (2008) 'Activating mutations in ALK provide a therapeutic target in neuroblastoma', *Nature*, 455(7215), pp. 975-8.

Gilbert, S.F. (2000) *Developmental Biology, 6th edition*. Sunderland (MA): Sinauer Associates.

Gilmore, T.D. (2006) 'Introduction to NF-kappaB: players, pathways, perspectives', *Oncogene*, 25(51), pp. 6680-4.

Gogolin, S., Ehemann, V., Becker, G., Brueckner, L.M., Dreidax, D., Bannert, S., Nolte, I., Savelyeva, L., Bell, E. and Westermann, F. (2013) 'CDK4 inhibition restores G(1)-S arrest in MYCN-amplified neuroblastoma cells in the context of doxorubicin-induced DNA damage', *Cell Cycle*, 12(7), pp. 1091-104.

Goldschneider, D., Horvilleur, E., Plassa, L.-F., Guillaud-Bataille, M., Million, K., Wittmer-Dupret, E., Danglot, G., Thé, H.d., Bénard, J., May, E. and Douc-Rasy, S. (2006a) 'Expression of C-terminal deleted p53 isoforms in neuroblastoma', *Nucleic Acids Research*, 34(19), pp. 5603-5612.

Goldschneider, D., Horvilleur, E., Plassa, L.F., Guillaud-Bataille, M., Million, K., Wittmer-Dupret, E., Danglot, G., de The, H., Benard, J., May, E. and Douc-

Rasy, S. (2006b) 'Expression of C-terminal deleted p53 isoforms in neuroblastoma', *Nucleic Acids Res*, 34(19), pp. 5603-12.
Gossen, M. and Bujard, H. (1992) 'Tight control of gene expression in mammalian cells by tetracycline-responsive promoters', *Proc Natl Acad Sci U S A*, 89(12), pp. 5547-51.
Grandori, C., Cowley, S.M., James, L.P. and Eisenman, R.N. (2000) 'The Myc/Max/Mad network and the transcriptional control of cell behavior', *Annu Rev Cell Dev Biol*, 16, pp. 653-99.
Gstaiger, M., Jordan, R., Lim, M., Catzavelos, C., Mestan, J., Slingerland, J. and Krek, W. (2001) 'Skp2 is oncogenic and overexpressed in human cancers', *Proceedings of the National Academy of Sciences*, 98(9), pp. 5043-5048.
Gu, W. and Roeder, R.G. (1997) 'Activation of p53 sequence-specific DNA binding by acetylation of the p53 C-terminal domain', *Cell*, 90(4), pp. 595-606.
Gu, W., Shi, X.L. and Roeder, R.G. (1997) 'Synergistic activation of transcription by CBP and p53', *Nature*, 387(6635), pp. 819-23.
Guardavaccaro, D., Kudo, Y., Boulaire, J., Barchi, M., Busino, L., Donzelli, M., Margottin-Goguet, F., Jackson, P.K., Yamasaki, L. and Pagano, M. (2003) 'Control of meiotic and mitotic progression by the F box protein beta-Trcp1 in vivo', *Dev Cell*, 4(6), pp. 799-812.
Guccione, E., Martinato, F., Finocchiaro, G., Luzi, L., Tizzoni, L., Dall' Olio, V., Zardo, G., Nervi, C., Bernard, L. and Amati, B. (2006) 'Myc-binding-site recognition in the human genome is determined by chromatin context', *Nat Cell Biol*, 8(7), pp. 764-770.
Guglielmi, L., Cinnella, C., Nardella, M., Maresca, G., Valentini, A., Mercanti, D., Felsani, A. and D'Agnano, I. (2014) 'MYCN gene expression is required for the onset of the differentiation programme in neuroblastoma cells', *Cell Death Dis*, 5, p. e1081.
Guo, C., White, P.S., Hogarty, M.D., Brodeur, G.M., Gerbing, R., Stram, D.O. and Maris, J.M. (2000) 'Deletion of 11q23 is a frequent event in the evolution of MYCN single-copy high-risk neuroblastomas', *Med Pediatr Oncol*, 35(6), pp. 544-6.
Hanahan, D. and Weinberg, Robert A. (2011) 'Hallmarks of Cancer: The Next Generation', *Cell*, 144(5), pp. 646-674.
Hao, B., Zheng, N., Schulman, B.A., Wu, G., Miller, J.J., Pagano, M. and Pavletich, N.P. (2005) 'Structural basis of the Cks1-dependent recognition of p27(Kip1) by the SCF(Skp2) ubiquitin ligase', *Mol Cell*, 20(1), pp. 9-19.
Hasan, M.K., Nafady, A., Takatori, A., Kishida, S., Ohira, M., Suenaga, Y., Hossain, S., Akter, J., Ogura, A., Nakamura, Y., Kadomatsu, K. and Nakagawara, A. (2013) 'ALK is a MYCN target gene and regulates cell migration and invasion in neuroblastoma', *Sci. Rep.*, 3.
Hatton, K.S., Mahon, K., Chin, L., Chiu, F.C., Lee, H.W., Peng, D., Morgenbesser, S.D., Horner, J. and DePinho, R.A. (1996) 'Expression and activity of L-Myc in normal mouse development', *Mol Cell Biol*, 16(4), pp. 1794-804.
Heaney, M.L., Pierce, J. and Parsons, J.T. (1986) 'Site-directed mutagenesis of the gag-myc gene of avian myelocytomatosis virus 29: Biological activity and intracellular localization of structurally altered proteins', *Journal of Virology*, 60(1), pp. 167-176.
Henriksson, M. and Luscher, B. (1996) 'Proteins of the Myc network: essential regulators of cell growth and differentiation', *Adv Cancer Res*, 68, pp. 109-82.

Hero, B., Simon, T., Spitz, R., Ernestus, K., Gnekow, A.K., Scheel-Walter, H.G., Schwabe, D., Schilling, F.H., Benz-Bohm, G. and Berthold, F. (2008) 'Localized infant neuroblastomas often show spontaneous regression: results of the prospective trials NB95-S and NB97', *J Clin Oncol*, 26(9), pp. 1504-10.

Hershko, D.D. (2008) 'Oncogenic properties and prognostic implications of the ubiquitin ligase Skp2 in cancer', *Cancer*, 112(7), pp. 1415-24.

Hirai, M., Yoshida, S., Kashiwagi, H., Kawamura, T., Ishikawa, T., Kaneko, M., Ohkawa, H., Nakagawara, A., Miwa, M. and Uchida, K. (1999) '1q23 gain is associated with progressive neuroblastoma resistant to aggressive treatment', *Genes Chromosomes Cancer*, 25(3), pp. 261-9.

Hiramatsu, Y., Kitagawa, K., Suzuki, T., Uchida, C., Hattori, T., Kikuchi, H., Oda, T., Hatakeyama, S., Nakayama, K.I., Yamamoto, T., Konno, H. and Kitagawa, M. (2006) 'Degradation of Tob1 mediated by SCFSkp2-dependent ubiquitination', *Cancer Res*, 66(17), pp. 8477-83.

Hirvonen, H., Makela, T.P., Sandberg, M., Kalimo, H., Vuorio, E. and Alitalo, K. (1990) 'Expression of the myc proto-oncogenes in developing human fetal brain', *Oncogene*, 5(12), pp. 1787-97.

Hnisz, D., Abraham, Brian J., Lee, Tong I., Lau, A., Saint-André, V., Sigova, Alla A., Hoke, Heather A. and Young, Richard A. 'Super-Enhancers in the Control of Cell Identity and Disease', *Cell*, 155(4), pp. 934-947.

Hogarty, M.D. (2003) 'The requirement for evasion of programmed cell death in neuroblastomas with MYCN amplification', *Cancer Lett*, 197(1-2), pp. 173-9.

Hogarty, M.D., Norris, M.D., Davis, K., Liu, X., Evageliou, N.F., Hayes, C.S., Pawel, B., Guo, R., Zhao, H., Sekyere, E., Keating, J., Thomas, W., Cheng, N.C., Murray, J., Smith, J., Sutton, R., Venn, N., London, W.B., Buxton, A., Gilmour, S.K., Marshall, G.M. and Haber, M. (2008) 'ODC1 is a critical determinant of MYCN oncogenesis and a therapeutic target in neuroblastoma', *Cancer Res*, 68(23), pp. 9735-45.

Hu, M.C., Lee, D.F., Xia, W., Golfman, L.S., Ou-Yang, F., Yang, J.Y., Zou, Y., Bao, S., Hanada, N., Saso, H., Kobayashi, R. and Hung, M.C. (2004) 'IkappaB kinase promotes tumorigenesis through inhibition of forkhead FOXO3a', *Cell*, 117(2), pp. 225-37.

Huang, H., Regan, K.M., Wang, F., Wang, D., Smith, D.I., van Deursen, J.M. and Tindall, D.J. (2005) 'Skp2 inhibits FOXO1 in tumor suppression through ubiquitin-mediated degradation', *Proc Natl Acad Sci U S A*, 102(5), pp. 1649-54.

Huang, H., Zhao, W. and Yang, D. (2012) 'Stat3 induces oncogenic Skp2 expression in human cervical carcinoma cells', *Biochem Biophys Res Commun*, 418(1), pp. 186-90.

Huang, Y., Shen, X., Zou, Q., Wang, S., Tang, S. and Zhang, G. (2011) 'Biological functions of microRNAs: a review', *Journal of Physiology and Biochemistry*, 67(1), pp. 129-139.

Huang, Y.C. and Hung, W.C. (2006) '1,25-dihydroxyvitamin D3 transcriptionally represses p45Skp2 expression via the Sp1 sites in human prostate cancer cells', *J Cell Physiol*, 209(2), pp. 363-9.

Huber, K. (2006) 'The sympathoadrenal cell lineage: specification, diversification, and new perspectives', *Dev Biol*, 298(2), pp. 335-43.

Huber, K., Combs, S., Ernsberger, U., Kalcheim, C. and Unsicker, K. (2002) 'Generation of neuroendocrine chromaffin cells from sympathoadrenal

progenitors: beyond the glucocorticoid hypothesis', *Ann N Y Acad Sci*, 971, pp. 554-9.
Imaki, H., Nakayama, K., Delehouzee, S., Handa, H., Kitagawa, M., Kamura, T. and Nakayama, K.I. (2003) 'Cell cycle-dependent regulation of the Skp2 promoter by GA-binding protein', *Cancer Res*, 63(15), pp. 4607-13.
Ingvarsson, S., Asker, C., Axelson, H., Klein, G. and Sumegi, J. (1988) 'Structure and expression of B-myc, a new member of the myc gene family', *Molecular and Cellular Biology*, 8(8), pp. 3168-3174.
Inuzuka, H., Gao, D., Finley, L.W., Yang, W., Wan, L., Fukushima, H., Chin, Y.R., Zhai, B., Shaik, S., Lau, A.W., Wang, Z., Gygi, S.P., Nakayama, K., Teruya-Feldstein, J., Toker, A., Haigis, M.C., Pandolfi, P.P. and Wei, W. (2012) 'Acetylation-dependent regulation of Skp2 function', *Cell*, 150(1), pp. 179-93.
Iraci, N., Diolaiti, D., Papa, A., Porro, A., Valli, E., Gherardi, S., Herold, S., Eilers, M., Bernardoni, R., Della Valle, G. and Perini, G. (2011) 'A SP1/MIZ1/MYCN repression complex recruits HDAC1 at the TRKA and p75NTR promoters and affects neuroblastoma malignancy by inhibiting the cell response to NGF', *Cancer Res*, 71(2), pp. 404-12.
Irwin, M., Marin, M.C., Phillips, A.C., Seelan, R.S., Smith, D.I., Liu, W., Flores, E.R., Tsai, K.Y., Jacks, T., Vousden, K.H. and Kaelin Jr, W.G. (2000) 'Role for the p53 homologue p73 in E2F-1-induced apoptosis', *Nature*, 407(6804), pp. 645-648.
Iwahara, T., Fujimoto, J., Wen, D., Cupples, R., Bucay, N., Arakawa, T., Mori, S., Ratzkin, B. and Yamamoto, T. (1997) 'Molecular characterization of ALK, a receptor tyrosine kinase expressed specifically in the nervous system', *Oncogene*, 14(4), pp. 439-49.
James, M.K., Ray, A., Leznova, D. and Blain, S.W. (2008) 'Differential modification of p27Kip1 controls its cyclin D-cdk4 inhibitory activity', *Mol Cell Biol*, 28(1), pp. 498-510.
Janoueix-Lerosey, I., Lequin, D., Brugieres, L., Ribeiro, A., de Pontual, L., Combaret, V., Raynal, V., Puisieux, A., Schleiermacher, G., Pierron, G., Valteau-Couanet, D., Frebourg, T., Michon, J., Lyonnet, S., Amiel, J. and Delattre, O. (2008) 'Somatic and germline activating mutations of the ALK kinase receptor in neuroblastoma', *Nature*, 455(7215), pp. 967-70.
Jeffers, J.R., Parganas, E., Lee, Y., Yang, C., Wang, J., Brennan, J., MacLean, K.H., Han, J., Chittenden, T., Ihle, J.N., McKinnon, P.J., Cleveland, J.L. and Zambetti, G.P. (2003) 'Puma is an essential mediator of p53-dependent and -independent apoptotic pathways', *Cancer Cell*, 4(4), pp. 321-8.
Ji, P., Goldin, L., Ren, H., Sun, D., Guardavaccaro, D., Pagano, M. and Zhu, L. (2006) 'Skp2 contains a novel cyclin A binding domain that directly protects cyclin A from inhibition by p27Kip1', *J Biol Chem*, 281(33), pp. 24058-69.
Ji, P., Jiang, H., Rekhtman, K., Bloom, J., Ichetovkin, M., Pagano, M. and Zhu, L. (2004) 'An Rb-Skp2-p27 Pathway Mediates Acute Cell Cycle Inhibition by Rb and Is Retained in a Partial-Penetrance Rb Mutant', *Molecular Cell*, 16(1), pp. 47-58.
Ji, P., Sun, D., Wang, H., Bauzon, F. and Zhu, L. (2007) 'Disrupting Skp2-cyclin A interaction with a blocking peptide induces selective cancer cell killing', *Mol Cancer Ther*, 6(2), pp. 684-91.
Jiang, F., Caraway, N.P., Li, R. and Katz, R.L. (2005a) 'RNA silencing of S-phase kinase-interacting protein 2 inhibits proliferation and centrosome amplification in lung cancer cells', *Oncogene*, 24(21), pp. 3409-18.

Jiang, H., Chang, F.C., Ross, A.E., Lee, J., Nakayama, K., Nakayama, K. and Desiderio, S. (2005b) 'Ubiquitylation of RAG-2 by Skp2-SCF links destruction of the V(D)J recombinase to the cell cycle', *Mol Cell*, 18(6), pp. 699-709.

Kamura, T., Hara, T., Kotoshiba, S., Yada, M., Ishida, N., Imaki, H., Hatakeyama, S., Nakayama, K. and Nakayama, K.I. (2003) 'Degradation of p57Kip2 mediated by SCFSkp2-dependent ubiquitylation', *Proc Natl Acad Sci U S A*, 100(18), pp. 10231-6.

Kamura, T., Hara, T., Matsumoto, M., Ishida, N., Okumura, F., Hatakeyama, S., Yoshida, M., Nakayama, K. and Nakayama, K.I. (2004) 'Cytoplasmic ubiquitin ligase KPC regulates proteolysis of p27(Kip1) at G1 phase', *Nat Cell Biol*, 6(12), pp. 1229-35.

Katase, N., Lefeuvre, M., Tsujigiwa, H., Fujii, M., Ito, S., Tamamura, R., Buery, R.R., Gunduz, M. and Nagatsuka, H. (2013) 'Knockdown of Dkk-3 decreases cancer cell migration and invasion independently of the Wnt pathways in oral squamous cell carcinomaderived cells', *Oncol Rep*, 29(4), pp. 1349-55.

Katayose, Y., Kim, M., Rakkar, A.N., Li, Z., Cowan, K.H. and Seth, P. (1997) 'Promoting apoptosis: a novel activity associated with the cyclin-dependent kinase inhibitor p27', *Cancer Res*, 57(24), pp. 5441-5.

Kato, G.J., Barrett, J., Villa-Garcia, M. and Dang, C.V. (1990) 'An amino-terminal c-Myc domain required for neoplastic transformation activates transcription', *Molecular and Cellular Biology*, 10(11), pp. 5914-5920.

Keller, U.B., Old, J.B., Dorsey, F.C., Nilsson, J.A., Nilsson, L., MacLean, K.H., Chung, L., Yang, C., Spruck, C., Boyd, K., Reed, S.I. and Cleveland, J.L. (2007) 'Myc targets Cks1 to provoke the suppression of p27Kip1, proliferation and lymphomagenesis', *EMBO J*, 26(10), pp. 2562-74.

Kenney, A.M., Widlund, H.R. and Rowitch, D.H. (2004) 'Hedgehog and PI-3 kinase signaling converge on Nmyc1 to promote cell cycle progression in cerebellar neuronal precursors', *Development*, 131(1), pp. 217-228.

Kim, J.Y., Kim, H.J., Park, J.H., Park, D.I., Cho, Y.K., Sohn, C.I., Jeon, W.K., Kim, B.I., Kim, D.H., Chae, S.W. and Sohn, J.H. (2014) 'Epidermal growth factor upregulates Skp2/Cks1 and p27(kip1) in human extrahepatic cholangiocarcinoma cells', *World J Gastroenterol*, 20(3), pp. 755-73.

Kim, S.Y., Herbst, A., Tworkowski, K.A., Salghetti, S.E. and Tansey, W.P. (2003) 'Skp2 regulates Myc protein stability and activity', *Mol Cell*, 11(5), pp. 1177-88.

Kitagawa, M., Higashi, H., Suzuki-Takahashi, I., Segawa, K., Hanks, S.K., Taya, Y., Nishimura, S. and Okuyama, A. (1995) 'Phosphorylation of E2F-1 by cyclin A-cdk2', *Oncogene*, 10(2), pp. 229-36.

Kitagawa, M., Lee, S.H. and McCormick, F. (2008) 'Skp2 suppresses p53-dependent apoptosis by inhibiting p300', *Mol Cell*, 29(2), pp. 217-31.

Klebe, G. (2006) 'Virtual ligand screening: strategies, perspectives and limitations', *Drug Discovery Today*, 11(13–14), pp. 580-594.

Knoepfler, P.S., Cheng, P.F. and Eisenman, R.N. (2002) 'N-myc is essential during neurogenesis for the rapid expansion of progenitor cell populations and the inhibition of neuronal differentiation', *Genes Dev*, 16(20), pp. 2699-712.

Knudson, A.G., Jr. and Strong, L.C. (1972) 'Mutation and cancer: neuroblastoma and pheochromocytoma', *Am J Hum Genet*, 24(5), pp. 514-32.

Kohl, N.E., Legouy, E., DePinho, R.A., Nisen, P.D., Smith, R.K., Gee, C.E. and Alt, F.W. (1986) 'Human N-myc is closely related in organization and nucleotide sequence to c-myc', *Nature*, 319(6048), pp. 73-7.

Koivomagi, M., Ord, M., Iofik, A., Valk, E., Venta, R., Faustova, I., Kivi, R., Balog, E.R., Rubin, S.M. and Loog, M. (2013) 'Multisite phosphorylation networks as signal processors for Cdk1', *Nat Struct Mol Biol*, 20(12), pp. 1415-24.

Koivomagi, M., Valk, E., Venta, R., Iofik, A., Lepiku, M., Balog, E.R., Rubin, S.M., Morgan, D.O. and Loog, M. (2011) 'Cascades of multisite phosphorylation control Sic1 destruction at the onset of S phase', *Nature*, 480(7375), pp. 128-31.

Koomoa, D.L., Geerts, D., Lange, I., Koster, J., Pegg, A.E., Feith, D.J. and Bachmann, A.S. (2013) 'DFMO/eflornithine inhibits migration and invasion downstream of MYCN and involves p27Kip1 activity in neuroblastoma', *Int J Oncol*, 42(4), pp. 1219-28.

Koppen, A., Ait-Aissa, R., Hopman, S., Koster, J., Haneveld, F., Versteeg, R. and Valentijn, L.J. (2007) 'Dickkopf-1 is down-regulated by MYCN and inhibits neuroblastoma cell proliferation', *Cancer Lett*, 256(2), pp. 218-28.

Kossatz, U., Dietrich, N., Zender, L., Buer, J., Manns, M.P. and Malek, N.P. (2004) 'Skp2-dependent degradation of p27kip1 is essential for cell cycle progression', *Genes Dev*, 18(21), pp. 2602-7.

Kroemer, G., Zamzami, N. and Susin, S.A. (1997) 'Mitochondrial control of apoptosis', *Immunol Today*, 18(1), pp. 44-51.

Krueger, U., Bergauer, T., Kaufmann, B., Wolter, I., Pilk, S., Heider-Fabian, M., Kirch, S., Artz-Oppitz, C., Isselhorst, M. and Konrad, J. (2007) 'Insights into effective RNAi gained from large-scale siRNA validation screening', *Oligonucleotides*, 17(2), pp. 237-50.

Kumps, C., Fieuw, A., Mestdagh, P., Menten, B., Lefever, S., Pattyn, F., De Brouwer, S., Sante, T., Schulte, J.H., Schramm, A., Van Roy, N., Van Maerken, T., Noguera, R., Combaret, V., Devalck, C., Westermann, F., Laureys, G., Eggert, A., Vandesompele, J., De Preter, K. and Speleman, F. (2013) 'Focal DNA copy number changes in neuroblastoma target MYCN regulated genes', *PLoS One*, 8(1), p. e52321.

Kundu, T.K. and Rao, M.R.S. (1999) 'CpG islands in chromatin organization and gene expression', *Journal of Biochemistry*, 125(2), pp. 217-222.

Kuphal, S., Lodermeyer, S., Bataille, F., Schuierer, M., Hoang, B.H. and Bosserhoff, A.K. (2006) 'Expression of Dickkopf genes is strongly reduced in malignant melanoma', *Oncogene*, 25(36), pp. 5027-36.

Kurland, J.F. and Tansey, W.P. (2004) 'Crashing waves of destruction: The cell cycle and APCCdh1 regulation of SCFSkp2', *Cancer Cell*, 5(4), pp. 305-306.

Kushner, B.H., Kramer, K., Modak, S., Qin, L.X. and Cheung, N.K. (2010) 'Differential impact of high-dose cyclophosphamide, topotecan, and vincristine in clinical subsets of patients with chemoresistant neuroblastoma', *Cancer*, 116(12), pp. 3054-60.

Lane, D.P. (1992) 'Cancer. p53, guardian of the genome', *Nature*, 358(6381), pp. 15-6.

Larrea, M.D., Liang, J., Da Silva, T., Hong, F., Shao, S.H., Han, K., Dumont, D. and Slingerland, J.M. (2008) 'Phosphorylation of p27Kip1 regulates assembly and activation of cyclin D1-Cdk4', *Mol Cell Biol*, 28(20), pp. 6462-72.

Lasorella, A., Iavarone, A. and Israel, M.A. (1996) 'Id2 specifically alters regulation of the cell cycle by tumor suppressor proteins', *Mol Cell Biol*, 16(6), pp. 2570-8.

Lastowska, M., Roberts, P., Pearson, A.D., Lewis, I., Wolstenholme, J. and Bown, N. (1997) 'Promiscuous translocations of chromosome arm 17q in human neuroblastomas', *Genes Chromosomes Cancer*, 19(3), pp. 143-9.

Li, W., Bengtson, M.H., Ulbrich, A., Matsuda, A., Reddy, V.A., Orth, A., Chanda, S.K., Batalov, S. and Joazeiro, C.A. (2008) 'Genome-wide and functional annotation of human E3 ubiquitin ligases identifies MULAN, a mitochondrial E3 that regulates the organelle's dynamics and signaling', *PLoS One*, 3(1), p. e1487.

Li, X., Zhao, Q., Liao, R., Sun, P. and Wu, X. (2003) 'The SCF(Skp2) ubiquitin ligase complex interacts with the human replication licensing factor Cdt1 and regulates Cdt1 degradation', *J Biol Chem*, 278(33), pp. 30854-8.

Lill, N.L., Grossman, S.R., Ginsberg, D., DeCaprio, J. and Livingston, D.M. (1997) 'Binding and modulation of p53 by p300/CBP coactivators', *Nature*, 387(6635), pp. 823-7.

Lin, C.H., Guo, Y., Ghaffar, S., McQueen, P., Pourmorady, J., Christ, A., Rooney, K., Ji, T., Eskander, R., Zi, X. and Hoang, B.H. (2013) 'Dkk-3, a secreted wnt antagonist, suppresses tumorigenic potential and pulmonary metastasis in osteosarcoma', *Sarcoma*, 2013, p. 147541.

Lin, C.Y., Loven, J., Rahl, P.B., Paranal, R.M., Burge, C.B., Bradner, J.E., Lee, T.I. and Young, R.A. (2012) 'Transcriptional amplification in tumor cells with elevated c-Myc', *Cell*, 151(1), pp. 56-67.

Lin, H.-K., Chen, Z., Wang, G., Nardella, C., Lee, S.-W., Chan, C.-H., Yang, W.-L., Wang, J., Egia, A., Nakayama, K.I., Cordon-Cardo, C., Teruya-Feldstein, J. and Pandolfi, P.P. 'Skp2 targeting suppresses tumorigenesis by Arf-p53-independent cellular senescence', *Nature*, 464(7287), pp. 374-379.

Lin, H.K., Chen, Z., Wang, G., Nardella, C., Lee, S.W., Chan, C.H., Yang, W.L., Wang, J., Egia, A., Nakayama, K.I., Cordon-Cardo, C., Teruya-Feldstein, J. and Pandolfi, P.P. (2010a) 'Skp2 targeting suppresses tumorigenesis by Arf-p53-independent cellular senescence', *Nature*, 464(7287), pp. 374-9.

Lin, H.K., Wang, G., Chen, Z., Teruya-Feldstein, J., Liu, Y., Chan, C.H., Yang, W.L., Erdjument-Bromage, H., Nakayama, K.I., Nimer, S., Tempst, P. and Pandolfi, P.P. (2009) 'Phosphorylation-dependent regulation of cytosolic localization and oncogenic function of Skp2 by Akt/PKB', *Nat Cell Biol*, 11(4), pp. 420-32.

Lin, R.J., Lin, Y.C., Chen, J., Kuo, H.H., Chen, Y.Y., Diccianni, M.B., London, W.B., Chang, C.H. and Yu, A.L. (2010b) 'microRNA signature and expression of Dicer and Drosha can predict prognosis and delineate risk groups in neuroblastoma', *Cancer Res*, 70(20), pp. 7841-50.

Lipinski, C.A., Lombardo, F., Dominy, B.W. and Feeney, P.J. (2001) 'Experimental and computational approaches to estimate solubility and permeability in drug discovery and development settings', *Adv Drug Deliv Rev*, 46(1-3), pp. 3-26.

Lisztwan, J., Marti, A., Sutterlüty, H., Gstaiger, M., Wirbelauer, C. and Krek, W. (1998) 'Association of human CUL-1 and ubiquitin-conjugating enzyme CDC34 with the F-box protein p45(SKP2): Evidence for evolutionary conservation in the subunit composition of the CDC34-SCF pathway', *EMBO Journal*, 17(2), pp. 368-383.

Littlewood, T.D., Hancock, D.C., Danielian, P.S., Parker, M.G. and Evan, G.I. (1995) 'A modified oestrogen receptor ligand-binding domain as an improved switch for the regulation of heterologous proteins', *Nucleic Acids Res*, 23(10), pp. 1686-90.

Liu, J., Furukawa, M., Matsumoto, T. and Xiong, Y. (2002) 'NEDD8 Modification of CUL1 Dissociates p120CAND1, an Inhibitor of CUL1-SKP1 Binding and SCF Ligases', *Molecular Cell*, 10(6), pp. 1511-1518.

Liu, T., Tee, A.E.L., Porro, A., Smith, S.A., Dwarte, T., Liu, P.Y., Iraci, N., Sekyere, E., Haber, M., Norris, M.D., Diolaiti, D., Della Valle, G., Perini, G. and Marshall, G.M. (2007) 'Activation of tissue transglutaminase transcription by histone deacetylase inhibition as a therapeutic approach for Myc oncogenesis', *Proceedings of the National Academy of Sciences*, 104(47), pp. 18682-18687.

Liu, Y., Hedvat, C.V., Mao, S., Zhu, X.H., Yao, J., Nguyen, H., Koff, A. and Nimer, S.D. (2006) 'The ETS protein MEF is regulated by phosphorylation-dependent proteolysis via the protein-ubiquitin ligase SCFSkp2', *Mol Cell Biol*, 26(8), pp. 3114-23.

Look, A.T., Hayes, F.A., Nitschke, R., McWilliams, N.B. and Green, A.A. (1984) 'Cellular DNA content as a predictor of response to chemotherapy in infants with unresectable neuroblastoma', *N Engl J Med*, 311(4), pp. 231-5.

Lundberg, A.S. and Weinberg, R.A. (1998) 'Functional inactivation of the retinoblastoma protein requires sequential modification by at least two distinct cyclin-cdk complexes', *Mol Cell Biol*, 18(2), pp. 753-61.

Lutz, W., Stohr, M., Schurmann, J., Wenzel, A., Lohr, A. and Schwab, M. (1996) 'Conditional expression of N-myc in human neuroblastoma cells increases expression of alpha-prothymosin and ornithine decarboxylase and accelerates progression into S-phase early after mitogenic stimulation of quiescent cells', *Oncogene*, 13(4), pp. 803-12.

Lydeard, J.R., Schulman, B.A. and Harper, J.W. (2013) 'Building and remodelling Cullin-RING E3 ubiquitin ligases', *EMBO Rep*, 14(12), pp. 1050-61.

Maestro, R., Dei Tos, A.P., Hamamori, Y., Krasnokutsky, S., Sartorelli, V., Kedes, L., Doglioni, C., Beach, D.H. and Hannon, G.J. (1999) 'Twist is a potential oncogene that inhibits apoptosis', *Genes Dev*, 13(17), pp. 2207-17.

Majello, B., Napolitano, G., Giordano, A. and Lania, L. (1999) 'Transcriptional regulation by targeted recruitment of cyclin-dependent CDK9 kinase in vivo', *Oncogene*, 18(32), pp. 4598-605.

Malumbres, M. and Barbacid, M. (2005) 'Mammalian cyclin-dependent kinases', *Trends Biochem Sci*, 30(11), pp. 630-41.

Malumbres, M., Harlow, E., Hunt, T., Hunter, T., Lahti, J.M., Manning, G., Morgan, D.O., Tsai, L.-H. and Wolgemuth, D.J. (2009) 'Cyclin-dependent kinases: a family portrait', *Nat Cell Biol*, 11(11), pp. 1275-1276.

Malynn, B.A., de Alboran, I.M., O'Hagan, R.C., Bronson, R., Davidson, L., DePinho, R.A. and Alt, F.W. (2000) 'N-myc can functionally replace c-myc in murine development, cellular growth, and differentiation', *Genes Dev*, 14(11), pp. 1390-9.

Mamillapalli, R., Gavrilova, N., Mihaylova, V.T., Tsvetkov, L.M., Wu, H., Zhang, H. and Sun, H. (2001) 'PTEN regulates the ubiquitin-dependent degradation of the CDK inhibitor p27KIP1 through the ubiquitin E3 ligase SCFSKP2', *Current Biology*, 11(4), pp. 263-267.

Maris, J.M. (2010) 'Recent advances in neuroblastoma', *N Engl J Med*, 362(23), pp. 2202-11.

Maris, J.M., Hogarty, M.D., Bagatell, R. and Cohn, S.L. (2007) 'Neuroblastoma', *The Lancet*, 369(9579), pp. 2106-2120.

Maris, J.M., Mosse, Y.P., Bradfield, J.P., Hou, C., Monni, S., Scott, R.H., Asgharzadeh, S., Attiyeh, E.F., Diskin, S.J., Laudenslager, M., Winter, C., Cole, K.A., Glessner, J.T., Kim, C., Frackelton, E.C., Casalunovo, T., Eckert, A.W., Capasso, M., Rappaport, E.F., McConville, C., London, W.B., Seeger, R.C., Rahman, N., Devoto, M., Grant, S.F., Li, H. and Hakonarson, H. (2008) 'Chromosome 6p22 locus associated with clinically aggressive neuroblastoma', *N Engl J Med*, 358(24), pp. 2585-93.

Maris, J.M., Weiss, M.J., Guo, C., Gerbing, R.B., Stram, D.O., White, P.S., Hogarty, M.D., Sulman, E.P., Thompson, P.M., Lukens, J.N., Matthay, K.K., Seeger, R.C. and Brodeur, G.M. (2000) 'Loss of heterozygosity at 1p36 independently predicts for disease progression but not decreased overall survival probability in neuroblastoma patients: a Children's Cancer Group study', *J Clin Oncol*, 18(9), pp. 1888-99.

Marti, A., Wirbelauer, C., Scheffner, M. and Krek, W. (1999) 'Interaction between ubiquitin-protein ligase SCFSKP2 and E2F-1 underlies the regulation of E2F-1 degradation', *Nat Cell Biol*, 1(1), pp. 14-9.

Martínez-Cerdeño, V., Lemen, J.M., Chan, V., Wey, A., Lin, W., Dent, S.R. and Knoepfler, P.S. (2012) 'N-Myc and GCN5 Regulate Significantly Overlapping Transcriptional Programs in Neural Stem Cells', *PLoS ONE*, 7(6), p. e39456.

Masuda, A., Osada, H., Yatabe, Y., Kozaki, K., Tatematsu, Y., Takahashi, T., Hida, T., Takahashi, T. and Takahashi, T. (2001) 'Protective function of p27(KIP1) against apoptosis in small cell lung cancer cells in unfavorable microenvironments', *Am J Pathol*, 158(1), pp. 87-96.

Matsuo, T., Seth, P. and Thiele, C.J. (2001) 'Increased expression of p27Kip1 arrests neuroblastoma cell growth', *Med Pediatr Oncol*, 36(1), pp. 97-9.

Mattern, M.R., Wu, J. and Nicholson, B. (2012) 'Ubiquitin-based anticancer therapy: Carpet bombing with proteasome inhibitors vs surgical strikes with E1, E2, E3, or DUB inhibitors', *Biochimica et Biophysica Acta (BBA) - Molecular Cell Research*, 1823(11), pp. 2014-2021.

McGrath, D.A., Balog, E.R.M., Kõivomägi, M., Lucena, R., Mai, M.V., Hirschi, A., Kellogg, D.R., Loog, M. and Rubin, S.M. (2013) 'Cks confers specificity to phosphorylation-dependent CDK signaling pathways', *Nat Struct Mol Biol*, 20(12), pp. 1407-1414.

McMahon, S.B., Van Buskirk, H.A., Dugan, K.A., Copeland, T.D. and Cole, M.D. (1998) 'The Novel ATM-Related Protein TRRAP Is an Essential Cofactor for the c-Myc and E2F Oncoproteins', *Cell*, 94(3), pp. 363-374.

McMahon, S.B., Wood, M.A. and Cole, M.D. (2000) 'The essential cofactor TRRAP recruits the histone acetyltransferase hGCN5 to c-Myc', *Mol Cell Biol*, 20(2), pp. 556-62.

Mendez, J., Zou-Yang, X.H., Kim, S.Y., Hidaka, M., Tansey, W.P. and Stillman, B. (2002) 'Human origin recognition complex large subunit is degraded by ubiquitin-mediated proteolysis after initiation of DNA replication', *Mol Cell*, 9(3), pp. 481-91.

Mishra, A., Godavarthi, S.K. and Jana, N.R. (2009) 'UBE3A/E6-AP regulates cell proliferation by promoting proteasomal degradation of p27', *Neurobiol Dis*, 36(1), pp. 26-34.

Mitra, J. and Enders, G.H. (2004) 'Cyclin A/Cdk2 complexes regulate activation of Cdk1 and Cdc25 phosphatases in human cells', *Oncogene*, 23(19), pp. 3361-7.

Molenaar, J.J., Ebus, M.E., Geerts, D., Koster, J., Lamers, F., Valentijn, L.J., Westerhout, E.M., Versteeg, R. and Caron, H.N. (2009) 'Inactivation of CDK2 is synthetically lethal to MYCN over-expressing cancer cells', *Proceedings of the National Academy of Sciences*, 106(31), pp. 12968-12973.

Monclair, T., Brodeur, G.M., Ambros, P.F., Brisse, H.J., Cecchetto, G., Holmes, K., Kaneko, M., London, W.B., Matthay, K.K., Nuchtern, J.G., von Schweinitz, D., Simon, T., Cohn, S.L. and Pearson, A.D. (2009) 'The International Neuroblastoma Risk Group (INRG) staging system: an INRG Task Force report', *J Clin Oncol*, 27(2), pp. 298-303.

Montagnoli, A., Fiore, F., Eytan, E., Carrano, A.C., Draetta, G.F., Hershko, A. and Pagano, M. (1999a) 'Ubiquitination of p27 is regulated by Cdk-dependent phosphorylation and trimeric complex formation', *Genes and Development*, 13(9), pp. 1181-1189.

Montagnoli, A., Fiore, F., Eytan, E., Carrano, A.C., Draetta, G.F., Hershko, A. and Pagano, M. (1999b) 'Ubiquitination of p27 is regulated by Cdk-dependent phosphorylation and trimeric complex formation', *Genes Dev*, 13(9), pp. 1181-9.

Moreira, I.S., Fernandes, P.A. and Ramos, M.J. (2007) 'Hot spots--a review of the protein-protein interface determinant amino-acid residues', *Proteins*, 68(4), pp. 803-12.

Moro, L., Arbini, A.A., Marra, E. and Greco, M. (2006) 'Up-regulation of Skp2 after prostate cancer cell adhesion to basement membranes results in BRCA2 degradation and cell proliferation', *J Biol Chem*, 281(31), pp. 22100-7.

Mosse, Y.P., Laudenslager, M., Khazi, D., Carlisle, A.J., Winter, C.L., Rappaport, E. and Maris, J.M. (2004) 'Germline PHOX2B mutation in hereditary neuroblastoma', *Am J Hum Genet*, 75(4), pp. 727-30.

Mosse, Y.P., Laudenslager, M., Longo, L., Cole, K.A., Wood, A., Attiyeh, E.F., Laquaglia, M.J., Sennett, R., Lynch, J.E., Perri, P., Laureys, G., Speleman, F., Kim, C., Hou, C., Hakonarson, H., Torkamani, A., Schork, N.J., Brodeur, G.M., Tonini, G.P., Rappaport, E., Devoto, M. and Maris, J.M. (2008) 'Identification of ALK as a major familial neuroblastoma predisposition gene', *Nature*, 455(7215), pp. 930-5.

Müller, D., Bouchard, C., Rudolph, B., Steiner, P., Stuckmann, I., Saffrich, R., Ansorge, W., Huttner, W. and Eilers, M. (1997) 'Cdk2-dependent phosphorylation of p27 facilitates its MSc-induced release from cyclin E/cdk2 complexes', *Oncogene*, 15(21), pp. 2561-2576.

Munoz, J.P., Sanchez, J.R. and Maccioni, R.B. (2003) 'Regulation of p27 in the process of neuroblastoma N2A differentiation', *J Cell Biochem*, 89(3), pp. 539-49.

Muraji, T., Okamoto, E., Fujimoto, J., Suita, S. and Nakagawara, A. (1993) 'Combined determination of N-myc oncogene amplification and DNA ploidy in neuroblastoma. Complementary prognostic indicators', *Cancer*, 72(9), pp. 2763-8.

Muth, D., Ghazaryan, S., Eckerle, I., Beckett, E., Pöhler, C., Batzler, J., Beisel, C., Gogolin, S., Fischer, M., Henrich, K.-O., Ehemann, V., Gillespie, P., Schwab, M. and Westermann, F. (2010) 'Transcriptional Repression of SKP2 Is Impaired in MYCN-Amplified Neuroblastoma', *Cancer Research*, 70(9), pp. 3791-3802.

Nakagawara, A., Arima-Nakagawara, M., Scavarda, N.J., Azar, C.G., Cantor, A.B. and Brodeur, G.M. (1993) 'Association between high levels of

expression of the TRK gene and favorable outcome in human neuroblastoma', *N Engl J Med*, 328(12), pp. 847-54.
Nakagawara, A. and Ohira, M. (2004) 'Comprehensive genomics linking between neural development and cancer: neuroblastoma as a model', *Cancer Lett*, 204(2), pp. 213-24.
Nakamura, M., Matsuo, T., Stauffer, J., Neckers, L. and Thiele, C.J. (2003) 'Retinoic acid decreases targeting of p27 for degradation via an N-myc-dependent decrease in p27 phosphorylation and an N-myc-independent decrease in Skp2', *Cell Death Differ*, 10(2), pp. 230-239.
Nakayama, K.-I., Hatakeyama, S. and Nakayama, K. (2001) 'Regulation of the Cell Cycle at the G1–S Transition by Proteolysis of Cyclin E and p27Kip1', *Biochemical and Biophysical Research Communications*, 282(4), pp. 853-860.
Nakayama, K., Ishida, N., Shirane, M., Inomata, A., Inoue, T., Shishido, N., Horii, I., Loh, D.Y. and Nakayama, K. (1996) 'Mice lacking p27(Kip1) display increased body size, multiple organ hyperplasia, retinal dysplasia, and pituitary tumors', *Cell*, 85(5), pp. 707-20.
Nakayama, K., Nagahama, H., Minamishima, Y.A., Matsumoto, M., Nakamichi, I., Kitagawa, K., Shirane, M., Tsunematsu, R., Tsukiyama, T., Ishida, N., Kitagawa, M., Nakayama, K. and Hatakeyama, S. (2000) 'Targeted disruption of Skp2 results in accumulation of cyclin E and p27(Kip1), polyploidy and centrosome overduplication', *EMBO J*, 19(9), pp. 2069-81.
Nakayama, K., Nagahama, H., Minamishima, Y.A., Miyake, S., Ishida, N., Hatakeyama, S., Kitagawa, M., Iemura, S., Natsume, T. and Nakayama, K.I. (2004) 'Skp2-mediated degradation of p27 regulates progression into mitosis', *Dev Cell*, 6(5), pp. 661-72.
Nakayama, K.I. and Nakayama, K. (2006a) 'Ubiquitin ligases: cell-cycle control and cancer', *Nat Rev Cancer*, 6(5), pp. 369-381.
Nakayama, K.I. and Nakayama, K. (2006b) 'Ubiquitin ligases: cell-cycle control and cancer', *Nat Rev Cancer*, 6(5), pp. 369-81.
Nakazawa, M. (1993) 'The prognostic significance of DNA ploidy for neuroblastoma', *Surg Today*, 23(3), pp. 215-9.
Nero, T.L., Morton, C.J., Holien, J.K., Wielens, J. and Parker, M.W. (2014) 'Oncogenic protein interfaces: small molecules, big challenges', *Nat Rev Cancer*, 14(4), pp. 248-262.
Nesbit, C.E., Tersak, J.M. and Prochownik, E.V. (1999) 'MYC oncogenes and human neoplastic disease', *Oncogene*, 18(19), pp. 3004-16.
Nie, Z., Hu, G., Wei, G., Cui, K., Yamane, A., Resch, W., Wang, R., Green, Douglas R., Tessarollo, L., Casellas, R., Zhao, K. and Levens, D. 'c-Myc Is a Universal Amplifier of Expressed Genes in Lymphocytes and Embryonic Stem Cells', *Cell*, 151(1), pp. 68-79.
O'Neill, S., Ekstrom, L., Lastowska, M., Roberts, P., Brodeur, G.M., Kees, U.R., Schwab, M. and Bown, N. (2001) 'MYCN amplification and 17q in neuroblastoma: evidence for structural association', *Genes Chromosomes Cancer*, 30(1), pp. 87-90.
Ohira, M., Oba, S., Nakamura, Y., Hirata, T., Ishii, S. and Nakagawara, A. (2005) 'A review of DNA microarray analysis of human neuroblastomas', *Cancer Lett*, 228(1-2), pp. 5-11.
Old, J.B., Kratzat, S., Hoellein, A., Graf, S., Nilsson, J.A., Nilsson, L., Nakayama, K.I., Peschel, C., Cleveland, J.L. and Keller, U.B. (2010) 'Skp2 directs Myc-mediated suppression of p27Kip1 yet has modest effects on Myc-driven lymphomagenesis', *Mol Cancer Res*, 8(3), pp. 353-62.

Opel, D., Poremba, C., Simon, T., Debatin, K.M. and Fulda, S. (2007) 'Activation of Akt predicts poor outcome in neuroblastoma', *Cancer Res*, 67(2), pp. 735-45.

Ora, I. and Eggert, A. (2011) 'Progress in treatment and risk stratification of neuroblastoma: impact on future clinical and basic research', *Semin Cancer Biol*, 21(4), pp. 217-28.

Ott, C.J., Kopp, N., Bird, L., Paranal, R.M., Qi, J., Bowman, T., Rodig, S.J., Kung, A.L., Bradner, J.E. and Weinstock, D.M. (2012) 'BET bromodomain inhibition targets both c-Myc and IL7R in high-risk acute lymphoblastic leukemia', *Blood*, 120(14), pp. 2843-52.

Otto, T., Horn, S., Brockmann, M., Eilers, U., Schüttrumpf, L., Popov, N., Kenney, A.M., Schulte, J.H., Beijersbergen, R., Christiansen, H., Berwanger, B. and Eilers, M. (2009) 'Stabilization of N-Myc Is a Critical Function of Aurora A in Human Neuroblastoma', *Cancer Cell*, 15(1), pp. 67-78.

Park, M.S., Rosai, J., Nguyen, H.T., Capodieci, P., Cordon-Cardo, C. and Koff, A. (1999) 'p27 and Rb are on overlapping pathways suppressing tumorigenesis in mice', *Proc Natl Acad Sci U S A*, 96(11), pp. 6382-7.

Pastorino, J.G., Chen, S.T., Tafani, M., Snyder, J.W. and Farber, J.L. (1998) 'The overexpression of Bax produces cell death upon induction of the mitochondrial permeability transition', *J Biol Chem*, 273(13), pp. 7770-5.

Penas, C., Ramachandran, V. and Ayad, N.G. (2011) 'The APC/C Ubiquitin Ligase: From Cell Biology to Tumorigenesis', *Front Oncol*, 1, p. 60.

Peng, J., Zhu, Y., Milton, J.T. and Price, D.H. (1998) 'Identification of multiple cyclin subunits of human P-TEFb', *Genes Dev*, 12(5), pp. 755-62.

Perry, J. and Kornbluth, S. (2007) 'Cdc25 and Wee1: analogous opposites?', *Cell Division*, 2(1), p. 12.

Petroni, M., Veschi, V., Gulino, A. and Giannini, G. (2012) 'Molecular mechanisms of MYCN-dependent apoptosis and the MDM2-p53 pathway: an Achille's heel to be exploited for the therapy of MYCN-amplified neuroblastoma', *Front Oncol*, 2, p. 141.

Petroni, M., Veschi, V., Prodosmo, A., Rinaldo, C., Massimi, I., Carbonari, M., Dominici, C., McDowell, H.P., Rinaldi, C., Screpanti, I., Frati, L., Bartolazzi, A., Gulino, A., Soddu, S. and Giannini, G. (2011) 'MYCN sensitizes human neuroblastoma to apoptosis by HIPK2 activation through a DNA damage response', *Mol Cancer Res*, 9(1), pp. 67-77.

Petroski, M.D. and Deshaies, R.J. (2005) 'Function and regulation of cullin-RING ubiquitin ligases', *Nat Rev Mol Cell Biol*, 6(1), pp. 9-20.

Philipp-Staheli, J., Payne, S.R. and Kemp, C.J. (2001) 'p27(Kip1): regulation and function of a haploinsufficient tumor suppressor and its misregulation in cancer', *Exp Cell Res*, 264(1), pp. 148-68.

Pines, J. (1994) 'The cell cycle kinases', *Semin Cancer Biol*, 5(4), pp. 305-13.

Pirity, M., Blanck, J.K. and Schreiber-Agus, N. (2006) 'Lessons learned from Myc/Max/Mad knockout mice', *Curr Top Microbiol Immunol*, 302, pp. 205-34.

Prochownik, E.V. and Vogt, P.K. (2010) 'Therapeutic Targeting of Myc', *Genes & Cancer*, 1(6), pp. 650-659.

Pugh, T.J., Morozova, O., Attiyeh, E.F., Asgharzadeh, S., Wei, J.S., Auclair, D., Carter, S.L., Cibulskis, K., Hanna, M., Kiezun, A., Kim, J., Lawrence, M.S., Lichenstein, L., McKenna, A., Pedamallu, C.S., Ramos, A.H., Shefler, E., Sivachenko, A., Sougnez, C., Stewart, C., Ally, A., Birol, I., Chiu, R., Corbett, R.D., Hirst, M., Jackman, S.D., Kamoh, B., Khodabakshi, A.H., Krzywinski, M., Lo, A., Moore, R.A., Mungall, K.L., Qian, J., Tam, A.,

Thiessen, N., Zhao, Y., Cole, K.A., Diamond, M., Diskin, S.J., Mosse, Y.P., Wood, A.C., Ji, L., Sposto, R., Badgett, T., London, W.B., Moyer, Y., Gastier-Foster, J.M., Smith, M.A., Guidry Auvil, J.M., Gerhard, D.S., Hogarty, M.D., Jones, S.J., Lander, E.S., Gabriel, S.B., Getz, G., Seeger, R.C., Khan, J., Marra, M.A., Meyerson, M. and Maris, J.M. (2013) 'The genetic landscape of high-risk neuroblastoma', *Nat Genet*, 45(3), pp. 279-84.

Puissant, A., Frumm, S.M., Alexe, G., Bassil, C.F., Qi, J., Chanthery, Y.H., Nekritz, E.A., Zeid, R., Gustafson, W.C., Greninger, P., Garnett, M.J., McDermott, U., Benes, C.H., Kung, A.L., Weiss, W.A., Bradner, J.E. and Stegmaier, K. (2013) 'Targeting MYCN in neuroblastoma by BET bromodomain inhibition', *Cancer Discov*, 3(3), pp. 308-23.

Qi, Y., Gregory, M.A., Li, Z., Brousal, J.P., West, K. and Hann, S.R. (2004) 'p19ARF directly and differentially controls the functions of c-Myc independently of p53', *Nature*, 431(7009), pp. 712-7.

Radke, S., Pirkmaier, A. and Germain, D. (2005) 'Differential expression of the F-box proteins Skp2 and Skp2B in breast cancer', *Oncogene*, 24(21), pp. 3448-58.

Reichert, M., Saur, D., Hamacher, R., Schmid, R.M. and Schneider, G. (2007) 'Phosphoinositide-3-Kinase Signaling Controls S-Phase Kinase–Associated Protein 2 Transcription via E2F1 in Pancreatic Ductal Adenocarcinoma Cells', *Cancer Research*, 67(9), pp. 4149-4156.

Riley, R.D., Heney, D., Jones, D.R., Sutton, A.J., Lambert, P.C., Abrams, K.R., Young, B., Wailoo, A.J. and Burchill, S.A. (2004) 'A Systematic Review of Molecular and Biological Tumor Markers in Neuroblastoma', *Clinical Cancer Research*, 10(1), pp. 4-12.

Rodier, G., Coulombe, P., Tanguay, P.L., Boutonnet, C. and Meloche, S. (2008) 'Phosphorylation of Skp2 regulated by CDK2 and Cdc14B protects it from degradation by APC(Cdh1) in G1 phase', *EMBO J*, 27(4), pp. 679-91.

Rodier, G., Makris, C., Coulombe, P., Scime, A., Nakayama, K., Nakayama, K.I. and Meloche, S. (2005) 'p107 inhibits G1 to S phase progression by down-regulating expression of the F-box protein Skp2', *J Cell Biol*, 168(1), pp. 55-66.

Rose, A.E., Wang, G., Hanniford, D., Monni, S., Tu, T., Shapiro, R.L., Berman, R.S., Pavlick, A.C., Pagano, M., Darvishian, F., Mazumdar, M., Hernando, E. and Osman, I. (2011) 'Clinical relevance of SKP2 alterations in metastatic melanoma', *Pigment Cell Melanoma Res*, 24(1), pp. 197-206.

Rosenbaum, H., Webb, E., Adams, J.M., Cory, S. and Harris, A.W. (1989) 'N-myc transgene promotes B lymphoid proliferation, elicits lymphomas and reveals cross-regulation with c-myc', *EMBO J*, 8(3), pp. 749-55.

Ross, R.A., Biedler, J.L. and Spengler, B.A. (2003) 'A role for distinct cell types in determining malignancy in human neuroblastoma cell lines and tumors', *Cancer Lett*, 197(1-2), pp. 35-9.

Rounbehler, R.J., Li, W., Hall, M.A., Yang, C., Fallahi, M. and Cleveland, J.L. (2009) 'Targeting ornithine decarboxylase impairs development of MYCN-amplified neuroblastoma', *Cancer Res*, 69(2), pp. 547-53.

Sahai, E. and Marshall, C.J. (2002) 'RHO-GTPases and cancer', *Nat Rev Cancer*, 2(2), pp. 133-142.

Saito-Ohara, F., Imoto, I., Inoue, J., Hosoi, H., Nakagawara, A., Sugimoto, T. and Inazawa, J. (2003) 'PPM1D is a potential target for 17q gain in neuroblastoma', *Cancer Res*, 63(8), pp. 1876-83.

Sakamuro, D. and Prendergast, G.C. (1999) 'New Myc-interacting proteins: a second Myc network emerges', *Oncogene*, 18(19), pp. 2942-54.
Salghetti, S.E., Kim, S.Y. and Tansey, W.P. (1999) 'Destruction of Myc by ubiquitin-mediated proteolysis: Cancer-associated and transforming mutations stabilize Myc', *EMBO Journal*, 18(3), pp. 717-726.
Santo, E.E., Stroeken, P., Sluis, P.V., Koster, J., Versteeg, R. and Westerhout, E.M. (2013) 'FOXO3a is a major target of inactivation by PI3K/AKT signaling in aggressive neuroblastoma', *Cancer Res*, 73(7), pp. 2189-98.
Sarmento, L.M., Huang, H., Limon, A., Gordon, W., Fernandes, J., Tavares, M.J., Miele, L., Cardoso, A.A., Classon, M. and Carlesso, N. (2005) 'Notch1 modulates timing of G1-S progression by inducing SKP2 transcription and p27 Kip1 degradation', *J Exp Med*, 202(1), pp. 157-68.
Schleiermacher, G., Michon, J., Ribeiro, A., Pierron, G., Mosseri, V., Rubie, H., Munzer, C., Benard, J., Auger, N., Combaret, V., Janoueix-Lerosey, I., Pearson, A., Tweddle, D.A., Bown, N., Gerrard, M., Wheeler, K., Noguera, R., Villamon, E., Canete, A., Castel, V., Marques, B., de Lacerda, A., Tonini, G.P., Mazzocco, K., Defferrari, R., de Bernardi, B., di Cataldo, A., van Roy, N., Brichard, B., Ladenstein, R., Ambros, I., Ambros, P., Beiske, K., Delattre, O. and Couturier, J. (2011) 'Segmental chromosomal alterations lead to a higher risk of relapse in infants with MYCN-non-amplified localised unresectable/disseminated neuroblastoma (a SIOPEN collaborative study)', *Br J Cancer*, 105(12), pp. 1940-8.
Schleiermacher, G., Mosseri, V., London, W.B., Maris, J.M., Brodeur, G.M., Attiyeh, E., Haber, M., Khan, J., Nakagawara, A., Speleman, F., Noguera, R., Tonini, G.P., Fischer, M., Ambros, I., Monclair, T., Matthay, K.K., Ambros, P., Cohn, S.L. and Pearson, A.D. (2012) 'Segmental chromosomal alterations have prognostic impact in neuroblastoma: a report from the INRG project', *Br J Cancer*, 107(8), pp. 1418-22.
Schmid, P., Schulz, W.A. and Hameister, H. (1989) 'Dynamic expression pattern of the myc protooncogene in midgestation mouse embryos', *Science*, 243(4888), pp. 226-9.
Schneider, G., Saur, D., Siveke, J.T., Fritsch, R., Greten, F.R. and Schmid, R.M. (2006) 'IKKalpha controls p52/RelB at the skp2 gene promoter to regulate G1- to S-phase progression', *EMBO J*, 25(16), pp. 3801-12.
Schonherr, C., Ruuth, K., Kamaraj, S., Wang, C.L., Yang, H.L., Combaret, V., Djos, A., Martinsson, T., Christensen, J.G., Palmer, R.H. and Hallberg, B. (2012) 'Anaplastic Lymphoma Kinase (ALK) regulates initiation of transcription of MYCN in neuroblastoma cells', *Oncogene*, 31(50), pp. 5193-5200.
Schramm, A., Köster, J., Marschall, T., Martin, M., Schwermer, M., Fielitz, K., Büchel, G., Barann, M., Esser, D., Rosenstiel, P., Rahmann, S., Eggert, A. and Schulte, J.H. (2013) 'Next-generation RNA sequencing reveals differential expression of MYCN target genes and suggests the mTOR pathway as a promising therapy target in MYCN-amplified neuroblastoma', *International Journal of Cancer*, 132(3), pp. E106-E115.
Schulman, B.A., Carrano, A.C., Jeffrey, P.D., Bowen, Z., Kinnucan, E.R., Finnin, M.S., Elledge, S.J., Harper, J.W., Pagano, M. and Pavletich, N.P. (2000) 'Insights into SCF ubiquitin ligases from the structure of the Skp1-Skp2 complex', *Nature*, 408(6810), pp. 381-6.
Schulte, J.H., Lindner, S., Bohrer, A., Maurer, J., De Preter, K., Lefever, S., Heukamp, L., Schulte, S., Molenaar, J., Versteeg, R., Thor, T., Kunkele, A., Vandesompele, J., Speleman, F., Schorle, H., Eggert, A. and

Schramm, A. (2013a) 'MYCN and ALKF1174L are sufficient to drive neuroblastoma development from neural crest progenitor cells', *Oncogene*, 32(8), pp. 1059-65.

Schulte, J.H., Pentek, F., Hartmann, W., Schramm, A., Friedrichs, N., Ora, I., Koster, J., Versteeg, R., Kirfel, J., Buettner, R. and Eggert, A. (2009) 'The low-affinity neurotrophin receptor, p75, is upregulated in ganglioneuroblastoma/ganglioneuroma and reduces tumorigenicity of neuroblastoma cells in vivo', *Int J Cancer*, 124(10), pp. 2488-94.

Schulte, J.H., Schulte, S., Heukamp, L.C., Astrahantseff, K., Stephan, H., Fischer, M., Schramm, A. and Eggert, A. (2013b) 'Targeted Therapy for Neuroblastoma: ALK Inhibitors', *Klin Padiatr*, 225(6), pp. 303-8.

Schwab, M., Alitalo, K., Klempnauer, K.H., Varmus, H.E., Bishop, J.M., Gilbert, F., Brodeur, G., Goldstein, M. and Trent, J. (1983) 'Amplified DNA with limited homology to myc cellular oncogene is shared by human neuroblastoma cell lines and a neuroblastoma tumour', *Nature*, 305(5931), pp. 245-8.

Schwab, M., Varmus, H.E. and Bishop, J.M. (1985a) 'Human N-myc gene contributes to neoplastic transformation of mammalian cells in culture', *Nature*, 316(6024), pp. 160-162.

Schwab, M., Varmus, H.E. and Bishop, J.M. (1985b) 'Human N-myc gene contributes to neoplastic transformation of mammalian cells in culture', *Nature*, 316(6024), pp. 160-2.

Scott, D., Elsden, J., Pearson, A. and Lunec, J. (2003) 'Genes co-amplified with MYCN in neuroblastoma: silent passengers or co-determinants of phenotype?', *Cancer Lett*, 197(1-2), pp. 81-6.

Scott, Daniel C., Sviderskiy, Vladislav O., Monda, Julie K., Lydeard, John R., Cho, Shein E., Harper, J.W. and Schulman, Brenda A. (2014) 'Structure of a RING E3 Trapped in Action Reveals Ligation Mechanism for the Ubiquitin-like Protein NEDD8', *Cell*, 157(7), pp. 1671-1684.

Seeger, R.C., Danon, Y.L., Rayner, S.A. and Hoover, F. (1982) 'Definition of a Thy-1 determinant on human neuroblastoma, glioma, sarcoma, and teratoma cells with a monoclonal antibody', *J Immunol*, 128(2), pp. 983-9.

Segerstrom, L., Baryawno, N., Sveinbjornsson, B., Wickstrom, M., Elfman, L., Kogner, P. and Johnsen, J.I. (2011) 'Effects of small molecule inhibitors of PI3K/Akt/mTOR signaling on neuroblastoma growth in vitro and in vivo', *Int J Cancer*, 129(12), pp. 2958-65.

Sheaff, R.J., Groudine, M., Gordon, M., Roberts, J.M. and Clurman, B.E. (1997) 'Cyclin E-CDK2 is a regulator of p27(Kip1)', *Genes and Development*, 11(11), pp. 1464-1478.

Sherr, C.J. and Roberts, J.M. (1999) 'CDK inhibitors: positive and negative regulators of G1-phase progression', *Genes Dev*, 13(12), pp. 1501-12.

Shimada, H., Ambros, I.M., Dehner, L.P., Hata, J., Joshi, V.V. and Roald, B. (1999) 'Terminology and morphologic criteria of neuroblastic tumors: recommendations by the International Neuroblastoma Pathology Committee', *Cancer*, 86(2), pp. 349-63.

Shimada, H., Chatten, J., Newton, W.A., Jr., Sachs, N., Hamoudi, A.B., Chiba, T., Marsden, H.B. and Misugi, K. (1984) 'Histopathologic prognostic factors in neuroblastic tumors: definition of subtypes of ganglioneuroblastoma and an age-linked classification of neuroblastomas', *J Natl Cancer Inst*, 73(2), pp. 405-16.

Shimada, H., Stram, D.O., Chatten, J., Joshi, V.V., Hachitanda, Y., Brodeur, G.M., Lukens, J.N., Matthay, K.K. and Seeger, R.C. (1995) 'Identification

of subsets of neuroblastomas by combined histopathologic and N-myc analysis', *J Natl Cancer Inst*, 87(19), pp. 1470-6.

Shiota, M., Izumi, H., Onitsuka, T., Miyamoto, N., Kashiwagi, E., Kidani, A., Hirano, G., Takahashi, M., Naito, S. and Kohno, K. (2008) 'Twist and p53 reciprocally regulate target genes via direct interaction', *Oncogene*, 27(42), pp. 5543-53.

Sholler, G.L., Gerner, E.W., Bergendahl, G., LaFleur, B.J., VanderWerff, A., Ashikaga, T., Ferguson, F., Roberts, W., Eslin, D., Kaplan, J., Kraveka, J.M., Mitchell, D., Neville, K., Wada, R., Parikh, N., Sender, L., Higgins, T. and Bachmann, A. (2013) 'Phase I trial of relapsed neuroblastoma with DFMO alone and in combination with etoposide. [abstract]. In: Proceedings of the 104th Annual Meeting of the American Association for Cancer Research', *Cancer Research*, 73.

Signoretti, S., Di Marcotullio, L., Richardson, A., Ramaswamy, S., Isaac, B., Rue, M., Monti, F., Loda, M. and Pagano, M. (2002) 'Oncogenic role of the ubiquitin ligase subunit Skp2 in human breast cancer', *J Clin Invest*, 110(5), pp. 633-41.

Sitry, D., Seeliger, M.A., Ko, T.K., Ganoth, D., Breward, S.E., Itzhaki, L.S., Pagano, M. and Hershko, A. (2002) 'Three different binding sites of Cks1 are required for p27-ubiquitin ligation', *J Biol Chem*, 277(44), pp. 42233-40.

Sjostrom, S.K., Finn, G., Hahn, W.C., Rowitch, D.H. and Kenney, A.M. (2005) 'The Cdk1 complex plays a prime role in regulating N-myc phosphorylation and turnover in neural precursors', *Dev Cell*, 9(3), pp. 327-38.

Skehan, P., Storeng, R., Scudiero, D., Monks, A., McMahon, J., Vistica, D., Warren, J.T., Bokesch, H., Kenney, S. and Boyd, M.R. (1990) 'New colorimetric cytotoxicity assay for anticancer-drug screening', *J Natl Cancer Inst*, 82(13), pp. 1107-12.

Slack, A., Chen, Z., Tonelli, R., Pule, M., Hunt, L., Pession, A. and Shohet, J.M. (2005) 'The p53 regulatory gene MDM2 is a direct transcriptional target of MYCN in neuroblastoma', *Proc Natl Acad Sci U S A*, 102(3), pp. 731-6.

Slack, A.D., Chen, Z., Ludwig, A.D., Hicks, J. and Shohet, J.M. (2007) 'MYCN-directed centrosome amplification requires MDM2-mediated suppression of p53 activity in neuroblastoma cells', *Cancer Res*, 67(6), pp. 2448-55.

Soucy, T.A., Smith, P.G., Milhollen, M.A., Berger, A.J., Gavin, J.M., Adhikari, S., Brownell, J.E., Burke, K.E., Cardin, D.P., Critchley, S., Cullis, C.A., Doucette, A., Garnsey, J.J., Gaulin, J.L., Gershman, R.E., Lublinsky, A.R., McDonald, A., Mizutani, H., Narayanan, U., Olhava, E.J., Peluso, S., Rezaei, M., Sintchak, M.D., Talreja, T., Thomas, M.P., Traore, T., Vyskocil, S., Weatherhead, G.S., Yu, J., Zhang, J., Dick, L.R., Claiborne, C.F., Rolfe, M., Bolen, J.B. and Langston, S.P. (2009) 'An inhibitor of NEDD8-activating enzyme as a new approach to treat cancer', *Nature*, 458(7239), pp. 732-6.

Spencer, C.A. and Groudine, M. (1991) 'Control of c-myc regulation in normal and neoplastic cells', *Adv Cancer Res*, 56, pp. 1-48.

Spitz, R., Hero, B., Ernestus, K. and Berthold, F. (2003a) 'Deletions in chromosome arms 3p and 11q are new prognostic markers in localized and 4s neuroblastoma', *Clin Cancer Res*, 9(1), pp. 52-8.

Spitz, R., Hero, B., Ernestus, K. and Berthold, F. (2003b) 'Gain of distal chromosome arm 17q is not associated with poor prognosis in neuroblastoma', *Clin Cancer Res*, 9(13), pp. 4835-40.

Spitz, R., Hero, B., Simon, T. and Berthold, F. (2006) 'Loss in chromosome 11q identifies tumors with increased risk for metastatic relapses in localized and 4S neuroblastoma', *Clin Cancer Res*, 12(11 Pt 1), pp. 3368-73.

Staller, P., Peukert, K., Kiermaier, A., Seoane, J., Lukas, J., Karsunky, H., Moroy, T., Bartek, J., Massague, J., Hanel, F. and Eilers, M. (2001) 'Repression of p15INK4b expression by Myc through association with Miz-1', *Nat Cell Biol*, 3(4), pp. 392-399.

Stanton, B.R., Perkins, A.S., Tessarollo, L., Sassoon, D.A. and Parada, L.F. (1992) 'Loss of N-myc function results in embryonic lethality and failure of the epithelial component of the embryo to develop', *Genes Dev*, 6(12A), pp. 2235-47.

Stewart, H.J., Horne, G.A., Bastow, S. and Chevassut, T.J. (2013) 'BRD4 associates with p53 in DNMT3A-mutated leukemia cells and is implicated in apoptosis by the bromodomain inhibitor JQ1', *Cancer Med*, 2(6), pp. 826-35.

Storlazzi, C.T., Lonoce, A., Guastadisegni, M.C., Trombetta, D., D'Addabbo, P., Daniele, G., L'Abbate, A., Macchia, G., Surace, C., Kok, K., Ullmann, R., Purgato, S., Palumbo, O., Carella, M., Ambros, P.F. and Rocchi, M. (2010) 'Gene amplification as double minutes or homogeneously staining regions in solid tumors: origin and structure', *Genome Res*, 20(9), pp. 1198-206.

Strieder, V. and Lutz, W. (2003) 'E2F proteins regulate MYCN expression in neuroblastomas', *J Biol Chem*, 278(5), pp. 2983-9.

Suenaga, Y., Islam, S.M., Alagu, J., Kaneko, Y., Kato, M., Tanaka, Y., Kawana, H., Hossain, S., Matsumoto, D., Yamamoto, M., Shoji, W., Itami, M., Shibata, T., Nakamura, Y., Ohira, M., Haraguchi, S., Takatori, A. and Nakagawara, A. (2014) 'NCYM, a Cis-antisense gene of MYCN, encodes a de novo evolved protein that inhibits GSK3beta resulting in the stabilization of MYCN in human neuroblastomas', *PLoS Genet*, 10(1), p. e1003996.

Sugihara, E., Kanai, M., Matsui, A., Onodera, M., Schwab, M. and Miwa, M. (2004) 'Enhanced expression of MYCN leads to centrosome hyperamplification after DNA damage in neuroblastoma cells', *Oncogene*, 23(4), pp. 1005-9.

Sugihara, E., Kanai, M., Saito, S., Nitta, T., Toyoshima, H., Nakayama, K., Nakayama, K.I., Fukasawa, K., Schwab, M., Saya, H. and Miwa, M. (2006) 'Suppression of centrosome amplification after DNA damage depends on p27 accumulation', *Cancer Res*, 66(8), pp. 4020-9.

Sugiyama, A., Kume, A., Nemoto, K., Lee, S.Y., Asami, Y., Nemoto, F., Nishimura, S. and Kuchino, Y. (1989) 'Isolation and characterization of s-myc, a member of the rat myc gene family', *Proceedings of the National Academy of Sciences of the United States of America*, 86(23), pp. 9144-9148.

Sun, Y. (2003) 'Targeting E3 ubiqutin ligases for cancer therapy', *Cancer Biology and Therapy*, 2(6), pp. 621-627.

Sutterluty, H., Chatelain, E., Marti, A., Wirbelauer, C., Senften, M., Muller, U. and Krek, W. (1999) 'p45SKP2 promotes p27Kip1 degradation and induces S phase in quiescent cells', *Nat Cell Biol*, 1(4), pp. 207-14.

Suzuki, T., Bogenmann, E., Shimada, H., Stram, D. and Seeger, R.C. (1993) 'Lack of high-affinity nerve growth factor receptors in aggressive neuroblastomas', *J Natl Cancer Inst*, 85(5), pp. 377-84.

Taguchi, T., Kato, Y., Baba, Y., Nishimura, G., Tanigaki, Y., Horiuchi, C., Mochimatsu, I. and Tsukuda, M. (2004) 'Protein levels of p21, p27, cyclin

E and Bax predict sensitivity to cisplatin and paclitaxel in head and neck squamous cell carcinomas', *Oncol Rep*, 11(2), pp. 421-6.
Takeda, D.Y. and Dutta, A. (2005) 'DNA replication and progression through S phase', 24(17), pp. 2827-2843.
Tanaka, M., Kigasawa, H., Kato, K., Ijiri, R., Nishihira, H., Aida, N., Ohama, Y. and Tanaka, Y. (2010) 'A prospective study of a long-term follow-up of an observation program for neuroblastoma detected by mass screening', *Pediatr Blood Cancer*, 54(4), pp. 573-8.
Tanaka, S., Tajiri, T., Noguchi, S., Shono, K., Ihara, K., Hara, T. and Suita, S. (2004) 'Clinical significance of a highly sensitive analysis for gene dosage and the expression level of MYCN in neuroblastoma', *J Pediatr Surg*, 39(1), pp. 63-8.
Tang, X.X., Zhao, H., Kung, B., Kim, D.Y., Hicks, S.L., Cohn, S.L., Cheung, N.-K., Seeger, R.C., Evans, A.E. and Ikegaki, N. (2006a) 'The MYCN Enigma: Significance of MYCN Expression in Neuroblastoma', *Cancer Research*, 66(5), pp. 2826-2833.
Tang, X.X., Zhao, H., Kung, B., Kim, D.Y., Hicks, S.L., Cohn, S.L., Cheung, N.K., Seeger, R.C., Evans, A.E. and Ikegaki, N. (2006b) 'The MYCN enigma: significance of MYCN expression in neuroblastoma', *Cancer Res*, 66(5), pp. 2826-33.
Tang, X.X., Zhao, H., Robinson, M.E., Cnaan, A., London, W., Cohn, S.L., Cheung, N.K., Brodeur, G.M., Evans, A.E. and Ikegaki, N. (2000a) 'Prognostic significance of EPHB6, EFNB2, and EFNB3 expressions in neuroblastoma', *Med Pediatr Oncol*, 35(6), pp. 656-8.
Tang, X.X., Zhao, H., Robinson, M.E., Cohen, B., Cnaan, A., London, W., Cohn, S.L., Cheung, N.K., Brodeur, G.M., Evans, A.E. and Ikegaki, N. (2000b) 'Implications of EPHB6, EFNB2, and EFNB3 expressions in human neuroblastoma', *Proc Natl Acad Sci U S A*, 97(20), pp. 10936-41.
Tansey, W.P. (2014) 'Mammalian MYC Proteins and Cancer', *New Journal of Science*, 2014, p. 27.
Tateishi, K., Omata, M., Tanaka, K. and Chiba, T. (2001) 'The NEDD8 system is essential for cell cycle progression and morphogenetic pathway in mice', *J Cell Biol*, 155(4), pp. 571-9.
Taylor, W.R. and Stark, G.R. (2001) 'Regulation of the G2/M transition by p53', *Oncogene*, 20(15), pp. 1803-15.
Tedesco, D., Lukas, J. and Reed, S.I. (2002) 'The pRb-related protein p130 is regulated by phosphorylation-dependent proteolysis via the protein-ubiquitin ligase SCF(Skp2)', *Genes Dev*, 16(22), pp. 2946-57.
Teng, Y., Ross, J.L. and Cowell, J.K. (2014) 'The involvement of JAK-STAT3 in cell motility, invasion, and metastasis', *JAKSTAT*, 3(1), p. e28086.
ThermoScientific (2004) 'Instructions SCF-Skp2 E3 Ligase: p27 degradation Redistribution Assay®'.
Timmerbeul, I., Garrett-Engele, C.M., Kossatz, U., Chen, X., Firpo, E., Grunwald, V., Kamino, K., Wilkens, L., Lehmann, U., Buer, J., Geffers, R., Kubicka, S., Manns, M.P., Porter, P.L., Roberts, J.M. and Malek, N.P. (2006) 'Testing the importance of p27 degradation by the SCFskp2 pathway in murine models of lung and colon cancer', *Proc Natl Acad Sci U S A*, 103(38), pp. 14009-14.
Tomasini, R., Seux, M., Nowak, J., Bontemps, C., Carrier, A., Dagorn, J.C., Pebusque, M.J., Iovanna, J.L. and Dusetti, N.J. (2005) 'TP53INP1 is a novel p73 target gene that induces cell cycle arrest and cell death by modulating p73 transcriptional activity', *Oncogene*, 24(55), pp. 8093-104.

Toyoshima, H. and Hunter, T. (1994) 'p27, a novel inhibitor of G1 cyclin-Cdk protein kinase activity, is related to p21', *Cell*, 78(1), pp. 67-74.

Trochet, D., Bourdeaut, F., Janoueix-Lerosey, I., Deville, A., de Pontual, L., Schleiermacher, G., Coze, C., Philip, N., Frebourg, T., Munnich, A., Lyonnet, S., Delattre, O. and Amiel, J. (2004) 'Germline mutations of the paired-like homeobox 2B (PHOX2B) gene in neuroblastoma', *Am J Hum Genet*, 74(4), pp. 761-4.

Tsai, Y.S., Chang, H.C., Chuang, L.Y. and Hung, W.C. (2005) 'RNA silencing of Cks1 induced G2/M arrest and apoptosis in human lung cancer cells', *IUBMB Life*, 57(8), pp. 583-9.

Tsvetkov, L.M., Yeh, K.H., Lee, S.J., Sun, H. and Zhang, H. (1999) 'p27(Kip1) ubiquitination and degradation is regulated by the SCF(Skp2) complex through phosphorylated Thr187 in p27', *Curr Biol*, 9(12), pp. 661-4.

Tumilowicz, J.J., Nichols, W.W., Cholon, J.J. and Greene, A.E. (1970) 'Definition of a continuous human cell line derived from neuroblastoma', *Cancer Res*, 30(8), pp. 2110-8.

Ubersax, J.A., Woodbury, E.L., Quang, P.N., Paraz, M., Blethrow, J.D., Shah, K., Shokat, K.M. and Morgan, D.O. (2003) 'Targets of the cyclin-dependent kinase Cdk1', *Nature*, 425(6960), pp. 859-64.

Ungermannova, D., Gao, Y. and Liu, X. (2005) 'Ubiquitination of p27Kip1 requires physical interaction with cyclin E and probable phosphate recognition by SKP2', *J Biol Chem*, 280(34), pp. 30301-9.

Uribesalgo, I., Buschbeck, M., Gutiérrez, A., Teichmann, S., Demajo, S., Kuebler, B., Nomdedéu, J.F., Marté-N-Caballero, J., Roma, G., Benitah, S.A. and Di Croce, L. (2011) 'E-box-independent regulation of transcription and differentiation by MYC', *Nature Cell Biology*, 13(12), pp. 1443-1449.

Valentijn, L.J., Koppen, A., van Asperen, R., Root, H.A., Haneveld, F. and Versteeg, R. (2005) 'Inhibition of a New Differentiation Pathway in Neuroblastoma by Copy Number Defects of N-myc, Cdc42, and nm23 Genes', *Cancer Research*, 65(8), pp. 3136-3145.

Valentijn, L.J., Koster, J., Haneveld, F., Aissa, R.A., van Sluis, P., Broekmans, M.E., Molenaar, J.J., van Nes, J. and Versteeg, R. (2012) 'Functional MYCN signature predicts outcome of neuroblastoma irrespective of MYCN amplification', *Proc Natl Acad Sci U S A*, 109(47), pp. 19190-5.

Valsesia-Wittmann, S., Magdeleine, M., Dupasquier, S., Garin, E., Jallas, A.C., Combaret, V., Krause, A., Leissner, P. and Puisieux, A. (2004) 'Oncogenic cooperation between H-Twist and N-Myc overrides failsafe programs in cancer cells', *Cancer Cell*, 6(6), pp. 625-30.

van den Heuvel, S. and Harlow, E. (1993) 'Distinct roles for cyclin-dependent kinases in cell cycle control', *Science*, 262(5142), pp. 2050-4.

van Noesel, M.M., Pieters, R., Voute, P.A. and Versteeg, R. (2003) 'The N-myc paradox: N-myc overexpression in neuroblastomas is associated with sensitivity as well as resistance to apoptosis', *Cancer Lett*, 197(1-2), pp. 165-72.

Van Roy, N., Laureys, G., Van Gele, M., Opdenakker, G., Miura, R., van der Drift, P., Chan, A., Versteeg, R. and Speleman, F. (1997) 'Analysis of 1;17 translocation breakpoints in neuroblastoma: implications for mapping of neuroblastoma genes', *Eur J Cancer*, 33(12), pp. 1974-8.

Vermeulen, J., De Preter, K., Mestdagh, P., Laureys, G., Speleman, F. and Vandesompele, J. (2010) 'Predicting outcomes for children with neuroblastoma', *Discov Med*, 10(50), pp. 29-36.

Vervoorts, J., Luscher-Firzlaff, J.M., Rottmann, S., Lilischkis, R., Walsemann, G., Dohmann, K., Austen, M. and Luscher, B. (2003) 'Stimulation of c-MYC transcriptional activity and acetylation by recruitment of the cofactor CBP', *EMBO Rep*, 4(5), pp. 484-90.

Villunger, A., Michalak, E.M., Coultas, L., Mullauer, F., Bock, G., Ausserlechner, M.J., Adams, J.M. and Strasser, A. (2003) 'p53- and drug-induced apoptotic responses mediated by BH3-only proteins puma and noxa', *Science*, 302(5647), pp. 1036-8.

Vlach, J., Hennecke, S. and Amati, B. (1997) 'Phosphorylation-dependent degradation of the cyclin-dependent kinase inhibitor p27(Kip1)', *EMBO Journal*, 16(17), pp. 5334-5344.

von der Lehr, N., Johansson, S., Wu, S., Bahram, F., Castell, A., Cetinkaya, C., Hydbring, P., Weidung, I., Nakayama, K., Nakayama, K.I., Soderberg, O., Kerppola, T.K. and Larsson, L.G. (2003) 'The F-box protein Skp2 participates in c-Myc proteosomal degradation and acts as a cofactor for c-Myc-regulated transcription', *Mol Cell*, 11(5), pp. 1189-200.

Wakamatsu, Y., Watanabe, Y., Nakamura, H. and Kondoh, H. (1997) 'Regulation of the neural crest cell fate by N-myc: promotion of ventral migration and neuronal differentiation', *Development*, 124(10), pp. 1953-62.

Wang, C., Liu, Z., Woo, C.W., Li, Z., Wang, L., Wei, J.S., Marquez, V.E., Bates, S.E., Jin, Q., Khan, J., Ge, K. and Thiele, C.J. (2012a) 'EZH2 Mediates epigenetic silencing of neuroblastoma suppressor genes CASZ1, CLU, RUNX3, and NGFR', *Cancer Res*, 72(1), pp. 315-24.

Wang, H., Bauzon, F., Ji, P., Xu, X., Sun, D., Locker, J., Sellers, R.S., Nakayama, K., Nakayama, K.I., Cobrinik, D. and Zhu, L. (2010a) 'Skp2 is required for survival of aberrantly proliferating Rb1-deficient cells and for tumorigenesis in Rb1+/- mice', *Nat Genet*, 42(1), pp. 83-8.

Wang, I.C., Chen, Y.J., Hughes, D., Petrovic, V., Major, M.L., Park, H.J., Tan, Y., Ackerson, T. and Costa, R.H. (2005) 'Forkhead box M1 regulates the transcriptional network of genes essential for mitotic progression and genes encoding the SCF (Skp2-Cks1) ubiquitin ligase', *Mol Cell Biol*, 25(24), pp. 10875-94.

Wang, Q., Hii, G., Shusterman, S., Mosse, Y., Winter, C.L., Guo, C., Zhao, H., Rappaport, E., Hogarty, M.D. and Maris, J.M. (2003) 'ID2 expression is not associated with MYCN amplification or expression in human neuroblastomas', *Cancer Res*, 63(7), pp. 1631-5.

Wang, S., Raven, J.F. and Koromilas, A.E. (2010b) 'STAT1 Represses Skp2 Gene Transcription to Promote p27Kip1 Stabilization in Ras-Transformed Cells', *Molecular Cancer Research*, 8(5), pp. 798-805.

Wang, X., Gorospe, M., Huang, Y. and Holbrook, N.J. (1997) 'p27Kip1 overexpression causes apoptotic death of mammalian cells', *Oncogene*, 15(24), pp. 2991-7.

Wang, X.C., Tian, L.L., Tian, J. and Jiang, X.Y. (2012b) 'Overexpression of SKP2 promotes the radiation resistance of esophageal squamous cell carcinoma', *Radiat Res*, 177(1), pp. 52-8.

Wang, X.C., Tian, L.L., Tian, J., Wu, H.L. and Meng, A.M. (2009a) 'Overexpression of Cks1 is associated with poor survival by inhibiting apoptosis in breast cancer', *J Cancer Res Clin Oncol*, 135(10), pp. 1393-401.

Wang, Z., Gerstein, M. and Snyder, M. (2009b) 'RNA-Seq: a revolutionary tool for transcriptomics', *Nat Rev Genet*, 10(1), pp. 57-63.

Watanabe, N., Arai, H., Nishihara, Y., Taniguchi, M., Watanabe, N., Hunter, T. and Osada, H. (2004) 'M-phase kinases induce phospho-dependent ubiquitination of somatic Wee1 by SCFbeta-TrCP', *Proc Natl Acad Sci U S A*, 101(13), pp. 4419-24.

Wei, J.S., Song, Y.K., Durinck, S., Chen, Q.R., Cheuk, A.T., Tsang, P., Zhang, Q., Thiele, C.J., Slack, A., Shohet, J. and Khan, J. (2008) 'The MYCN oncogene is a direct target of miR-34a', *Oncogene*, 27(39), pp. 5204-13.

Wei, W., Ayad, N.G., Wan, Y., Zhang, G.J., Kirschner, M.W. and Kaelin, W.G., Jr. (2004) 'Degradation of the SCF component Skp2 in cell-cycle phase G1 by the anaphase-promoting complex', *Nature*, 428(6979), pp. 194-8.

Wei, Z., Jiang, X., Qiao, H., Zhai, B., Zhang, L., Zhang, Q., Wu, Y., Jiang, H. and Sun, X. (2013) 'STAT3 interacts with Skp2/p27/p21 pathway to regulate the motility and invasion of gastric cancer cells', *Cell Signal*, 25(4), pp. 931-8.

Weiss, W.A., Aldape, K., Mohapatra, G., Feuerstein, B.G. and Bishop, J.M. (1997) 'Targeted expression of MYCN causes neuroblastoma in transgenic mice', *EMBO J*, 16(11), pp. 2985-95.

Wenzel, A., Cziepluch, C., Hamann, U., Schurmann, J. and Schwab, M. (1991) 'The N-Myc oncoprotein is associated in vivo with the phosphoprotein Max(p20/22) in human neuroblastoma cells', *EMBO J*, 10(12), pp. 3703-12.

Wenzel, A. and Schwab, M. (1995) 'The mycN/max protein complex in neuroblastoma. Short review', *Eur J Cancer*, 31A(4), pp. 516-9.

Westermann, F., Henrich, K.-O., Wei, J.S., Lutz, W., Fischer, M., König, R., Wiedemeyer, R., Ehemann, V., Brors, B., Ernestus, K., Leuschner, I., Benner, A., Khan, J. and Schwab, M. (2007) 'High Skp2 Expression Characterizes High-Risk Neuroblastomas Independent of MYCN Status', *Clinical Cancer Research*, 13(16), pp. 4695-4703.

Westermann, F., Muth, D., Benner, A., Bauer, T., Henrich, K.O., Oberthuer, A., Brors, B., Beissbarth, T., Vandesompele, J., Pattyn, F., Hero, B., Konig, R., Fischer, M. and Schwab, M. (2008) 'Distinct transcriptional MYCN/c-MYC activities are associated with spontaneous regression or malignant progression in neuroblastomas', *Genome Biol*, 9(10), p. R150.

Wirbelauer, C., Sutterluty, H., Blondel, M., Gstaiger, M., Peter, M., Reymond, F. and Krek, W. (2000) 'The F-box protein Skp2 is a ubiquitylation target of a Cul1-based core ubiquitin ligase complex: evidence for a role of Cul1 in the suppression of Skp2 expression in quiescent fibroblasts', *EMBO J*, 19(20), pp. 5362-75.

Woo, C.W., Tan, F., Cassano, H., Lee, J., Lee, K.C. and Thiele, C.J. (2008) 'Use of RNA interference to elucidate the effect of MYCN on cell cycle in neuroblastoma', *Pediatr Blood Cancer*, 50(2), pp. 208-12.

Wu, J., Lee, S.W., Zhang, X., Han, F., Kwan, S.Y., Yuan, X., Yang, W.L., Jeong, Y.S., Rezaeian, A.H., Gao, Y., Zeng, Y.X. and Lin, H.K. (2013) 'Foxo3a transcription factor is a negative regulator of Skp2 and Skp2 SCF complex', *Oncogene*, 32(1), pp. 78-85.

Wu, J., Zhang, X., Zhang, L., Wu, C.Y., Rezaeian, A.H., Chan, C.H., Li, J.M., Wang, J., Gao, Y., Han, F., Jeong, Y.S., Yuan, X., Khanna, K.K., Jin, J., Zeng, Y.X. and Lin, H.K. (2012a) 'Skp2 E3 ligase integrates ATM activation and homologous recombination repair by ubiquitinating NBS1', *Mol Cell*, 46(3), pp. 351-61.

Wu, L., Grigoryan, A.V., Li, Y., Hao, B., Pagano, M. and Cardozo, T.J. (2012b) 'Specific small molecule inhibitors of Skp2-mediated p27 degradation', *Chem Biol*, 19(12), pp. 1515-24.

Xu, M., Sheppard, K.A., Peng, C.Y., Yee, A.S. and Piwnica-Worms, H. (1994) 'Cyclin A/CDK2 binds directly to E2F-1 and inhibits the DNA-binding activity of E2F-1/DP-1 by phosphorylation', *Mol Cell Biol*, 14(12), pp. 8420-31.

Xu, S., Abbasian, M., Patel, P., Jensen-Pergakes, K., Lombardo, C.R., Cathers, B.E., Xie, W., Mercurio, F., Pagano, M., Giegel, D. and Cox, S. (2007) 'Substrate Recognition and Ubiquitination of SCFSkp2/Cks1 Ubiquitin-Protein Isopeptide Ligase', *Journal of Biological Chemistry*, 282(21), pp. 15462-15470.

Xue, C., Haber, M., Flemming, C., Marshall, G.M., Lock, R.B., MacKenzie, K.L., Gurova, K.V., Norris, M.D. and Gudkov, A.V. (2007) 'p53 Determines Multidrug Sensitivity of Childhood Neuroblastoma', *Cancer Research*, 67(21), pp. 10351-10360.

Yada, M., Hatakeyama, S., Kamura, T., Nishiyama, M., Tsunematsu, R., Imaki, H., Ishida, N., Okumura, F., Nakayama, K. and Nakayama, K.I. (2004) 'Phosphorylation-dependent degradation of c-Myc is mediated by the F-box protein Fbw7', *EMBO Journal*, 23(10), pp. 2116-2125.

Yam, C.H., Ng, R.W., Siu, W.Y., Lau, A.W. and Poon, R.Y. (1999) 'Regulation of cyclin A-Cdk2 by SCF component Skp1 and F-box protein Skp2', *Mol Cell Biol*, 19(1), pp. 635-45.

Yang, Z., He, N. and Zhou, Q. (2008) 'Brd4 recruits P-TEFb to chromosomes at late mitosis to promote G1 gene expression and cell cycle progression', *Mol Cell Biol*, 28(3), pp. 967-76.

Yokoi, S., Yasui, K., Mori, M., Iizasa, T., Fujisawa, T. and Inazawa, J. (2004) 'Amplification and overexpression of SKP2 are associated with metastasis of non-small-cell lung cancers to lymph nodes', *Am J Pathol*, 165(1), pp. 175-80.

Yu, A.L., Gilman, A.L., Ozkaynak, M.F., London, W.B., Kreissman, S.G., Chen, H.X., Smith, M., Anderson, B., Villablanca, J.G., Matthay, K.K., Shimada, H., Grupp, S.A., Seeger, R., Reynolds, C.P., Buxton, A., Reisfeld, R.A., Gillies, S.D., Cohn, S.L., Maris, J.M. and Sondel, P.M. (2010) 'Anti-GD2 antibody with GM-CSF, interleukin-2, and isotretinoin for neuroblastoma', *N Engl J Med*, 363(14), pp. 1324-34.

Yu, J., Wang, Z., Kinzler, K.W., Vogelstein, B. and Zhang, L. (2003) 'PUMA mediates the apoptotic response to p53 in colorectal cancer cells', *Proc Natl Acad Sci U S A*, 100(4), pp. 1931-6.

Yu, J. and Zhang, L. (2008) 'PUMA, a potent killer with or without p53', *Oncogene*, 27 Suppl 1, pp. S71-83.

Yu, Z.K., Gervais, J.L. and Zhang, H. (1998) 'Human CUL-1 associates with the SKP1/SKP2 complex and regulates p21(CIP1/WAF1) and cyclin D proteins', *Proc Natl Acad Sci U S A*, 95(19), pp. 11324-9.

Zeller, K.I., Jegga, A.G., Aronow, B.J., O'Donnell, K.A. and Dang, C.V. (2003) 'An integrated database of genes responsive to the Myc oncogenic transcription factor: identification of direct genomic targets', *Genome Biol*, 4(10), p. R69.

Zetterberg, A., Larsson, O. and Wiman, K.G. (1995) 'What is the restriction point?', *Curr Opin Cell Biol*, 7(6), pp. 835-42.

Zhan, F., Colla, S., Wu, X., Chen, B., Stewart, J.P., Kuehl, W.M., Barlogie, B. and Shaughnessy, J.D., Jr. (2007) 'CKS1B, overexpressed in aggressive

disease, regulates multiple myeloma growth and survival through SKP2- and p27Kip1-dependent and -independent mechanisms', *Blood*, 109(11), pp. 4995-5001.

Zhang, H., Kobayashi, R., Galaktionov, K. and Beach, D. (1995) 'p19Skp1 and p45Skp2 are essential elements of the cyclin A-CDK2 S phase kinase', *Cell*, 82(6), pp. 915-25.

Zhang, L. and Wang, C. (2006) 'F-box protein Skp2: a novel transcriptional target of E2F', *Oncogene*, 25(18), pp. 2615-27.

Zhao, H., Bauzon, F., Fu, H., Lu, Z., Cui, J., Nakayama, K., Nakayama, K.I., Locker, J. and Zhu, L. (2013) 'Skp2 deletion unmasks a p27 safeguard that blocks tumorigenesis in the absence of pRb and p53 tumor suppressors', *Cancer Cell*, 24(5), pp. 645-59.

Zheng, N., Schulman, B.A., Song, L., Miller, J.J., Jeffrey, P.D., Wang, P., Chu, C., Koepp, D.M., Elledge, S.J., Pagano, M., Conaway, R.C., Conaway, J.W., Harper, J.W. and Pavletich, N.P. (2002) 'Structure of the Cul1-Rbx1-Skp1-F boxSkp2 SCF ubiquitin ligase complex', *Nature*, 416(6882), pp. 703-9.

Zhu, X.H., Nguyen, H., Halicka, H.D., Traganos, F. and Koff, A. (2004) 'Noncatalytic requirement for cyclin A-cdk2 in p27 turnover', *Mol Cell Biol*, 24(13), pp. 6058-66.

Zimmerman, K.A., Yancopoulos, G.D., Collum, R.G., Smith, R.K., Kohl, N.E., Denis, K.A., Nau, M.M., Witte, O.N., Toran-Allerand, D., Gee, C.E. and et al. (1986) 'Differential expression of myc family genes during murine development', *Nature*, 319(6056), pp. 780-3.

Zuo, T., Liu, R., Zhang, H., Chang, X., Liu, Y., Wang, L., Zheng, P. and Liu, Y. (2007) 'FOXP3 is a novel transcriptional repressor for the breast cancer oncogene SKP2', *J Clin Invest*, 117(12), pp. 3765-73.

Appendix I

Western blotting buffers:

10x Electrophoresis buffer

30.3g Tris-Base (Sigma)
144.1g Glycine (Sigma)
10g SDS (Sigma)

Transfer buffer

3.03g Tris-Base
14.14g Glycine
200 ml Methanol
Made up to 1 litre with ddH_20

10x TBS Tween

90g NaCl (Sigma)
60g Tris-Base
1 litre ddH_20
pH 7.5 with HCl
5ml Tween 20 (Sigma)

Appendix II

Publications:

Evans L, Chen L, Milazzo G, Gherardi S, Perini G, Willmore E, Newell DR, Tweddle DA: SKP2 is a direct transcriptional target of MYCN and potential target in neuroblastoma.

- *Submitted to Cell Cycle for publication.*

Shouksmith A, **Evans LE**, Massa B, Willmore E, Tweddle DA, Miller DC, Newell DR, Griffin RJ, Golding BT: Synthesis of putative small-molecule inhibitors of the SCF^{SKP2} E2 ligase complex.

- *Submitted to Aust. J. Chem for publication*

Conference poster presentations:

L.Evans, E.Willmore, D.R.Newell, D.A.Tweddle*. "An investigation into the potential therapeutic benefit of targeting SKP2 in neuroblastoma".*

- Neuroblastoma society symposium, 2011, London, UK.
- Advances in neuroblastoma research (ANR) Conference, 2012, Toronto, Canada.
- National Cancer Research Institute (NCRI) cancer conference, 2012, Liverpool, UK
- American Association for Cancer Research (AACR), Annual Meeting 2013, Washington DC
- Neuroblastoma society symposium, 2013, Liverpool, UK.

Conference oral presentations:

- North East postgraduate conference, 2013, Newcastle upon Tyne, UK.
- SIOPEN Annual General Assembly, 2013, Paris, France.